# Nonlinear Resonant MHD Waves in Solar Plasmas

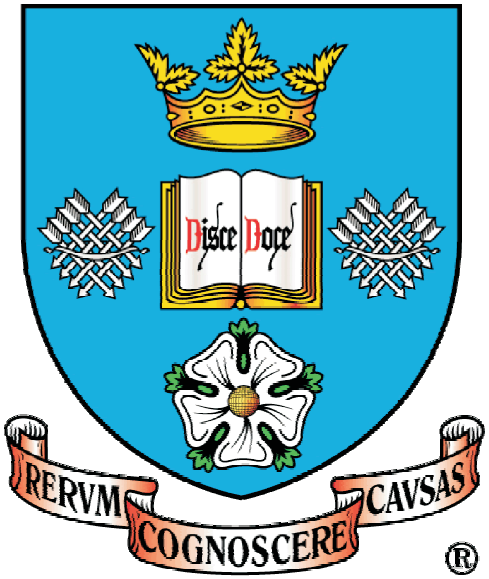


The University of Sheffield

Christopher Clack

Department of Applied Mathematics

Submission for the degree of Doctor of Philosophy

April 15, 2010

## Acknowledgements

This thesis could not have been completed without the enduring help and encouragement from many people.

My first thank you goes to my supervisor Dr Istvan Ballai. Not only did he open my eyes to solar physics, but his commitment for physical understanding, accuracy and completeness has shaped my thinking and approach to work. I next want to thank Prof. Michael S. Ruderman for his excellent scientific and mathematical guidance. Our many discussions often led me to new conclusions and a deeper understanding of mathematics and physics. Thirdly, I want to extend my gratitude to Prof. Robertus von Fáy-Siebenbürgen for convincing me Sheffield was the place to do my PhD and for our fascinating talks. I would also like to add a thank you to all the staff in the Applied mathematics department, all of whom answered any, and all, questions I had and made my life as a PhD student much easier.

I want to now thank people who are not staff, but have made my three years as a PhD student in Sheffield a delight. My office colleagues for the first two years: Alice, Andrew, Jennie, Jim and Phon. Without the laughter, chatter and mathematical discourse we all shared in that office I would not have survived the difficult first few months. I have often enjoyed lunch or coffee with many other friends in the department which has made my time here an experience as well as an education.

To my Dad, thank you! For our chats in my car when driving you to and from the hospital; encouraging me to continue my work, even when you were incredibly ill; wanting to see me succeed in whatever I chose to do; listening to me talk about my work, and asking inquisitive questions (which I couldn't always answer) right up until the end. You will be missed.

To the rest of my family: Mum, Dennis, Patrick, Timothy and Thomas, thank you all for putting up with my speeches about the Sun, and the magic of the maths that describes it. Each of you, in your own way, have contributed to how this thesis has been produced.

Finally, I want my biggest thank you to go to my beautiful and loving partner Sarah. You have been with me through it all; the choice of PhD; the extreme lows; the ecstatic highs; the conferences; the practice seminars; essentially, you name it you have been there. Thank you for all your support and keeping me in check with reality, even when I have been stressed, anxious or confused.

## Abstract

In solar physics many questions remain unanswered, such as the solar coronal heating problem in the solar atmosphere or magnetic field generation in the solar interior. However, there is a growing consensus that many different physical phenomena will combine to give a solution to these problems.

From the solar coronal heating point of view, one possible phenomenon to study is resonant absorption, which allows the natural transfer of wave energy to and from the background plasma. If the plasma is dissipative this energy can be converted into heat. One of the stumbling blocks when studying resonant absorption is that linear theory can *breakdown* around the resonant point. This causes a dilemma: use linear theory as an approximation regardless to try and find sensible solutions or try and solve the difficult, but realistic, nonlinear equations.

The present thesis will investigate the nonlinearity associated with resonant absorption. There are two different resonances in solar plasmas, one is the Alfvén resonance and the other is the slow resonance. Previous studies, in nonlinear theory, have concentrated mainly on the slow resonances as they are more affected by nonlinearity. We will study both the Alfvén and the slow resonances. The present thesis will analytically investigate these resonances in anisotropic, dispersive and dissipative plasmas - typical conditions of the solar upper atmosphere.

The second manifestation of nonlinearity is the generation of a mean shear flow outside the layer enclosing the resonant surface. We will derive the governing equations for this generated flow at the Alfvén resonance. These flows (like all flows) are completely determined by the boundary conditions and we produce an example flow.

The thesis culminates by studying *coupled resonances*; when the distance between an Alfvén and slow resonance is so small (in comparison to the incoming wave) they act as if they interact with an incoming wave simultaneously. We derive the governing equations for the absorption of fast magnetoacoustic waves at the coupled resonance, and then numerically analyse the coefficient of wave energy absorption to compare with the results found for single resonances. We find that the absorption of fast magnetoacoustic waves is far more efficient under coronal conditions compared with chromospheric conditions despite an increase in absorption due to the coupled resonance.

# Contents

# List of Figures

# List of Tables

# 1
# Introduction

*The present chapter is an introduction to the thesis. We begin by familiarizing ourselves with the Sun and its overall properties. Drawing on both theoretical and observational evidence we describe the types of possible magnetohydrodynamic waves and different heating mechanisms available in the solar atmosphere. Additionally, the concept of solar magnetism is discussed. The chapter then points out and conveys the importance of nonlinearity within physics and why it is critical to the work presented in the present thesis. The last section will describe the outline of the present thesis and what we intend to cover.*

*The Sun is a mass of incandescent gas, a gigantic nuclear furnace;*
*where hydrogen is built into helium at temperatures of millions of degrees...*
**(Why does the Sun shine?, They Might Be Giants)**

## 1.1 Overall properties of the Sun

The Sun is a fairly ordinary yellow dwarf star; however, its close proximity to Earth makes it unique as it is the only star we can observe in high resolution. Studying the Sun is not only of immense importance for the understanding of stars, stellar plasmas and the galaxy, but also serves as a natural laboratory for processes such as fusion, heating, magnetic dynamo, etc. A list of the Sun's overall properties are given in Table 1.1 along with the corresponding properties for the Earth for comparison[1].

Table 1.1: Some of the overall properties of the Sun and Earth.

| Property | Sun | Earth | Ratio |
|---|---|---|---|
| **Mean diameter** | $1.392 \times 10^9$ m | $1.274 \times 10^7$ m | 109 |
| **Surface area** | $6.088 \times 10^{18}$ m$^2$ | $5.101 \times 10^{14}$ m$^2$ | 11,935 |
| **Volume** | $1.412 \times 10^{27}$ m$^3$ | $1.083 \times 10^{21}$ m$^3$ | 1,303,786 |
| **Mass** | $1.989 \times 10^{30}$ kg | $5.974 \times 10^{24}$ kg | 332,943 |
| **Average density** | $1.408 \times 10^3$ kgm$^{-3}$ | $5.515 \times 10^3$ kgm$^{-3}$ | 0.273 |
| **Escape velocity** | 617.7 kms$^{-1}$ | 11.186 kms$^{-1}$ | 55 |
| **Rotation velocity** | 1997 ms$^{-1}$ | 465 ms$^{-1}$ | 4.3 |

The numbers when dealing with the Sun can be enormous, so we draw attention to the ratios in Table 1.1. The Sun is approximately $4.5 \times 10^9$ (4.5 billion) years old, and loses about $10^9$ kg of mass a second. The majority of the mass loss is through nuclear fusion; the process which produces the Sun's energy. Some other interesting facts about our closest star are: the mean distance between the Earth and Sun is $1.49 \times 10^{11}$ m [93 million miles or 1 Astronomical Unit (AU)], which takes light 8 minutes to travel; the radiation emitted by the Sun amounts to about 1 kWm$^{-2}$ at the Earth's surface; the *average* rotational period of the Sun is 28 days; and the temperature at the Sun's *surface* (the surface we see with the naked eye - not recommended!) is about 5700 K.

The Sun is is a huge ball of plasma held together, and compressed, under its own gravitational attraction. It consists of hydrogen (H) [90%], helium (He) [10%] and a tiny proportion of other heavier elements [1%]. Figure 1.1 shows the percentage composition of the photosphere in terms of the 10 most abundant elements. Within the Sun the heavier elements (C, N and O) are present in roughly the same proportions as on Earth, which alludes to a common ancestor such as the interior of an older star.

The Sun is usually divided into two main regions, the *interior* and *outer atmosphere*. The divide comes naturally from the fact that there is a visible *surface* to the Sun, known as the *photosphere*, beneath which lies the interior and above it the outer atmosphere. The photosphere is simply the layer above which the gases are too cool or too thin to radiate a significant amount of light and is, therefore, the surface most readily visible to the naked eye. A schematic representation of the structure of the Sun is given in Fig. 1.2.

[1]Note that the rotational velocity in the table refers to the equatorial speed.

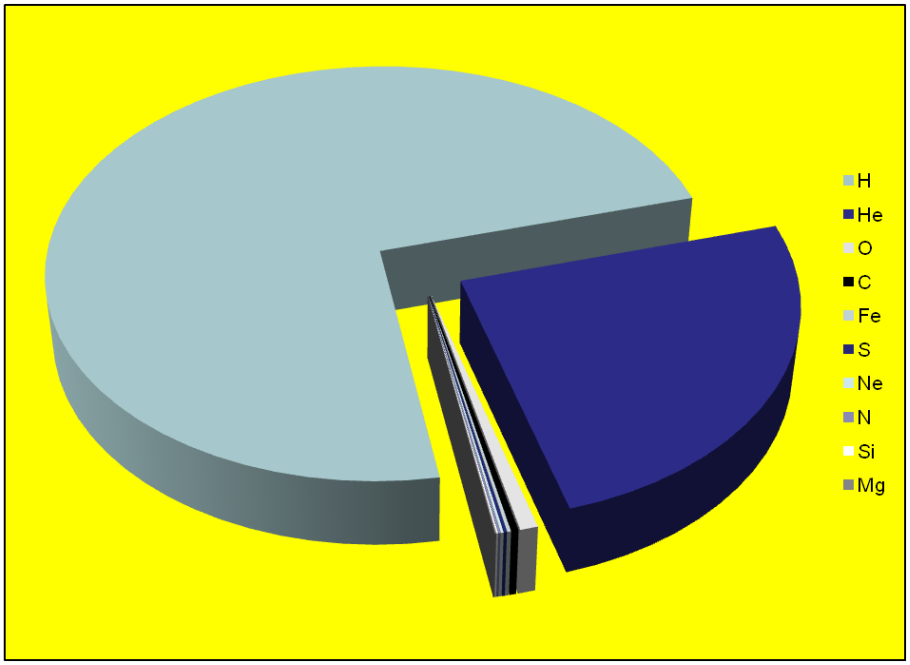


Figure 1.1: The photospheric composition of the photosphere's 10 most abundant elements. H $\approx$ 74%, He $\approx$ 25% and the rest contribute $\approx$ 1%.

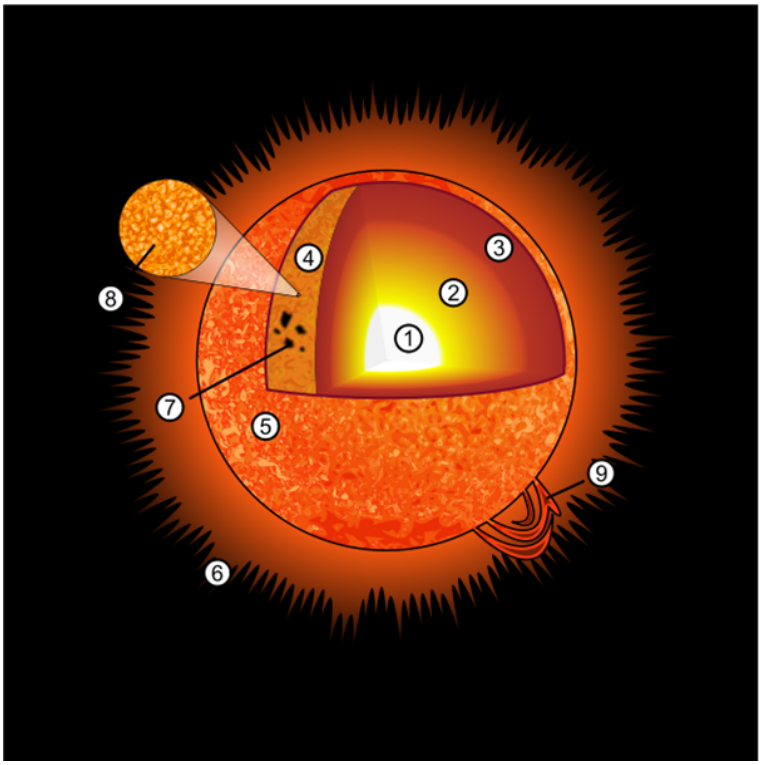


Figure 1.2: Schematic representation of the structure of the Sun and major features in its atmosphere: 1. Core; 2. Radiative zone; 3. Convection zone; 4. Photosphere; 5. Chromosphere; 6. Corona; 7. Sunspots; 8. Granules; 9. Prominence (Pbroks13, 2009).

### 1.1.1 Interior

The *interior* of the Sun is shielded from our view due to the opacity of the photosphere. However, we know that the solar interior is made up of four separate regions defined by the dominant processes taking place. The regions in question are called the core, the radiative zone, the tachocline and the convective zone.

The *core* contains half the mass of the Sun in only 1/5 of its volume and generates practically all of the energy. This energy is produced by fusing hydrogen into helium (nuclear fusion). The temperature and density in the core are $1.6 \times 10^7$ K (160 million degrees Celsius) and $1.6 \times 10^5$ kgm$^{-3}$ (approximately 10 times the density of gold), respectively. At these extraordinary temperatures and densities, the protons are so close together that (after quantum tunnelling) the strong nuclear force can overcome the electrostatic repulsion between the protons. This results in fusion and a mass loss, which corresponds to the energy released. The core burns up to $5 \times 10^9$ kg (5 million tonnes) of hydrogen a second. This process is extremely slow, taking (on average) the order of ten million years to complete a single cycle. In one cycle, the hydrogen is converted to helium according to the reaction:

$$4\,^1\mathrm{H} \rightarrow {}^4\mathrm{He} + 2e^+ + 26.7\,\mathrm{MeV},$$

where the energy is released in the form of two high-frequency $\gamma$-rays (26.2 MeV) and two neutrinos (0.5 MeV) [1 MeV $\approx 1.602 \times 10^{-13}$ J]. To put things into context, this results in a power density of just $193 \times 10^{-6}$ Wkg$^{-1}$, whereas a human body produces heat at a rate of approximately 1.2 Wkg$^{-1}$ (approximately 6000 times greater). However, the Sun is much much more massive than a human body!

The neutrinos are so minuscule that they escape the core (and the entire Sun) unimpeded. The $\gamma$-rays' (or photons') journeys are much more extravagant. They travel outwards by radiative diffusion (the $\gamma$-rays are absorbed, emitted and re-emitted many times by atoms, as well as being scattered by electrons resulting in the random walk motion). When they reach the edge of the core - where nuclear fusion can no longer be sustained (about 25% of the distance to the photosphere, in other words 175000 km from the centre of the Sun), they enter a new region called the *radiative zone*.

Inside the radiative zone, the $\gamma$-rays continue their radiative diffusion. This radiation causes the $\gamma$-rays' frequency to increase. The radiative zone extends to about $75 - 85\%$ of the distance to the photosphere and over this distance the temperature drops from 7 million K to 2 million K. The density also drops, from $2 \times 10^4$ kgm$^{-3}$ to $2 \times 10^2$ kgm$^{-3}$ (a fifth of the density of water). Eventually, at the top of the radiative zone there is a very thin transition region - known as the *solar tachocline*.

The solar tachocline is the transition layer where the plasma goes from being quiescent and radiative to being convectively unstable. The instability is caused by a steep temperature gradient. The tachocline is conjectured to be the place where the *solar dynamo* exists and produces the solar magnetic field. It is also at this point that *differential rotation* in the Sun begins. Below the tachocline the Sun rotates essentially as a solid body, but above this point it rotates differentially; with the poles rotating slower than the equator (see Fig. 1.3).

The *convection zone* extends from the solar tachocline to the photosphere. In this region the $\gamma$-rays that originated in the core are nearly at the end of their journey out of the Sun. Heat is transferred in this region by 'blobs' of hot plasma rising (expanding and cooling) and blobs of cooler plasma falling in a convective motion. The change in density in the convection zone

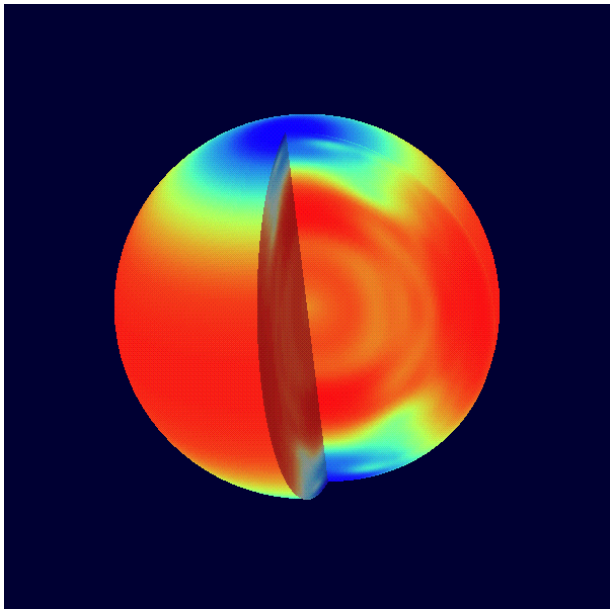

Figure 1.3: Model of the differential rotation of the Sun. The colour spectrum is defined from blue (slowest) to red (fastest).

takes it to $2 \times 10^{-4}$ kgm$^{-3}$ (0.017% the density of air at mean sea level) at the photosphere. The temperature at the top of the convection zone is 5800 K. It is only above the photosphere that the plasma becomes *optically thin* meaning the photons can finally be released from the Sun and head out towards outer space. This journey, from the solar core to the photosphere (which would take 2 seconds in free space), has taken the photons $10^7$ (10 million) years to complete.

### 1.1.2 Outer atmosphere

The outer atmosphere is the part of the Sun we can observe directly with, e.g. the ultraviolet (UV), visible or infrared (IR) spectrum. The solar atmosphere (like the solar interior) can be divided into four regions, however, instead of being defined by the dominant processes taking place within the regions, they are defined by the evolution of temperature and density in the regions. The regions of the solar atmosphere are known as the photosphere, the chromosphere, the transition region and the corona. A table of the *average* densities of the regions of the outer atmosphere (including the solar wind) is given in Table 1.2 (with the solar core as a comparison).

Table 1.2: Typical densities and temperatures throughout the solar outer atmosphere.

| Region | Number density ($m^{-3}$) | Mass density ($kgm^{-3}$) | Temperature (K) |
|---|---|---|---|
| **Core** | $10^{32}$ | 167,300 | $1.6 \times 10^7$ |
| **Photosphere** | $10^{23}$ | $2 \times 10^{-4}$ | 5,700 |
| **Chromosphere** | $10^{18}$ | $2 \times 10^{-9}$ | 10,000 |
| **Transition region** | $10^{15}$ | $2 \times 10^{-12}$ | 100,000 |
| **Corona** | $5 \times 10^{14}$ | $10^{-12}$ | $2 \times 10^6$ |
| **At 1AU** | $10^7$ | $2 \times 10^{-20}$ | $10^5$ |
| **In interstellar medium** | $10^6$ | $2 \times 10^{-21}$ | N/A |

The lowest part, the *photosphere*, is an extremely thin (of the order of a few 100 km) layer of plasma at approximately 5700 K. This layer is opaque and emits most of the solar radiation. It is the 'surface' of the Sun we can see from Earth with the naked eye. The photosphere has a plethora of features within it; Fig. 1.2 shows two of them; *sunspots* and *granules*. Figure 1.4 gives a high resolution observation of a pair of sunspots and granulation. Sunspots are regions of intense magnetic activity where convection is inhibited by strong magnetic fields. Since magnetic fields exert a pressure, the plasma pressure inside a sunspot does not need to be as great as the plasma pressure elsewhere in the photosphere such that the total pressure remains constant, therefore, the sunspot radiates less light than the rest of the photosphere and so looks darker (note, if you were to block out the rest of the photosphere and look at a sunspot you would still go blind!). The granules are cells of convective motions, and we can actually observe *meso- super*-granules, which are much larger than individual granulations. These granulations are constantly changing thanks to the convective motion below; it looks similar to the top of a pan of boiling water. The photosphere is a very dynamic region, observations show that the entire region oscillates with a period peaked around 3– and 5– minutes. This global oscillation is used to probe the inner structure of the Sun using helio-seismological techniques.

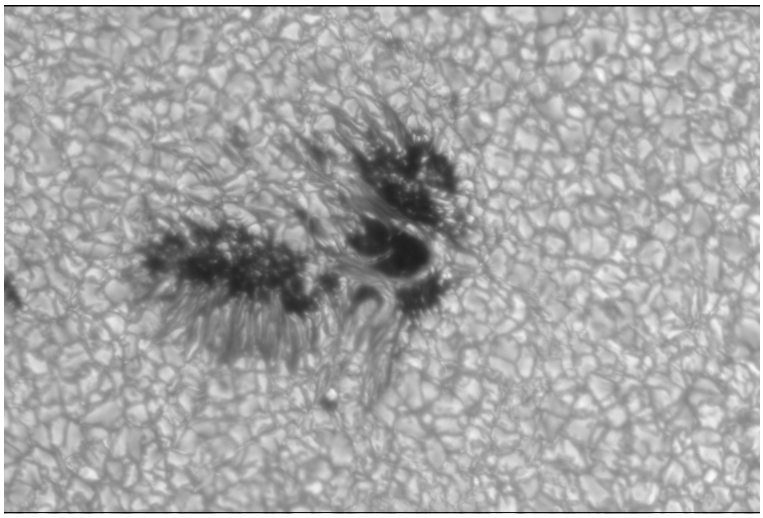

Figure 1.4: Detailed observation of a sunspot and photospheric granulation (courtesy of A. Hanslmeier, SVST at La Palma).

The layer above the photosphere is the *chromosphere* (originating from the Greek word for 'colour'). This region can be split into three further regions the *lower*, *middle* and *upper* chromosphere. The lower chromosphere extends from the photosphere to above the *temperature minimum* ($0-700$ km above the photosphere), the middle chromosphere is located within the relatively temperature stable region between $700-1700$ km above the photosphere and the upper chromosphere begins with a jump in temperature followed by a steady increase in temperature to the transition region ($1700-2300$ km above the photosphere). The chromosphere can be observed in, e.g. $H_\alpha$ (656.28 nm) or $H_\beta$ (486.13 nm) [1 nm=$10^{-9}$ m]. The chromosphere is abundant in various magnetic activities and exhibits features such as a network of magnetic field elements, bright plages around sunspots, dark filaments observed on the disk and prominences on the limb (see Fig. 1.2).

The *transition region* is located between $2300-2800$ km above the photosphere and is so-called because there is a steep transition in temperature from 20,000 K to 500,000 K. The transition region

is highly inhomogeneous and acts as a buffer zone between the corona and the much cooler chromosphere. We can observe the transition region from space using, e.g. CIV and OVI emission lines, which are in the UV spectrum.

The final region of the outer atmosphere is the *solar corona* which is the hottest region of the solar outer atmosphere (see Fig. 1.5 for the temperature change from the photosphere to the corona). The corona extends from 2800 km above the photosphere right out beyond 1AU ($15\times10^{10}$ m) via the *solar wind*. The corona (only visible during total solar eclipses before the space age) takes its name from the Latin word for 'crown'. The corona has many features such as streamers, polar plumes, coronal arcades, coronal mass ejections (CMES), flares, coronal rain and the solar wind, which are all manifestations of the magnetic field at coronal level. The frequency of these magnetic entities vary with the solar cycle which repeats, on average, every 11 years (see Fig. 1.6 which shows the number and location of sunspots with time).

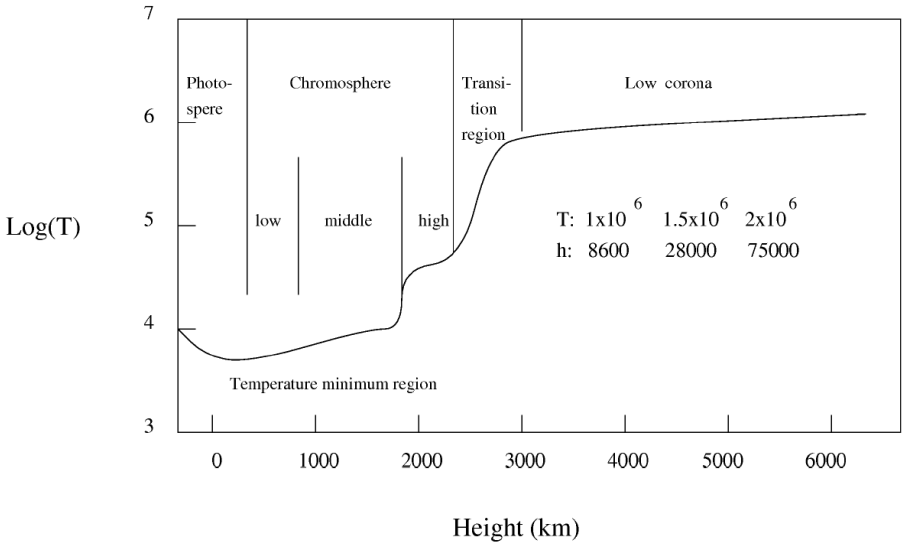


Figure 1.5: The variation of temperature with height throughout the solar outer atmosphere. The temperature is represented on a logarithmic scale. Image reproduced from Athay (1976).

Although the solar atmosphere's regions seem to contain plasma with vastly different physical properties, in reality the entire atmosphere is permeated by the solar magnetic field. Magnetism is the key to understanding the Sun (especially its atmosphere). Magnetic field is produced inside the Sun by the flow of electrically charged ions and electrons (thought to originate in the solar tachocline). Sunspots are places where very intense magnetic lines break through the photosphere. The sunspot cycle results from the recycling of magnetic fields by the flow of material in the interior. The prominences seen floating above the surface of the Sun are supported, and threaded through, by magnetic fields. The streamers and coronal loops seen in the corona are shaped by magnetic fields. Magnetic fields are at the root of virtually all of the features we see on the Sun. Magnetic field lines loop through the solar atmosphere and interior to form a complicated web of magnetic structures. Many of these structures are visible in the solar chromosphere and corona. However, the magnetic field is usually measured in the photosphere. For a more detailed review of the solar magnetic field, we refer to, e.g. Balogh and Thompson (2009); Parker (2009) [and references therein].

We have covered the overall features of the Sun in this section, however, each item included

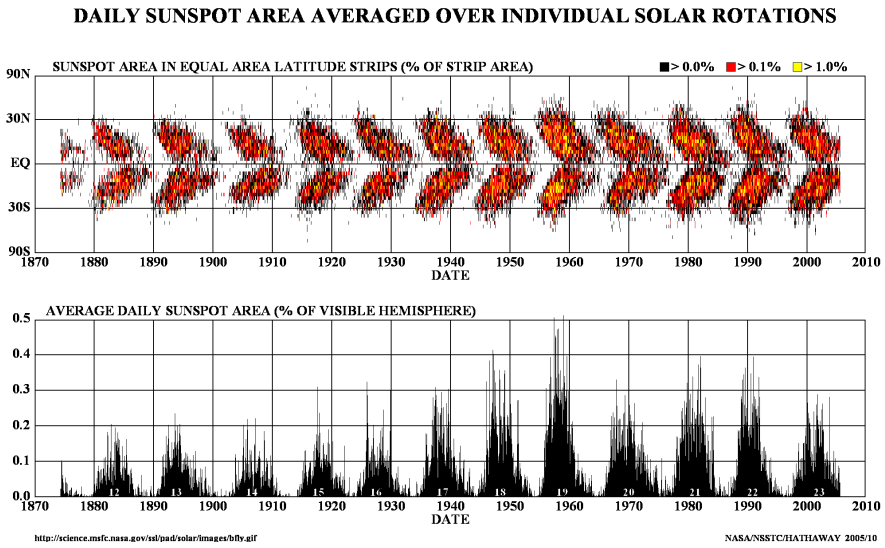


Figure 1.6: The butterfly diagram, and average daily sunspot plot of solar sunspots for several solar cycles (courtesy of David Hathaway, NASA).

here can be expanded and explained in greater detail. For the sake of brevity, we refer to four example books which cover the structure of the Sun further, namely Priest (1984), Mariska (1992), Golub and Pasachoff (1997) and Aschwanden (2004).

## 1.2 MHD Waves

The dynamical response of the plasma in the solar atmosphere to the rapid changes in the interior can be manifested through wave propagation within the solar atmosphere. Many of these waves are in the magnetohydrodynamic (MHD) spectrum. In this section we give a qualitative discussion of the MHD waves present in the solar atmosphere based on theory and observations, however, we do not derive any dispersion relations or mathematical models giving the evolution of the waves. In Sect. 2.2 we will deal with the mathematics and theory of unbounded homogeneous MHD waves, this is also where we will derive the dispersion relations. The section is intended as an introduction into the different types of MHD waves and where they are observed within the solar atmosphere. In addition, we will, briefly, discuss the history of the observations of global oscillations.

Ordinary sound waves in air owe their existence to the restoring force created by a gas pressure gradient. If we introduce a magnetic field to this system we create two more restoring forces, the magnetic tension and magnetic pressure gradient. If we assume that the plasma is homogeneous (every element of the plasma is identical to any other element) and infinite, the ideal MHD equations predict the existence of three different types of waves called the *slow magnetoacoustic*, *Alfvén* and *fast magnetoacoustic* waves (if gravitational and non-inertial forces are neglected).

The slow magnetoacoustic (or just simply slow waves) waves are driven by the magnetic and plasma pressure interacting destructively, whereas the fast magnetoacoustic (FMA) waves are produced when the magnetic and gas pressure interact constructively. The Alfvén wave has an intermediate wave speed, and is entirely driven by the magnetic tension. A polar diagram of the

phase speeds of these three wave types is given in Fig 1.7[2]. We can see from Fig. 1.7 that slow

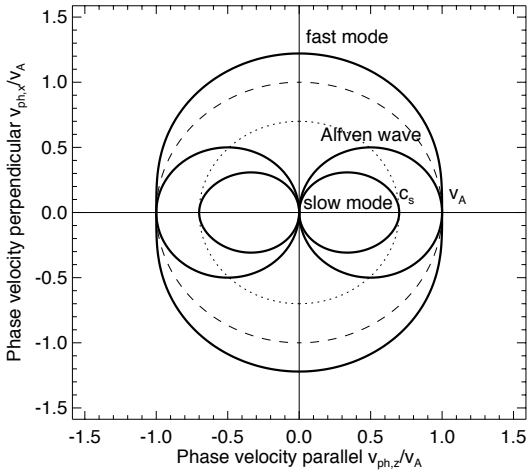


Figure 1.7: Polar plot of the phase speeds of the three types of MHD waves. The magnetic field lines lie parallel to the horizontal axis. Here the sound speed ($c_S$) is 70% of the Alfvén speed ($v_A$). The Alfvén speed and sound speed are given by the dashed and dotted line, respectively (Aschwanden, 2004).

waves travel fastest at very small angles off parallel to the magnetic field lines and fast waves travel in any direction, with a larger speed when they propagate perpendicular to the ambient magnetic field lines. Alfvén waves have a preference to transport energy along field lines and never across them (analogous to vibrations on a guitar string). The properties of these three waves are given quantitatively in Sect. 2.2.

It was recognised a long time ago that solar and space plasmas are in fact inhomogeneous, with physical properties varying over length scales much smaller than the scales determined by the gravitational stratification. Homogenous plasmas have a spectrum of linear eigenmodes which can be divided into the slow, fast and Alfvén subspectra (as described above). The slow and fast subspectra have discrete eigenmodes whereas the Alfvén subspectrum is infinitely degenerated[3]. When a transversal inhomogeneity is introduced the three subspectra are changed. The infinite degeneracy of the Alfvén point spectrum is lifted and replaced by the Alfvén continuum along with the possibility of discrete Alfvén modes occurring, the accumulation point of the slow magnetoacoustic eigenvalues is spread out into the slow continuum and a number of discrete slow modes may occur. Finally, the fast magnetoacoustic point spectrum accumulates at infinity (see, e.g. Goedbloed, 1975, 1984). Excitation of local Alfvén or slow oscillations provides a means for dissipating the wave energy far more efficiently in a weakly dissipative plasma than damping within a uniform plasma.

The solar atmosphere is highly structured throughout. In the case of the atmosphere we have large gradients which are created by the magnetic field. The magnetic field tends to accumulate in entities known as *flux tubes* and this imposes a strict ordering. The process of emergence of flux tubes is believed to be caused by the massive convective motions below the photosphere. Within the photosphere itself, stratification is dominated by the pressure and density gradients. In the light of all this structuring, we would expect there to be an abundance of MHD oscillations and waves present within the solar atmosphere. A detailed summary of the magnetic structuring within the solar atmosphere and an observational review of the waves they support can be found

[2]The derivation of the dispersion relations needed to plot this diagram is given in Sect. 2.2.
[3]An infinite number of discrete points

in, e.g. Roberts (1988); Zirker (1993); Nakariakov and Verwichte (2005); Banerjee et al. (2007); Erdélyi (2008). The observed MHD waves may play a role in complicated problems of the solar atmosphere, e.g. the heating of magnetic structures in the solar upper atmosphere.

Global oscillations of the Sun were first observed by Leighton et al. (1962) who detected oscillations with periods of around 5−minutes. These oscillations were not understood until they were viewed in conjunction with the observations of Deubner (1975) and the theoretical studies by Ulrich (1970); Leibacher and Stein (1971). These 5−minute oscillations are, in fact, global acoustic modes throughout the Sun, the so-called *pressure* or *p*-modes. After the p-modes were isolated, several new branches of solar physics began namely, *helio-* and *astro- seismology*. A detailed review of helio- and astro- seismology can be found in, e.g. Erdélyi (2006); Thompson (2006); DiMauro (2008); Korzennik (2008); Thompson and Zharkov (2008).

Beckers and Tallant (1969) were the first to detect oscillations within sunspots and since then even greater complexity has been discovered. A 3−minute and 5−minute oscillation exist in most sunspots' umbrae, where the 3−minute mode is more intense. The penumbrae also exhibit oscillations, but they tend to have periods of 4−minutes or longer (see, e.g. Lites, 1988). Zirin and Stein (1972) first detected so-called *penumbral waves* which are waves that have coherent wave fronts and appear to be produced within the umbra and then propagate across the penumbra with speeds of around $20 - 35$ kms$^{-1}$. Within the photosphere and chromosphere there is a hierarchy of magnetic structures ranging from sunspots (with scales of the order of $10^7$ m), to pores and knots (of the order of $10^5$ m) and right down to intense magnetic flux tubes (which can be of the order of $10^2 - 10^3$ m). These intense magnetic flux tubes have drawn large amounts of theoretical attention because they are thin; this allows the *thin tube approximation* to be applied, simplifying the governing equations considerably. The thin tube approximation was first used by, e.g. Spruit (1981); Spruit and Roberts (1983); Thomas (1985), but is still used today within solar physics by, e.g. Ballai et al. (2006); Goossens et al. (2008); Ballai et al. (2008); Erdélyi and Morton (2009).

Rigorous analytical studies of MHD waves began in the 1970s, but was developed further in the study by Roberts (1981a); where they studied MHD waves at a magnetic surface in an unbounded homogeneous plasma and derived the dispersion relations for the magnetoacoustic waves described in the present section. The work was continued in Roberts (1981b); Edwin and Roberts (1982); Roberts and Mangeney (1982); Edwin and Roberts (1983); Roberts et al. (1984). These studies extended the investigation of MHD waves to cases where the plasma environment was a magnetic slab, and furthered this by considering a magnetic tube. The critical finding of these seminal studies was the introduction of the concept of an interface or discontinuity in an otherwise homogeneous plasma; this led to the conclusion there are two further types of waves, the so-called *surface* and *body* waves, which can propagate within and along magnetic structures. Surface waves are geometrically confined to the surface of the slab / tube and the body waves are geometrically confined within the slab / tube (see Fig 1.8). Surface and body waves can be further sub-divided. The first and second modes are *sausage* and *kink* modes, respectively, while the third mode is the fluting mode. Sausage modes do not displace the symmetry axis of the tube, whereas the kink modes move the axis with the motion (see Fig 1.9). Fluting modes have much less energy compared with the energy of a kink mode (Terradas et al., 2007), so they are not considered in the present thesis. In nature true discontinuities do not exist, however, large gradients may develop due to a structuring being present which may act like a discontinuity. Kink modes have been observed in the solar corona by, e.g. Nakariakov et al. (1999); Aschwanden et al. (1999a); Ofman and Wang (2008); Erdélyi and Taroyan (2008); O'Shea and Doyle (2009) while sausage modes have

been observed in coronal loops by, e.g. Aschwanden (2003); Erdélyi and Taroyan (2008). Alfvén waves avoided detection for many years, indeed on several occasions when they were believed to be observed (Tomczyk et al., 2007; DePontieu et al., 2007), the waves turned out to be kink modes (van Doorsselaere et al., 2008). However, recently, Alfvén waves were correctly detected in the solar lower atmosphere by Jess et al. (2009).

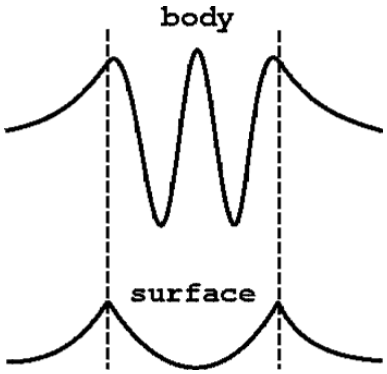


Figure 1.8: Schematic diagram of surface and body waves. Both waves are evanescent outside the inner structure. Surface waves have maximum energy at the interface, while, in the case of body waves, the energy remains inside the structure.

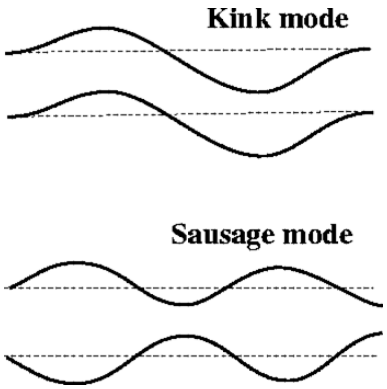


Figure 1.9: Schematic diagram of kink and sausage modes. The kink mode oscillates so that the symmetry axis is perturbed, whereas sausage modes do not alter the symmetry axis.

The further we move from the photosphere the more dominant the magnetic pressure becomes over the gas pressure. Consequently, the Alfvén speed (i.e. the propagation speed of Alfvén waves) increases rapidly with height. The corona is a region where the magnetic field dominates the physics and the plasma tends to accumulate preferentially along the magnetic field lines. This gives an ideal medium for MHD waves to propagate. Figure 1.10 shows typical *coronal arcades* where MHD waves propagate in abundance (see discussion above about kink and sausage mode propagation). It has been proposed that MHD waves may provide some of the heating required to maintain the high temperatures observed in the solar corona; in particular, the heating of coronal loops and arcades. A brief review of these, and other types of heating mechanisms, is included in the next section.

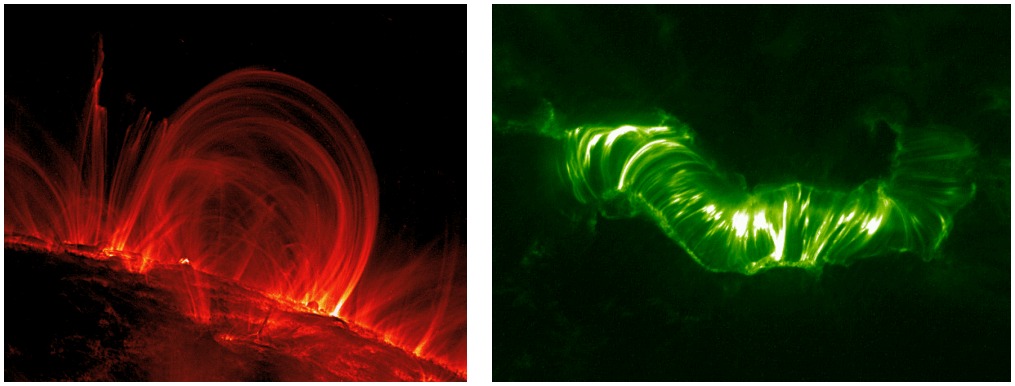

Figure 1.10: Coronal arcades within the solar corona. The left image is seen in 171Å and the right is viewed in 195Å, which corresponds to temperatures of $10^6$ K and $1.5 \times 10^6$ K, respectively (TRACE images).

## 1.3 Heating Mechanisms

The solar corona is a tenuous hot plasma with an average temperature of the order of $1 - 2 \times 10^6$ K. This very high temperature is reached far above the photosphere which has a temperature of only a few thousand degrees Kelvin. Explaining this extremely high temperature is one of the fundamental problems remaining in solar physics; the so-called *coronal heating problem*. The source of the energy producing the heating is simple and was outlined sixty years ago; the only available source of suprathermal energy to heat the corona comes from the mechanical work of the convection flows (see, e.g. Biermann, 1946; Schatzman, 1949; Alfvén, 1950; Piddington, 1956; Osterbrock, 1961). The elusive part of this problem is the precise nature of the connection between the energy within the convection flows and the solar corona.

The general consensus is that this *connection* is provided by the magnetic field. This idea was proposed after it was identified that active regions (particularly coronal loops) have the highest heating requirements implying that the kinetic energy within the convection flows is transferred to the magnetic field lines by shuffling their *footpoints*. If the characteristic time scale ($t_p$) of the shuffling is introduced and we define the Alfvén transit time as $t_A = l_{loop}/v_A$ (where $l_{loop}$ is the characteristic length of the magnetic flux tube and $v_A$ is the Alfvén phase velocity) we can distinguish between two different regimes.

If $t_p \gg t_A$ the shuffling is thought to be slow; building up magnetic stress, resulting in the magnetic flux tube being *twisted* or *braided*. The energy can be released via magnetic relaxation, magnetic reconnection (*nano-*, *micro- flaring*) or by a cascade of magnetic energy to very small length scales (see, e.g. Parker, 1972; van Ballegooijen, 1985; Biskamp, 1986; Priest and Forbes, 1992; Parker, 1993; Priest, 1997; Jain et al., 2006; Sarkar and Walsh, 2008; Birn et al., 2009). These heating mechanisms are collectively known as *DC heating*. The present thesis will not consider DC heating mechanisms, for further details we refer to, e.g Walsh and Ireland (2003); Erdélyi (2004); Erdélyi and Ballai (2007).

Fast shuffling corresponds to $t_p \ll t_A$; generating magnetoacoustic and Alfvén waves. Due to the sharp gradients near the footpoints, the majority of MHD waves bounce back and forth along the magnetic flux tubes. The loop essentially acts as a leaking resonant cavity in which wave dissipation can occur by means of turbulence enhancement, resonant absorption and phase mixing (see, e.g. Dobrowolny et al., 1980; Hasegawa and Uberoi, 1982; Heyvaerts and Priest, 1983;

Goossens, 1994; Matthaeus et al., 1994; Ruderman et al., 1998; Dmitruk and Gómez, 1999; Vasquez, 2005; Mocanu et al., 2008; Galtier, 2009). These processes are the so-called *AC heating mechanisms*. There is increasing agreement that all these processes act simultaneously to different degrees of efficiency throughout the solar corona. The agreement comes as observational data confirms the abundance of MHD wave propagation in the solar atmosphere, along with the complexity of the magnetic configuration enabling magnetic heating to occur (see, e.g. Doschek et al., 1976; Feldman et al., 1976; Cheng et al., 1979; Mariska et al., 1979; Acton et al., 1981; Jess et al., 2009; Vasheghani et al., 2009). However, even with recent advancements in spatial and temporal resolution we can still not observe the small scales needed to definitively conclude which dissipative processes are acting most efficiently within the solar atmosphere.

For all AC heating mechanisms a wave has to arrive at the region where they are to be dissipated. In the past the assumption was that the waves propagate from the photosphere below due to the magnetic shuffling. If this was the case, the only wave to arrive in the solar corona would be the Alfvén wave because the sharp gradients within the transition region would cause the magnetoacoustic slow waves to shock and fast waves to be reflected dissipating their energy rapidly - but both slow and fast waves have been observed in the solar corona (see, e.g. Ofman and Wang, 2008; Wang et al., 2009). However, there is another possible explanation: MHD waves are produced *within* the solar corona itself by, e.g. reconnection events or instabilities eliminating the difficulties of travelling to the corona via the transition region (see, e.g. Roussev et al., 2001a,b,c).

Historically phase mixing and resonant absorption have attracted intense research. These mechanisms can only occur when there is a transversal inhomogeneity within the plasma medium where the waves propagate. The phase mixing dissipation mechanism is due to the spontaneous decay of the free oscillations of the system. When the oscillations on different magnetic surfaces are initially excited in phase (coherently) the system will gradually evolve such that the oscillations become out of phase with the neighbouring magnetic surfaces; since each magnetic surface vibrates with a specific (and different) eigenfrequency. A consequence of this is the development of large gradients across these magnetic surfaces. This process leads to the creation of progressively smaller length scales and at some point will reach the limit where resistivity and viscosity operate enabling wave damping to occur. In contrast, resonant absorption involves the excitation of a single magnetic surface (when considering a single driving frequency); and since this thesis concentrates on resonant absorption a full introduction to this topic is given in Chapter 2.

## 1.4 Importance of nonlinearity

In general, to describe realistic physical processes accurately we need a nonlinear mathematical model. A classical example is modelling a flexible wooden stick. If we apply a transversal force on both ends of the stick we know, instinctively, that the stick will bend and if the forces are large enough the stick will break. However, if we use linear equations in our model the stick will just continue to bend forever; a nonlinear term is needed to explain why the stick would break.

Due to the limited mathematical framework available, only a few (simplified) nonlinear systems can be described in an analytical way. Numerical simulations have provided greater accessibility and have even given the answers to many problems, nevertheless nonlinearity and its effects remain an open question. Linearisation is an approximative device used in the study of physical systems which can give the underlying properties of a process. However, there are many cases in

which linearisation and the subsequent treatment of a system is not sufficient (such as the problem illustrated above). Indeed, new phenomena frequently occur in nonlinear problems which cannot exist in linear systems.

Solutions to nonlinear theories within MHD can be divided into three distinct classes:

- Properties of arbitrarily large disturbances are deduced straight from the full MHD equations. Integral inequalities are considered to yield bounds on flow quantities; such as the energy of the disturbances (which gives the stability criteria for growth or decay with time). These theories are advantageous because they supply mathematically rigorous results without incorporating too many assumptions. These criteria can correspond closely to the observed stability boundaries within the solar environment.

- Numerical simulations attempt to follow the evolution of an initial disturbance by direct computation of the MHD equations. Considerable success has been achieved within this field; and with the extraordinary speed at which computers are advancing further development is predicted, despite the complexity and sensitivity of numerical procedures.

- Weakly nonlinear theory is based on the idea that the linearised MHD equations provide a fundamental approximation for *very small*[4] finite amplitude perturbations. Successive approximations may then be introduced by asymptotic expansion of ascending powers of the characteristic dimensionless amplitude of the perturbation. This theory has been very successful in providing further understanding of processes taking place with the solar atmosphere.

Most of these theories have been developed with full regard to mathematical rigour, producing significant results for specific limiting cases. Other theories employ more heuristic methods in questions such as; convergence of the amplitude expansions; or the validity of their truncation of expansion. The success of modelling realistic physical problems which cannot be solved rigorously can be the only justification for adopting a non-rigorous approach.

Within the context of space physics intense research has been invested into various problems regarding nonlinear MHD waves in inhomogeneous plasmas. For example, there is an interest in explaining the Alfvén resonator within Earth's ionosphere (see, e.g. Sydorenko et al., 2008), rapid pulsations in the Sun's corona (see, e.g. Roberts et al., 1984; Rui-Xiang et al., 2003) and interpretting observed phenomena in galactic jets in terms of MHD waves (see, e.g. Roberts, 1987; Das et al., 2005). Other areas which have drawn significant attention include: the formation of shock waves and nonlinear interactions generating waves (see, e.g. Wentzel, 1977; Nakariakov and Oraevsky, 1995; Nakariakov et al., 1997; Wang and Lin, 2003; Chandran, 2008); the appearance of solitons (see, e.g. Roberts and Mangeney, 1982; Belmonte-Beitia et al., 2007; Erdélyi and Fedun, 2007; Pokhotelov et al., 2007; Fedun et al., 2008); examining wave phenomena in the solar wind (see, e.g. Mann, 1995; Ballai et al., 2003; Li and Li, 2007). A great effort, in recent years, has been paid to try to understand wave absorption and heating of the outer atmosphere of the solar atmosphere (see, e.g. Ruderman and Goossens, 1993; Ruderman et al., 1997b,c,d; Ballai and Erdélyi, 1998; Ballai et al., 1998a,b; Erdélyi and Ballai, 1999, 2001; Clack and Ballai, 2008, 2009a,b; Clack et al., 2009a,b).

[4]This refers to the characteristic dimensionless amplitude of oscillation being much smaller than a characteristic scale; so it depends on the wave being studied and the physics of the problem. It will be quantified by a nonlinear parameter introduced in Chapter 2.

In the context of resonant absorption, the majority of the work has been carried out from a linear point of view which is a direct result of the difficulties met when considering the highly nonlinear nature of the MHD equations. Although the driven MHD waves are assumed to be linear far away from the resonant magnetic surface, the near-resonant behaviour of the waves in the vicinity of the resonant position may cause linear theory to breakdown; hence we need the introduction of nonlinear theory.

## 1.5 Outline of thesis

At the thesis' core are the concepts of resonance, anisotropy, dispersion, dissipation and nonlinearity. We aim to assess the processes taking place at resonance in highly anisotropic, dispersive and weakly dissipative plasmas. We achieve this in three steps:

- Studying the *nonlinear theory of resonant slow waves*.
- Investigating the *nonlinear theory of resonant Alfvén waves*.
- Applying our theories to the *nonlinear resonant absorption of fast magnetoacoustic waves*.

The present analysis restricts itself, in the most part, to a *static* background equilibrium. This restriction is easily relaxed by assuming a steady flow parallel to the magnetic surfaces ($v_0$). In chapter 6 we, briefly, investigate the effect of equilibrium flows on wave energy absorption.

In Chapter 2 we introduce, in great detail, the concept of MHD equations and MHD waves and resonant absorption stressing the role resonant absorption has in physics. We review the various types of dissipation available in the solar atmosphere and discuss which dissipative processes are most efficient in different scenarios. The Hall term in the generalised Ohm's law is explained in detail; including the reasoning behind its importance to this thesis. We present an overview of the linear and nonlinear approaches to resonant absorption ignited, in the context of solar physics, by Ionson (1978), Sakurai et al. (1991b) and Ruderman et al. (1997d), respectively. We introduce the equilibrium model and the mathematical techniques and tools required to tackle the nonlinear resonant absorption problem.

In Chapter 3 we derive the nonlinear governing equation for the slow resonances in highly anisotropic and dispersive plasmas. We also formulate the *implicit* connection formulae for the jump in quantities across the resonance. This study is applicable to wave heating in the solar upper atmosphere. The results of this chapter were published in Phys. Plasmas (Clack and Ballai, 2008).

In Chapter 4 we investigate the upper limit of linear resonant Alfvén waves in the solar atmosphere. We derive the standard *linear* governing equation (when nonlinearity is taken into account). We prove that for large Reynolds numbers, applicable to the solar atmosphere, waves remain linear in the vicinity of the Alfvén resonant surface if they are linear far from the resonance. The results presented in this chapter are based on published research in Astron. Astrophys. (Clack et al., 2009b).

Chapter 5 is devoted to the second manifestation of nonlinearity; the generation of mean shear flows outside of the layer enclosing the Alfvén resonance. The technique of *Reynolds decomposition* is utilised to find the mean and fluctuating parts of variables. The *explicit* connection formulae for the derivatives of the mean shear flow are calculated across the resonance. We introduce a simple

model flow to estimate the magnitude of the shear flows produced. The results of this chapter has been published in Phys. Plasmas (Clack and Ballai, 2009a).

In Chapter 6 we apply the results found in Chapters 3 and 4 to study the resonant absorption of laterally impinging fast magnetoacoustic waves. In the case of the slow resonance, we assume weak nonlinearity and find successively higher order harmonics; after the third order approximation the outgoing wave is found to be *non-monochromatic*. For the Alfvén resonance there is no such difficulty since the governing equation of wave dynamics at the resonance is linear. We derive the *coefficient of wave energy absorption* at each resonance and investigate the effect of equilibrium flow on the wave energy absorption. The results of this paper were published in Phys. Plasmas (Clack and Ballai, 2009b).

Chapter 7 studies a new concept; called *coupled resonance*. In this scenario, the slow and Alfvén resonances are close enough together such that the incoming wave interacts with the Alfvén resonance followed by the transmitted wave interacting with the slow resonance before decaying. This is proposed as a possible heating mechanism for the solar upper chromosphere. We find the outgoing coupled wave amplitude when a fast magnetoacoustic wave is driven into the region, and derive the coefficient of wave energy absorption. We numerically analyse the coefficients of wave energy absorption for the slow, Alfvén and coupled resonance in conditions typical for the solar upper atmosphere. The results from this chapter have been submitted to Astron. Astrophys. (Clack et al., 2009a).

Finally, in Chapter 8, we will summarise and list our main results, presenting our conclusions. In addition, we shall illustrate some further possible studies and investigations that can arise from the research presented in the thesis.

# 2

# MHD equations, waves and the concept of resonant absorption

*The present thesis deals with magnetohydrodynamic (MHD) waves in plasmas with transversal inhomogeneities. In this chapter we introduce the essential concepts and analytical methods required to carry out the investigations contained in this thesis. The first section introduces the fundamental MHD equations, along with the assumptions needed for them to be applicable within solar physics. The next section derives the dispersion relations for the basic linear MHD waves present in an unbounded homogeneous plasma, giving quantification of the qualitative discussion in Sect. 1.2. The third section describes resonant absorption (within the framework of solar physics) in detail; it discusses the manifestations and approaches of resonant absorption. It also details the applications for resonant absorption along with a review of the associated literature. The fourth section illustrates and explains the important roles of anisotropic and dispersive plasmas in relation to resonant absorption. The section will explain why some of the solar plasma is anisotropic and dispersive and what the qualitative effects could be. The next section introduces and performs the standard calculations for linear resonant interactions; the so-called F and G functions are derived. In the sixth section of this chapter we introduce dimensionless quantities known as the Reynolds numbers and the concept of nonlinearity parameters. The final section constructs the fundamental mathematical method required for a nonlinear approach to resonant absorption which is applied to an isotropic non-dispersive plasma. We also present the basis of method used throughout the thesis called matched asymptotic expansion, applied to resonant absorption in solar plasmas for the first time by Ruderman et al. (1997d).*

*Do not worry about your difficulties in Mathematics. I can assure you mine are still greater.*
**(Albert Einstein** 1879 – 1955**)**

## 2.1 Magnetohydrodynamics

In order to describe the large scale (macroscopic) behaviour of a fully ionised plasma, a combination of the equations of hydrodynamics (Navier–Stokes), a simplified version of Maxwell's equations, Ohm's law and the equation of state are used.

To build up the MHD theory describing the dynamics of plasmas a significant number of assumptions have to be applied, for a detailed review we refer to Priest (1984); Aschwanden (2004); Erdélyi and Ballai (2007). The MHD framework assumes that the plasma is treated as a continuum. The plasma is also considered to be a single fluid which is in local thermodynamic equilibrium, according to the Maxwell distribution function. This implies that the length scales of variations being studied have to be much greater than the typical kinetic plasma scales such as the ion and electron gyro-radius and time scales of variations have to be longer than the particle collision times. In classical MHD, used in the present thesis, relativistic effects are neglected because the characteristic speeds we are working with are much smaller than the speed of light. Hence, the displacement current in Maxwell's equations is neglected which means that electromagnetic waves are excluded from the model. Another important consequence of this assumption is that the magnetic energy density is much larger than the electric energy density.

The MHD equations express the laws of mass, momentum, magnetic induction and energy. The first equation to write down is the *mass continuity equation*

$$\frac{\partial \overline{\rho}}{\partial t} + \nabla \cdot (\overline{\rho}\mathbf{v}) = 0, \tag{2.1}$$

where $\overline{\rho}$ is the mass density and $\mathbf{v}$ is the local velocity vector. This is a typical conservation equation, balancing the rate of change of a quantity in a volume with the flux of the quantity through the surface that bounds the volume. If the effect of gravity and other non-inertial forces are neglected, the *momentum equation* may be written as

$$\overline{\rho}\frac{D\mathbf{v}}{Dt} = -\nabla\overline{p} + \frac{1}{\mu_0}(\nabla \times \mathbf{B}) \times \mathbf{B} + \mathcal{D}_\nu, \tag{2.2}$$

where $\overline{p}$ is the plasma pressure (assumed to be scalar), $\mathbf{B}$ is the magnetic field induction vector, $\mathcal{D}_\nu$ is the divergence of the viscosity tensor, $\mu_0$ is the magnetic permeability of free space and the operator

$$\frac{D}{Dt} = \frac{\partial}{\partial t} + (\mathbf{v} \cdot \nabla) \tag{2.3}$$

is the *convective* (material) derivative. In general, the plasma is subjected to a pressure gradient $\nabla\overline{p}$, a Lorentz force $\frac{1}{\mu_0}(\nabla \times \mathbf{B}) \times \mathbf{B}$ per unit volume and a resistance force due to the dissipative effect $\mathcal{D}_\nu$. The form of $\mathcal{D}_\nu$ depends on the particular waves being described and the plasma properties; this will be explained in full in Sect. 2.4.

The *induction equation* gives the evolution of the magnetic induction and is defined as

$$\frac{\partial \mathbf{B}}{\partial t} = \nabla \times (\mathbf{v} \times \mathbf{B}) + \eta\nabla^2\mathbf{B} + \overline{\mathbf{H}}, \tag{2.4}$$

where $\eta$ is the isotropic magnetic diffusivity (a parameter that quantifies the plasma motion across

magnetic field lines) and $\overline{\mathbf{H}}$ is the Hall term defined by

$$\overline{\mathbf{H}} = \frac{1}{\mu_0 e}\nabla \times \left(\frac{1}{n_e}\mathbf{B} \times \nabla \times \mathbf{B}\right). \tag{2.5}$$

Here $e$ is the electron charge and $n_e$ is the electron number density. The Hall term and the conditions under which this effect can be important will be discussed much further in Sect. 2.4. Equation (2.4) has to be supplemented by the equation expressing that the magnetic field is divergence-free (the *solenoidal constraint*)

$$\nabla \cdot \mathbf{B} = 0. \tag{2.6}$$

In spite of its simplicity Eq. (2.6) has important meanings. One meaning is based upon the concept of magnetic flux $\Phi = \oint \mathbf{B} \cdot d\mathbf{S}$ (where the integral is taken over a closed surface bounding a plasma element); if the integral is taken over a surface that completely encloses a volume then no net magnetic flux will cross the surface. Another meaning is that the magnetic field has no sources as magnetic monopoles, hence all magnetic field lines must be closed.

The system of equations is completed by two equations connecting the thermodynamic variables $\overline{p}$ and $\overline{\rho}$. The first is the *energy conservation equation* which can be written as

$$\frac{D}{Dt}\left(\frac{\overline{p}}{\overline{\rho}^{\gamma}}\right) = -\frac{\gamma - 1}{\overline{\rho}^{\gamma}}\mathcal{L}, \tag{2.7}$$

where $\mathcal{L}$ is the energy loss function (the net effect of all the sinks and sources of energy) and $\gamma$ is the ratio of specific heats or the adiabatic index. When the energy losses balance the gains, $\mathcal{L} \equiv 0$, the energy conservation equation becomes the *adiabatic equation*, i.e. the entropy of the system remains constant. The second equation is the *equation of state* of the solar plasma (considered to be a perfect gas)

$$\overline{p} = \frac{\widetilde{R}}{\widetilde{\mu}}\overline{\rho}\,\overline{T}, \tag{2.8}$$

where $\widetilde{R}$ is the gas constant, $\widetilde{\mu}$ is the mean atomic weight[1] and $T$ is the temperature.

The system of Eqs (2.1)–(2.8) are the full set of nonlinear visco-resistive MHD equations. The MHD equations presented here are nonlinear and difficult to solve except in simplified cases.

## 2.2 Unbounded homogeneous MHD waves

In the present section we derive the dispersion relations for slow, Alfvén and fast waves in an unbounded homogeneous isotropic plasma. The section can be thought of as the quantitative equivalent of Sect. 1.2. The dispersion relations supply some basic propagation properties of the waves.

The MHD equations (assuming an adiabatic energy equation) are linearised by writing $\overline{f}(x, y, z, t) \rightarrow f_0(x, y, z) + f(x, y, z, t)$, where $\overline{f}$ is any variable present within the system of MHD equations, $f_0$ is the *equilibrium* value of $\overline{f}$ and $f$ is the *Eulerian perturbation*. All perturbations are supposed to be much smaller than their equilibrium values. The equilibrium state is assumed to be static. Removing products of perturbations (which are assumed to be negligible) leads to the linearised MHD equations:

$$\frac{\partial \rho}{\partial t} + \rho_0 \nabla \cdot \mathbf{v} = 0, \tag{2.9}$$

[1] In the literature it is common to find $\widetilde{R}/\widetilde{\mu}$ replaced with $\widetilde{R}^* = \widetilde{R}/\widetilde{\mu}$, and for it still to be called the gas constant.

$$\rho_0 \frac{\partial \mathbf{v}}{\partial t} = -\nabla p + \frac{1}{\mu}\left[(\nabla \times \mathbf{B}_0) \times \mathbf{b} + (\nabla \times \mathbf{b}) \times \mathbf{B}_0\right] + \rho_0 \overline{\nu} \nabla^2 \mathbf{v}, \tag{2.10}$$

$$\frac{\partial \mathbf{b}}{\partial t} = \nabla \times (\mathbf{v} \times \mathbf{B}_0) + \overline{\eta} \nabla^2 \mathbf{b},^2 \tag{2.11}$$

$$\frac{\partial p}{\partial t} + \mathbf{v} \cdot \nabla p_0 = \frac{\gamma p_0}{\rho_0}\left(\frac{\partial \rho}{\partial t} + \mathbf{v} \cdot \nabla \rho_0\right), \tag{2.12}$$

where $\mathbf{b} = (b_x, b_y, b_z)$ is the perturbation of magnetic field. The ideal linearised MHD equations are produced by assuming $\overline{\nu} = \overline{\eta} = 0$ (where $\overline{\nu}$ is the coefficient of kinematic viscosity and $\overline{\eta}$ is the coefficient of magnetic diffusivity).

In an unbounded homogeneous medium permeated by a uniform magnetic field $B_0\hat{\mathbf{z}}$ linear compressional waves are governed by the system (see, e.g. Lighthill, 1960; Cowling, 1976)

$$\frac{\partial^2 (\nabla \cdot \mathbf{v})}{\partial t^2} = (c_S^2 + v_A^2)\nabla^2 (\nabla \cdot \mathbf{v}) - v_A^2 \nabla^2 \left(\frac{\partial v_z}{\partial z}\right), \tag{2.13}$$

$$\frac{\partial^2 v_z}{\partial t^2} = c_S^2 \frac{\partial (\nabla \cdot \mathbf{v})}{\partial z}, \tag{2.14}$$

where $c_S$ is the sound speed, $v_A$ is the Alfvén speed[3], $\mathbf{v} = (v_x, v_y, v_z)$ and $\nabla^2$ is the three-dimensional Laplacian operator. Equations (2.13) and (2.14) can be reduced, by means of algebraic manipulation, to

$$\frac{\partial^4 (\nabla \cdot \mathbf{v})}{\partial t^4} - (c_S^2 + v_A^2)\frac{\partial^2}{\partial t^2}\nabla^2 (\nabla \cdot \mathbf{v}) + c_S^2 v_A^2 \frac{\partial^2}{\partial z^2}\nabla^2 (\nabla \cdot \mathbf{v}) = 0. \tag{2.15}$$

Writing $\Theta := \nabla \cdot \mathbf{v}$, we Fourier analyse the perturbations and write

$$\Theta = \hat{\Theta}(x) e^{i(\omega t - ly - kz)}, \tag{2.16}$$

for frequency $\omega$, and wavenumbers $l$ and $k$. If the ansatz in Eq. (2.16) is applied to Eq. (2.15), it can be seen that $\hat{\Theta}(x)$ satisfies

$$\frac{d^2 \hat{\Theta}}{dx^2} - (l^2 + m_0^2)\hat{\theta} = 0, \tag{2.17}$$

where the magnetoacoustic parameter, $m_0^2$, is defined as

$$m_0^2 = \frac{(k^2 c_S^2 - \omega^2)(k^2 v_A^2 - \omega^2)}{(c_S^2 + v_A^2)(k^2 c_T^2 - \omega^2)}, \quad \text{where} \quad c_T^2 = \frac{c_S^2 v_A^2}{c_S^2 + v_A^2} \quad \text{is the } \textit{tube} \text{ (cusp) speed.}$$

If we Fourier analyse the $x$-dependence in $\hat{\Theta}$, by writing $\hat{\Theta} \sim e^{inx}$, then Eq. (2.17) becomes

$$n^2 + l^2 + m_0^2 = 0,$$

that is

$$\omega^4 - \overline{\mathbf{k}}^2 (c_S^2 + v_A^2)\omega^2 + \overline{\mathbf{k}}^2 k^2 c_S^2 v_A^2 = 0, \tag{2.18}$$

for propagation vector $\overline{\mathbf{k}} = (n, l, k)$. Equation (2.18) is the dispersion relation for the slow and fast

[2] There is no Hall term in the induction equation as we consider isotropic plasmas, so the Hall currents are negligible in comparison to the direct conduction.

[3] As the sound and Alfvén speeds are not used explicitly here, we show their definitions later in Sect. 2.5.

magnetoacoustic waves. Solving Eq. (2.18) (for $\omega^2$) yields

$$\frac{\omega^2}{\mathbf{k}^2} = \frac{1}{2}\left(c_S^2 + v_A^2 \pm \sqrt{(c_S^2 + v_A^2)^2 - 4c_S^2 v_A^2 \cos^2\theta}\right), \tag{2.19}$$

where $\theta$ is the angle between the direction of wave propagation and the magnetic field.

The trivial solution of Eq. (2.15) [$\nabla \cdot \mathbf{v} = 0$], for which $v_z = 0$ and neglecting pressure changes (to linear order), describes the (shear) Alfvén modes with the dispersion relation

$$\frac{\omega^2}{\mathbf{k}^2} = v_A^2 \cos^2\theta. \tag{2.20}$$

Once the dependence of $\omega$ is known the phase diagrams for the magnetoacoustic and Alfvén waves can be drawn (see Fig. 1.7).

## 2.3 Resonant absorption

The process of resonance was discovered and described first by Galileo Galilei whilst he was studying pendulums in the early 1600s; to be accurate he discovered the *mechanical resonance*. Nearly 300 years later in 1899 Nikola Tesla (inspired by the work of Galilei) designed and started work on the *magnifying transmitter*. The principle behind this device was to transmit a signal which would be amplified by the natural frequencies of the ionosphere, essentially utilising *magnetic resonance*. It is claimed that they were successful in broadcasting enough power (using this method) over 26 miles to light 10,000 Watts worth of incandescent light bulbs. Later in his life Tesla also claimed to have produced an oscillator that "you could put in your overcoat pocket" which could destroy a building by resonance if it was tuned into the natural frequency of a building, however, these claims were never verified.

More recently, resonance hit headlines when the *Millenium bridge* (in London) was found to swing more and more vigorously when people walked on it. All the processes of resonance rely on one idea: if you drive a system at its natural frequency the system will become more and more excited as the driving continually deposits energy at the natural frequency. The resonance can be suppressed by damping mechanisms. Figure 2.1 shows a plot of a driven system for varying strengths of damping; the resonance occurs when the driving frequency matches the natural frequency of the system. *Resonant absorption* occurs when the resonance creates a transfer of energy from (or to) the driver to (or from) the system.

In the solar atmosphere (and other space plasmas) when excited and propagating MHD waves interact with an inhomogeneous plasma, the waves can transfer energy to / from the plasma. When the plasma gives up its energy (heat) to the wave, instabilities can be formed, however, this is not studied in this thesis. As mentioned (briefly) in Sect. 1.3 waves transfer their energy to the background plasma by the externally driven waves resonantly interacting with the local oscillation eigenmodes. In Fig. 2.2 we show a schematic picture of resonant absorption; inside the inhomogeneous layer (marked by the thick black lines) the local oscillation eigenmodes are constantly changing, and at a particular frequency the incoming wave will resonantly interact with one of the eigenmodes resulting in resonant absorption (providing the frequency of the incoming wave matches the local frequency of the plasma). Theoretically MHD resonance can take two basic manifestations:

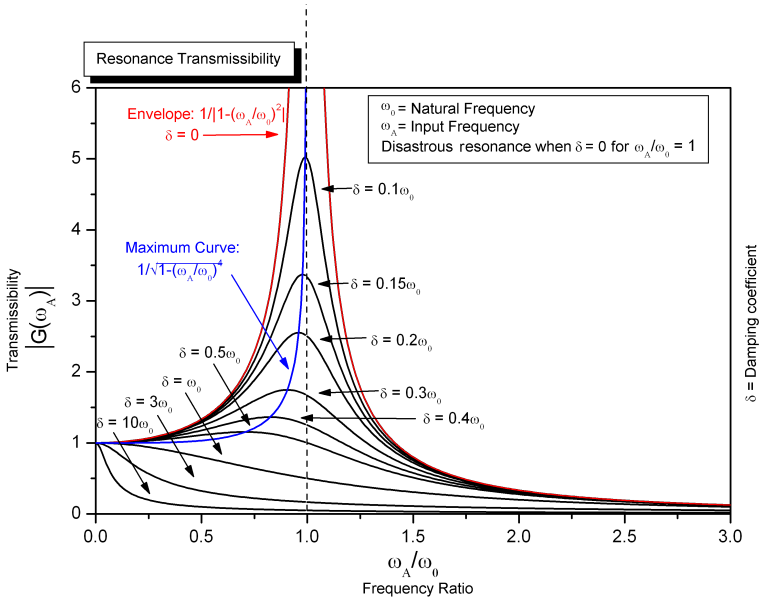


Figure 2.1: The transmissibility (output/input) plotted against the frequency ratio of a driven system. Resonance occurs when the ratio between the driving and natural frequencies is unity. Progressive damping is shown by the black lines. The damping coefficient, $\delta$, is a multiple of the natural frequency, $\omega_0$, which leads to the dimensionless damping ratio, $c = \delta/\omega_0$. Hence, the larger c (and $\delta$) the more effective the damping. The red line represents the envelope of oscillations and the blue line represents the maximum growth curve (Ogata, 2003).

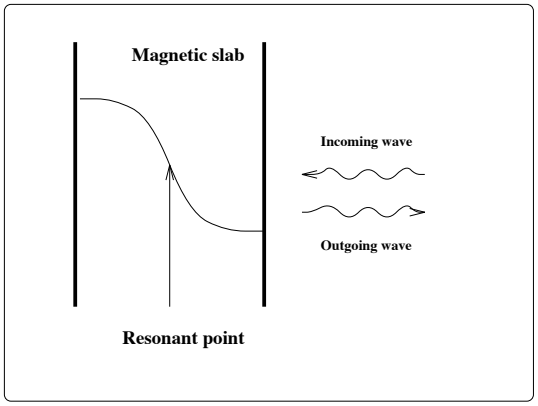


Figure 2.2: A schematic representation of laterally driven resonant absorption in a plasma slab. The thick black lines represent the boundaries of an inhomogeneous layer and the curved line within represents the changing frequency of local oscillation eigenmodes (Erdélyi, 1996).

- The first type is analogous to a resonant cavity in acoustic or optical physics. These models have the wave confined to a waveguide, e.g. a coronal loop with photospheric boundaries (acting as partial reflectors). This type of absorption was studied by, e.g. Davila (1987); Nocera and Ruderman (1998); O'Shea et al. (2007).

- The second type involves an external driver that excites the plasma oscillations. This causes resonant absorption to occur. There are two classes for the driven problem: *direct driving* and *indirect driving*. Direct driving involves shaking the magnetic field lines explicitly, e.g. at their photospheric footpoints (see, e.g. Ruderman et al., 1997a,b; Tirry et al., 1997; DeGroof and Goossens, 2000; DeGroof et al., 2002) whereas indirect driving is when a carrier wave

is needed to transport the energy across the magnetic surfaces (see, e.g. Poedts et al., 1989, 1990a,c,d; Sakurai et al., 1991a; Goossens and Poedts, 1992; Erdélyi, 1997).

At the position where the resonant condition is satisfied the global wave motion will be locally in resonance with the external driver on a particular magnetic surface (Ionson, 1978). In the context of plasma physics, a resonance will occur if the frequency of external waves matches a frequency in the slow or Alfvén continuum (explained earlier). Analytical solutions and connection formulae for resonant Alfvén and slow MHD waves in linear ideal MHD were first derived by Sakurai et al. (1991b). They assumed that the ideal MHD conservation law remained valid in dissipative MHD and subsequently obtained analytical solutions in dissipative MHD in terms of Hankel functions of order $1/3$. Goossens et al. (1992) derived the jump conditions and the conservation law for resonant slow and Alfvén waves in steady equilibrium states in linear ideal MHD. Goossens et al. (1995) showed that the ideal MHD connection formulae found by Sakurai et al. (1991b) remain valid in dissipative MHD. They obtained an elegant formulation of the dissipative solutions in terms of so-called F and G functions. This formulation helps to understand the basic physics of driven resonant waves. In addition, the jump conditions and the conservation law make it possible to compute the amount of absorbed wave energy without solving the dissipative MHD equations. Ruderman and Roberts (2002) uncovered the equations that show resonant absorption at work in damping solar coronal loop oscillations.

The absorption of resonant Alfvén waves has been studied intensively for the past few decades. Here, for the sake of brevity, we list only three of the areas investigated (which are relevant to this thesis). Resonant absorption was studied as a means of supplementary heating of fusion plasmas, but was later rejected due to technical difficulties (see, e.g. Tataronis and Grossmann, 1973; Grossmann and Tataronis, 1973; Chen and Hasegawa, 1974; Hasegawa and Chen, 1976; Goedbloed, 1984; Poedts et al., 1989; van Eester et al., 1991; Elfimov, 2000). Resonant absorption has been investigated as a mechanism of heating and damping coronal loops (see, e.g. Hollweg, 1984; Ionson, 1985; Erdélyi and Goossens, 1995; Belien et al., 1999; Goossens et al., 2002; Ruderman and Roberts, 2002; Aschwanden et al., 2003; Andries et al., 2005; Dymova and Ruderman, 2006; Terradas et al., 2008). Thirdly, resonance has been thought of as a candidate for the absorption of $p$-modes in sunspots (see, e.g. Hollweg, 1988; Lou, 1990; Chitre and Davila, 1991; Goossens and Poedts, 1992; Spruit and Bogdan, 1992; Keppens et al., 1994).

As stated earlier, resonant absorption of MHD waves has an extraordinary range of applications and has been studied within the context of controlled nuclear fusion reactors, astrophysics and magnetospheric physics. For controlled nuclear fusion, resonant absorption has been applied to the tasks of supplying a supplementary heating mechanism in order to achieve the high temperatures required for ignition and as a mechanism to damp global Alfvén waves that are destabilized by fusion-born $\alpha$-particles. The applications to astrophysics are a possible mechanism for heating magnetic loops in solar and stellar coronae, the absorption of p-modes by sunspots and the Alfvén resonance present in spiral galactic arms. Within the framework of magnetospheric physics we can apply resonance to study flow instabilities and as a diagnostic tool for investigating magnetospheric properties.

## 2.4 Anisotropic and dispersive plasmas

The solar and space plasmas are far from being an ideal environment with the plasma dynamics being affected by many dissipative and dispersive effects. The dissipative processes of in-

terest in this thesis are viscosity, electrical resistivity and thermal conduction, while dispersive effects are considered to be described by the Hall term in the generalized Ohm's law. In plasmas where the magnetic field dominates over any other gas quantities, the dissipative processes are anisotropic[4] and require a different treatment from their isotropic counterparts. Dissipative processes are weak in the solar atmosphere; this means that the diffusion coefficients are small. The rate of dissipation, however, is dependent on the local spatial scales. Traditionally, the local spatial scales would be determined by the internal dynamics, so that the plasma configuration can be treated within the framework of ideal MHD. Many phenomena (e.g. resonant absorption, current sheets or turbulence) are inherently non-ideal and nonlinear as they are strongly influenced by dissipative and dispersive effects. In particular, dissipation is important to nonlinear dynamical processes because large-scale motions rapidly lead to small-scale structures being formed, which corresponds to singularities in the ideal theory.

We consider three types of dissipation and one type of dispersion in the present thesis. Viscosity and thermal conductivity are linked to hydrodynamical processes, while electrical conductivity and Hall dispersion are connected to the presence of the magnetic field. In the context of solar physics, the general effect of dissipation and dispersion is to relax the accumulation of wave energy in a system. The relaxation can be performed by, e.g.; converting the wave energy at resonance to heat by viscous or resistive dissipation or thermal conduction (via resonant absorption), or the dispersion of energy over a larger area by Hall conduction. The relaxation caused by dissipation and dispersion prevents the formation of singularities (entities abhorred by nature).

In our derivations we will assume that dissipative and dispersive coefficients are constants. Let us now, first, discuss how the physical processes in question become anisotropic. The key quantities in our discussion are the products $\omega_i\tau_i$ and $\omega_e\tau_e$, where $\omega_{i(e)}$ is the ion (electron) cyclotron frequency and $\tau_{i(e)}$ is the mean ion (electron) collision time. The product $\omega_i\tau_i$ is important for viscosity, whereas, the product $\omega_e\tau_e$ is important for thermal and electrical conductivity as well as Hall dispersion. If the condition $\omega_i\tau_i \ll 1$ is satisfied, viscosity is thought to be isotropic and as such $\mathcal{D}_v$ in Eq. (2.2) can be written as

$$\mathcal{D}_v = \overline{\rho\nu}\left(\nabla^2\mathbf{v} + \frac{1}{3}\nabla\left(\nabla\cdot\mathbf{v}\right)\right), \tag{2.21}$$

where $\overline{\nu}$ is the kinematic shear viscosity coefficient. If, in addition, we have $\omega_e\tau_e \ll 1$ then thermal conductivity and Hall dispersion are negligible when compared with the isotropic viscosity. Hence, the isotropic MHD equations are represented by Eqs (2.1)–(2.8) with Eq. (2.21) substituted for $\mathcal{D}_v$ and $\mathbf{H} = \mathcal{L} = 0$. This situation reflects the conditions met in the lower part of the solar atmosphere.

In the upper part of the atmosphere (upper part of chromosphere, corona and solar wind) we have $\omega_i\tau_i \geq 1$ and so the viscous force is given in its most general form, by Braginskii's viscosity tensor, which comprises of five terms. Its divergence can be written as (Braginskii, 1965; Erdélyi, 1996)

$$\nabla\cdot\mathbf{S} = \overline{\eta}_0\nabla\cdot\mathbf{S}_0 + \overline{\eta}_1\nabla\cdot\mathbf{S}_1 + \overline{\eta}_2\nabla\cdot\mathbf{S}_2 - \overline{\eta}_3\nabla\cdot\mathbf{S}_3 - \overline{\eta}_4\nabla\cdot\mathbf{S}_4, \tag{2.22}$$

where $\overline{\eta}_0$ is the coefficient of compressional viscosity, $\overline{\eta}_1$ and $\overline{\eta}_2$ are the coefficients of shear viscosity and $\overline{\eta}_3$ and $\overline{\eta}_4$ are the coefficients of dispersion. Hence, the terms proportional to $\overline{\eta}_0$, $\overline{\eta}_1$ and $\overline{\eta}_2$ in Eq. (2.22) describe viscous dissipation, while terms proportional to $\overline{\eta}_3$ and $\overline{\eta}_4$ are non-

[4]The tendency for a process to be directionally dependent.

dissipative and describe the wave dispersion related to the finite ion gyroradius, hence, will be ignored in what follows (and in the rest of this thesis). The quantities $\mathbf{S}_0$, $\mathbf{S}_1$ and $\mathbf{S}_2$ are given by

$$\mathbf{S}_0 = \left(\mathbf{b}' \otimes \mathbf{b}' - \frac{1}{3}\mathrm{I}\right)\left[3\mathbf{b}' \cdot \nabla(\mathbf{b}' \cdot \mathbf{v}) - \nabla \cdot \mathbf{v}\right], \tag{2.23}$$

$$\mathbf{S}_1 = \nabla \otimes \mathbf{v} + (\nabla \otimes \mathbf{v})^{\mathrm{T}} - \mathbf{b}' \otimes \mathbf{W} - \mathbf{W} \otimes \mathbf{b}' + (\mathbf{b}' \otimes \mathbf{b}' - \mathrm{I})\,\nabla \cdot \mathbf{v} + (\mathbf{b}' \otimes \mathbf{b}' + \mathrm{I})\,\mathbf{b}' \cdot \nabla\,(\mathbf{b}' \cdot \mathbf{v}), \tag{2.24}$$

$$\mathbf{S}_2 = \mathbf{b}' \otimes \mathbf{W} + \mathbf{W} \otimes \mathbf{b}' - 4\,(\mathbf{b}' \otimes \mathbf{b}')\,\mathbf{b}' \cdot \nabla\,(\mathbf{b}' \cdot \mathbf{v}), \tag{2.25}$$

$$\mathbf{W} = \nabla\,(\mathbf{b}' \cdot \mathbf{v}) + (\mathbf{b}' \cdot \nabla)\,\mathbf{v}. \tag{2.26}$$

Here $\mathbf{v} = (u, v, w)$ is the local velocity vector, $\mathbf{b}' = \mathbf{B}_0/B_0$ is the unit vector in the direction of the magnetic field, $\mathbf{I}$ is the unit tensor and $\otimes$ indicates the dyadic product of two vectors. The superscript 'T' denotes a transposed tensor.

The first viscosity coefficient, $\overline{\eta}_0$, (*compressional viscosity*) has the following approximate expression (see, e.g. Ruderman, 2000)

$$\overline{\eta}_0 = \frac{\rho_0 k_B T_0 \tau_i}{m_p}, \tag{2.27}$$

where $\rho_0$ and $T_0$ are the equilibrium density and temperature, $m_p$ is the proton mass and $k_B$ is the Boltzmann constant. When $\omega_i\tau_i \gg 1$ the other viscosity coefficients are given by the approximate expressions

$$\overline{\eta}_1 = \frac{\overline{\eta}_0}{4\,(\omega_i\tau_i)^2}, \quad \overline{\eta}_2 = 4\overline{\eta}_1. \tag{2.28}$$

The viscosity described by the sum of the second and third terms in Eq. (2.22) is known as *the shear viscosity*. For conditions typical of the solar upper atmosphere $\omega_i\tau_i$ is of the order of $10^5 - 10^6$, so according to Eq. (2.28) the term proportional to $\overline{\eta}_0$ in Eq. (2.22) is much larger than the second and third terms. However, it has been long understood that the compressional viscosity does not remove the Alfvén singularity (see e.g., Erdélyi and Goossens, 1995; Mocanu et al., 2008) while this task is done by shear viscosity. Hence, when studying slow magnetoacoustic waves in the solar upper atmosphere we write $\mathcal{D}_\nu$ in Eq. (2.2) as

$$\mathcal{D}_\nu = \overline{\eta}_0 \nabla \cdot \mathbf{S}_0, \tag{2.29}$$

whereas when studying Alfvén waves in the solar upper atmosphere we must rewrite $\mathcal{D}_\nu$ as

$$\mathcal{D}_\nu = \overline{\eta}_1 \nabla \cdot \mathbf{S}_1 + \overline{\eta}_2 \nabla \cdot \mathbf{S}_2. \tag{2.30}$$

If the condition $\omega_e\tau_e \geq 1$ is satisfied then we have to consider anisotropic thermal conduction. This process appears as a term in the energy loss function, $\mathcal{L}$, in Eq. (2.7). The expression for heat flux involves three thermal conduction coefficients $\overline{\kappa}_\parallel$, $\overline{\kappa}_\perp$ and $\overline{\kappa}_\wedge$. The thermal coefficient in the magnetic surface and parallel (perpendicular) to magnetic field lines is $\overline{\kappa}_\parallel$ ($\overline{\kappa}_\perp$) and the thermal coefficient normal to the magnetic surface is $\overline{\kappa}_\wedge$. When $\omega_e\tau_e \gg 1$ the following estimations are valid

$$\frac{\overline{\kappa}_\perp}{\overline{\kappa}_\parallel} \approx (\omega_e\tau_e)^{-2}, \quad \frac{\overline{\kappa}_\wedge}{\overline{\kappa}_\parallel} \approx (\omega_e\tau_e)^{-1}. \tag{2.31}$$

Since in the solar upper atmosphere $\omega_e\tau_e \sim 10^5$, the perpendicular and normal components of the heat flux can be neglected in comparison to the parallel component. In this case, for Alfvén waves,

we neglect the thermal conduction completely as it does not significantly alter the wave dynamics (since the dominant motions are perpendicular to the magnetic field lines). On the other hand, for slow waves we must include the thermal conduction, but we only retain the parallel component. As a result, we write the heat flux as

$$\mathbf{q} = -\overline{\kappa}_{\parallel}\mathbf{b}'\left(\mathbf{b}'\cdot\nabla\overline{T}\right), \tag{2.32}$$

and the energy loss function will become $\mathcal{L} = \nabla\cdot\mathbf{q}$ (where $\overline{T}$ is the temperature).

The condition $\omega_e\tau_e \geq 1$ means that Hall dispersion needs to be considered. Mathematically, the Hall currents in Eq. (2.4) arise when off-diagonal terms in the conductivity tensor are considered. Physically, this pseudo-diffusion manifests itself by the ions and electrons slowly drifting away from their parent magnetic field lines. Hall currents are only relevant to plasma dynamics occurring on length scales shorter than the *ion inertial length* (ion skin depth), $d_i = c/\omega_i$, where c is the speed of light (Huba, 1995). The Hall term itself is very complicated, as can be seen by its form in Eq. (2.5), however it can be simplified by estimating the magnitude of each term and then retaining only the largest. This process must be carried out for slow and Alfvén waves separately; and is shown in Appendix A. It is found that Hall dispersion plays a key role when considering nonlinear resonant slow waves, however, plays no significant role when investigating resonant Alfvén waves because the largest Hall terms in the perpendicular direction relative to the ambient magnetic field identically cancel.

The final dissipative process to be discussed in this thesis is electrical conductivity. The dissipative coefficient is isotropic provided $\omega_e\tau_e \ll 1$ (only satisfied in the lower photosphere). This process describes the decay of the magnetic field due to magnetic diffusivity. When $\omega_e\tau_e \geq 1$ the dissipative coefficient becomes anisotropic, however, the parallel and perpendicular components only differ by a factor of 2, so in our investigations we use only one of the components for both without loss of generality. For further details on possible dissipative processes and their importance, we refer to Braginskii (1965); Priest (1984); Hollweg (1985); Porter et al. (1994); Ruderman et al. (1997b, 2000); Goossens et al. (2006); Clack et al. (2009b).

All dissipative and dispersive effects strongly depend on the plasma parameters (such as temperature, density, magnetic field strength and pressure) and their magnitude and importance can be obtained once plasma parameters are known. If the density is measured in $\mathrm{kgm}^{-3}$ and the temperature is measured in K, then the dissipative coefficients are given as

- The kinematic viscosity coefficient of a fully-ionised hydrogen plasma is (Chapman, 1954)

$$\overline{\nu} = \frac{2.21\times10^{-16}T^{5/2}}{\overline{\rho}\ln\Lambda}(\mathrm{m}^2\mathrm{s}^{-1}).$$

- The isotropic magnetic diffusivity coefficient is given by (Spitzer, 1962)

$$\overline{\eta} = 5.2\times10^{7}\ln\Lambda T^{-3/2}(\mathrm{m}^2\mathrm{s}^{-1}).$$

- The coefficient of the parallel component of thermal conductivity can be written as (Priest, 1984)

$$\overline{\kappa}_{\parallel} = \frac{1.8\times10^{-10}T^{5/2}}{\ln\Lambda}(\mathrm{Wm}^{-1}\mathrm{K}^{-1}).$$

- The coefficients of Braginskii's viscosity tensor are given by Eqs (2.27) and (2.28).

The term $\ln\Lambda$ is known as the *Coulomb logarithm*; it generally has a value between 5 and 22 and has a weak dependence on temperature and density. For most of the work in this thesis, it would be adequate to take $\ln\Lambda \approx 20$.

It should be noted that viscosity, magnetic diffusivity, thermal conduction and Hall dispersion affect all waves, however, for particular physical cases, some are negligible compared to others. In all subsequent chapters we will present a rigorous reasoning for our choices of dissipative and dispersive processes and / or will refer to the scalings displayed above.

## 2.5 Resonant interaction of linear MHD waves

This section reviews the method, which was first developed by Sakurai et al. (1991b), for studying resonant absorption of MHD waves within a linear framework. The method is based on a series of simple concepts: dissipation is important in a thin layer called the dissipative layer[5] embracing the resonant surface, outside this dissipative layer we suppose that the plasma is homogeneous and its dynamics is described by the ideal MHD equations. Figure 2.3 is a schematic picture of what this method entails. The method produces connection formulae across the resonant position, so the ideal MHD equations can be used over the whole domain with the exception of the resonant layer and here the connection formulae can be used to *jump* over the resonance.

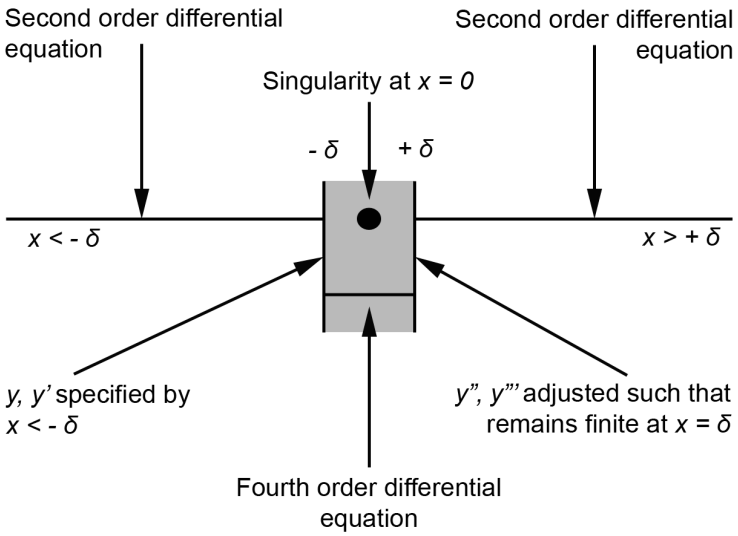


Figure 2.3: Schematic illustration of the methodology used in deriving the connection formulae across the resonant layer. Here the horizontal line is taken to be the $x-$direction and $\delta$ is the width of the dissipative layer (either Alfvén or slow).

The system of MHD equations (2.1)–(2.8) must be linearly perturbed, so that linear resonant absorption can be studied. Every quantity $\overline{f}$ can be written as the sum of its equilibrium part $f_0$ and its Eulerian perturbation $f$ (as defined in Sect. 2.2). We neglect the stratification effects due to gravity. In order to have a linear description it is assumed that $|f| \ll |f_0|$, implying that the product of two perturbed quantities can be neglected. The linearised system of dissipative MHD

[5]The dissipative layer is a thin strip of plasma enclosing the resonant position where dissipation is dominant over other forces. Later on, we will consider the dissipative layer to be the strip where nonlinearity, dispersion and dissipation are all of equal importance.

is written as in the system of Eqs (2.9)–(2.12). Part of the basic physics of the resonant MHD waves can be understood in the context of linear ideal MHD, so we set $\overline{\nu} = \overline{\eta} = 0$ in the system of Eqs (2.9)–(2.12). Cartesian coordinates are adopted and it is assumed that the equilibrium quantities depend on the transversal coordinate, $x$, only. The equilibrium magnetic field is unidirectional and is aligned with the $z-$axis. The total pressure balance is given by

$$\frac{d}{dx}\left(p_0 + \frac{B_0^2}{2\mu_0}\right) = 0. \tag{2.33}$$

The coordinate system is aligned in such a way that the wave vector $\mathbf{k}$ lies in the $xz-$plane. The wave vector has two components with respect to $\mathbf{B}_0$. Since equilibrium quantities depend on $x$ only we can Fourier-analyse the perturbed quantities with respect to the other coordinate and set them proportional to $\exp(ikz)$. The perturbations also oscillate with the same real frequency, hence these quantities are considered to be proportional to $\exp(-i\omega t)$, with $\omega > 0$. The frequency and phase speed are related by $\omega = Vk$ where $k$ is the wave vector in the direction of propagation. The Lagrangian displacement, $\hat{\xi}$, is introduced as $\mathbf{v} = -i\omega\hat{\xi}$ and the Eulerian perturbation of total pressure is $P = p + \mathbf{B}\cdot\mathbf{b}/\mu_0$ (where the second term on the right-hand side denotes the magnetic pressure).

All but two of the perturbed quantities can be eliminated by algebraic means from Eqs (2.9)–(2.12). It is then found that the normal component of the displacement and the total pressure perturbation satisfy a pair of first order differential equations

$$D\frac{d\hat{\xi}_x}{dx} = -CP, \quad \frac{dP}{dx} = \rho_0 D_A \hat{\xi}_x, \tag{2.34}$$

where the coefficients $D_A$, $D_C$, $D$ and $C$ take the form

$$D_A = \omega^2 - \omega_A^2, \quad D_C = \left(c_S^2 + v_A^2\right)\left(\omega^2 - \omega_C^2\right),$$

$$D = \rho_0 D_A D_C, \quad C = \omega^4 - k^2 D_C. \tag{2.35}$$

All the other perturbed quantities can be computed once $\hat{\xi}_x$ and $P$ are known. The symbols used in Eqs (2.34)–(2.35) denote the adiabatic speed of sound, $c_S$, the Alfvén speed, $v_A$, the local Alfvén frequency, $\omega_A$, and the local cusp frequency, $\omega_C$. The squares of these quantities are defined as

$$c_S^2 = \frac{\gamma p_0}{\rho_0}, \quad v_A^2 = \frac{B_0^2}{\mu_0\rho_0}, \quad \omega_A^2 = k^2 v_A^2\cos^2\alpha, \quad \omega_C^2 = \frac{c_S^2\omega_A^2}{c_S^2 + v_A^2},$$

and $\alpha$ is the angle between the magnetic field vector and the $z-$axis.

The pair of differential equations (2.34) supplemented with boundary conditions defines an eigenvalue problem with $\omega^2$ as the eigenvalue. The system has regular singularities at zeros of the coefficient $D$, i.e. for the values of $x$ such that

$$\omega^2 = \omega_A^2(x), \quad \omega^2 = \omega_C^2(x), \tag{2.36}$$

which constitutes the conditions for an Alfvén and slow resonance, respectively. Since $\omega_A^2(x)$ and $\omega_C^2(x)$ are functions of position, the equalities (2.36) define two continuous ranges of frequencies

$$\{\min[\omega_A(x)], \max[\omega_A(x)]\}, \quad \{\min[\omega_C(x)], \max[\omega_C(x)]\},$$

that correspond to mobile regular singularities of the differential equations (2.34). These two frequency ranges are known as the *Alfvén* and the *slow continua*, respectively (see Sect. 1.2 for full details). In what follows, we restrict ourselves to the slow continuum by choosing the magnetic field parallel to the z-axis, i.e. $\alpha = 0$ (to study the details for the Alfvén continuum refer to, e.g. Goossens et al., 1995). This assumption means that there will be no component of the wave vector perpendicular to the equilibrium magnetic field.

Let $x = x_c$ be the position of the singular point. We introduce a new spatial variable, defined as $s = x - x_c$. Elimination of the total pressure, $P$, from the system (2.34) leads to an ordinary differential equation for the x-component of the displacement, $\hat{\xi}_x$,

$$\frac{d}{ds}\left[\frac{D}{C}\frac{d\hat{\xi}_x}{ds}\right] + \rho_0 D_A \hat{\xi}_x = 0.$$

If, instead, the normal component of displacement is eliminated from the system (2.34), a differential equation for $P$ is recovered in the form

$$\frac{1}{C}\frac{d}{ds}\left[\frac{1}{\rho_0 D_A}\frac{dP}{ds}\right] + \frac{1}{D}P = 0.$$

Series expansion of the coefficient functions $D_A$ and $D_C$ gives a simplified version of the system (2.34) which is valid in the interval $[-s_C, s_C]$ around the resonant position. Here the linear Taylor expansion is a valid approximation of $\omega^2 - \omega_C^2(x)$, hence $s_C$ (i.e. the interval around the slow resonance) has to satisfy the condition

$$s_C \ll \left|\frac{2(\omega_C^2)_0'}{(\omega_C^2)_0''}\right|,$$

where the prime denotes the derivative with respect to $s$. It can easily be seen that the expansion of $D_C$ starts with a term in $s$, while the series expansion of the other coefficients start with a constant term. Thus, the governing equation for $\hat{\xi}_x$ can be written as

$$\widetilde{\alpha}\frac{d}{ds}\left(s\frac{d\hat{\xi}_x}{ds}\right) + \widetilde{\beta}\hat{\xi}_x = 0, \tag{2.37}$$

where $\widetilde{\alpha}$ and $\widetilde{\beta}$ are two non-zero constants. The indicial equation of (2.37) has a double root $\widetilde{\upsilon}_{1,2} = 0$, meaning that one of the two independent solutions must have a logarithmic dependence[6]. Since the interval only contains one singular point the solution may be written as

$$\hat{\xi}_x(s) = \begin{cases} S_1 f(s) + R_1 \left(f(s)\ln|s| + g(s)\right), & s < 0, \\ S_2 f(s) + R_2 \left(f(s)\ln|s| + g(s)\right), & s > 0. \end{cases}$$

Here $S_1$, $S_2$, $R_1$, $R_2$ are constants and $f(s)$ and $g(s)$ are analytical functions of $s$. The regular solution $f(s)$ is called the *small* solution and the solution containing the $\ln|s|$ is called the *large* solution. It has been shown that the large variable has to be continuous, whereas the small solution may jump: $R_1 = R_2$, $S_1 \neq S_2$ (Goedbloed, 1983; Goossens and Ruderman, 1995). The solution for $\hat{\xi}_x$

[6]Determined by using the technique of reduction of order

then takes the form

$$\hat{\xi}_x(s) = R\,(f(s)\ln|s| + g(s)) + \begin{cases} S_1 f(s), & s < 0, \\ S_2 f(s), & s > 0. \end{cases} \tag{2.38}$$

For the total pressure, $P$, the governing equation is of the form

$$\hat{\alpha}\frac{d^2P}{ds^2} + \frac{\hat{\beta}}{s}P = 0, \tag{2.39}$$

where again $\hat{\alpha}$ and $\hat{\beta}$ are constants. The indicial equation yields two roots, $\hat{v}_1 = 0$ and $\hat{v}_2 = 1$. The root $\hat{v}_2 = 1$ gives rise to a $s\ln|s|$ contribution to the solution which for $|s| \ll 1$ can be neglected compared to the constant term. It can be shown that for this equilibrium configuration the total pressure perturbation has no logarithmic singularity (Sakurai et al., 1991b). If the method presented in Sakurai et al. (1991b) is followed it is obtained that the total pressure is constant across the singularity and this constitutes a conservation law used later in the thesis.

The dominant singularity for slow waves, however, resides in the component of the displacement parallel to the equilibrium magnetic field lines, described by

$$s\hat{\xi}_z = \frac{kc_S^2}{\rho_0\Delta(c_S^2 + v_A^2)}P, \tag{2.40}$$

where

$$\Delta = -\frac{d}{ds}\left[\omega_C^2(s)\right]_0,$$

so $\hat{\xi}_z$ has a $1/s$ singularity and a $\delta(s)$ contribution which dominates the $\ln|s|$ singularity and the jump found for $\hat{\xi}_x$ and $P$. Due to the singularities in Eq. (2.34), the solutions and their derivatives diverge at the resonant position $s = 0$. Therefore, the ideal MHD approximation fails to give physically acceptable results at the resonance. The singularities can be removed by considering non-ideal (dissipative) effects. In spite of the fact that under solar conditions non-ideal effects are weak in the vicinity of the resonant position they play a vital role. Sufficiently far from $s = 0$ (denoted as the *outer region*), the ideal MHD solution is an excellent approximation of the actual solution. However, near the resonant position (the *inner region*) the character of the solution changes and the assumption of ideal MHD is invalid. In this region a dissipative, small-scale solution must be found. Moreover, the Taylor expansions of equilibrium quantities are valid in a region far wider than the inner region creating an *overlap region* which is used to match the solutions from the inner and outer regions.

Using a similar technique as presented in the ideal case, all but two of the variables can be eliminated from the linearised dissipative MHD equations, leading to an almost identical system of equations for the x-component of the displacement and the total pressure as in Eq. (2.34). The only difference is that now the coefficient function $D_C$ is expressed as

$$D_{\tilde{C}} = \left(c_S^2 + v_A^2\right)\left(\tilde{\omega}^2 - \omega_C^2\right),$$

where $\tilde{\omega}^2$ is the differential operator

$$\tilde{\omega}^2 = \omega^2\left[1 - \frac{i}{\omega}\left(\overline{\nu} + \frac{\omega_C^2}{\omega_A^2}\overline{\eta}\right)\frac{d^2}{ds^2}\right].$$

Now the system, which is the dissipative counterpart of Eq. (2.34), is not singular at $s = 0$,

however, the order of these differential equations is raised from *two* (in ideal MHD) to *six* (in dissipative MHD). This rise in order is noted in Fig. 2.3.

In the vicinity of the ideal resonant position the equations describing the evolution of the longitudinal and transversal displacement and the total pressure can be simplified by using first order Taylor polynomials for the coefficient functions (see, e.g. Goossens and Ruderman, 1995; Ballai, 2000)

$$\left[s\Delta - i\omega\left(\overline{\nu} + \frac{\omega_C^2}{\omega_A^2}\overline{\eta}\right)\frac{d^2}{ds^2}\right]\frac{d\hat{\xi}_x}{ds} = \frac{\omega_C^4}{\rho_0 v_A^2 \omega_A^2}P, \tag{2.41}$$

$$\left[s\Delta - i\omega\left(\overline{\nu} + \frac{\omega_C^2}{\omega_A^2}\overline{\eta}\right)\frac{d^2}{ds^2}\right]\frac{dP}{ds} = 0, \tag{2.42}$$

$$\left[s\Delta - i\omega\left(\overline{\nu} + \frac{\omega_C^2}{\omega_A^2}\overline{\eta}\right)\frac{d^2}{ds^2}\right]\hat{\xi}_z = \frac{ikc_S^2}{\rho_0(c_S^2 + v_A^2)\omega_C^2}P. \tag{2.43}$$

Dissipation is only important when the terms on the left-hand sides of (2.41)–(2.43) are of the same order, i.e.

$$\frac{s\Delta}{i\omega\left(\overline{\nu} + \frac{\omega_C^2}{\omega_A^2}\overline{\eta}\right)} = \mathcal{O}(1).$$

This results in an isotropic dissipative layer with a thickness $\widetilde{\delta}_c$ given by

$$\widetilde{\delta}_c = \left[\frac{\omega}{|\Delta|}\left(\overline{\nu} + \frac{\omega_C^2}{\omega_A^2}\overline{\eta}\right)\right]^{1/3}, \tag{2.44}$$

a result first discovered by Sakurai et al. (1991b) (here, as elsewhere in the thesis, the values for constants are all calculated at the resonant position). In view of the very large Reynolds numbers[7] in the solar atmosphere the inequality

$$\frac{s_C}{\widetilde{\delta}_c} \gg 1$$

is very important in the present discussion. It implies that the interval where the simplified version of the dissipative equations are valid contains the dissipative layer and two overlap regions, one to the left and one to the right of the dissipative layer. Following Goossens and Ruderman (1995), it is convenient to introduce another new scaled variable $r = s/\widetilde{\delta}_c$, which is of the order of unity within the dissipative layer, but in view of the inequality $s_C/\widetilde{\delta}_c \gg 1$, $s \to \pm s_C$ corresponds to $r \to \pm\infty$. The jump of a quantity Q across the dissipative layer can be calculated by

$$[Q] = \lim_{s\to 0}\{Q(s) - Q(-s)\}.$$

Written in the new variable (r) the system (2.41)–(2.43) takes the form

$$\left(\frac{d^2}{dr^2} + i\,\mathrm{sgn}(\Delta)r\right)\frac{d\hat{\xi}_x}{dr} = \frac{i\omega_C^4}{\rho_0|\Delta|\omega_A^2 v_A^2}P, \tag{2.45}$$

$$\left(\frac{d^2}{dr^2} + i\,\mathrm{sgn}(\Delta)r\right)\frac{dP}{dr} = 0, \tag{2.46}$$

$$\left(\frac{d^2}{dr^2} + i\,\mathrm{sgn}(\Delta)r\right)\hat{\xi}_z = -\frac{kc_S^2}{\rho_0|\Delta|\widetilde{\delta}_c\omega_C^2(c_S^2 + v_A^2)}P. \tag{2.47}$$

[7]Reynolds numbers are a measure of the efficiency of dissipation. The larger the number the *weaker* the dissipation. This will be discussed in full in Sect. 2.6.

The solutions to a system of ODEs of this type were first given analytical form by Sakurai et al. (1991b) in terms of Hankel functions of a complex argument. Goossens et al. (1995) came up with a more elegant form where the solutions take the form of constants multiplied by the generalized F and G functions, which are given by

$$F(r) = \int_0^\infty \exp\left(iqr\ \mathrm{sgn}(\Delta) - \frac{q^3}{3}\right) dq, \tag{2.48}$$

$$G(r) = \int_0^\infty \frac{e^{-q^3/3}}{q} \left[\exp(iqr\ \mathrm{sgn}(\Delta)) - 1\right] dq. \tag{2.49}$$

Equation (2.46) shows that the ideal conservation law for the cusp singularity remains valid in dissipative MHD. Finally, the jumps in $\hat{\xi}_x$ and P across the dissipative layer are

$$[\hat{\xi}_x] = -i\pi \frac{\omega_C^4}{\rho_0 |\Delta| \omega_A^2 v_A^2} P, \tag{2.50}$$

$$[P] = 0. \tag{2.51}$$

The above two relations are important because in knowing them a solution of the full MHD system does not need to be found inside the dissipative layer for determining the solution everywhere else in the domain, hence, the solution in the dissipative layer can be circumvented by the use of connection formulae (jumps) written for the x-component of the displacement and the total pressure perturbation. Using the asymptotic behaviour of $F(r)$ and $G(r)$, computed by, e.g. Goossens et al. (1995), it follows that the asymptotic behaviour of $\hat{\xi}_z$ for $|r| \to \infty$ is given by

$$\hat{\xi}_z = \frac{ikc_S^2}{r\tilde{\delta}_c \Delta \rho_0 (c_S^2 + v_A^2) \omega_C^2} P, \tag{2.52}$$

which recovers the $r^{-1}$ behaviour of $\mathrm{Im}(\hat{\xi}_z)$ far away from the ideal resonance position. It should be observed that the connection formulae for $\hat{\xi}_x$ and P are both *independent* of the dissipative coefficients, thus the amount of energy absorbed is also independent of those coefficients.

## 2.6 The nonlinearity parameter and Reynolds numbers

A nonlinear description of resonant absorption requires the introduction of some characteristic quantities used throughout the present thesis. For our further mathematical consideration we introduce: the *dimensionless amplitude of perturbations* ($\epsilon$) far away from the ideal resonant position[8]; the *characteristic spatial scale* ($l_{ch}$) which is usually taken to be the characteristic scale of inhomogeneity ($l_{inh}$), but can sometimes be taken to be equal to the wavelength of the wave being studied; the *characteristic speed* ($v_{ch}$) which is usually taken to be the order of the phase speed of the global MHD wave ($V$); the *characteristic scale of dissipation* ($l_{diss}$) predicted to be of the order of $R^{-1/3} l_{ch}$ (see, e.g. Ruderman and Goossens, 1993), where R is the total Reynolds number (defined later).

If it is assumed that the characteristic scale of the perturbations along the dissipative layer is of the order $l_{inh}$ then linear theory predicts that the perturbations of large variables in the dissipative layer are of the order of $\epsilon l_{inh}/l_{diss} = \epsilon R^{1/3}$ (see, e.g. Hollweg, 1987; Goossens et al., 1995; Ruderman et al., 1997d). Therefore, waves with small dimensionless amplitude far from resonance can

[8] In this thesis $\epsilon$ is always assumed to be small far away from the ideal resonant position ($\epsilon \ll 1$).

grow in magnitude near the resonant position. As a direct result, linear theory can breakdown and, hence, nonlinear theory may become important in the dissipative layer.

To measure the magnitude of dissipative coefficients we introduce the dimensionless *Reynolds numbers*. In isotropic plasmas where waves are damped by the classical viscosity and resistivity, the Reynolds numbers are defined as

$$R_e = \frac{\nu_{ch} l_{ch}}{\overline{\nu}}, \quad R_m = \frac{\nu_{ch} l_{ch}}{\overline{\eta}}, \quad \frac{1}{R_i} = \frac{1}{R_e} + \frac{1}{R_m}, \tag{2.53}$$

where $R_e$, $R_m$, $R_i$ are the isotropic *viscous*, *magnetic* and *total* Reynolds numbers, respectively. For anisotropic plasmas we have to define two different sets of Reynolds numbers. For slow waves, which are susceptible to thermal conduction and compressional viscosity, we have

$$R_{e(c)} = \frac{\nu_{ch} l_{ch} \rho_{0_c}}{\overline{\eta}_0}, \quad P_e = \frac{\nu_{ch} l_{ch} \rho_{0_c} \widetilde{R}}{\overline{\kappa}_{\parallel}}, \quad \frac{1}{R_c} = \frac{1}{R_{e(c)}} + \frac{1}{P_e}, \tag{2.54}$$

where $R_{e(c)}$, $P_e$, $R_c$ are the anisotropic *compressional* viscous Reynolds number, *Péclet number* and *compressional* total Reynolds number, respectively. Here $\widetilde{R}$ is the gas constant and $\rho_{0_c} = \rho_0(x_c)$ is the density evaluated at the slow ideal resonant position. Alfvén waves are influenced by shear viscosity and resistivity, so we define

$$R_{e(a)} = \frac{\nu_{ch} l_{ch} \rho_{0_a}}{\overline{\eta}_1}, \quad R_m = \frac{\nu_{ch} l_{ch}}{\overline{\eta}}, \quad \frac{1}{R_a} = \frac{1}{R_{e(a)}} + \frac{1}{R_m}, \tag{2.55}$$

where $R_{e(a)}$, $R_m$, $R_a$ are the anisotropic *shear* viscous, magnetic and *shear* total Reynolds numbers, respectively. Here $\rho_{0_a} = \rho_0(x_a)$ is the density evaluated at the Alfvén ideal resonant position.

When Eqs (2.53)–(2.55) are calculated for the solar atmosphere using the parameters given in Sect. 2.4 we find that, for the solar photosphere and lower chromosphere, $R_i \sim 10^6 - 10^8$ and, for the solar upper chromosphere and corona, $R_c \sim 10^2 - 10^3$ and $R_a \sim 10^{10} - 10^{12}$. Originally, these total Reynolds numbers were introduced based on intuition, simplicity and linear theory (see, e.g. Sakurai et al., 1991b; Goossens et al., 1995; Goossens and Ruderman, 1995; Clack et al., 2009b). However, it turned out that using these definitions the *strength* of dissipation is the same order of magnitude as the inverse of the total Reynolds numbers.

In an isotropic plasma, if $g$ is a *large* variable[9] the typical largest quadratic nonlinear term in the system of MHD equations is of the form $g\partial g/\partial z$, while the typical dissipative term is of the form $\overline{\nu}\partial^2 g/\partial x^2$. Here $\overline{\nu}$ could be replaced by $\overline{\eta}$ since they are of the same order of magnitude, however, to follow convention we use the viscosity coefficient ($\overline{\nu}$)[10]. At the beginning of this section, we discussed that large variables are of the order of $\epsilon R^{1/3}$ in the isotropic dissipative layer, but linear theory also predicts that $\partial/\partial z = \mathcal{O}(l_{inh}^{-1})$, $\partial/\partial x = \mathcal{O}(l_{diss}^{-1})$ and $\overline{\nu} = \mathcal{O}(R_i^{-1} l_{inh})$ (see, e.g. Ruderman and Goossens, 1993). These scalings allow us to estimate the ratio of the largest nonlinear and dissipative terms[11], resulting in the *isotropic nonlinearity parameter*

$$N_i = \frac{g\partial g/\partial z}{\overline{\nu}\partial^2 g/\partial x^2} = \mathcal{O}(\epsilon R_i^{2/3}). \tag{2.56}$$

Therefore, if the condition $N_i \ll 1$ is satisfied then linear theory is applicable. On the other

[9] Linear theory shows that *large* variables have an ideal singularity $(x - x_r)^{-1}$ in the vicinity of $x = x_r$.
[10] This convention will be continued throughout this section and thesis.
[11] The largest nonlinear and dissipative terms are related to velocity.

hand, if $N_i \geq 1$ then nonlinearity has to be taken into account when studying resonant waves in the isotropic dissipative layers. This inequality implies very restrictive conditions, even for very small values of amplitude. For example, a dimensionless amplitude $\epsilon \sim 0.01$ implies that linear theory is valid provided $R_i \ll 10^3$. In the solar photosphere it is known that $R_i \sim 10^6$, hence it is not at all obvious from the outset that linear theory is adequate (Ruderman et al., 1997d). Nonlinearity becomes important in the vicinity of resonance (where it will have the same order of magnitude as dissipation).

In anisotropic plasmas we have two separate nonlinearity parameters, a unique one for each of the Alfvén and slow resonances as the two waves have different dominating dissipative processes acting upon them. For Alfvén waves the procedure is identical to the one undertaken to produce the isotropic nonlinearity parameter in Eq. (2.56) leading to the *anisotropic Alfvén nonlinearity parameter*

$$N_a = \frac{g\partial g/\partial z}{\overline{\eta}_1 \partial^2 g/\partial x^2} = \mathcal{O}(\epsilon R_a^{2/3}). \tag{2.57}$$

It is clear that Eqs (2.56) and (2.57) are similar in their form. At the slow resonance, anisotropy changes the characteristic scale of dissipation and so $l_{diss}$ becomes the order of $R_c^{-1} l_{inh}$. In addition, the linear theory developed by Ruderman and Goossens (1996) predicts that large variables in the dissipative layer are of the order of $\epsilon R_c$. Since the plasma is anisotropic, and the dominant dissipative processes are along the magnetic field lines, the largest dissipative terms are of the form $\overline{\eta}_0 \partial^2 g/\partial z^2$. Taking the ratio of the largest nonlinear and dissipative terms leads to the *anisotropic slow nonlinearity parameter*

$$N_c = \frac{g\partial g/\partial z}{\overline{\eta}_0 \partial^2 g/\partial z^2} = \mathcal{O}(\epsilon R_c^2). \tag{2.58}$$

Hence, if the conditions $N_a \ll 1$ and $N_c \ll 1$ are satisfied linear theory is a valid approximation for anisotropic plasmas. However, if $N_a \geq 1$ or $N_c \geq 1$ then linear theory may breakdown. For example, a dimensionless amplitude $\epsilon \sim 0.01$ implies that linear theory is valid provided $R_a \ll 10^3$ or $R_c \ll 10$. We know that $R_a \sim 10^{12}$ and $R_c \sim 10^2$ in the solar corona (see, e.g. Priest, 1984; Goossens and Ruderman, 1995; Aschwanden, 2004), hence it is likely a nonlinear theory is needed.

We should note here that the MHD equations also contain cubic order nonlinearity. In this case, the largest nonlinear terms would be of the form $g^2 \partial g/\partial z$. If, for any reason, a nonlinear theory is not found when using the nonlinearity parameters from Eqs (2.56)–(2.58) a theory based on cubic nonlinearity should be attempted. For the Alfvén resonance, this implies *cubic nonlinearity parameters* of the form

$$N_i^{(h)} = \frac{g^2 \partial g/\partial z}{\overline{\nu} \partial^2 g/\partial x^2} = \mathcal{O}(\epsilon^2 R_i), \quad N_a^{(h)} = \frac{g^2 \partial g/\partial z}{\overline{\eta}_1 \partial^2 g/\partial x^2} = \mathcal{O}(\epsilon^2 R_a), \tag{2.59}$$

where the superscript '(h)' identifies the nonlinearity parameters to be of a higher order of nonlinearity compared to the standard parameters. Cubic nonlinearity can only be used when quadratic nonlinearity does not result in a nonlinear theory, since cubic nonlinearity is weaker than its quadratic counterpart.

In order to obtain nonlinearity and dissipation of the same order in the dissipative layer, we assume that the nonlinearity parameter is of the order of unity when deriving the governing equations for waves inside the dissipative layer. For example, for the isotropic nonlinearity parameter

we have $N_i = \epsilon R_i^{2/3} = \mathcal{O}(1)$, i.e. $R_i = \mathcal{O}(\epsilon^{-3/2})$. Hence, according to Eq. (2.53) we rescale the isotropic dissipative coefficients as

$$\overline{\nu} = \epsilon^{3/2}\nu, \quad \overline{\eta} = \epsilon^{3/2}\eta. \tag{2.60}$$

This type of scaling is widely applied to problems where nonlinearity and dissipation are chosen to be of the same order (see, e.g. Edwin and Roberts, 1986; Ruderman et al., 1997d; Nakariakov and Roberts, 1999; Ballai et al., 2003; Clack and Ballai, 2009a). In a similar manner, we must rescale the dissipative coefficients for the anisotropic Alfvén and slow dissipative layers. For the anisotropic Alfvén dissipative layer we have $N_a = \epsilon R_a^{2/3} = \mathcal{O}(1)$, i.e. $R_a = \mathcal{O}(\epsilon^{-3/2})$, so the dissipative coefficients are rescaled as

$$\overline{\eta}_1 = \epsilon^{3/2}\eta_1, \quad \overline{\eta} = \epsilon^{3/2}\eta. \tag{2.61}$$

In the anisotropic slow dissipative layer we have $N_c = \epsilon R_c^2 = \mathcal{O}(1)$, i.e. $R_c = \mathcal{O}(\epsilon^{-1/2})$, hence we rescale as

$$\overline{\eta}_0 = \epsilon^{1/2}\eta_0, \quad \overline{\kappa}_{\parallel} = \epsilon^{1/2}\kappa_{\parallel}. \tag{2.62}$$

Finally, if we consider cubic nonlinearity we have $N_i^{(h)} = \epsilon^2 R_i = \mathcal{O}(1)$, i.e. $R_i = \mathcal{O}(\epsilon^{-2})$ and $N_a^{(h)} = \epsilon^2 R_a = \mathcal{O}(1)$, i.e. $R_a = \mathcal{O}(\epsilon^{-2})$, thus the dissipative coefficients in this case are rescaled as

$$\overline{\nu} = \epsilon^2\nu, \quad \overline{\eta} = \epsilon^2\eta,$$

$$\overline{\eta}_1 = \epsilon^2\eta_1, \quad \overline{\eta} = \epsilon^2\eta. \tag{2.63}$$

To summarize, we have introduced Reynolds numbers as a measure of the efficiency of dissipation in the solar atmosphere. We have used these Reynolds numbers in combination with the dimensionless amplitude of perturbations ($\epsilon$) to derive the nonlinearity parameters. In turn, we have used these parameters to stretch the dissipative coefficients in the dissipative layer. The Reynolds numbers, nonlinearity parameters and scaling to be used in different scenarios are listed below:

- When studying resonant waves in isotropic plasmas use Eqs (2.53), (2.56) and (2.60).
- Investigation of slow waves in anisotropic plasmas utilises Eqs (2.54), (2.58) and (2.62).
- For Alfvén waves in anisotropic plasmas use Eqs (2.55), (2.57) and (2.61).
- If cubic nonlinearity has to be considered use the appropriate Reynolds numbers with Eqs (2.59) and (2.63).

## 2.7 Methodology for deriving the nonlinear theory of resonant waves

The calculations carried out in the present thesis require a series of generic mathematical suppositions and methods which will be presented through the nonlinear treatment of resonant slow waves in isotropic plasmas first derived in the seminal work by Ruderman et al. (1997d). Accordingly, new concepts and ideas will be added throughout the section which are critical for the

thesis. The idea is to draw similarities and differences between this theory and the ones derived later on in the thesis.

It is well-known that in nonlinear theory perturbations cannot be Fourier-analysed. Therefore, it is convenient to use the components of velocity, $\mathbf{v}$, instead of the Lagrangian displacements, $\hat{\xi}$, as the unknown variables. In Sect. 2.5 we showed that in linear theory all perturbed quantities are Fourier-analysed with respect to the spatial coordinate $z$. All perturbations were then taken to be proportional to $\exp[i(kz - \omega t)]$. Hence, the solution of the linear dissipative MHD equations was found in the form of a propagating wave with a wavelength $L = 2\pi/k$, with all perturbed quantities depending on the combination $\theta = z - Vt$ of the independent variables $z$ and $t$, rather than on $z$ and $t$ separately. Throughout this thesis, the concept of parallel and perpendicular components of the velocity and magnetic field perturbation relative to the equilibrium magnetic field lines is adopted. The definitions of these new quantities are

$$\begin{pmatrix} v_{\parallel} \\ b_{\parallel} \end{pmatrix} = \begin{pmatrix} v & w \\ b_y & b_z \end{pmatrix} \begin{pmatrix} \sin\alpha \\ \cos\alpha \end{pmatrix}, \qquad \begin{pmatrix} v_{\perp} \\ b_{\perp} \end{pmatrix} = \begin{pmatrix} v & -w \\ b_y & -b_z \end{pmatrix} \begin{pmatrix} \cos\alpha \\ \sin\alpha \end{pmatrix}. \tag{2.64}$$

Here $u, v, w$ are the $x, y, z$—components of the velocity perturbations. During our calculations it is assumed that the equilibrium magnetic field $\mathbf{B}_0$ is unidirectional and lies in the $yz$-plane, and $\alpha$ is the angle between $\mathbf{B}_0$ and the $z$-axis. In an attempt to match the linear formulation as closely as possible only solutions in the form of plane periodic propagating waves with permanent shape are considered, implying that all perturbed quantities depend only on $\theta$, and they are periodic with respect to $\theta$.

In order to derive the governing equations for wave motions in the dissipative layer a version of the method of *matched asymptotic expansions* is used (see, e.g. Nayfeh, 1981; Bender and Ország, 1991). This method entails finding the so-called *outer* and *inner* expansions and then matching them in the overlap regions. This nomenclature is well adopted for the situation here. The outer expansion is the solution outside the dissipative layer and the inner expansion is the solution inside the dissipative layer.

With the new variable, $\theta$, the isotropic version of the system of equations (2.1)–(2.8) can be easily rewritten. Since we are assuming an isotropic plasma, Sect. 2.6 suggests the use of Eqs (2.53), (2.56) and (2.60). Upon obtaining the scalar versions of Eqs (2.1)–(2.8) we find that they contain terms proportional to $\epsilon^{1/2}$ and this inspires us to seek solutions in the outer region represented by asymptotic expansions containing terms of the order $\epsilon$, $\epsilon^{3/2}$ and higher. By carrying out calculations we derive, in the first order, a system of two linear partial differential equations for $u^{(1)}$ and $P^{(1)}$ which are singular at the Alfvén and slow resonant positions for which the solutions can be found in the form of Fröbenius expansions. All other variables can be written in terms of $u^{(1)}$ and $P^{(1)}$. The salient properties of the first order of approximation is that $P$, $v_{\perp}$ and $b_{\perp}$ are regular, $u$ and $b_x$ possess logarithmic singularities and $\rho$, $p$, $v_{\parallel}$ and $b_{\parallel}$ are the most singular with a $1/x$ singularity. Continuing calculations to higher orders of approximations we find the dominant singularities remain in the perturbations denoted in the first order of approximation. Therefore, the whole outer solution for each variable can be written in asymptotic form.

Now that the outer expansions are known, the inner expansions need to be derived (which gives the solution in the dissipative layer). The inner and outer expansions then need to be matched in order to derive the governing equation for the perturbations inside the isotropic dissipative layer. The thickness of the isotropic dissipative layer is of the order of $l_{inh}R^{-1/3}$ and we

have assumed that $R = \mathcal{O}(\epsilon^{-3/2})$, so it is convenient to introduce a stretched variable to replace the transverse coordinate in the dissipative layer $\xi = \epsilon^{-1/2}x$. Equations (2.1)–(2.8) then need to be written in terms of the new variable, $\xi$, as well as the variable $\theta$, introduced earlier. The matching of outer and inner expansions is carried out as follows:

1. Find the inner ($f^i$) and outer ($f^o$) expansions.

2. Obtain the inner expansion of the outer expansion $[(f^o)^i]$ and the outer expansion of the inner expansion $[(f^i)^o]$. To obtain the inner expansion of the outer expansion $x = \epsilon^{1/2}\xi$ is substituted into the outer expansion and then re-expanded in power series of $\epsilon$ at fixed $\xi$. The outer expansion of the inner expansion is obtained by substituting $\xi = \epsilon^{-1/2}x$ and then re-expanding in power series of $\epsilon$ at fixed $x$.

3. Make the inner expansion of the outer expansion and the outer expansion of the inner expansion coincide in the overlap region $[(f^o)^i = (f^i)^o]$ to define the matching condition. The matching condition is that the outer expansion of the inner expansion coincides with the inner expansion of the outer expansion when $x = \epsilon^{1/2}\xi$ is substituted into the former[12] (or, equivalently, $\xi = \epsilon^{-1/2}x$ into the latter).

Ruderman et al. (1997d) found (using the method of matched asymptotic expansions) the inner expansion of all perturbed quantities, however, their derivation was cumbersome and required detailed mathematical analysis. In the present thesis, we employ the method of *simplified* matched asymptotic expansions (see, e.g. Goossens et al., 1995; Ballai et al., 1998b; Clack and Ballai, 2008). Since we study only weakly dissipative plasmas, dissipation is only relevant in a thin layer enclosing the resonant position. This allowed us to use the linear MHD equations to find the governing equation outside the dissipative layer. Inside the dissipative layer the amplitudes of perturbations grow, but (critically) they are assumed to still be small such that asymptotic expansions can be carried out. We know that $|\ln\epsilon| \ll \epsilon^{-m}$ for any $m > 0$ with $\epsilon \to +0$, thus, we assume that $\ln^t\epsilon$ ($t \geq 1$) is of the order of unity and is not used in the expansions. Bearing this in mind we find that the inner expansions of small variables ($P$, $v_\perp$, $b_\perp$, $u_x$ and $b_x$) should be of the same form as their outer expansions, i.e. asymptotic series starting with a term proportional to $\epsilon$, whereas large variables ($\rho$, $p$, $v_\parallel$ and $b_\parallel$) should be of the form of an asymptotic expansion with the leading term being proportional to $\epsilon^{1/2}$.

The first order approximation yields a linear homogeneous system of equations for the variables with subscript '1'. We find that the total pressure perturbation is independent of the transversal coordinate $\xi$, which parallels the result found in linear theory. In addition, an equation relating $u^{(1)}$ and $v_\parallel^{(1)}$ is recovered. The second order approximation gives a linear non-homogeneous system of equations for the variables with the superscript '2', which contains a compatibility condition. Once these equations have been rewritten and manipulated accordingly, the governing

[12]The use of the method of matched asymptotic expansions in its classical form requires a closed analytical solution for the inner expansion. Since a closed analytical solution has not been obtained, a slightly modified method has been employed - use the inner expansion of the outer expansion as an asymptotic boundary condition for the inner expansion (see, e.g. Ruderman et al., 1995). In addition, the inner expansion of the outer expansion is used as a guide line for prescribing the form of the inner expansion

equation of perturbations inside the dissipative layer is obtained to be

$$\Delta_c \xi \frac{\partial v_\parallel^{(1)}}{\partial \theta} - \frac{V\left[(\gamma+1)v_{A_c}^2 + 3c_{S_c}^2\right] v_{A_c}^2 \cos\alpha}{\left(v_{A_c}^2 + c_{S_c}^2\right)^2} v_\parallel^{(1)} \frac{\partial v_\parallel^{(1)}}{\partial \theta} + V\left(\nu + \frac{c_{T_c}^2}{v_{A_c}^2}\eta\right)\frac{\partial^2 v_\parallel^{(1)}}{\partial \xi^2} = \frac{V c_{S_c}^2 \cos\alpha}{\rho_{0_c}\left(v_{A_c}^2 + c_{S_c}^2\right)} \frac{dP^{(1)}}{d\theta}. \tag{2.65}$$

where

$$\Delta_c = -\cos^2\alpha \left(\frac{dc_T^2}{dx}\right)_c.$$

In Eq (2.65) the *driving term* is considered to be $P^{(1)}$, and is assumed to be a known function which is defined by the external conditions. Once the solution of the governing equation is known, the normal component of velocity can be obtained from the equation relating $v_\parallel$ to $u^{(1)}$. Equation (2.65) is identical to the governing equation found by Ruderman et al. (1997d), which used the full matched asymptotic expansions. Inspired by this result (and the results of other studies, e.g. Goossens et al., 1995; Ballai et al., 1998b), we will continue to use the simplified matched asymptotic expansions technique throughout the present thesis. If the amplitude of perturbations are sufficiently small the nonlinear term in Eq. (2.65) can be neglected. Hence, the corresponding equation of linear MHD is recovered (see, e.g. Sakurai et al., 1991b).

The next task is to compute the connection formulae across the isotropic dissipative layer, which is defined as

$$[f] = \lim_{\epsilon \to +0} \{f^o(\epsilon) - f^o(-\epsilon)\}, \tag{2.66}$$

where $f^o$ is the outer expansion of the variable $f$. When investigating resonant slow waves we found that the jump in the total pressure was zero. This result parallels the continuity of total pressure found in the linear theory, for cartesian geometry in Sect. 2.5 [see, Eq. (2.51)] and for cylindrical geometry in, e.g. Sakurai et al. (1991b). In order to obtain a nonlinear analog to the connection formulae for the normal component of velocity found in linear theory we need to introduce new dimensionless variables $\sigma_i$ for the transversal coordinate and $q_i$ for the parallel component of velocity perturbations. Outside the dissipative layer the approximations $u \approx \epsilon u^{(1)}$, $P \approx \epsilon P^{(1)}$ can be used. In the new variables Eq. (2.65) can be rewritten in a dimensionless form. Using the dimensionless form of Eq. (2.65) it is possible to deduce the connection formula for the normal component of the velocity perturbations. The system of two linear equations outside the dissipative layer and the connection formulae constitute the complete system of equations and boundary conditions, which must be solved simultaneously with the dimensionless nonlinear governing equation inside the isotropic dissipative layer.

# 3

# Nonlinear theory of resonant slow waves in strongly anisotropic and dispersive plasmas

*The present chapter is devoted to deriving the equation that governs the dynamics of nonlinear resonant slow waves in highly anisotropic and dispersive plasmas. The solar corona is a typical example of a plasma with strongly anisotropic transport processes. The main dissipative mechanisms in the solar corona acting on slow magnetoacoustic waves are the anisotropic thermal conductivity and viscosity. Ballai et al. (1998b) developed the nonlinear theory of driven slow resonant waves in such a regime. In the present chapter the nonlinear behaviour of driven magnetohydrodynamic waves in the slow dissipative layer in plasmas with strongly anisotropic viscosity and thermal conductivity is expanded by considering dispersive effects due to Hall currents. Our analysis shows that the nonlinear governing equation describing the dynamics of nonlinear resonant slow waves is supplemented by a term which describes nonlinear dispersion and is of the same order of magnitude as nonlinearity and dissipation. The connection formulae are found to be similar to their non-dispersive counterparts. The results of the present chapter have been published in Physics of Plasmas (Clack and Ballai, 2008).*

*Mathematicians stand on each other's shoulders.*
**(Carl Friedrich Gauss** 1777 – 1855**)**

## 3.1 Introduction

Ionson (1978) suggested, for the first time, that resonant MHD waves may be a means to heat magnetic loops in the solar corona. Since then, resonant absorption of MHD waves has become a popular and successful mechanism for providing some of the heating of the solar corona (see, e.g. Poedts et al., 1990b; Ofman and Davila, 1995; Belien et al., 1999). A driven problem for resonant MHD waves occurs when there is an external (or internal) source of energy that excites the plasma oscillations (see Sect. 2.3). If there is a small amount of dissipation present in the system, after some time the system will attain a steady state in which all perturbed quantities will oscillate with the same frequency $\omega$. Two types of driving are possible. First, direct driving, was described in Sect. 2.3. In the context of resonant absorption, this type of driving was studied by, e.g. Ruderman et al. (1997a), Ruderman et al. (1997b) and Tirry et al. (1997). Secondly, in the case of indirect or lateral driving, the energy source can be either outside or inside the system. This energy source excites fast or slow magnetosonic waves which propagate across and along magnetic surfaces and reach the resonant magnetic surface where their energy is partly dissipated due to resonant coupling with localized Alfvén or slow waves. The lateral driving problem was studied by, e.g. Davila (1987) for planar geometry and by, e.g. Erdélyi (1997) for cylindrical geometry. In the present chapter, we consider only the lateral driven case (for a comprehensive background to lateral driving see, e.g. Poedts et al., 1989, 1990a,c,d). An important property of these waves is that their damping rate is independent of the values of the dissipative coefficients, a situation characteristic for dissipative systems with large Reynolds numbers. As a result, the damping rate of near resonant MHD waves can be many orders of magnitudes larger than the damping rate of MHD waves with the same frequencies in homogeneous plasmas. The damping allows the waves energy to be converted into heat, which has made resonant absorption a subject of intense study.

Most studies on driven resonant MHD waves use isotropic viscosity and / or electrical resistivity. However, the solar corona is a well-known example of a plasma where viscosity is strongly anisotropic (Hollweg, 1985). Hollweg and Yang (1988) studied the laterally driven problem in the cold plasma approximation. They found that anisotropic viscosity does not remove the Alfvén singularity (if the Braginskii's viscosity tensor is approximated by its first term only). However, it is shown in Sect. 2.4 that Braginskii's full viscosity tensor does remove the Alfvén singularity via its shear viscosity component.

For the case of slow resonant waves the situation is different. The laterally driven linear slow resonant waves in plasmas with strongly anisotropic viscosity and thermal conductivity was studied first by Ruderman and Goossens (1996). They successfully showed that anisotropic viscosity and / or thermal conductivity removes the singularity at the slow resonance present in ideal plasmas. They also obtained the explicit connection formulae, which are identical to those found in the case of plasmas with isotropic viscosity and finite electrical resistivity (see, e.g. Sakurai et al., 1991b). This fact supports the hypothesis that in weakly dissipative plasmas the connection formulae are independent of the exact form of dissipative processes present in the dissipative layer.

The laterally driven nonlinear slow resonant waves in plasmas with strongly anisotropic viscosity and thermal conductivity was first studied by Ballai et al. (1998b). They found that nonlinearity was crucial in the dissipative layer. The governing equation for slow wave dynamics in the dissipative layer was derived and the *implicit* connection formulae were found (explicit connection formulae have only been found for linear theory and for the limit of strong nonlinearity, see, e.g. Ruderman, 2000). The governing equation was almost identical to that found by Ruderman

et al. (1997d), however the dissipative term was laterally dependent ($\theta$) rather than normally dependent ($\xi$). The implicit connection formulae found coincide with those found in plasmas with isotropic viscosity and finite electrical resistivity (Ruderman et al., 1997d).

A drawback of previous studies on resonant absorption is that even though anisotropy is considered, dispersion (by, e.g. Hall effect) is neglected. This approximation is acceptable only for lowest regions of the solar atmosphere. The solar corona is known to be strongly magnetized, hence the Hall term can be comparable with other effects considered in the process of resonance. The present chapter will extend the nonlinear theory of resonant slow MHD waves in the dissipative layer with strongly anisotropic viscosity and thermal conductivity to include Hall dispersion and show that the effect of this new addition is of the same order of magnitude as nonlinearity and dissipation near resonance.

## 3.2 Fundamental equations

In what follows we use the visco-thermal MHD equations with strongly anisotropic viscosity and thermal conductivity. We assume that the plasma is strongly magnetised, so that the conditions $\omega_e\tau_e \gg 1$ and $\omega_i\tau_i \gg 1$ are satisfied. Due to the strong magnetic field, transport processes are anisotropic. Under these conditions, for slow waves, it is a good approximation to retain only the first term of Braginskii's expression for viscosity (Hollweg, 1985) given by Eq. (2.29) and the definitions from Eqs (2.23) and (2.27). As discussed in Sect. 2.4, in a strongly magnetised plasma the thermal conductivity parallel to the magnetic field lines dwarfs the perpendicular component so the heat flux is supplied by Eq. (2.32).

In the solar corona the finite electrical resistivity can be neglected as it is several orders of magnitude smaller than the dissipative coefficients considered here (see, e.g. Erdélyi and Goossens, 1995). The visco-thermal MHD equations are given by Eqs (2.1)–(2.8), with $\mathcal{L} = \nabla \cdot \mathbf{q}$ substituted into Eq. (2.7). This substitution transforms the energy equation into the *thermal equation*

$$\frac{\partial \overline{T}}{\partial t} + \mathbf{v}\cdot\nabla\overline{T} + (\gamma-1)\overline{T}\nabla\cdot\mathbf{v} = \frac{\gamma-1}{\widetilde{R}\overline{\rho}}\left\{\nabla\cdot\left[\overline{\kappa}_{\parallel}\mathbf{b}'(\mathbf{b}'\cdot\nabla\overline{T})\right] + \frac{1}{3}\overline{\eta}_0 Q^2\right\}, \tag{3.1}$$

where

$$Q = 3\mathbf{b}'\cdot(\mathbf{b}'\cdot\nabla)\mathbf{v} - \nabla\cdot\mathbf{v}.$$

The first term (in the braces) on the right hand side of Eq. (3.1) describes heating due to thermal conductivity, while the second term gives the viscous heating. In addition to the thermal equation being formed, the total pressure is modified by the viscosity, to give

$$\overline{P} = \overline{p} + \frac{\mathbf{B}^2}{2\mu_0} + \frac{\overline{\eta}_0}{3}Q. \tag{3.2}$$

The propagation of compressional linear and nonlinear MHD waves in Hall plasmas has been studied by, e.g. Baranov and Ruderman (1974); Ruderman (1976, 1987, 2002); Ballai et al. (2003); Miteva et al. (2004). As stated in Sect. 2.4, Hall MHD is only relevant to plasma dynamics occurring on length scales of the order of the ion inertial length ($d_i = c/\omega_i$). For the present chapter this would require that $d_i = \mathcal{O}(\delta_c)$, where $\delta_c$ is the thickness of the *anisotropic* slow dissipative layer. Indeed, starting from the upper chromosphere this condition is satisfied and the lengths involved in the problem are of the order of $10 - 100$m.

We adopt a Cartesian coordinate system, and limit our analysis to a static background equilibrium ($\mathbf{v}_0 = 0$). We assume that all equilibrium quantities depend on $x$ only. The equilibrium magnetic field, $\mathbf{B}_0$, is unidirectional and lies in the $yz-$plane. The equilibrium quantities must satisfy the condition of total pressure balance as given by Eq. (2.33). In addition we assume that the wave propagation is independent of $y$ ($\partial/\partial y = 0$). In linear theory of driven waves all perturbed quantities oscillate with the same frequency $\omega$ (see Sect. 2.5) so we seek solutions in the form of propagating waves, where these waves depend on the combination $\theta = z - Vt$, with $V = \omega/k$ where $k = (k_x^2 + k_y^2 + k_z^2)^{1/2}$. In the context of resonant absorption (of slow waves) the phase velocity ($V$) must match the projection of the cusp velocity ($c_T$) onto the $z$-axis when $x = x_c$. To define the resonant position mathematically it is convenient to introduce the angle ($\alpha$) between the $z-$axis and the direction of the equilibrium magnetic field, so that the components of the equilibrium magnetic field are

$$B_{0y} = B_0 \sin\alpha, \quad B_{0z} = B_0 \cos\alpha. \tag{3.3}$$

The definition of the *slow* resonant position can now be written mathematically as

$$V = c_T\,(x_c)\cos\alpha. \tag{3.4}$$

In a nonlinear regime the perturbations cannot be Fourier-analysed, however, in an attempt to adhere as closely to linear theory as possible we look for travelling wave solutions and assume all perturbed quantities depend on $\theta = z - Vt$ where $V$ is given by Eq. (3.4). The perturbations of the physical quantities are defined by

$$\overline{\rho} = \rho_0 + \rho, \quad \overline{p} = p_0 + p, \quad \overline{T} = T_0 + T \quad \mathbf{B} = \mathbf{B}_0 + \mathbf{b}, \quad \overline{\mathbf{H}} = \mathbf{H}_0 + \mathbf{H}, \quad \overline{P} = P_0 + \widetilde{P} \tag{3.5}$$

Simple calculations using Eqs (2.5) and (3.5) yields that $\mathbf{H}_0 = 0$. To make the mathematical analysis more concise and to make the physics more transparent we define the components of velocity and magnetic field that are parallel and perpendicular to the equilibrium magnetic field as in Eq. (2.64). In Sect. 2.6 we discussed, at length, the Reynolds numbers and dissipative coefficient stretching required in different scenarios. In this particular scenario, we need to use the Reynolds numbers defined by Eq. (2.54), the nonlinearity parameter in Eq. (2.58) and the stretched dissipative coefficients supplied by Eq. (2.62). In addition, we must also consider the *coefficient of Hall conduction*, defined as $\overline{\chi} = \overline{\eta}\omega_e\tau_e$ (although $\overline{\eta}$ is small enough, in the solar corona, to be neglected in comparison to $\overline{\eta}_0$, here it is multiplied by the product $\omega_e\tau_e$ which is very large under coronal conditions). Similar to the previous dissipative coefficients, we introduce the scaling

$$\overline{\chi} = \epsilon^{1/2}\chi. \tag{3.6}$$

With all these new notations we rewrite the MHD equations as

$$V\frac{\partial\rho}{\partial\theta} - \frac{\partial(\rho_0 u)}{\partial x} - \rho_0\frac{\partial w}{\partial\theta} = \frac{\partial(\rho u)}{\partial x} + \frac{\partial(\rho w)}{\partial\theta}, \tag{3.7}$$

$$\rho_0 V\frac{\partial u}{\partial\theta}-\frac{\partial\widetilde{P}}{\partial x}+\frac{B_0\cos\alpha}{\mu_0}\frac{\partial b_x}{\partial\theta}=\overline{\rho}\left(u\frac{\partial u}{\partial x}+w\frac{\partial w}{\partial\theta}\right)-\rho V\frac{\partial u}{\partial\theta}$$
$$-\frac{b_x}{\mu_0}\frac{\partial b_x}{\partial x}-\frac{b_z}{\mu_0}\frac{\partial b_x}{\partial\theta}-\epsilon^{1/2}\left(\frac{\partial}{\partial x}b_x'+\frac{\partial}{\partial\theta}b_z'\right)(\eta_0 b_x' Q)\,, \quad (3.8)$$

$$\frac{\partial}{\partial\theta}\left(\rho_0 V v_\perp+\widetilde{P}\sin\alpha+\frac{B_0\cos\alpha}{\mu_0}b_\perp\right)=\overline{\rho}\left(u\frac{\partial v_\perp}{\partial x}+w\frac{\partial v_\perp}{\partial\theta}\right)-\rho V\frac{\partial v_\perp}{\partial\theta}$$
$$-\frac{b_x}{\mu_0}\frac{\partial b_\perp}{\partial x}-\frac{b_z}{\mu_0}\frac{\partial b_\perp}{\partial\theta}-\epsilon^{1/2}\left(\frac{\partial}{\partial x}b_x'+\frac{\partial}{\partial\theta}b_z'\right)(\eta_0 b_\perp' Q)\,, \quad (3.9)$$

$$\frac{\partial}{\partial\theta}\left(\rho_0 V v_\parallel-\widetilde{P}\cos\alpha+\frac{B_0\cos\alpha}{\mu_0}b_\parallel\right)+\frac{b_x}{\mu_0}\frac{dB_0}{dx}=\overline{\rho}\left(u\frac{\partial v_\parallel}{\partial x}+w\frac{\partial v_\parallel}{\partial\theta}\right)$$
$$-\rho V\frac{\partial v_\parallel}{\partial\theta}-\frac{b_x}{\mu_0}\frac{\partial b_\parallel}{\partial x}-\frac{b_z}{\mu_0}\frac{\partial b_\parallel}{\partial\theta}-\epsilon^{1/2}\left(\frac{\partial}{\partial x}b_x'+\frac{\partial}{\partial\theta}b_z'\right)\left(\eta_0 b_\parallel' Q\right), \quad (3.10)$$

$$Vb_x+B_0 u\cos\alpha=wb_x-ub_z-\epsilon^{1/2}\chi\frac{\partial b_\parallel}{\partial\theta}\cos\alpha\sin\alpha, \quad (3.11)$$

$$\frac{\partial}{\partial\theta}\left(Vb_\perp+B_0 v_\perp\cos\alpha\right)=\frac{\partial(ub_\perp)}{\partial x}+\frac{\partial(wb_\perp)}{\partial\theta}-b_x\frac{\partial v_\perp}{\partial x}-b_z\frac{\partial v_\perp}{\partial\theta}-\epsilon^{1/2}\chi\frac{\partial^2 b_\parallel}{\partial x\partial\theta}\cos\alpha, \quad (3.12)$$

$$\frac{\partial}{\partial\theta}\left(Vb_\parallel+B_0 v_\parallel\cos\alpha\right)-\frac{\partial(B_0 u)}{\partial x}-B_0\frac{\partial w}{\partial\theta}=\frac{\partial(ub_\parallel)}{\partial x}$$
$$+\frac{\partial(wb_\parallel)}{\partial\theta}-b_x\frac{\partial v_\parallel}{\partial x}-b_z\frac{\partial v_\parallel}{\partial\theta}-\epsilon^{1/2}\frac{\chi}{\rho_0}\frac{\partial b_\parallel}{\partial\theta}\frac{\partial\rho}{\partial x}\sin\alpha, \quad (3.13)$$

$$\frac{\gamma T_0 p}{c_S^2}-T_0\rho-\rho_0 T=\rho T, \quad (3.14)$$

$$\frac{\partial b_x}{\partial x}+\frac{\partial b_z}{\partial\theta}=0, \quad (3.15)$$

$$V\frac{\partial T}{\partial\theta}-u\frac{dT_0}{dx}-(\gamma-1)T_0\left(\frac{\partial u}{\partial x}+\frac{\partial w}{\partial\theta}\right)=u\frac{\partial T}{\partial x}+w\frac{\partial T}{\partial\theta}+(\gamma-1)T\left(\frac{\partial u}{\partial x}+\frac{\partial w}{\partial\theta}\right)$$
$$-\epsilon^{1/2}\frac{\gamma-1}{\overline{\rho}\widetilde{R}}\left\{\frac{1}{3}\eta_0 Q^2+\left(\frac{\partial}{\partial x}b_x'+\frac{\partial}{\partial\theta}b_z'\right)\kappa_\parallel\left[b_x'\left(\frac{dT_0}{dx}+\frac{\partial T}{\partial x}\right)+b_z'\frac{\partial T}{\partial\theta}\right]\right\}, \quad (3.16)$$

$$\widetilde{P}=p+\frac{1}{2\mu_0}\left(b_x^2+b_\perp^2+b_\parallel^2+2B_0 b_\parallel\right)+\frac{1}{3}\epsilon^{1/2}\eta_0 Q, \quad (3.17)$$

$$Q=3b_x'\left(b_x'\frac{\partial u}{\partial x}+b_z'\frac{\partial u}{\partial\theta}\right)+3b_\parallel'\left(b_x'\frac{\partial v_\parallel}{\partial x}+b_z'\frac{\partial v_\parallel}{\partial\theta}\right)-\left(\frac{\partial u}{\partial x}+\frac{\partial w}{\partial\theta}\right). \quad (3.18)$$

We should state that in Eqs (3.11)–(3.13) we have used the coefficient of Hall conduction ($\chi$) which does not contribute to the total Reynolds number because it is the multiplier of dispersive terms rather than dissipative ones. The derivation of the expressions of the Hall terms in the induction equation can be found in Appendix A. The largest terms of Braginskii's viscosity tensor are derived in Appendix B. These terms are used in deriving the governing equation in the next section.

The set of Eqs (3.7)–(3.18), will be used in the next section to derive the governing equation for

wave motion in the anisotropic slow dissipative layer.

## 3.3 Deriving the governing equation in the dissipative layer

In order to derive the governing equation inside the anisotropic slow dissipative layer we employ the method of simplified matched asymptotic expansions introduced in Sect. 2.7. We only consider a weakly dissipative plasmas so viscosity and thermal conductivity are only important in the narrow dissipative layer (here dissipation and nonlinearity are of the same order) embracing the resonant position. Far away from the dissipative layer the amplitudes of perturbations are small, so we use linear ideal MHD equations in order to describe the wave motion far away from the dissipative layer. The full set of nonlinear dissipative MHD equations are used for describing wave motion *inside* the dissipative layer where the amplitudes are much larger than those far away from the dissipative layer. We therefore look for solutions in the form of asymptotic expansions. The equilibrium quantities change only slightly across the dissipative layer so it is possible to approximate them by the first non-vanishing term in their Taylor series expansion with respect to $x$. Similar to linear theory, we assume the expansions of equilibrium quantities are valid in a region embracing the ideal resonant position which is assumed to be wider than the dissipative layer.

Before deriving the nonlinear governing equation we ought to make a note. In linear theory, perturbations of physical quantities are harmonic functions of $\theta$ and their mean values vanish over a period. In nonlinear theory, however, the perturbations of variables can have non-zero values as a result of nonlinear interaction of different harmonics. Due to the nonlinear absorption of wave momentum, a mean shear flow can be generated outside the dissipative layer, as shown by Ruderman et al. (1997d) for slow waves in an isotropic plasma. In our scenario a mean shear flow is created outside the dissipative layer, but as there is no perpendicular component to viscosity the oscillating plasma can slide past each other without friction which produces a mean flow with infinite amplitude. However, boundaries can prevent such oscillations. Therefore, if it is assumed such boundaries exist there will be no generation of mean shear flow; a procedure carried out by Ballai et al. (1998b) when they studied slow waves in anisotropic *non*-dispersive plasmas. Since Hall currents do not halt the production of mean shear flows we will do the same.

The first step in our mathematical description is the derivation of governing equations outside the dissipative layer where the dynamics is described by ideal and linear MHD. It is clear that Eqs (3.7)–(3.18) contain terms proportional to $\epsilon^{1/2}$, therefore, the solution in the outer region is represented by asymptotic expansions of the form

$$f = \epsilon f^{(1)} + \epsilon^{3/2} f^{(2)} + \dots, \tag{3.19}$$

where $f$ denotes any perturbed quantity (with the exception of the $y-$ and $z-$components of the velocity). Substitution of expansion (3.19) into the ideal ($\overline{\eta}_0 = \overline{\kappa}_{\parallel} = \overline{\chi} = 0$) version of the system of Eqs (3.7)–(3.18) leads to several orders of approximation. In the first order approximation a system of linear equations with the superscript '1' is obtained, where all but two of the variables can be eliminated by algebraic means. This leads to a system of two equations for $u^{(1)}$ and $P^{(1)}$

$$\frac{\partial u^{(1)}}{\partial x} = \frac{V}{\widetilde{F}} \frac{\partial P^{(1)}}{\partial \theta}, \quad \frac{\partial P^{(1)}}{\partial x} = \frac{\rho_0 A}{V} \frac{\partial u^{(1)}}{\partial \theta}, \tag{3.20}$$

where the coefficients are given as

$$\widetilde{F} = \frac{\rho_0 A C}{V^4 - V^2(v_A^2 + c_S^2) + v_A^2 c_S^2 \cos^2\alpha}, \tag{3.21}$$

$$A = V^2 - v_A^2 \cos^2\alpha, \quad C = (v_A^2 + c_S^2)\left(V^2 - c_T^2 \cos^2\alpha\right). \tag{3.22}$$

It is clear that the quantities $A$ and $C$ vanish at the Alfvén and slow resonant positions, respectively. Thus, these two positions are regular singular points of the system (3.20). The remaining variables can be expressed in terms of $u^{(1)}$ and $P^{(1)}$,

$$v_\perp^{(1)} = -\frac{V\sin\alpha}{\rho_0 A}P^{(1)}, \quad v_\parallel^{(1)} = \frac{V c_S^2 \cos\alpha}{\rho_0 C}P^{(1)}, \tag{3.23}$$

$$b_x^{(1)} = -\frac{B_0\cos\alpha}{V}u^{(1)}, \quad b_\perp^{(1)} = \frac{B_0\cos\alpha\sin\alpha}{\rho_0 A}P^{(1)}, \tag{3.24}$$

$$\frac{\partial b_\parallel^{(1)}}{\partial\theta} = \frac{B_0\left(V^2 - c_S^2\cos^2\alpha\right)}{\rho_0 C}\frac{\partial P^{(1)}}{\partial\theta} + \frac{u^{(1)}}{V}\frac{dB_0}{dx}, \tag{3.25}$$

$$\frac{\partial p^{(1)}}{\partial\theta} = \frac{V^2 c_S^2}{C}\frac{\partial P^{(1)}}{\partial\theta} - \frac{u^{(1)}B_0}{\mu_0 V}\frac{dB_0}{dx}, \quad \frac{\partial\rho^{(1)}}{\partial\theta} = \frac{V^2}{C}\frac{\partial P^{(1)}}{\partial\theta} + \frac{u^{(1)}}{V}\frac{d\rho_0}{dx}, \tag{3.26}$$

$$\frac{\partial T^{(1)}}{\partial\theta} = \frac{(\gamma-1)T_0 V^2}{\rho_0 C}\frac{\partial P^{(1)}}{\partial\theta} + \frac{u^{(1)}}{\gamma V\widetilde{R}}\frac{dc_S^2}{dx}. \tag{3.27}$$

Note that Eq. (3.20) coincides with the previously presented Eq. (2.34). The above equations are similar to those found in a non-dispersive plasma (Ballai et al., 1998b), because the dissipative and dispersive terms do not appear in the linear limit.

Eliminating $P^{(1)}$ from system (3.20) and then the introducing the Fourier series for the periodic functions leads to

$$\frac{\partial}{\partial x}\left(\widetilde{F}\frac{\partial\widehat{u}^{(1)}}{\partial x}\right) + k^2\rho_0 A\widehat{u}^{(1)} = 0. \tag{3.28}$$

Here $\widehat{u}^{(1)}(x,k)$ is a coefficient function in the Fourier series for $u^{(1)}(x,z)$ with respect to $z$, and $k = 2\pi n/L$ where $n$ is the index of the terms in the Fourier series. The position $x = 0$[1] is a regular singular point, so the solution of (3.28) can be found in the form of Fröbenius expansion in the variable $x$ with the form

$$\widehat{u}^{(1)} = A_r(k)U_r(x,k) + A_s(k)U_s(x,k). \tag{3.29}$$

$A_r(k)$ and $A_s(k)$ are arbitrary functions of $k$. The regular ($U_r$) and singular solutions ($U_s$) are defined by

$$\begin{aligned} U_r &= 1 + U_{r_1}x + U_{r_2}x^2 + \ldots, \\ U_s &= U_r\ln|x| + U_{s_1}x + U_{s_2}x^2 + \ldots. \end{aligned} \tag{3.30}$$

The expressions for the coefficients described above are not shown here as they are not used in what follows. Note that the coefficients in Eqs (3.29)–(3.30) are generally different for $x < 0$ and $x > 0$.

It can be shown (for full details see, e.g. Ruderman et al., 1997d; Ballai et al., 1998b; Clack and Ballai, 2008) that in the vicinity of the slow resonance the variables $P^{(1)}$, $v_\perp^{(1)}$ and $b_\perp^{(1)}$ behave as a

[1]We will always be able to translate the coordinate system such that the resonant position is at $x = 0$.

series of the form

$$f^{(1)} = f_1^{(1)}(\theta) + f_2^{(1)}(\theta)x\ln|x| + f_3^{(1)}(\theta)x + \dots, \tag{3.31}$$

the variables $u^{(1)}$ and $b_x^{(1)}$ have series solutions of the form

$$g^{(1)} = g_1^{(1)}(\theta)\ln|x| + g_2^{(1)}(\theta) + g_3^{(1)}(\theta)x\ln|x| + g_4^{(1)}(\theta)x + \dots, \tag{3.32}$$

and the variables $\rho^{(1)}$, $p^{(1)}$, $T^{(1)}$ $\nu_{\|}^{(1)}$ and $b_{\|}^{(1)}$ can be written as

$$h^{(1)} = h_1^{(1)}(\theta)x^{-1} + h_2^{(1)}(\theta)\ln|x| + h_3^{(1)}(\theta) + \dots. \tag{3.33}$$

Equations (3.31)–(3.33) repeat the well-known results of linear theory that in the vicinity of the slow resonant position the variables $P^{(1)}$, $\nu_{\perp}^{(1)}$ and $b_{\perp}^{(1)}$ are regular, $u^{(1)}$ and $b_x^{(1)}$ possess a logarithmic singularity, and $\rho^{(1)}$, $p^{(1)}$, $T^{(1)}$, $\nu_{\|}^{(1)}$ and $b_{\|}^{(1)}$ possess a $1/x$ singularity. In particular, the last five variables are the most singular. Proceeding in the same way, the solutions of subsequent higher order approximations can be found and the dominant singular behaviour persists to higher approximations. With all the information gathered the outer expansions can be written out in the form

$$\begin{aligned} f = \epsilon&\left[f_1^{(1)}(\theta) + f_2^{(1)}(\theta)x\ln|x| + f_3^{(1)}(\theta)x + \dots\right] \\ &+ \epsilon\left[f_1^{(2)}(\theta)\ln|x| + f_2^{(2)}(\theta) + \dots\right] + \sum_{n=3}^{\infty}\epsilon^{(n+1)/2}\left[f_1^{(n)}x^{2-n} + \dots\right], \end{aligned} \tag{3.34}$$

for $P$, $\widetilde{\nu}_{\perp}$ and $b_{\perp}$,

$$\begin{aligned} g = \epsilon&\left[g_1^{(1)}(\theta)\ln|x| + g_2^{(1)}(\theta) + g_3^{(1)}(\theta)x\ln|x| + g_4^{(1)}(\theta)x + \dots\right] \\ &+ \epsilon^{3/2}\left[g_1^{(2)}(\theta)\ln^2|x| + g_2^{(2)}(\theta)\ln|x| + g_3^{(2)}(\theta) + \dots\right] \\ &+ \sum_{n=3}^{\infty}\epsilon^{(n+1)/2}\left[g_1^{(n)}(\theta)x^{1-n} + g_2^{(n)}(\theta)x^{2-n}\ln|x| + g_3^{(n)}(\theta)x^{2-n} + \dots\right], \end{aligned} \tag{3.35}$$

for $u$ and $b_x$ and

$$\begin{aligned} h = \epsilon&\left[h_1^{(1)}(\theta)x^{-1} + h_2^{(1)}(\theta)\ln|x| + h_3^{(1)}(\theta) + \dots\right] + \epsilon^{3/2}\left[h_1^{(2)}(\theta)x^{-1}\ln|x| + h_2^{(2)}(\theta)x^{-1} + \dots\right] \\ &+ \sum_{n=3}^{\infty}\epsilon^{(n+1)/2}\left[h_1^{(n)}(\theta)x^{-n} + h_2^{(n)}(\theta)x^{1-n}\ln|x| + h_3^{(n)}(\theta)x^{1-n} + \dots\right], \end{aligned} \tag{3.36}$$

for $\rho$, $p$, $T$, $\widetilde{\nu}_{\|}$ and $b_{\|}$. The dots inside the braces denote terms that are of higher order with respect to $x$. In general, the coefficient functions of $\theta$ in Eqs (3.34)–(3.36) are different for $x < 0$ and $x > 0$.

Now let us concentrate on the solution in the dissipative layer. The thickness of the anisotropic slow dissipative layer is of the order $l_{inh}R^{-1}$. We have assumed that $R \sim \epsilon^{-1/2}$ so we obtain $l_{inh}R^{-1} = \mathcal{O}(\epsilon^{1/2}l_{inh})$. The implication of this scaling is that we have to introduce a new stretched variable to replace the transversal coordinate in the dissipative layer, so we are going to use $\xi = \epsilon^{-1/2}x$. Equations (3.7)–(3.18) are not rewritten here as they are easily obtained by the substitution of

$$\frac{\partial}{\partial x} = \epsilon^{-1/2}\frac{\partial}{\partial \xi}, \tag{3.37}$$

for all derivatives. The equilibrium quantities still depend on $x$, not $\xi$ (their expression is valid in a wider region than the characteristic scale of dissipation). All equilibrium quantities are expanded around the ideal resonant position ($x = x_c$) as

$$f_0 = f_{0_c} + \xi \left(\frac{\partial f_0}{\partial \xi}\right)_c + \ldots \approx f_{0_c} + \epsilon^{1/2} \xi \left(\frac{df_0}{dx}\right)_c , \tag{3.38}$$

where $f_0$ is any equilibrium quantity and the subscript 'c' indicates the equilibrium quantity has been evaluated at the resonant point (we can always make $x_c = 0$ by proper translation of the coordinate system).

We seek the solution to the set of equations obtained from Eqs (3.7)–(3.18) by the substitution of $x = \epsilon^{1/2}\xi$ into variables in the form of power series of $\epsilon$. These equations contain powers of $\epsilon^{1/2}$, so we use this quantity as an expansion parameter. To derive the form of the inner expansions of different quantities we have to analyze the outer solutions. First, since $v_\perp$ and $b_\perp$ are regular at $x = x_c$ we can write their inner expansions in the form of their outer expansions, namely Eq. (3.19). The quantity $\widetilde{P}$ is the sum of the perturbation of total pressure $P$, which is regular at $x = x_c$, and the dissipative term proportional to $Q$. From Eq. (3.18) it is obvious that $Q$ behaves as $x^{-1}$ in the vicinity of $x = x_c$. Far away from the dissipative layer, $Q$ is of the order $\epsilon$. Since the thickness of the anisotropic slow dissipative layer is of the order $\epsilon^{1/2} l_{inh}$, $Q$ is of the order $\epsilon^{1/2}$ in the dissipative layer. However, Eq. (3.17) clearly shows the term proportional to $Q$ contains a multiplier ($\epsilon^{1/2}$) which implies the contribution of $\widetilde{P}$ supplied by the dissipative term is of the order $\epsilon$. As a consequence, we write the inner expansion of $\widetilde{P}$ in the form of its outer expansion [Eq. (3.19)]. The amplitudes of large variables in the dissipative layer are of the order $\epsilon^{1/2}$, so the inner expansion of the variables $v_\parallel$, $b_\parallel$, $p$, $\rho$ and $T$ is

$$g = \epsilon^{1/2} g^{(1)} + \epsilon g^{(2)} + \ldots . \tag{3.39}$$

The quantities $u$ and $b_x$ behave as $\ln|x|$ in the vicinity of $x = x_c$, which suggests that they have expansions with terms of the order of $\epsilon \ln \epsilon$ in the dissipative layer. Ruderman et al. (1997d) showed that, strictly speaking, the inner expansions of all variables have to contain terms proportional to $\epsilon \ln \epsilon$ and $\epsilon^{3/2} \ln \epsilon$. However, in the simplified version of matched asymptotic expansions, we consider $\ln \epsilon$ as a quantity of the order of unity. This enables us to write the inner expansions for $u$ and $b_x$ in the form of Eq. (3.19).

We now substitute the expansion (3.19) for $u$, $b_x$, $\widetilde{P}$, $v_\perp$, $b_\perp$ and the expansion given by (3.39) for $v_\parallel$, $b_\parallel$, $p$, $\rho$, $T$ into the set of equations obtained from Eqs (3.7)–(3.18) after substitution of $x = \epsilon^{1/2}\xi$. The first order approximation (terms proportional to $\epsilon$), yields a linear homogeneous system of equations for the terms with superscript '1'. The important result that follows from this set of equations is that

$$\widetilde{P}^{(1)} = \widetilde{P}^{(1)}(\theta), \tag{3.40}$$

that is to say $\widetilde{P}^{(1)}$ does not change across the anisotropic slow dissipative layer. This result parallels the result found in linear theory (see, e.g. Sakurai et al., 1991b; Goossens et al., 1995) and nonlinear theory (see, e.g. Ruderman et al., 1997d; Ballai et al., 1998b). Subsequently, all remaining variables can be expressed in terms of $u^{(1)}$, $v_\parallel^{(1)}$ and $\widetilde{P}^{(1)}$ as

$$v_\perp^{(1)} = \frac{c_{s_c}^2 \sin\alpha}{\rho_{0_c} V v_{A_c}^2} \widetilde{P}^{(1)}(\theta), \quad b_x^{(1)} = -\frac{B_{0_c}\cos\alpha}{V} u^{(1)}, \tag{3.41}$$

$$b_{\perp}^{(1)} = -\frac{B_{0_c} c_{S_c}^2 \sin\alpha\cos\alpha}{\rho_{0_c} V^2 v_{A_c}^2}\widetilde{P}^{(1)}(\theta), \quad b_{\parallel}^{(1)} = -\frac{B_{0_c} V}{v_{A_c}^2\cos\alpha}v_{\parallel}^{(1)}, \tag{3.42}$$

$$p^{(1)} = \frac{\rho_{0_c} V}{\cos\alpha}v_{\parallel}^{(1)}, \quad \rho^{(1)} = \frac{\rho_{0_c} V}{c_{S_c}^2\cos\alpha}v_{\parallel}^{(1)}, \quad T^{(1)} = \frac{(\gamma-1)T_{0_c} V}{c_{S_c}^2\cos\alpha}v_{\parallel}^{(1)}. \tag{3.43}$$

In addition, we find that the equation that relates $u^{(1)}$ and $v_{\parallel}^{(1)}$ is

$$\frac{\partial u^{(1)}}{\partial\xi} + \frac{V^2}{v_{A_c}^2\cos\alpha}\frac{\partial v_{\parallel}^{(1)}}{\partial\theta} = 0. \tag{3.44}$$

We can verify whether Eqs (3.41)–(3.44) are correct, by substituting $V = c_{T_c}\cos\alpha$ into Eqs (3.23)–(3.27). If the equations are identical then we have carried out our calculations properly. The reason for this is that dissipation and dispersion do not appear in the first order approximation, so we should recover the result from linear theory.

In the second order approximation we use only the expressions obtained from Eqs (3.7), (3.10), (3.13), (3.14), (3.16) and (3.17). Employing Eqs (3.40)–(3.44), we replace the variables in the first order approximation. The equations obtained in the second order approximation are

$$\rho_{0_c}\left(\frac{\partial u^{(2)}}{\partial\xi} + \frac{\partial v_{\parallel}^{(2)}}{\partial\theta}\cos\alpha\right) - V\frac{\partial\rho^{(2)}}{\partial\theta} = -u^{(1)}\left(\frac{d\rho_0}{dx}\right)_c - \frac{v_{A_c}^2\cos\alpha}{v_{A_c}^2 + c_{S_c}^2}\left(\frac{d\rho_0}{dx}\right)_c \xi\frac{\partial v_{\parallel}^{(1)}}{\partial\theta}$$
$$+ \frac{c_{S_c}^2\sin^2\alpha}{V v_{A_c}^2}\frac{d\widetilde{P}}{d\theta} - \frac{\rho_{0_c} V}{c_{S_c}^2}\left(\frac{u^{(1)}}{\cos\alpha}\frac{\partial v_{\parallel}^{(1)}}{\partial\xi} + \frac{2v_{A_c}^2 + c_{S_c}^2}{c_{S_c}^2 + v_{A_c}^2}v_{\parallel}^{(1)}\frac{\partial v_{\parallel}^{(1)}}{\partial\theta}\right), \tag{3.45}$$

$$\frac{\partial}{\partial\theta}\left(V v_{\parallel}^{(2)} + \frac{B_{0_c}\cos\alpha}{\mu_0\rho_{0_c}}b_{\parallel}^{(2)}\right) = \frac{\cos\alpha}{\rho_{0_c}}\frac{d\widetilde{P}^{(1)}}{d\theta} + \frac{B_{0_c}\cos\alpha}{\mu_0 V\rho_{0_c}}u^{(1)}\left(\frac{dB_0}{dx}\right)_c$$
$$+ \frac{V}{B_{0_c}}\left[\left(\frac{dB_0}{dx}\right)_c - \frac{B_{0_c}}{\rho_{0_c}}\left(\frac{d\rho_0}{dx}\right)_c\right]\xi\frac{\partial v_{\parallel}^{(1)}}{\partial\theta} - \left(\frac{\eta_0\cos^2\alpha}{\rho_{0_c}}\right)\frac{2v_{A_c}^2 + 3c_{S_c}^2}{v_{A_c}^2 + c_{S_c}^2}\frac{\partial^2 v_{\parallel}^{(1)}}{\partial\theta^2}, \tag{3.46}$$

$$V\frac{\partial b_{\parallel}^{(2)}}{\partial\theta} - B_{0_c}\frac{\partial u^{(2)}}{\partial\xi} = u^{(1)}\left(\frac{dB_0}{dx}\right)_c - \frac{V^2}{v_{A_c}^2\cos\alpha}\left(\frac{dB_0}{dx}\right)_c\xi\frac{\partial v_{\parallel}^{(1)}}{\partial\theta} - \frac{B_{0_c}c_{S_c}^2\sin^2\alpha}{\rho_{0_c}V v_{A_c}^2}\frac{d\widetilde{P}^{(1)}}{d\theta}$$
$$+ \frac{B_{0_c}v_{A_c}^2}{V\left(v_{A_c}^2 + c_{S_c}^2\right)}\left(u^{(1)}\frac{\partial v_{\parallel}^{(1)}}{\partial\xi}\cos\alpha - \frac{V^2}{v_{A_c}^2}v_{\parallel}^{(1)}\frac{\partial v_{\parallel}^{(1)}}{\partial\theta}\right) + \chi\frac{B_{0_c}\sin\alpha}{v_{A_c}^2 + c_{S_c}^2}\frac{\partial v_{\parallel}^{(1)}}{\partial\xi}\frac{\partial v_{\parallel}^{(1)}}{\partial\theta}, \tag{3.47}$$

$$V\frac{\partial T^{(2)}}{\partial\theta} - (\gamma-1)T_{0_c}\left(\frac{\partial u^{(2)}}{\partial\xi} + \frac{\partial v_{\parallel}^{(2)}}{\partial\theta}\cos\alpha\right) = u^{(1)}\left(\frac{dT_0}{dx}\right)_c$$
$$+ (\gamma-1)\left[\frac{v_{A_c}^2\cos\alpha}{T_{0_c}\left(v_{A_c}^2 + c_{S_c}^2\right)}\xi\left(\frac{dT_0}{dx}\right)_c\frac{\partial v_{\parallel}^{(1)}}{\partial\theta} - \frac{c_{S_c}^2\sin^2\alpha}{\rho_{0_c}V v_{A_c}^2}\frac{d\widetilde{P}}{d\theta} - \frac{(\gamma-1)V\kappa_{\parallel}\cos\alpha}{\rho_{0_c}\widetilde{R}c_{S_c}^2}\frac{\partial^2 v_{\parallel}}{\partial\theta^2}\right.$$
$$\left. + \frac{V}{c_{S_c}^2}\left(\frac{u^{(1)}}{\cos\alpha}\frac{\partial v_{\parallel}^{(1)}}{\partial\xi} + \frac{\gamma v_{A_c}^2 + c_{S_c}^2}{v_{A_c}^2 + c_{S_c}^2}v_{\parallel}^{(1)}\frac{\partial v_{\parallel}^{(1)}}{\partial\theta}\right)\right], \tag{3.48}$$

$$\frac{\gamma T_{0_c}}{c_{S_c}^2} p^{(2)} - T_{0_c}\rho^{(2)} - \rho_{0_c} T^{(2)} = \frac{\rho_{0_c} V}{c_{S_c}^2 \cos\alpha}\left[\left(\frac{dT_0}{dx}\right)_c + \frac{(\gamma-1)T_{0_c}}{\rho_{0_c}}\left(\frac{d\rho_0}{dx}\right)\right]\xi v_\parallel^{(1)} + \frac{(\gamma-1)T_{0_c}\rho_{0_c} v_{A_c}^2}{c_{S_c}^2\left(v_{A_c}^2 + c_{S_c}^2\right)}\left(v_\parallel^{(1)}\right)^2, \quad (3.49)$$

$$p^{(2)} + \frac{B_{0_c}}{\mu} B_\parallel^{(2)} = \frac{\rho_{0_c} V}{B_{0_c}\cos\alpha}\left(\frac{dB_0}{dx}\right)_c \xi v_\parallel^{(1)} - \left(\frac{\eta_0\cos\alpha}{3}\right)\frac{3c_{S_c}^2 + 2v_{A_c}^2}{v_{A_c}^2 + c_{S_c}^2}\frac{\partial v_\parallel^{(1)}}{\partial\theta} - \frac{\rho_{0_c} c_{S_c}^2}{2\left(v_{A_c}^2 + c_{S_c}^2\right)}\left(v_\parallel^{(1)}\right)^2. \quad (3.50)$$

In deriving the above system we have used the fact that

$$Q^{(1)} = \frac{3c_{S_c}^2 + 2v_{A_c}^2}{v_{A_c}^2 + c_{S_c}^2}\frac{\partial v_\parallel^{(1)}}{\partial\theta}\cos\alpha, \quad (3.51)$$

obtained from Eq. (3.18) in the first order of approximation. With the exception of Eq. (3.47), which has the addition of the Hall term, these equations are identical to those found by Ballai et al. (1998b). The left-hand sides of the set of Eqs (3.45)–(3.51) could be obtained from the left-hand sides of the first order approximation by substituting variables with the superscript '2' for those with superscript '1'. The first order of approximation possesses a non-trivial solution, so Eqs (3.45)–(3.51) are compatible only if the right-hand sides of Eqs (3.45)–(3.51) satisfy a compatibility condition. To derive the compatibility condition we express $\rho^{(2)}$ and $b_\parallel^{(2)}$ in terms of $u^{(2)}$, $v_\parallel^{(2)}$, $u^{(1)}$, $v_\parallel^{(1)}$ and $\widetilde{P}^{(1)}$, using Eqs (3.46) and (3.48)–(3.50). Subsequently, we substitute these expressions into Eqs (3.45) and (3.47), to obtain

$$\frac{\partial u^{(2)}}{\partial\xi} + \frac{V^2}{v_{A_c}^2\cos\alpha}\frac{\partial v_\parallel^{(2)}}{\partial\theta} = \frac{V\left(v_{A_c}^2 + c_{S_c}^2\sin^2\alpha\right)}{\rho_{0_c} v_{A_c}^4\cos^2\alpha}\frac{d\widetilde{P}^{(1)}}{d\theta} + \frac{V}{v_{A_c}^2 + c_{S_c}^2} v_\parallel^{(1)}\frac{\partial v_\parallel^{(1)}}{\partial\theta} + \frac{V^2}{v_{A_c}^2\cos\alpha}\left[\frac{2}{B_{0_c}}\left(\frac{dB_0}{dx}\right)_c - \frac{1}{\rho_{0_c}}\left(\frac{d\rho_0}{dx}\right)_c\right]\xi\frac{\partial v_\parallel^{(1)}}{\partial\theta} - \frac{\eta_0 V\cos\alpha}{\rho_{0_c} v_{A_c}^2}\left(\frac{2v_{A_c}^2 + 3c_{S_c}^2}{v_{A_c}^2 + c_{S_c}^2}\right)\frac{\partial^2 v_\parallel^{(1)}}{\partial\theta^2} - \frac{V}{c_{S_c}^2\cos\alpha} u^{(1)}\frac{\partial v_\parallel^{(1)}}{\partial\xi} - \frac{\chi\sin\alpha}{v_{A_c}^2 + c_{S_c}^2}\frac{\partial v_\parallel^{(1)}}{\partial\xi}\frac{\partial v_\parallel^{(1)}}{\partial\theta}, \quad (3.52)$$

$$\frac{\partial u^{(2)}}{\partial\xi} + \frac{V^2}{v_{A_c}^2\cos\alpha}\frac{\partial v_\parallel^{(2)}}{\partial\theta} = \frac{c_{S_c}^2\sin^2\alpha}{\rho_{0_c} V v_{A_c}^2}\frac{d\widetilde{P}^{(1)}}{d\theta} - \frac{V^2}{T_{0_c} c_{S_c}^2\cos\alpha}\left(\frac{dT_0}{dx}\right)_c\xi\frac{\partial v_\parallel^{(1)}}{\partial\theta} - \frac{V}{c_{S_c}^2\cos\alpha} u^{(1)}\frac{\partial v_\parallel}{\partial\xi} - \frac{V\left(2c_{S_c}^2 + (\gamma+1)v_{A_c}^2\right)}{c_{S_c}^2\left(v_{A_c}^2 + c_{S_c}^2\right)} v_\parallel^{(1)}\frac{\partial v_\parallel^{(1)}}{\partial\theta} + \frac{V\cos\alpha}{\gamma\rho_{0_c} c_{S_c}^2}\left[\frac{2\gamma\eta_0}{3}\left(\frac{2v_{A_c}^2 + 3c_{S_c}^2}{v_{A_c}^2 + c_{S_c}^2}\right) + \frac{(\gamma-1)^2\kappa_\parallel}{\widetilde{R}}\right]\frac{\partial^2 v_\parallel^{(1)}}{\partial\theta^2}. \quad (3.53)$$

It can be seen that Eqs (3.52) and (3.53) have identical left-hand sides. Extracting these two equations we derive the governing equation (which is the equation connecting $v_\parallel^{(1)}$ and $\widetilde{P}^{(1)}$)

$$\Delta\xi\frac{\partial v_\parallel^{(1)}}{\partial\theta} - \alpha v_\parallel^{(1)}\frac{\partial v_\parallel^{(1)}}{\partial\theta} + \frac{V^3\lambda}{v_{A_c}^2 + c_{S_c}^2}\frac{\partial^2 v_\parallel^{(1)}}{\partial\theta^2} + \Omega\frac{\partial v_\parallel^{(1)}}{\partial\xi}\frac{\partial v_\parallel^{(1)}}{\partial\theta} = \frac{V c_{S_c}^2\cos\alpha}{\rho_{0_c}\left(v_{A_c}^2 + c_{S_c}^2\right)}\frac{d\widetilde{P}^{(1)}}{d\theta}, \quad (3.54)$$

where we have used the notation

$$a = \frac{V\left[(\gamma+1)v_{A_c}^2 + 3c_{S_c}^2\right]v_{A_c}^2\cos\alpha}{\left(v_{A_c}^2 + c_{S_c}^2\right)^2}, \quad \lambda = \frac{\eta_0\left(2v_{A_c}^2 + 3c_{S_c}^2\right)^2}{3\rho_{0_c}v_{A_c}^2 c_{S_c}^2} + \frac{(\gamma-1)^2\kappa_{\parallel}\left(v_{A_c}^2 + c_{S_c}^2\right)}{\gamma\rho_{0_c}\widetilde{R}c_{S_c}^2},$$

$$\Omega = \frac{\chi c_{S_c}^2 v_{A_c}^2}{\left(v_{A_c}^2 + c_{S_c}^2\right)^2}\cos\alpha\sin\alpha, \quad \Delta = -\cos^2\alpha\left(\frac{dc_T^2}{dx}\right)_c.$$

Equation (3.54) differs from its counterpart found by Ballai et al. (1998b) only by the last term of the left-hand side representing Hall dispersion. If we linearize Eq. (3.54) and take $v_{\parallel}^{(1)}$ proportional to $\exp(ik\theta)$, we arrive at the linear equation for the parallel velocity obtained in linear theory by Ruderman and Goossens (1996).

Equation (3.54) is the complete nonlinear governing equation for the parallel velocity in the anisotropic slow dissipative layer. The function $\widetilde{P}^{(1)}$ in this equation is determined by the solution outside the dissipative layer and is thought to be the driving term. We should note here that the dispersion (the last term on the left-hand side) appears as a nonlinear term (*nonlinear* dispersion).

## 3.4 Nonlinear connection formulae

In linear dissipative MHD it is assumed that when dissipative effects are weak they are only important in the thin dissipative layer that embraces the ideal resonant position (see, e.g. Sakurai et al., 1991b; Hollweg, 1988; Hollweg and Yang, 1988; Goossens et al., 1995). Outside this layer, ideal MHD can be employed to describe the plasma motion. The dissipative layer is treated as a surface of discontinuity (see discussion in Sect. 2.5). In order to solve Eq. (3.20) boundary conditions are needed for the variables $u$ and $P$ at this surface of discontinuity. In linear theory these conditions are described by the explicit connection formulae that determine the jumps in the quantities $u$ and $P$. In order to derive the nonlinear counterpart of connection formulae for the anisotropic slow dissipative layer, we define the jump of a function as in Eq. (2.66). The thickness of the anisotropic slow dissipative layer ($\delta_c$) is determined by the condition that the first and third terms in Eq. (3.54) are of the same order, i.e.

$$\delta_c = \frac{V^3 k\lambda}{\left(v_{A_c}^2 + c_{S_c}^2\right)|\Delta|}, \tag{3.55}$$

where $k$ is the wave number. It is instructive to introduce a new, dimensionless variable [$\sigma_c = (x - x_c)/\delta_c$] in the dissipative layer. Let $x_0$ be the characteristic width of the overlap regions of the dissipative layer (where both the linear ideal MHD equations and the nonlinear dissipative MHD equations are valid). One of the main reasons we have introduced the variable $\sigma_c$ is the property that $\sigma_c = \mathcal{O}(1)$ in the dissipative layer, while $|x| \to x_0$ corresponds to $|\sigma_c| \to \infty$. This provides us with the second definition of the jump in the function $f(x)$ across the dissipative layer,

$$[f] = \lim_{\sigma_c \to +\infty}\{f(\sigma_c) - f(-\sigma_c)\}. \tag{3.56}$$

The first connection formula can be obtained in a straightforward way by taking into account that the variable $\widetilde{P}^{(1)}$ does not change across the dissipative layer, so there cannot be any jump in the total pressure,

$$\left[\,\overline{P}\,\right] = 0. \tag{3.57}$$

This connection formula is the same as obtained previously by linear and nonlinear theories.

In order to derive the second connection formula we use the approximate relations $u \approx \epsilon u^{(1)}$, $v_{\parallel} \approx \epsilon^{1/2} v_{\parallel}^{(1)}$, $\widetilde{P} \approx \epsilon \widetilde{P}^{(1)}$ and introduce the new dimensionless variable, $q_c$, defined as

$$q_c = \epsilon^{1/2} \frac{kV\delta_c \cos\alpha}{v_{A_c}^2} \widetilde{v}_{\parallel}^{(1)}. \tag{3.58}$$

In the new variable, Eq. (3.44) is rewritten as

$$\frac{\partial u}{\partial \sigma_c} = -\frac{V}{k\cos^2\alpha} \frac{\partial q}{\partial \theta}, \tag{3.59}$$

and Eq. (3.54) becomes

$$\mathrm{sgn}(\Delta_c)\sigma_c \frac{\partial q_c}{\partial \theta} - \Lambda q_c \frac{\partial q_c}{\partial \theta} + k^{-1} \frac{\partial^2 q_c}{\partial \theta^2} + \Psi \frac{\partial q_c}{\partial \sigma_c} \frac{\partial q_c}{\partial \theta} = \frac{kV^4}{\rho_{0_c} v_{A_c}^2 |\Delta_c|} \frac{d\widetilde{P}}{d\theta}, \tag{3.60}$$

where

$$\Lambda = R_c^2 \frac{v_{A_c}^4 |\Delta_c| \left[(\gamma+1)v_{A_c}^2 + 3c_{S_c}^2\right]}{kV^8}, \quad \text{and} \quad \Psi = R_c^2 \frac{\chi |\Delta_c|^2 c_{S_c}^2 v_{A_c}^2 (v_{A_c}^2 + c_{S_c}^2)\sin\alpha}{kV^{13}}. \tag{3.61}$$

It is worth mentioning that we have used a slightly different Reynolds number ($R_c$) to the one used in previous sections of this chapter. Here it is defined as $R_c^* = V/k\lambda$. When $kl_{inh} = \mathcal{O}(1)$ (in fact our analysis is valid when $\epsilon^{1/2} \ll kl_{inh} \ll \epsilon^{-1/2}$), the total Reynolds number used in this section is of the same order of magnitude as that used in the previous sections of this chapter, and the criterion of nonlinearity coincides with that obtained in Sect. 2.6 from the qualitative analysis. It is easy to show that the estimations

$$q_c = \mathcal{O}(\epsilon^{1/2} kl_{inh} R_c^{-1}), \quad \delta_c = \mathcal{O}(l_{inh} R_c^{-1}), \quad \Lambda = \mathcal{O}(R_c^2 k^{-1} l_{inh}^{-1}), \quad \Psi = \mathcal{O}(R_c^2 k^{-1} l_{inh}^{-2}),$$

are valid. The ratios of the nonlinear to dissipative term ($N_c$), dispersive to dissipative term ($D_d$) and dispersive to nonlinear term ($D_n$) in Eq. (3.60) are

$$N_c = \mathcal{O}(\epsilon^{1/2} R_c kl_{inh}), \quad D_d = \mathcal{O}(\epsilon^{1/2} R_c^2 kl_{inh}^{-1}), \quad D_n = \mathcal{O}(R_c l_{inh}^{-2}).$$

The parameters $N_c$ and $D_d$ can be considered as nonlinearity and dispersive parameters, respectively. Nonlinearity (dispersion) is important if $N_c \gtrsim 1$ ($D_d \gtrsim 1$). When $N_c \ll 1$ ($D_d \ll 1$) the nonlinear (dispersive) term in Eq. (3.60) can be neglected. Dispersion dominates nonlinearity if $D_n > 1$. In the opposite case ($D_n < 1$) nonlinearity dominates dispersion. With the above scalings in mind, it is obvious that the physical background of this chapter is applicable for relatively short inhomogeneity scales.

Following linear studies, the outer solution reveals that $v_{\parallel} = \mathcal{O}(x^{-1})$ as $x \to 0$. Thus, to match the outer and inner solutions in the overlap regions the asymptotic relation $q_c = \mathcal{O}(\sigma_c^{-1})$ as $|\sigma_c| \to \infty$ must be valid. It then directly follows from Eq. (3.60) that $q_c$ takes the form

$$q_c \simeq \frac{kV^4 P_c(\theta)}{\rho_{0_c} v_{A_c}^2 \Delta_c \sigma_c}. \tag{3.62}$$

for $|\sigma_c| \to \infty$. From Eqs (3.59) and (3.62) it is obtained that when $\sigma_c \to \pm\infty$,

$$u = -\frac{V c_{S_e}^4 \cos^2\alpha}{\rho_{0_e}\Delta_c\left(v_{A_e}^2 + c_{S_e}^2\right)^2}\frac{dP_c}{d\theta}\ln|\sigma_c| + u_{\pm}(\theta) + \mathcal{O}(\sigma_c^{-1}), \tag{3.63}$$

where

$$u_+(\theta) - u_-(\theta) = -\frac{V}{k\cos^2\alpha}\mathcal{P}\int_{-\infty}^{\infty}\frac{\partial q_c}{\partial\theta}\,d\sigma_c. \tag{3.64}$$

The symbol of *Cauchy principal part* ($\mathcal{P}$) is used because the integral is divergent at infinity. The matching conditions yield

$$[u_c] = -\frac{V}{k\cos^2\alpha}\mathcal{P}\int_{-\infty}^{\infty}\frac{\partial q_c}{\partial\theta}\,d\sigma_c. \tag{3.65}$$

Equation (3.65) is the nonlinear analog for the implicit connection formula for the normal component of velocity. The main difference between the linear and the nonlinear connection formula is that while in the linear version the jumps are expressed explicitly in terms of $\widetilde{P}(\theta)$ and equilibrium quantities, in the nonlinear version the jump in the normal component of velocity, $u$, is expressed implicitly in terms of an unknown quantity $q_c$. The connection formula (3.65) is identical to that found by Ruderman et al. (1997d) in the limit of weak nonlinearity for non-dispersive plasmas and by Ballai et al. (1998b) for anisotropic plasmas. To find solutions in the dissipative layer we have to use Eqs (3.20) and (3.60) simultaneously. The boundary conditions for the outer solution are provided by Eqs (3.57) and (3.65).

## 3.5 Conclusions

In the present chapter we have further developed the nonlinear theory of resonant slow MHD waves in the dissipative layer in one-dimensional planar geometry in plasmas with strongly anisotropic viscosity and thermal conductivity by considering dispersive effects. The plasma motion outside the dissipative layer is described by the set of linear, ideal MHD equations. This set of equations can be reduced to Eq. (3.20) for the component of the velocity in the direction of the inhomogeneity ($u$) and the perturbation of total pressure ($P$). The wave motion in the anisotropic slow dissipative layer is governed by Eq. (3.60) for the quantity $q_c$, which is the dimensionless component of the velocity parallel to the equilibrium magnetic field defined by Eq. (3.58).

The dissipative layer is considered as a surface of discontinuity when solving Eq. (3.20) to describe the wave motion outside the dissipative layer. The jumps across the dissipative layer are given by Eqs. (3.57) and (3.65), thus providing the boundary conditions at the surface of discontinuity. In stark contrast to linear theory, the jump in $u$ is not solvable analytically, as it is given in terms of a infinite integral of $q_c$; which in turn is determined by Eq. (3.60). Since this equation has not been solved analytically we must solve Eqs (3.20) and (3.60) simultaneously when studying resonant slow waves that are nonlinear in the anisotropic dissipative layer.

From the fact that $q_c$ forms part of the jump, it is clear that dispersion must play a role in the wave absorption at the slow resonance. Since $q_c$ is found by solving Eq. (3.60) and as it contains a dispersive term, the overall form of $q_c$ is changed. This effect is likely to be small as it is the same order of magnitude as nonlinearity, which has been shown to have a decreasing effect on absorption (see, e.g. Ruderman et al., 1997c; Ballai et al., 1998a). We will tackle this very problem later in Chapter 6 of the present thesis.

# 4

# The validity of nonlinear resonant Alfvén waves in space plasmas

*In the approximation of linear dissipative MHD it can be shown that driven MHD waves in magnetic plasmas with high Reynolds number exhibit a near resonant behaviour if the frequency of the wave becomes equal to the local Alfvén (or slow) frequency of a magnetic surface. This near resonant behaviour is confined to a thin region, known as the dissipative layer, which embraces the resonant magnetic surface. Although driven MHD waves have small dimensionless amplitude far away from the resonant surface, this near-resonant behaviour in the dissipative layer may cause a breakdown of linear theory. In the present chapter, we aim to study the nonlinear effects in Alfvén dissipative layer. The method of simplified matched asymptotic expansions developed for nonlinear slow resonant waves is used to describe nonlinear effects inside the Alfvén dissipative layer. The nonlinear corrections to resonant waves in the Alfvén dissipative layer are derived and it is proved that at the Alfvén resonance (with isotropic / anisotropic dissipation) wave dynamics can be described by the linear theory with great accuracy. The results of the present chapter were published in Astronomy and Astrophysics (Clack et al., 2009b).*

*I have always believed that astrophysics should be the extrapolation of laboratory physics, that we must begin from the present universe and work our way backward to progressively more remote and uncertain epochs.*
**(Hannes Alfvén** 1908 – 1995**)**

## 4.1 Introduction

One particular aspect of the solar physics that has attracted much attention since the 1940s is the very high temperature of the solar corona compared with the much cooler lower regions of the solar atmosphere requiring the existence of some mechanism(s) which keeps the solar corona hot against the radiative cooling. One of the possible theories proposed is the transfer of omnipresent waves' energy into thermal energy by resonant absorption or resonant coupling of waves (see, e.g. Poedts et al., 1990a; Sakurai et al., 1991b; Goossens et al., 1995). Waves which were initially observed sporadically mainly in radio wavelengths (see, e.g. Kai and Takayanagi, 1973; Aschwanden et al., 1992) are now observed in abundance in all wavelengths, especially in (extreme) ultraviolet (see, e.g. DeForest and Gurman, 1998; Aschwanden et al., 1999a; Nakariakov et al., 1999; Robbrecht et al., 2001; King et al., 2003; Erdélyi and Taroyan, 2008; Mariska et al., 2008). Since the plasma is non-ideal, waves can lose their energy through transport processes, however, the time over which the waves dissipate their energy is far too long. In order to have an effective and localized energy conversion, the plasma must exhibit transversal inhomogeneities relative to the direction of the ambient magnetic field. According to the accepted wave theories, effective energy transfer between an energy carrying wave and the plasma occurs if the frequency of the wave matches one of the frequencies in the slow or Alfvén continua, i.e. at the slow or Alfvén resonances.

Given the complexity of the mathematical approach, most theories describing resonant waves are limited to the linear regime (see Sect. 2.5). Perturbations, in these theories, are considered to be just small deviations from an equilibrium despite the highly nonlinear character of MHD equations describing the dynamics of waves and the complicated interaction between waves and plasmas. Initial numerical investigations of resonant waves in a nonlinear limit (see, e.g. Ofman and Davila, 1995) unveiled that the account of nonlinearity introduces new physical effects which cannot be described in the linear framework. The first attempts to describe the nonlinear resonant waves analytically appeared after the papers by Ruderman et al. (1997c,d) which were followed by further analysis by, e.g. Ballai et al. (1998b); Ruderman (2000); Clack and Ballai (2008), however, all these investigations focused on the resonant slow waves only. These studies revealed that nonlinearity does affect the absorption of waves.

The present chapter analytically studies the validity of nonlinear resonant Alfvén wave. We will obtain governing equations using techniques made familiar in Chapter 3. Dissipation is a key ingredient of the problem of resonance. As mentioned in Sect. 2.5 and 2.7, dissipation removes singularities in mathematical solutions. From a physical point of view, dissipation is important as it is the mechanism which relaxes the accumulation of energy at the resonant surface and eventually contributes to the global process of heating.

## 4.2 Fundamental equations and assumptions

For describing mathematically the nonlinear resonant Alfvén waves we use the visco-resistive MHD equations. In spite of the presence of dissipation we use the adiabatic equation as an approximation of the energy equation. Numerical studies by Poedts et al. (1994) in linear MHD have shown that dissipation due to viscosity and finite electrical conductivity in the energy equation does not alter significantly the behaviour of resonant MHD waves in the driven problem.

We discussed in Sect. 2.4 that when the product of the ion (electron) gyrofrequency [$\omega_{i(e)}$] and

the ion (electron) collision time [$\tau_{i(e)}$] is much greater than one the viscosity and finite electrical conductivity become anisotropic and viscosity is given by the Braginskii viscosity tensor (see Sect. 2.4 for definition and Appendix B for derivation of dominant terms). The components of the viscosity tensor that remove the Alfvén singularity are the shear components. The parallel and perpendicular components of anisotropic finite electrical conductivity only differ by a factor of 2, therefore, we will consider only one of them without loss of generality.

The dynamics of waves in our model is described by the visco-resistive MHD equations given by Eqs (2.1)–(2.8) with $\mathcal{D}_\nu$ taking the form given in Eq. (2.30) and $\mathcal{L} = \overline{\mathbf{H}} = 0$. Note that even though anisotropy has been considered the Hall term has been neglected. We neglect the Hall term from the induction equation, which can be of the order of diffusion term in the solar corona, because the largest Hall terms in the perpendicular direction relative to the ambient magnetic field identically cancel. The components of the Hall term in the normal and parallel directions relative to the ambient magnetic field have no effect on the dynamics of Alfvén waves in dissipative layers, hence these too are neglected. For full details on the Hall term and the reasoning behind neglecting it we refer to Appendix A.

We adopt a physical set up identical to that in the Chapter 3 (see discussion in Sect. 3.2). However, instead of the resonant position being at $x_c$ (the slow resonant position), it is at the Alfvén resonant position $x = x_a$. The definition of the resonant position can now be written mathematically as

$$V = v_A\,(x_a)\cos\alpha, \tag{4.1}$$

In what follows we can take $x_a = 0$ without loss of generality. The perturbations of the physical quantities are defined by

$$\overline{\rho} = \rho_0 + \rho, \quad \overline{p} = p_0 + p, \quad \mathbf{B} = \mathbf{B}_0 + \mathbf{b}, \quad P = p + \frac{\mathbf{B}_0\cdot\mathbf{b}}{\mu_0} + \frac{\mathbf{b}^2}{2\mu_0}, \tag{4.2}$$

where $P$ is the perturbation of total pressure.

The dominant dynamics of resonant Alfvén waves, in linear MHD, resides in the components of the perturbed magnetic field and velocity that are perpendicular to the equilibrium magnetic field and to the $x-$direction. This dominant behaviour is created by an $x^{-1}$ singularity in the spatial solution of these quantities at the Alfvén resonance (Sakurai et al., 1991b; Goossens and Ruderman, 1995); these variables are known as *large variables*. The $x-$component of velocity, the components of magnetic field normal and parallel to the equilibrium magnetic field, plasma pressure and density are also singular, however, their singularity is proportional to $\ln|x|$. In addition, the quantities $P$ and the component of $\mathbf{v}$ that is parallel to the equilibrium magnetic field are regular; all these variables are called *small variables*.

The definition of the components of velocity and magnetic field that are in the $yz-$plane and are either parallel or perpendicular to the equilibrium magnetic field is supplied by Eq. (2.64). The characteristic scale of inhomogeneity ($l_{inh}$) and Reynolds numbers used in the present chapter were introduced in Sect. 2.6. The Reynolds numbers are defined by Eq. (2.55). In nonlinear theory, when studying resonant behaviour in the dissipative layer we must scale the dissipative coefficients (see, e.g. Ruderman et al., 1997d; Ballai et al., 1998b; Clack and Ballai, 2008). The overall general scaling to be applied is

$$\overline{\eta} = R_a^{-1}\eta, \quad \overline{\eta}_1 = R_a^{-1}\eta_1. \tag{4.3}$$

Linear theory predicts that the characteristic thickness of the dissipative layer ($l_{diss}$) is of the order of $l_{inh}R_a^{-1/3}$ and we assume that this is true in the nonlinear regime, too. Hence, we must introduce a stretching transversal coordinate ($\xi$) in the dissipative layer defined as

$$\xi = R_a^{1/3} x. \tag{4.4}$$

We can rewrite Eqs (2.1)–(2.8) in the scalar form as

$$V\frac{\partial \rho}{\partial \theta} - \frac{\partial(\rho_0 u)}{\partial x} - \rho_0 \frac{\partial w}{\partial \theta} = \frac{\partial(\rho u)}{\partial x} + \frac{\partial(\rho w)}{\partial \theta}, \tag{4.5}$$

$$\rho_0 V\frac{\partial u}{\partial \theta} - \frac{\partial P}{\partial x} + \frac{B_0 \cos\alpha}{\mu_0}\frac{\partial b_x}{\partial \theta} = \overline{\rho}\left(u\frac{\partial u}{\partial x} + w\frac{\partial w}{\partial \theta}\right) - \rho V\frac{\partial u}{\partial \theta} - \frac{b_x}{\mu_0}\frac{\partial b_x}{\partial x} - \frac{b_z}{\mu_0}\frac{\partial b_x}{\partial \theta} - \overline{\eta}_1\frac{\partial^2 u}{\partial x^2}, \tag{4.6}$$

$$\frac{\partial}{\partial \theta}\left(\rho_0 V v_\perp + P\sin\alpha + \frac{B_0\cos\alpha}{\mu_0}b_\perp\right) = \overline{\rho}\left(u\frac{\partial v_\perp}{\partial x} + w\frac{\partial v_\perp}{\partial \theta}\right) - \rho V\frac{\partial v_\perp}{\partial \theta} - \frac{b_x}{\mu_0}\frac{\partial b_\perp}{\partial x} - \frac{b_z}{\mu_0}\frac{\partial b_\perp}{\partial \theta} - \overline{\eta}_1\frac{\partial^2 v_\perp}{\partial x^2}, \tag{4.7}$$

$$\frac{\partial}{\partial \theta}\left(\rho_0 V v_\parallel - P\cos\alpha + \frac{B_0\cos\alpha}{\mu_0}b_\parallel\right) = \overline{\rho}\left(u\frac{\partial v_\parallel}{\partial x} + w\frac{\partial v_\parallel}{\partial \theta}\right) - \frac{b_x}{\mu_0}\frac{dB_0}{dx} - \rho V\frac{\partial v_\parallel}{\partial \theta} - \frac{b_x}{\mu_0}\frac{\partial b_\parallel}{\partial x} - \frac{b_z}{\mu_0}\frac{\partial b_\parallel}{\partial \theta} - 4\overline{\eta}_1\frac{\partial^2 v_\parallel}{\partial x^2}, \tag{4.8}$$

$$Vb_x + B_0 u\cos\alpha = wb_x - ub_z + \overline{\eta}\left(\frac{\partial b_x}{\partial \theta} - \frac{\partial b_z}{\partial x}\right), \tag{4.9}$$

$$\frac{\partial}{\partial \theta}\left(Vb_\perp + B_0 v_\perp\cos\alpha\right) = \frac{\partial(ub_\perp)}{\partial x} + \frac{\partial(wb_\perp)}{\partial \theta} - b_x\frac{\partial v_\perp}{\partial x} - b_z\frac{\partial v_\perp}{\partial \theta} - \overline{\eta}\nabla^2 b_\perp, \tag{4.10}$$

$$\frac{\partial}{\partial \theta}\left(Vb_\parallel + B_0 v_\parallel\cos\alpha\right) - \frac{\partial(B_0 u)}{\partial x} - B_0\frac{\partial w}{\partial \theta} = \frac{\partial(ub_\parallel)}{\partial x} + \frac{\partial(wb_\parallel)}{\partial \theta} - b_x\frac{\partial v_\parallel}{\partial x} - b_z\frac{\partial v_\parallel}{\partial \theta} - \overline{\eta}\nabla^2 b_\parallel, \tag{4.11}$$

$$V\left(\frac{\partial p}{\partial \theta} - c_S^2\frac{\partial \rho}{\partial \theta}\right) - u\left(\frac{dp_0}{dx} - c_S^2\frac{d\rho_0}{dx}\right) = \frac{1}{\rho_0}\left\{V\left(\gamma p\frac{\partial \rho}{\partial \theta} - \rho\frac{\partial p}{\partial \theta}\right) - w\left[\gamma\overline{p}\frac{\partial \rho}{\partial \theta} - \overline{p}\frac{\partial p}{\partial \theta}\right] + u\left[\rho\frac{dp_0}{dx} - \gamma p\frac{d\rho_0}{dx} + \overline{\rho}\frac{\partial p}{\partial x} - \gamma\overline{p}\frac{\partial \rho}{\partial x}\right]\right\} \tag{4.12}$$

$$P = p + \frac{1}{2\mu_0}\left(b_x^2 + b_\perp^2 + b_\parallel^2 + 2B_0 b_\parallel\right), \tag{4.13}$$

$$\frac{\partial b_x}{\partial x} + \frac{\partial b_z}{\partial \theta} = 0. \tag{4.14}$$

In the above equations $\nabla = (\partial/\partial x, 0, \partial/\partial\theta)$ and $w = v_\parallel\cos\alpha - v_\perp\sin\alpha$.

Equations (4.5)-(4.14) will be used throughout the rest of the chapter to derive the governing equation for the resonant Alfvén waves inside the dissipative layer and to find the nonlinear corrections.

## 4.3 The governing equation in the Alfvén dissipative layer

In order to derive the governing equation for wave motions in the Alfvén dissipative layer we employ the method of matched asymptotic expansions (see, e.g. Nayfeh, 1981; Bender and Országh, 1991). A simplified version of the method of matched asymptotic expansions is adopted here. This method was introduced in Sect. 2.7 and utilized in Chapter 3. To begin deriving the governing equation we refer back to Sect. 2.6. Here we introduced the nonlinearity parameters for different scenarios. In this case we need Eq. (2.57). This implies that we stretch the dissipative coefficients as described by Eq. (2.61). We do not rewrite the MHD equations as they are easily obtained from Eqs (4.5)–(4.14) by substitution of Eq. (2.61).

As discussed in Chapter 2, far away from the dissipative layer the amplitudes of perturbations are small. So we use linear ideal MHD equations in order to describe the wave motion. The full set of nonlinear dissipative MHD equations are used for describing wave motion inside the *anisotropic Alfvén* dissipative layer where the amplitudes can be large. We, therefore, look for solutions in the form of asymptotic expansions. The equilibrium quantities change only slightly across the dissipative layer so it is possible to approximate them by the first non-vanishing term in their Taylor series expansion with respect to $x$.

Before deriving the nonlinear governing equation we ought to make a note. In linear theory, perturbations of physical quantities are harmonic functions of $\theta$ and their mean values over a period are zero. In nonlinear theory, however, the perturbations of variables can have non-zero mean values as a result of nonlinear interaction of different harmonics. Due to the absorption of wave momentum, a mean shear flow is generated outside the dissipative layer (see, e.g. Ofman and Davila, 1995). This result is true for our analysis also and we will deal with this phenomenon in Chapter 5.

The first step in our mathematical description is the derivation of governing equations outside the anisotropic Alfvén dissipative layer where the dynamics is described by ideal ($\overline{\eta}_1 = \overline{\eta} = 0$) and linear MHD. We use the expansion form of Eq. (3.19). Since the wave motion is described by the ideal linear MHD equations we recover the governing equations from Sect. 2.7, namely Eq. (3.20), which has regular singularities at the Alfvén resonance. Hence, the solutions can be obtained in terms of Fröbenius series with respect to $x$ (for details see Sect. 2.7). The remaining variables can all be expressed in terms of $u^{(1)}$ and $P^{(1)}$. The form of these variables is given by Eqs (3.23)–(3.27).

As the characteristic scale of dissipation is of the order of $l_{inh}R_a^{-1/3}$ and we have assumed that $R_a \sim \epsilon^{-3/2}$ we obtain that the thickness of the dissipative layer is $l_{inh}R_a^{-1/3} = \mathcal{O}(\epsilon^{1/2}l_{inh})$, implying the introduction of a new stretched variable to replace the transversal coordinate in the dissipative layer, which is defined as $\xi = \epsilon^{-1/2}x$. Again, for brevity, Eqs (4.5)–(4.14) are not rewritten as they can be obtained by the substitution of Eq. (3.37) for all derivatives. The equilibrium quantities still depend on $x$, not $\xi$, (their expression is valid in a wider region than the characteristic thickness of the dissipative layer). All equilibrium quantities are expanded around the ideal resonant position ($x = 0$) as

$$f_0 \approx f_{0_a} + \epsilon^{1/2}\xi \left(\frac{df_0}{dx}\right)_a, \tag{4.15}$$

where $f_0$ is any equilibrium quantity and the subscript 'a' indicates that the equilibrium quantity is evaluated at the Alfvén resonant point.

We seek the solution to the set of equations obtained from Eqs (4.5)–(4.14) by the substitution of $\overline{\eta}_1 = \epsilon^{3/2}\eta_1$, $\overline{\eta} = \epsilon^{3/2}\eta$ and $x = \epsilon^{1/2}\xi$ into variables in the form of power series of $\epsilon$. These equations contain powers of $\epsilon^{1/2}$, so we use this quantity as an expansion parameter. To derive the form of the inner expansions of different quantities we have to analyze the outer solutions. First, since $v_\parallel$ and $P$ are regular at $x = 0$ we can write their inner expansions in the form of their outer expansions [Eq. (3.19)]. The amplitudes of large variables in the dissipative layer are of the order of $\epsilon^{1/2}$, so the inner expansion of the variables $v_\perp$ and $b_\perp$ is given by Eq. (3.39). The quantities $u$, $b_x$, $b_\parallel$, $p$ and $\rho$ behave as $\ln|x|$ in the vicinity of $x = 0$, which suggests that they have expansions with terms of the order of $\epsilon \ln \epsilon$ in the dissipative layer. Strictly speaking, the inner expansions of all variables have to contain terms proportional to $\epsilon \ln \epsilon$ and $\epsilon^{3/2} \ln \epsilon$ (see, e.g. Ruderman et al., 1997d). In the simplified version of matched asymptotic expansions we consider $\ln \epsilon$ as a quantity of the order of unity (see, e.g. Ballai et al., 1998b; Clack and Ballai, 2008). This enables us to write the inner expansions for $u$, $b_x$, $b_\parallel$, $p$ and $\rho$ in the form of Eq. (3.19).

We now substitute the expansion (3.19) for $P$, $u$, $b_x$, $b_\parallel$, $v_\parallel$, $p$ and $\rho$ and the expansion given by Eq. (3.39) for $v_\perp$ and $b_\perp$ into the set of equations obtained from Eqs (4.5)–(4.14) after substitution of $x = \epsilon^{1/2}\xi$. The first order approximation (terms proportional to $\epsilon$), yields a linear homogeneous system of equations for the terms with superscript '1'. The important result that follows from this set of equations is that

$$P^{(1)} = P^{(1)}(\theta), \tag{4.16}$$

that is $P^{(1)}$ does not change across the dissipative layer. This result parallels the result found in linear theory (see, e.g. Sakurai et al., 1991b; Goossens et al., 1995) and nonlinear theories of slow resonance (see, e.g. Ruderman et al., 1997d; Ballai et al., 1998b; Clack and Ballai, 2008). Subsequently, all remaining variables can be expressed in terms of $u^{(1)}$, $v_\perp^{(1)}$ and $P^{(1)}$ as

$$b_x^{(1)} = -\frac{B_{0_a}\cos\alpha}{V}u^{(1)}, \quad b_\perp^{(1)} = -\frac{B_{0_a}V}{v_{A_a}^2\cos\alpha}v_\perp^{(1)}, \quad v_\parallel^{(1)} = \frac{c_{S_a}^2}{v_{A_a}^2}\frac{\cos\alpha}{\rho_{0_a}V}P^{(1)}, \tag{4.17}$$

$$\frac{\partial b_\parallel^{(1)}}{\partial\theta} = \frac{B_{0_a}\left(v_{A_a}^2 - c_{S_a}^2\right)}{\rho_{0_a}v_{A_a}^4}\frac{dP^{(1)}}{d\theta} + \frac{u^{(1)}}{V}\left(\frac{dB_0}{dx}\right)_a, \tag{4.18}$$

$$\frac{\partial p^{(1)}}{\partial\theta} = \frac{c_{S_a}^2}{v_{A_a}^2}\frac{dP^{(1)}}{d\theta} - \frac{u^{(1)}}{V}\frac{B_{0_a}}{\mu_0}\left(\frac{dB_0}{dx}\right)_a, \quad \frac{\partial\rho^{(1)}}{\partial\theta} = \frac{1}{v_{A_a}^2}\frac{dP^{(1)}}{d\theta} + \frac{u^{(1)}}{V}\left(\frac{d\rho_0}{dx}\right)_a. \tag{4.19}$$

The subscript '$a$' indicates that the equilibrium quantity has been calculated at $x = x_a = 0$. In addition, the relation that connects the normal and perpendicular components of velocity is

$$\frac{\partial u^{(1)}}{\partial\xi} - \sin\alpha\frac{\partial v_\perp^{(1)}}{\partial\theta} = 0. \tag{4.20}$$

In the second order approximation we only use the expressions obtained from Eqs (4.7) and (4.10)[1]. Employing Eqs (4.17)–(4.20), we replace the variables in the second order approximation which have superscript '1'. The equations obtained in the second order are

$$\frac{\partial P^{(1)}}{\partial\theta}\sin\alpha + \frac{B_{0_a}\cos\alpha}{\mu_0}\frac{\partial b_\perp^{(2)}}{\partial\theta} + V\rho_{0_a}\frac{\partial v_\perp^{(2)}}{\partial\theta} = \left[\frac{B_{0_a}V}{\mu_0 v_{A_a}^2}\left(\frac{dB_0}{dx}\right)_a - V\left(\frac{d\rho_0}{dx}\right)_a\right]\xi\frac{\partial v_\perp^{(1)}}{\partial\theta} - \eta_1\frac{\partial^2 v_\perp^{(1)}}{\partial\xi^2}, \tag{4.21}$$

[1]We only need these two equations because the dominant dynamics when studying resonant Alfvén waves are in the perpendicular components of magnetic field and velocity.

$$V\frac{\partial b_\perp^{(2)}}{\partial\theta} + B_{0_a}\cos\alpha\frac{\partial v_\perp^{(2)}}{\partial\theta} + \cos\alpha\left(\frac{dB_0}{dx}\right)_a \xi\frac{\partial v_\perp^{(1)}}{\partial\theta} = \eta\frac{B_{0_a}V}{v_{A_a}^2\cos\alpha}\frac{\partial^2 v_\perp^{(1)}}{\partial\xi^2}. \tag{4.22}$$

Once the variables with superscript '2' have been eliminated from the above two equations, the governing equation for resonant Alfvén waves inside the dissipative layer is derived as

$$\Delta_a\xi\frac{\partial v_\perp^{(1)}}{\partial\theta} + \frac{V}{\rho_{0_a}}(\eta_1 + \rho_{0_a}\eta)\frac{\partial^2 v_\perp^{(1)}}{\partial\xi^2} = -\frac{V\sin\alpha}{\rho_{0_a}}\frac{dP^{(1)}}{d\theta}, \tag{4.23}$$

where

$$\Delta_a = -\cos^2\alpha\left(\frac{dv_A^2}{dx}\right)_a.$$

It is clear that Eq. (4.23) does not contain nonlinear terms despite considering the full MHD system of equations. This result is in stark contrast with the results obtained for nonlinear slow resonance where the governing equation was found to be always nonlinear (see, e.g. Ruderman et al., 1997d; Ballai et al., 1998b; Clack and Ballai, 2008). The governing equation (4.23) suggests that resonant Alfvén waves can be described by the linear theory unless their amplitudes inside the dissipative layer is of the order of unity.

As the quadratic nonlinear terms cancel each other out, it is natural to take into account cubic nonlinearity (the system of MHD equations contain cubic nonlinear terms), where the nonlinearity parameter is defined as Eq. (2.59) and the stretched dissipative coefficients are given by Eq. (2.63). However, despite the higher order nonlinearity we arrive at the identical compatibility equations (4.21) and (4.22). This leads to a similar governing equation to the one derived for quadratic nonlinearity (4.23). We do not write out the calculations here as they are identical to the ones carried out for the quadratic nonlinearity, just with different stretched dissipative coefficients. These results require finding an explanation to the linear behaviour of waves inside the dissipative layer. The following section will be devoted to the study of nonlinear corrections in the Alfvén dissipative layer.

## 4.4 Nonlinear corrections in the Alfvén dissipative layer

Since we have assumed that waves have small dimensionless amplitude outside the dissipative layer, we will concentrate only on the solutions *inside* the anisotropic Alfvén dissipative layer. In our analysis we use the assumptions and equations presented in Sect. 4.3, however, we will not impose any relation between $\epsilon$ and $R$. Equations (4.3) and (4.4) will be used to define the scaled dissipative coefficients and stretching transversal coordinate in the dissipative layer. For simplicity we denote $\widetilde{\beta} = R_a^{-1/3}$. This means that our scaled dissipative coefficients and stretched transversal coordinate become

$$\overline{\eta}_1 = \widetilde{\beta}^3\eta_1, \quad \overline{\eta} = \widetilde{\beta}^3\eta, \quad \xi = \widetilde{\beta}^{-1}x. \tag{4.24}$$

The first step to accomplish our task is to rewrite Eqs (4.5)–(4.14) by substituting

$$\frac{\partial}{\partial x} = \widetilde{\beta}^{-1}\frac{\partial}{\partial\xi}, \quad \frac{\partial}{\partial z} = \frac{\partial}{\partial\theta}, \quad \text{and} \quad \frac{\partial}{\partial t} = -V\frac{\partial}{\partial\theta}. \tag{4.25}$$

All equilibrium quantities (which are still dependent on $x$, not $\xi$) will be approximated by the first non-vanishing term of their Taylor expansion [see, Eq. (4.15)].

The substitution of Eqs (4.15), (4.24)–(4.25) will transform Eqs (4.5)–(4.14) into

$$\rho_0\frac{\partial u}{\partial\xi}+\widetilde{\beta}u\frac{d\rho_0}{dx}+\frac{\partial(\rho u)}{\partial\xi}-\widetilde{\beta}\frac{\partial}{\partial\theta}\left[\overline{p}\,(V-w)\right]=0, \tag{4.26}$$

$$\frac{1}{\overline{\rho}}\left[\frac{\partial P}{\partial\xi}-\frac{b_x}{\mu_0}\frac{\partial b_x}{\partial\xi}-\frac{\widetilde{\beta}}{\mu_0}\left(B_0\cos\alpha+b_z\right)\frac{\partial b_x}{\partial\theta}\right]=\widetilde{\beta}\,(V-w)\frac{\partial u}{\partial\theta}-u\frac{\partial u}{\partial\xi}+\widetilde{\beta}^2\frac{\eta_1}{\rho_0}\frac{\partial^2 u}{\partial\xi^2}, \tag{4.27}$$

$$\frac{1}{\overline{\rho}}\left[\widetilde{\beta}\frac{\partial P}{\partial\theta}\sin\alpha+\frac{b_x}{\mu_0}\frac{\partial b_\perp}{\partial\xi}+\frac{\widetilde{\beta}}{\mu_0}\left(B_0\cos\alpha+b_z\right)\frac{\partial b_\perp}{\partial\theta}\right]=-\widetilde{\beta}\,(V-w)\frac{\partial v_\perp}{\partial\theta}+u\frac{\partial v_\perp}{\partial\xi}-\widetilde{\beta}^2\frac{\eta_1}{\rho_0}\frac{\partial^2 v_\perp}{\partial\xi^2}, \tag{4.28}$$

$$\frac{1}{\overline{\rho}}\left[\widetilde{\beta}\frac{\partial P}{\partial\theta}\cos\alpha-\frac{b_x}{\mu_0}\frac{\partial b_\parallel}{\partial\xi}-\frac{\widetilde{\beta}}{\mu_0}\left(B_0\cos\alpha+b_z\right)\frac{\partial b_\parallel}{\partial\theta}-\frac{\widetilde{\beta}}{\mu_0}\frac{dB_0}{dx}b_x\right]=$$
$$\widetilde{\beta}\,(V-w)\frac{\partial v_\parallel}{\partial\theta}-u\frac{\partial v_\parallel}{\partial\xi}+\widetilde{\beta}^2\frac{4\eta_1}{\rho_0}\frac{\partial^2 v_\parallel}{\partial\xi^2}, \tag{4.29}$$

$$\widetilde{\beta}\,(V-w)\frac{\partial b_x}{\partial\theta}+\widetilde{\beta}\left(B_0\cos\alpha+b_z\right)\frac{\partial u}{\partial\theta}+\widetilde{\beta}^2\eta\left(\frac{\partial^2}{\partial\xi^2}+\widetilde{\beta}^2\frac{\partial^2}{\partial\theta^2}\right)b_x=0, \tag{4.30}$$

$$\widetilde{\beta}\,(V-w)\frac{\partial b_\perp}{\partial\theta}-u\frac{\partial b_\perp}{\partial\xi}-b_\perp\left(\frac{\partial u}{\partial\xi}+\widetilde{\beta}\frac{\partial v_\parallel}{\partial\theta}\cos\alpha\right)+b_x\frac{\partial v_\perp}{\partial\xi}$$
$$+\widetilde{\beta}\left(B_0+b_\parallel\right)\frac{\partial v_\perp}{\partial\theta}\cos\alpha+\widetilde{\beta}^2\eta\left(\frac{\partial^2}{\partial\xi^2}+\widetilde{\beta}^2\frac{\partial^2}{\partial\theta^2}\right)b_\perp=0, \tag{4.31}$$

$$\widetilde{\beta}\,(V-w)\frac{\partial b_\parallel}{\partial\theta}-u\left(\frac{\partial b_\parallel}{\partial\xi}+\widetilde{\beta}\frac{dB_0}{dx}\right)+b_x\frac{\partial v_\parallel}{\partial\xi}-\widetilde{\beta}b_\perp\frac{\partial v_\parallel}{\partial\theta}$$
$$-\left(B_0+b_\parallel\right)\left(\frac{\partial u}{\partial\xi}-\widetilde{\beta}\frac{\partial v_\perp}{\partial\theta}\sin\alpha\right)+\widetilde{\beta}^2\eta\left(\frac{\partial^2}{\partial\xi^2}+\widetilde{\beta}^2\frac{\partial^2}{\partial\theta^2}\right)b_\parallel=0, \tag{4.32}$$

$$\left[\widetilde{\beta}\,(V-w)\frac{\partial}{\partial\theta}-u\frac{\partial}{\partial\xi}\right]\left(\frac{\overline{p}}{\overline{\rho}^\gamma}\right)=0, \tag{4.33}$$

$$P=p+\frac{B_0}{\mu_0}b_\parallel+\frac{1}{2\mu_0}\left(b_x^2+b_\perp^2+b_\parallel^2\right). \tag{4.34}$$

There is only one condition we need to impose when deriving the nonlinear corrections to resonant Alfvén waves in the anisotropic dissipative layer. This must be imported from the linear theory which predicts that in the dissipative layer 'large' variables have dimensionless amplitude of the order of $\epsilon R^{1/3}$ (see Sect. 2.5). We assume that the dimensionless amplitudes of the linear approximation of 'large' variables ($v_\perp$ and $b_\perp$) in the dissipative layer are small[2], such that

$$\epsilon\ll R_a^{-1/3}(=\widetilde{\beta}). \tag{4.35}$$

This condition ensures that the dimensionless amplitude of oscillations of large variables remains less than unity inside the dissipative layer. From a naive point of view the linear theory is applicable as soon as the oscillation amplitude is small. The example of slow resonant waves clearly

[2]This condition is critical. If we have the dimensionless amplitude of large variables inside the dissipative layer greater than unity our asymptotic analysis breaks down.

shows that this is not the case. The nonlinear effects become important in the isotropic slow dissipative layer as soon as $\epsilon \sim R_c^{-2/3}$, i.e. as soon as the oscillation amplitude in the dissipative layer, which is of the order of $\epsilon R^{1/3}$, is of the order of $R_c^{-1/3} \ll 1$. For example, in the corona perturbations with dimensionless amplitudes less than $10^{-4}$ can be considered by this theory. From Eq. (2.57) we would expect to see quadratic nonlinearity appear for waves with dimensionless amplitudes larger than $10^{-8}$ and from Eq. (2.59) we would expect to see cubic nonlinearity appear for waves with dimensionless amplitudes larger than $10^{-6}$. If we take $\epsilon \approx R_a^{-1/3}$ we find that inside the dissipative layer we have dimensionless amplitudes of the order of unity. This causes a breakdown in our theory, and therefore another approach would have to be adopted. At this time we do not know of an analytical study which can carry out this task without considering the full nonlinear MHD equations throughout the domain.

We now assume that all perturbations can be written as a regular asymptotic expansion of the form

$$\overline{f} = \overline{f}_0(x) + \epsilon \overline{f}_1(\xi, \theta) + \epsilon^2 \overline{f}_2(\xi, \theta) + \dots, \tag{4.36}$$

where $\overline{f}_0(x)$ represents the equilibrium value. Substitution of expansion (4.36) into the system (4.26)–(4.34) leads to a system of equations which contains the small parameter $\widetilde{\beta}$. This observation inspires us to look for the solution in the form of expansions with respect to $\widetilde{\beta}$. In order to cast large and small variables in this description we are going to use the following expansion for small variables ($u$, $b_x$, $v_\parallel$, $b_\parallel$, $\rho$, $p$ and $P$)

$$\overline{g}_1 = \overline{g}_1^{(1)} + \widetilde{\beta} \overline{g}_1^{(2)} + \dots, \tag{4.37}$$

while large variables ($v_\perp$ and $b_\perp$) will be expanded according to

$$\overline{h}_1 = \widetilde{\beta}^{-1} \overline{h}_1^{(1)} + \overline{h}_1^{(2)} + \dots. \tag{4.38}$$

The bar notation is used here to distinguish between these expansions and the expansions used in the previous sections and chapters. From this point on we drop the bar notation.

Substituting Eqs (4.37), (4.38) into the system (4.26)–(4.34), taking terms proportional to $\epsilon$ and then only retaining terms with the lowest power of $\widetilde{\beta}$, results in the set of linear equations

$$\rho_0 \frac{\partial v_{\perp 1}^{(1)}}{\partial \theta} \sin\alpha - \rho_0 \frac{\partial u_1^{(1)}}{\partial \xi} = 0, \tag{4.39}$$

$$\frac{\partial P_1^{(1)}}{\partial \xi} = 0, \tag{4.40}$$

$$\rho_0 V \frac{\partial v_{\perp 1}^{(1)}}{\partial \theta} + \frac{B_0 \cos\alpha}{\mu_0} \frac{\partial b_{\perp 1}^{(1)}}{\partial \theta} = 0, \tag{4.41}$$

$$\frac{\partial P_1^{(1)}}{\partial \theta} \cos\alpha - \rho_0 V \frac{\partial v_{\parallel 1}^{(1)}}{\partial \theta} - \frac{b_{x1}^{(1)}}{\mu_0} \left( \frac{dB_0}{dx} \right) - \frac{B_0 \cos\alpha}{\mu_0} \frac{\partial b_{\parallel 1}^{(1)}}{\partial \theta} = 0, \tag{4.42}$$

$$V \frac{\partial b_{x1}^{(1)}}{\partial \theta} + B_0 \cos\alpha \frac{\partial u_1^{(1)}}{\partial \theta} = 0, \tag{4.43}$$

$$V \frac{\partial b_{\perp 1}^{(1)}}{\partial \theta} + B_0 \cos\alpha \frac{\partial v_{\perp 1}^{(1)}}{\partial \theta} = 0, \tag{4.44}$$

$$B_0 \frac{\partial u_1^{(1)}}{\partial \xi} - B_0 \sin\alpha \frac{\partial v_{\perp 1}^{(1)}}{\partial \theta} = 0, \tag{4.45}$$

$$\rho_0 V \frac{\partial p_1^{(1)}}{\partial \theta} - \rho_0 c_S^2 V \frac{\partial \rho_1^{(1)}}{\partial \theta} + \rho_0 u_1^{(1)} \left[ c_S^2 \left( \frac{d\rho_0}{dx} \right) - \left( \frac{dp_0}{dx} \right) \right] = 0, \tag{4.46}$$

$$P_1^{(1)} - p_1^{(1)} - \frac{B_0}{\mu_0} b_{\parallel 1}^{(1)} = 0. \tag{4.47}$$

We have dropped the notation of the subscript 'a' but, all equilibrium quantities are still calculated at $x = 0$.

Using these equations we can express all dependent variables in terms of $u_1^{(1)}$, $v_{\perp 1}^{(1)}$ and $P_1^{(1)}$,

$$b_{x1}^{(1)} = -\frac{B_0 \cos\alpha}{V} u_1^{(1)}, \quad b_{\perp 1}^{(1)} = -\frac{B_0 V}{v_A^2 \cos\alpha} v_{\perp 1}^{(1)}, \quad v_{\parallel 1}^{(1)} = \frac{c_S^2}{v_A^2} \frac{\cos\alpha}{\rho_0 V} P_1^{(1)}, \tag{4.48}$$

$$\frac{\partial b_{\parallel 1}^{(1)}}{\partial \theta} = \frac{B_0 \left( v_A^2 - c_S^2 \right)}{\rho_0 v_A^4} \frac{dP_1^{(1)}}{d\theta} + \frac{u_1^{(1)}}{V} \left( \frac{dB_0}{dx} \right), \tag{4.49}$$

$$\frac{\partial p_1^{(1)}}{\partial \theta} = \frac{c_S^2}{v_A^2} \frac{dP_1^{(1)}}{d\theta} - \frac{u_1^{(1)}}{V} \frac{B_0}{\mu_0} \left( \frac{dB_0}{dx} \right), \quad \frac{\partial \rho_1^{(1)}}{\partial \theta} = \frac{1}{v_A^2} \frac{dP_1^{(1)}}{d\theta} + \frac{u_1^{(1)}}{V} \left( \frac{d\rho_0}{dx} \right). \tag{4.50}$$

It follows from Eq. (4.40) that

$$P_1^{(1)} = P_1^{(1)}(\theta). \tag{4.51}$$

Finally, we obtain the relation between $u_1^{(1)}$ and $v_{\perp 1}^{(1)}$,

$$\frac{\partial u_1^{(1)}}{\partial \xi} = \frac{\partial v_{\perp 1}^{(1)}}{\partial \theta} \sin\alpha. \tag{4.52}$$

Note that Eqs (4.48)–(4.52) are formally identical to Eqs (4.17)–(4.20) for the linear approximation in Sect. 4.3. This is not surprising as both methods are designed to replicate linear theory in the first order approximation.

Now that the first order terms are known we can proceed to derive the second and third order approximations with respect to $\epsilon$ [i.e. terms from the expansion of Eqs (4.26)–(4.34) that are proportional to $\epsilon^2$ and $\epsilon^3$, respectively]. First, we write out the second order approximations and substitute for all first order terms [i.e. terms of the form $f_1^{(1)}$] using Eqs (4.48)–(4.52). Secondly, we find (by solving the inhomogeneous system) the expansions of second order terms (terms with *subscript* '2'). Thirdly, we derive the second order relations between all variables, similar to the ones obtained in the first order approximation.

The equations representing the second order approximation with respect to $\epsilon$ (with variables in the first order substituted) are

$$\rho_0 \frac{\partial u_2}{\partial \xi} + \widetilde{\beta} \left[ \xi \left( \frac{d\rho_0}{dx} \right) \frac{\partial u_2}{\partial \xi} - V \frac{\partial \rho_2}{\partial \theta} + \rho_0 \left( \frac{\partial v_{\parallel 2}}{\partial \theta} \cos\alpha - \frac{\partial v_{\perp 2}}{\partial \theta} \sin\alpha \right) + \left( \frac{d\rho_0}{dx} \right) u_2 \right] = \frac{v_{\perp 1}^{(1)}}{v_A^2} \frac{dP_1^{(1)}}{d\theta} \sin\alpha + \mathcal{O}(\widetilde{\beta}), \tag{4.53}$$

$$\frac{\partial P_2}{\partial \xi} - \widetilde{\beta} \left[ \rho_0 V \frac{\partial u_2}{\partial \theta} + \frac{B_0 \cos\alpha}{\mu_0} \frac{\partial b_{x2}}{\partial \theta} \right] = \mathcal{O}(\widetilde{\beta}), \tag{4.54}$$

$$\frac{\partial P_2}{\partial\theta}\sin\alpha+\rho_0 V\frac{\partial v_{\perp 2}}{\partial\theta}+\frac{B_0\cos\alpha}{\mu_0}\frac{\partial b_{\perp 2}}{\partial\theta}+\widetilde{\beta}\left\{\xi\left[V\left(\frac{d\rho_0}{dx}\right)\frac{\partial v_{\perp 2}}{\partial\theta}+\frac{\cos\alpha}{\mu_0}\left(\frac{dB_0}{dx}\right)\frac{\partial b_{\perp 2}}{\partial\theta}\right]+\eta_1\frac{\partial^2 v_{\perp 2}}{\partial\xi^2}\right\}=\mathcal{O}(\widetilde{\beta}^{-1}),\quad(4.55)$$

$$\frac{\partial P_2}{\partial\theta}\cos\alpha-\rho_0 V\frac{\partial v_{\parallel 2}}{\partial\theta}-\frac{b_{x2}}{\mu}\left(\frac{dB_0}{dx}\right)-\frac{B_0\cos\alpha}{\mu_0}\frac{\partial b_{\parallel 2}}{\partial\theta}-\widetilde{\beta}\left\{4\eta_1\frac{\partial^2 v_{\parallel 2}}{\partial\xi^2}+\xi\left[V\left(\frac{d\rho_0}{dx}\right)\frac{\partial v_{\parallel 2}}{\partial\theta}+\frac{\cos\alpha}{\mu_0}\left(\frac{dB_0}{dx}\right)\frac{\partial b_{\parallel 2}}{\partial\theta}\right]\right\}=\widetilde{\beta}^{-1}\left[\frac{\cos\alpha\sin\alpha}{V}v_{\perp 1}^{(1)}\frac{dP_1^{(1)}}{d\theta}\right]+\mathcal{O}(1),\quad(4.56)$$

$$V\frac{\partial b_{x2}}{\partial\theta}+B_0\cos\alpha\frac{\partial u_2}{\partial\theta}+\widetilde{\beta}\left[\eta\frac{\partial^2 b_{x2}}{\partial\xi^2}+\xi\cos\alpha\left(\frac{dB_0}{dx}\right)\frac{\partial u_2}{\partial\theta}\right]=\mathcal{O}(1),\quad(4.57)$$

$$V\frac{\partial b_{\perp 2}}{\partial\theta}+B_0\cos\alpha\frac{\partial v_{\perp 2}}{\partial\theta}+\widetilde{\beta}\left[\eta\frac{\partial^2 b_{\perp 2}}{\partial\xi^2}+\xi\cos\alpha\left(\frac{dB_0}{dx}\right)\frac{\partial v_{\perp 2}}{\partial\theta}\right]=\mathcal{O}(\widetilde{\beta}^{-1}),\quad(4.58)$$

$$B_0\frac{\partial u_2}{\partial\xi}+\widetilde{\beta}\left\{\left[u_2+\xi\frac{\partial u_2}{\partial\xi}\right]\left(\frac{dB_0}{dx}\right)-B_0\sin\alpha\frac{\partial v_{\perp 2}}{\partial\theta}-V\frac{\partial b_{\parallel 2}}{\partial\theta}\right\}=\frac{B_0\sin\alpha}{\rho_0 v_A^2}v_{\perp 1}^{(1)}\frac{dP_1^{(1)}}{d\theta}+\mathcal{O}(\widetilde{\beta}),\quad(4.59)$$

$$\rho_0 V\frac{\partial p_2}{\partial\theta}-\rho_0 c_S^2 V\frac{\partial\rho_2}{\partial\theta}+\rho_0 u_2\left[c_S^2\left(\frac{d\rho_0}{dx}\right)-\left(\frac{dp_0}{dx}\right)\right]=\mathcal{O}(\widetilde{\beta}^{-1}),\quad(4.60)$$

$$P_2-p_2-\frac{B_0}{\mu_0}b_{\parallel 2}+\widetilde{\beta}\left[\frac{\xi}{\mu_0}\left(\frac{dB_0}{dx}\right)b_{\parallel 2}\right]=\widetilde{\beta}^{-2}\left[\frac{\rho_0}{2}{v_{\perp 1}^{(1)}}^2\right]+\mathcal{O}(\widetilde{\beta}^{-1}).\quad(4.61)$$

It is clear that nonlinear terms appear from this order of approximation and they are expressed in terms of variables obtained in the first order. The analysis of the system of Eqs (4.53)–(4.61) reveals that the expansions with respect to $\widetilde{\beta}$ has to be written in the form

$$g_2=\widetilde{\beta}^{-1}g_2^{(1)}+g_2^{(2)}+\widetilde{\beta}g_2^{(3)}+\ldots,\quad(4.62)$$

for $u_2$, $b_{x2}$, $v_{\perp 2}$, $b_{\perp 2}$ and $P_2$ and

$$h_2=\widetilde{\beta}^{-2}h_2^{(1)}+\widetilde{\beta}^{-1}h_2^{(2)}+h_2^{(3)}+\ldots,\quad(4.63)$$

for $v_{\parallel 2}$, $b_{\parallel 2}$, $p_2$ and $\rho_2$.

Here we need to make a note. It follows from Eqs (4.62) and (4.63) that the ratio of $\rho_2$ to $\rho_1$ is of the order of $\epsilon\widetilde{\beta}^{-2}$, and the same is true for $v_{\parallel 2}$, $b_{\parallel 2}$ and $p_2$. It seems to be inconsistent with the regular perturbation method where it is assumed that the next order approximation is always smaller than the previous one. However, this problem is only apparent. To show this we need to clarify the exact mathematical meaning of the statement "in the asymptotic expansion each subsequent term is much smaller than the previous one". To do this we introduce the nine-dimensional vector $\mathbf{U}=\left(u,v_\parallel,v_\perp,b_x,b_\parallel,b_\perp,P,p,\rho\right)$ and consider it as an element of a Banach space[3]. The norm in this space can be introduced in different ways. One possibility is

$$||\mathbf{U}||=\int_0^L d\theta\int_{-\infty}^{\infty}|\mathbf{U}|\,d\xi,\quad(4.64)$$

[3]We choose a Banach space because it is a vector space which has a norm such that every Cauchy sequence has a limit within the space.

where L is the period. The asymptotic expansion in the dissipative layer [Eq. (4.36)] can be rewritten as $\mathbf{U} = \mathbf{U}_0 + \epsilon\mathbf{U}_1 + \epsilon^2\mathbf{U}_2 + \ldots$. Then the mathematical formulation of the statement "each subsequent term is much smaller than the previous one" is $\|\mathbf{U}_{n+1}\| \ll \|\mathbf{U}_n\|$, $n = 1, 2, \ldots$. It is straightforward to verify that [in accordance with Eqs (4.37), (4.38), (4.62) and (4.63)] $\|\mathbf{U}_2\| \ll \|\mathbf{U}_1\|$.

Once the expansions (4.62) and (4.63) are substituted into Eqs (4.53)–(4.61), we can express the variables in this order of approximation as

$$b_{x2}^{(1)} = -\frac{B_0 \cos\alpha}{V} u_2^{(1)}, \quad b_{\|2}^{(1)} = -\frac{B_0}{2v_A^2} {v_{\perp 1}^{(1)}}^2, \quad v_{\|2}^{(1)} = \frac{\cos\alpha}{2V} {v_{\perp 1}^{(1)}}^2, \tag{4.65}$$

$$b_{\perp 2}^{(1)} = v_{\perp 2}^{(1)} = 0, \quad p_2^{(1)} = \rho_2^{(1)} = 0. \tag{4.66}$$

For the total pressure we obtain that

$$\frac{\partial P_2^{(1)}}{\partial \xi} = 0 \Longrightarrow P_2^{(1)} = P_2^{(1)}(\theta). \tag{4.67}$$

In addition, we obtain that the equation which determines $u_2^{(1)}$ is

$$\frac{\partial u_2^{(1)}}{\partial \xi} = -\frac{\cos^2\alpha}{V} v_{\perp 1}^{(1)} \frac{\partial v_{\perp 1}^{(1)}}{\partial \theta}. \tag{4.68}$$

Since the large variables in this order of approximation are $v_{\|2}$ and $b_{\|2}$, we can deduce that the linear order of approximation of resonant Alfvén waves in the dissipative layer excite *magnetoacoustic* modes in the second order of approximation. The excitation comes from the nonlinear term found in the second order approximation of the pressure equation, this drives the parallel components of the velocity and magnetic field perturbations. Since we are focussed on the Alfvén resonance only, these waves are not resonant. These waves act to cancel the very small pressure and density perturbations created by the first order approximation.

We now calculate the third order approximation with respect to $\epsilon$. On analyzing the third order system of equations we deduce that the large variables in this order of approximation are Alfvénic ($v_{\perp 3}^{(1)}$, $b_{\perp 3}^{(1)}$), so we only need the perpendicular components of momentum and induction equations given by Eqs (4.28) and (4.31), respectively. First, since some of the first order approximation terms contribute to the third order approximation in integral form we must introduce a new notation

$$U_1^{(1)} = \int u_1^{(1)} d\theta. \tag{4.69}$$

The third order approximation of the perpendicular component of momentum is

$$\begin{aligned} \frac{\partial P_3}{\partial \theta}\sin\alpha + \rho_0 V \frac{\partial v_{\perp 3}}{\partial \theta} + \frac{B_0\cos\alpha}{\mu_0}\frac{\partial b_{\perp 3}}{\partial \theta} + \widetilde{\beta}\left\{\xi\left[V\left(\frac{d\rho_0}{dx}\right)\frac{\partial v_{\perp 3}}{\partial \theta} + \frac{\cos\alpha}{\mu_0}\left(\frac{dB_0}{dx}\right)\frac{\partial b_{\perp 3}}{\partial \theta}\right]\right. \\ \left. + \eta_1 \frac{\partial^2 v_{\perp 3}}{\partial \xi^2}\right\} = \widetilde{\beta}^{-2}\left\{\frac{\partial v_{\perp 1}^{(1)}}{\partial \xi}\left[\frac{u_1^{(1)} P_1^{(1)}}{v_A^2} + \frac{u_1^{(1)} U_1^{(1)}}{V}\left(\frac{d\rho_0}{dx}\right)\right]\right\} + \mathcal{O}(\widetilde{\beta}^{-1}), \end{aligned} \tag{4.70}$$

while the perpendicular component of magnetic induction equation is

$$V\frac{\partial b_{\perp 3}}{\partial \theta} + B_0\cos\alpha\frac{\partial v_{\perp 3}}{\partial \theta} + \widetilde{\beta}\left[\eta\frac{\partial^2 b_{\perp 3}}{\partial \xi^2} + \xi\cos\alpha\left(\frac{dB_0}{dx}\right)\frac{\partial v_{\perp 3}}{\partial \theta}\right] = \mathcal{O}(\widetilde{\beta}^{-2}), \tag{4.71}$$

Note that in obtaining the third order approximations we have employed all the relations we have for variables in the first and second order of approximation.

Equations (4.70) and (4.71) clearly show that the nonlinear terms on the right-hand sides do not cancel. This implies that the expansion of $v_{\perp 3}$ and $b_{\perp 3}$ should be of the form

$$h_3 = \widetilde{\beta}^{-3} h_3^{(1)} + \widetilde{\beta}^{-2} h_3^{(2)} + \widetilde{\beta}^{-1} h_3^{(3)} + \dots . \tag{4.72}$$

We should state, for completeness, that if we derive the third order approximation for all the Eqs (4.26)-(4.34) we obtain the expansions for $u_3$, $b_{x3}$, $v_{\parallel 3}$, $b_{\parallel 3}$, $p_3$, $\rho_3$ and $P_3$ to be

$$g_3 = \widetilde{\beta}^{-2} g_3^{(1)} + \widetilde{\beta}^{-1} g_3^{(2)} + g_3^{(3)} + \dots . \tag{4.73}$$

The expansions calculated for all the variables can now be collected together and we can write the expansions for 'large' and 'small' variables in the dissipative layer when studying resonant Alfvén waves. Large variables ($v_\perp$ and $b_\perp$) have the expansion

$$h = \left(\frac{\epsilon}{\widetilde{\beta}}\right) h_1^{(1)} + \epsilon \left(\frac{\epsilon}{\widetilde{\beta}}\right) h_2^{(1)} + \left(\frac{\epsilon}{\widetilde{\beta}}\right)^3 h_3^{(1)} + \dots , \tag{4.74}$$

and the expansion of small variables ($u$, $b_x$, $v_\parallel$, $b_\parallel$, $p$, $\rho$ and $P$) is defined as

$$g = \epsilon g_1^{(1)} + \left(\frac{\epsilon}{\widetilde{\beta}}\right)^2 g_2^{(1)} + \epsilon \left(\frac{\epsilon}{\widetilde{\beta}}\right)^2 g_3^{(1)} + \dots . \tag{4.75}$$

Since Eq. (4.35) is the only condition enforced in the dissipative layer, we can state that

$$1 > \left(\frac{\epsilon}{\widetilde{\beta}}\right) > \left(\frac{\epsilon}{\widetilde{\beta}}\right)^2 > \left(\frac{\epsilon}{\widetilde{\beta}}\right)^3 > \dots . \tag{4.76}$$

Therefore, since both Eqs (4.74) and (4.75) contain successive higher powers of the parameter $\epsilon/\widetilde{\beta}$ we can deduce that [considering Eq. (4.76)] higher orders of approximation of large and small variables become increasingly insignificant in comparison to the linear order of approximation. So resonant Alfvén waves in the dissipative layer can be described accurately by linear theory if condition (4.35) is satisfied.

## 4.5 Conclusions

In the present chapter we have investigated the nonlinear behaviour of resonant Alfvén waves in the dissipative layer in one-dimensional planar geometry in plasmas with anisotropic dissipative coefficients, a situation applicable to solar coronal conditions. The plasma motion outside the dissipative layer is described by the set of linear, ideal MHD equations. The wave motion inside the dissipative layer is governed by Eq. (4.23). This equation is linear, despite taking into consideration (quadratic and cubic) nonlinearity. The Hall terms of the induction equation in the perpendicular direction relative to the ambient magnetic field cancel each other out.

The nonlinear corrections were calculated to explain why Eq. (4.23), describing the nonlinear behaviour of wave dynamics, is always linear. We found that, in the second order of approximation, magnetoacoustic modes are excited by the perturbations of the linear order of approximation. These secondary waves act to counteract the small pressure and density variations created

by the first order terms. In addition, these waves are not resonant in the Alfvén dissipative layer. In the third order approximation the perturbations become Alfvénic, however, these perturbations are much smaller than those in the linear order of approximation. Equations (4.74) and (4.75) describe the expansion of large and small variables, respectively; and demonstrate that all higher order approximations of both large and small variables at the Alfvén resonance are smaller than the linear order approximation, provided condition (4.35) is satisfied. This condition ensures that the oscillation amplitude remains small inside the dissipative layer. From a naive point of view the linear theory is applicable as soon as the oscillation amplitude is small. The example of slow resonant waves clearly shows that this is not the case (see discussion in Sect. 4.4). We also found that any dispersive effect due to the consideration of ions' inertial length (Hall effect) is absent from the governing equation.

This calculation of nonlinear corrections to resonant Alfvén waves in dissipative layers allows us to apply the already well-known linear theory for studying resonant Alfvén waves in the solar corona with great accuracy, where the governing equation, jump conditions and the absorption of wave energy are already derived (see, e.g. Sakurai et al., 1991b; Goossens et al., 1995; Erdélyi, 1998). It is interesting to note that this work can be transferred to isotropic plasma rather easily. Shear viscosity, supplied by Braginskii's viscosity tensor (see Appendix B), acts exactly as isotropic viscosity. Therefore, replacing $\eta_1$ by $\rho_{0_a}\nu$ in Eq. (4.23) provides the required governing equation for resonant Alfvén waves in isotropic plasmas. Moreover, the work on the nonlinear corrections presented in this chapter is also unaltered by anisotropy. This implies that we can consider resonant Alfvén waves in dissipative layers throughout the solar atmosphere and still use linear theory if condition (4.35) is satisfied. We will use the governing equation derived here in Chapter 5 to study the generated mean shear flow at the Alfvén resonance and in Chapter 6 to investigate the wave energy absorption at the Alfvén resonance.

# 5

# Mean shear flows generated by resonant Alfvén waves

*In the context of resonant absorption, nonlinearity has two different manifestations. The first is the reduction in amplitude of perturbations around the resonant point (wave energy absorption). The second is the generation of mean shear flows outside the dissipative layer surrounding the resonant point. Ruderman et al. (1997d) and Ballai et al. (2000) studied both these effects at the slow resonance in isotropic plasmas in cartesian and cylindrical geometry, respectively. We investigated nonlinearity at the Alfvén resonance in Chapter 4, however, we did not include the generation of mean shear flow. In this present chapter, we investigate the mean shear flow, analytically, and study its properties. We find that the flow generated is parallel to the magnetic surfaces and has a characteristic velocity proportional to* $\epsilon^{1/2}$*, where* $\epsilon$ *is the dimensionless amplitude of perturbations far away from the resonance. This is, qualitatively, similar to the flow generated at the slow resonance. The jumps in the derivatives of the parallel and perpendicular components of mean shear flow across the dissipative layer are derived. We estimate the generated mean shear flow to be of the order of* $10\mathrm{kms}^{-1}$ *in both the solar upper chromosphere and solar corona, however, the value strongly depends on the choice of boundary conditions. It is proposed that the generated mean shear flow can produce a Kelvin–Helmholtz instability (KHI) at the dissipative layer which can create turbulent motions. The KHI would be an addition to the KHI that may already exist due to the velocity field of the resonant Alfvén waves. This flow can also be superimposed onto existing large scale motions in the solar upper atmosphere. The results of the present chapter were published in Physics of Plasmas (Clack and Ballai, 2009a).*

*It is not enough to have a good mind. The main thing is to use it well.*
**(Rene Descartes** 1596 – 1650**)**

## 5.1 Introduction

It has long been established, from observations, that the solar corona is highly structured and inhomogeneous with temperatures of the order of $10^6$K. The solar corona is filled with a large number of discrete magnetic loops (coronal arcades) and there is an abundance of observational evidence showing that magnetohydrodynamic (MHD) waves propagate in, and across, these loops (see, e.g. Hassler et al., 1990; Saba and Strong, 1991; Young et al., 1999; Banerjee et al., 2007). In order to sustain such high temperatures whilst combatting optically thin radiation and thermal conduction there must exist some mechanism(s) acting as a source of steady heating. The last few decades saw a multitude of models proposed to tackle the complicated problem of coronal heating, such as heating by waves (e.g. resonant absorption, phase mixing) or heating by magnetic relaxation (e.g. reconnection). There is an increasing consensus that all these processes act simultaneously to different degrees of efficiency throughout the solar corona (see discussion in Sect. 1.3).

A new understanding of the process of resonant absorption became available after the study by Ruderman et al. (1997d) which was the first analytical study on the nonlinear aspect of resonant absorption. Not only was it shown that resonant absorption of slow waves was an inherently nonlinear phenomenon, they also showed that a mean shear flow is generated outside the dissipative layer. By their calculations, however, they still found the generated flow was much too large compared to the observed velocities. On the other hand, the authors did note that their results should be used with caution in the solar atmosphere as some of their assumptions were not fully realistic for that environment.

From the coronal heating point of view, the slow resonance studied by Ruderman et al. (1997d) is not expected to contribute significantly as the energy stored in slow waves is much less than the required energy to compensate the losses. In addition, it is difficult for slow waves to reach the corona, as they become shocked as they climb due to density stratification (although they can be generated locally). From this point of view, Alfvén waves and Alfvén resonance are of much greater interest as estimations show that the energy carried by Alfvén waves is much higher and they can reach the corona without significant damping. The validity of nonlinear resonant Alfvén waves (under coronal conditions) was studied in great detail in Chapter 4, where we showed that in coronal plasmas the nonlinear addition to the result found in linear MHD is so small that the linear approach can be used with great accuracy. Essentially we clarified the upper limit in which linear theory is applicable to resonant Alfvén waves.

Studies have been carried out to investigate the properties of shear flows generated by velocity field of Alfvén waves, however, nearly all of these have been numerical due to analytical complications when considering nonlinearity, turbulence and resonant absorption simultaneously. These studies have found that shear flows could give rise to a Kelvin–Helmholtz instability at the narrow dissipative layer (see, e.g. Ofman and Davila, 1995). This instability can drive turbulent motions and, in turn, locally enhance transport coefficients which can alter the efficiency of heating (see, e.g. Karpen et al., 1994; Ofman et al., 1994; Ofman and Davila, 1995). None of these investigations have studied the generation of mean shear flow at the Alfvén resonance by nonlinear interactions. The generation of mean shear flow can supply additional shear enhancing turbulent motions. Recent advancements in the understanding of nonlinear Alfvén resonance has inspired us to study of the generation of mean shear flows at the Alfvén resonance. In the present chapter we will derive the equations describing the generated mean shear flow outside the Alfvén

dissipative layer and estimate the magnitude of the shear flow. We already know (from, e.g. Ofman and Davila, 1995) that the plasma velocity at the dissipative layer may be reduced by the turbulent enhancement of the dissipative parameters, implying that for a given heating rate, the wave amplitude is reduced compared to the linear case. This means that any result we produce must be reduced when considered for the solar corona since turbulent motions are likely to be present and this will reduce the mean flow speed.

## 5.2 Governing equations and assumptions

To mathematically study the mean shear flow generated at resonance we use the visco-resistive MHD equations. We discussed in Sect. 2.4 that when the products $\omega_i\tau_i \gg 1, \omega_e\tau_e \gg 1$ are much greater than unity (as in the solar corona) the viscosity and finite electrical conductivity become anisotropic. Another possible additive to our model might be dispersive effects caused by Hall currents, however, in Appendix A we showed that this effect does not alter the MHD waves in the vicinity of the Alfvén resonance. We therefore use Eqs (2.1)–(2.8) with $\mathcal{D}_\nu$ taking the form of Eq (2.30) and $\overline{\mathbf{H}} = \mathcal{L} = 0$.

We use an identical physical set up as in Chapter 4 so that we can utilize the governing equation (4.23). Hence, we adopt Cartesian coordinates $x, y, z$ and limit our analysis to a static background equilibrium ($\mathbf{v}_0 = 0$). We, also, assume that all equilibrium quantities (terms with subscript '0') depend on $x$ only. The equilibrium magnetic field, $\mathbf{B}_0$, is unidirectional and lies in the $yz-$plane and the equilibrium quantities must satisfy the condition of total pressure balance. For simplicity we assume that the perturbations of all quantities are independent of $y$ ($\partial/\partial y = 0$). We note that since the magnetic field is not aligned with the $z-$axis, an Alfvén resonance can still exists. Even though the Alfvén resonance is governed by a linear equation, we must consider nonlinear effects to obtain the second manifestation of nonlinearity; the mean shear flow generated outside the dissipative layer.

We know that in linear theory of driven waves all perturbed quantities oscillate with the same frequency, $\omega$, which means that they can be Fourier-analysed and taken to be proportional to $\exp(i[kz-\omega t])$. We assume this extends to nonlinear theory. In the context of resonant absorption the phase velocity, $V$, must match the projection of the Alfvén velocity, $v_A$, onto the $z-$axis when $x = x_a$ where $x_a$ is the resonant position. We defined the Alfvén resonant position mathematically in Eq. (4.1). In what follows we can take $x_a = 0$ without loss of generality. The perturbations of the physical quantities are defined by Eq. (4.2). As it was shown in Chapter 4, the dominant dynamics of resonant Alfvén waves resides in the components of the perturbed magnetic field and velocity that are perpendicular to the equilibrium magnetic field and to the $x-$direction. This dominant behaviour is created by an $1/x$ singularity in the spatial solution of these quantities at the Alfvén resonance (see, e.g. Sakurai et al., 1991b; Goossens, 1994; Goossens et al., 1995; Clack et al., 2009b). The variables that are dominant inside the dissipative layer are known as *large variables*, while all other variables are known as *small variables*.

To help make the mathematical analysis more concise we define the components of velocity and magnetic field that are in the $yz-$plane and are either parallel or perpendicular to the equilibrium magnetic field as in Eq. (2.64). As we are studying resonant Alfvén waves in anisotropic plasmas we must adopt the Reynolds numbers given by Eq. (2.55), with the consequence of utilizing the nonlinearity parameter (2.57) and the stretched dissipative coefficients given in Eq. (2.61). We note that the aim of the present chapter is to study the generation of a mean shear flow outside

the Alfvén dissipative layer due to the nonlinear behaviour of driven resonant Alfvén waves in the dissipative layer. We are not interested in the effects of MHD waves that have large amplitude everywhere and require a nonlinear description in the whole space. We focus on waves that have small dimensionless amplitude $\epsilon \ll 1$ far away from the ideal Alfvén resonant point.

In the linear theory all perturbed quantities are harmonic functions of $\theta$, therefore their mean values over a period vanish. On the other hand, in nonlinear theory the perturbed variables can have nonzero mean values as a result of nonlinear interaction of different harmonics. Let us introduce the mean value of a function $f(\theta)$ over a wavelength $L$ as

$$\langle f \rangle = \frac{1}{L}\int_0^L f(\theta)\, d\theta. \tag{5.1}$$

It directly follows from Eqs (2.1) and (2.6) that

$$\langle \overline{\rho} u \rangle = \langle b_x \rangle = 0. \tag{5.2}$$

We can always define the background state in such a way that the mean values of density, pressure and magnetic field vanish:

$$\langle \rho \rangle = \langle p \rangle = \langle b_\parallel \rangle = \langle b_\perp \rangle = 0. \tag{5.3}$$

This is not possible for the velocity parallel and perpendicular to the equilibrium magnetic field (since we have assumed a static equilibrium). It is convenient, therefore, to divide $v_\parallel$ and $v_\perp$ into mean and oscillatory parts. Using the Reynolds decomposition we can write

$$U_\parallel = \langle v_\parallel \rangle, \quad \widetilde{v}_\parallel = v_\parallel - U_\parallel, \quad U_\perp = \langle v_\perp \rangle, \quad \widetilde{v}_\perp = v_\perp - U_\perp. \tag{5.4}$$

The quantities $U_\parallel$ and $U_\perp$ describe the mean flow parallel to the magnetic surfaces. The mean flow is generated by the nonlinear interaction of the harmonics in the Fourier expansion of the perturbed quantities with respect to $\theta$.

The Eqs (2.1)–(2.8) were rewritten to their scalar form in Eqs (4.5)–(4.14). The equations for $U_\perp$ and $U_\parallel$ are obtained by averaging Eqs (4.7) and (4.8), respectively, and then dividing by $\overline{\rho}$,

$$\begin{aligned}\frac{\overline{\eta}_1}{\overline{\rho}}\frac{d^2U_\perp}{dx^2} = {} & \left\langle u\frac{\partial v_\perp}{\partial x}\right\rangle + \left\langle v_\parallel \frac{\partial v_\perp}{\partial \theta}\right\rangle \cos\alpha - \left\langle \frac{1}{\overline{\rho}}\frac{\partial P}{\partial \theta}\right\rangle \sin\alpha - \frac{B_0\cos\alpha}{\mu_0}\left\langle \frac{1}{\overline{\rho}}\frac{\partial b_\perp}{\partial \theta}\right\rangle \\ & - \frac{1}{\mu_0}\left\langle \frac{b_x}{\overline{\rho}}\frac{\partial b_\perp}{\partial x}\right\rangle - \frac{\cos\alpha}{\mu_0}\left\langle \frac{b_\parallel}{\overline{\rho}}\frac{\partial b_\perp}{\partial \theta}\right\rangle + \frac{\sin\alpha}{\mu_0}\left\langle \frac{b_\perp}{\overline{\rho}}\frac{\partial b_\perp}{\partial \theta}\right\rangle. \end{aligned} \tag{5.5}$$

$$\begin{aligned}\frac{\overline{\eta}_1}{\overline{\rho}}\frac{d^2U_\parallel}{dx^2} = {} & \left\langle u\frac{\partial v_\parallel}{\partial x}\right\rangle + \left\langle v_\parallel \frac{\partial v_\perp}{\partial \theta}\right\rangle \cos\alpha + \left\langle \frac{1}{\overline{\rho}}\frac{\partial P}{\partial \theta}\right\rangle \cos\alpha - \frac{B_0\cos\alpha}{\mu_0}\left\langle \frac{1}{\overline{\rho}}\frac{\partial b_\parallel}{\partial \theta}\right\rangle \\ & - \frac{1}{\mu_0}\left\langle \frac{b_x}{\overline{\rho}}\frac{\partial b_\parallel}{\partial x}\right\rangle - \frac{\cos\alpha}{\mu_0}\left\langle \frac{b_\parallel}{\overline{\rho}}\frac{\partial b_\parallel}{\partial \theta}\right\rangle + \frac{\sin\alpha}{\mu_0}\left\langle \frac{b_\perp}{\overline{\rho}}\frac{\partial b_\parallel}{\partial \theta}\right\rangle - \frac{1}{\mu_0}\frac{dB_0}{dx}\left\langle \frac{b_x}{\overline{\rho}}\right\rangle, \end{aligned} \tag{5.6}$$

Equations (4.5)–(4.14), (5.5) and (5.6) will be used in the following sections in order to calculate the mean flow that is generated outside the dissipative layer by the resonant waves.

## 5.3 Solution of generated mean shear flow outside the Alfvén dissipative layer

To calculate the mean shear flow generated outside the dissipative layer we recall some results from Chapter 4. We used the method of simplified matched asymptotic expansions (see, e.g. Ballai et al., 1998b; Clack and Ballai, 2008; Clack et al., 2009b) in order to derive the equation governing resonant Alfvén waves in the dissipative layer. The solutions in the outer region, with the exception of $v_\perp$ and $v_\parallel$, are represented by asymptotic expansions of the form of Eq. (3.19). We shall show that resonant Alfvén waves create a shear flow with an amplitude proportional to $\epsilon^{1/2}$ outside the dissipative layer. As a consequence, we expand $\widetilde{v}_\perp$ and $\widetilde{v}_\parallel$ in the form of Eq. (3.19), and $U_\perp$ and $U_\parallel$ in the form

$$U_\perp = \epsilon^{1/2}U_\perp^{(0)} + \epsilon U_\perp^{(1)} + \epsilon^{3/2}U_\perp^{(2)} + \ldots, \quad U_\parallel = \epsilon^{1/2}U_\parallel^{(0)} + \epsilon U_\parallel^{(1)} + \epsilon^{3/2}U_\parallel^{(2)} + \ldots. \tag{5.7}$$

In addition, we found that substitution of Eq. (3.19) into Eqs (4.5)–(4.14) led, in the first order approximation, to a system of linear equations for the variables with the superscript '1'. When all variables are eliminated in favour of $u^{(1)}$ and $P^{(1)}$ we arrived at Eq. (3.20). The remaining variables are expressed in terms of $u^{(1)}$ and $P^{(1)}$ in Eqs (3.23)–(3.27). Note that in Eq. (3.23) the velocities in the parallel and perpendicular directions relative to the ambient magnetic field ($v_\perp$ and $v_\parallel$) should be replaced by their oscillatory counterparts ($\widetilde{v}_\perp$ and $\widetilde{v}_\parallel$).

From Eqs (3.23)–(3.27), we see that the quantity $\widetilde{v}_\parallel^{(1)}$ is regular, while all other quantities are singular. The quantities $u^{(1)}$, $b_x^{(1)}$, $b_\parallel^{(1)}$, $p^{(1)}$ and $\rho^{(1)}$ behave as $\ln|x|$, while $\widetilde{v}_\perp^{(1)}$ and $b_\perp^{(1)}$ behave as $1/x$, so they are the most singular. Carrying out calculations on Eqs (5.6) and (5.5), and utilizing Eqs (3.20), (3.23)–(3.27), we find that in the first and second order approximations we have

$$\frac{d^2U_\perp^{(0)}}{dx^2} = \frac{d^2U_\perp^{(1)}}{dx^2} = \frac{d^2U_\parallel^{(0)}}{dx^2} = \frac{d^2U_\parallel^{(1)}}{dx^2} = 0. \tag{5.8}$$

The functions $U_\perp^{(0)}(x)$, $U_\parallel^{(0)}(x)$, $U_\perp^{(1)}(x)$ and $U_\parallel^{(1)}(x)$ are all continuous at $x = 0$. Since Eq. (5.8) suggests that $U_\perp^{(0)}(x)$, $U_\parallel^{(0)}(x)$, $U_\perp^{(1)}(x)$ and $U_\parallel^{(1)}(x)$ are linear functions of $x$, we can include $U_\perp^{(1)}(x)$ and $U_\parallel^{(1)}(x)$ into $U_\perp^{(0)}(x)$ and $U_\parallel^{(0)}(x)$ and take $U_\perp^{(1)}(x) = U_\parallel^{(1)}(x) = 0$, without loss of generality. We choose a mobile coordinate system such that $U_\perp^{(0)}(0) = U_\parallel^{(0)}(0) = 0$, which, when used in conjunction with Eq. (5.8), leads to

$$U_\perp^{(0)} = V_\perp^{\pm}x, \quad U_\parallel^{(0)} = V_\parallel^{\pm}x, \tag{5.9}$$

where $V_\perp^{\pm}$ and $V_\parallel^{\pm}$ are constants and the superscripts '–' and '+' refer to $x < 0$ and $x > 0$, respectively.

Continuing in the same way we can find the solutions of the subsequent higher order approximations. At each step in the scheme of approximations we obtain equations with the left-hand sides equal to the left-hand sides of the equations found in the first order approximation. The right-hand sides of the equations are expressed in terms of variables of lower order approximations. In carrying out this process we obtain that

$$U_\parallel^{(n)} = O(x^{-n+1}), \quad U_\perp^{(n)} = O(x^{-n+1}), \quad n \geq 2. \tag{5.10}$$

This implies that the mean velocity starts to behave singularly from the third order approximation. Taking into account Eqs (5.9) and (5.10) we write the expansion for the mean velocity in the form

$$U_j = \epsilon^{1/2} V_j x + \sum_{n=1}^{\infty} \epsilon^{(n+2)/2} V_j^{(n)}(x) x^{-n}, \tag{5.11}$$

where subscript 'j' represents either the subscript '$\perp$' or '$\|$' and the functions $V_j(x)$ and $V_j^{(n)}(x)$ have finite limits at $|x| \to 0$. The most important property of expansion (5.11) is that the term of the lowest order approximation (proportional to $\epsilon^{1/2}$) is very small inside the dissipative layer, but becomes large far away from the resonance. It is also interesting to note that the remaining terms tend to zero far from resonance. This result is in complete agreement with the studies by, e.g. Ruderman et al. (1997d); Ballai et al. (2000) where they found the mean flow generated by resonant slow waves outside the dissipative layer to be proportional to $\epsilon^{1/2}$.

## 5.4 Solution of generated mean shear flow in the Alfvén dissipative layer

In this section we determine the inner expansion, which is the solution inside the dissipative layer. The thickness of the dissipative layer is of the order of $l_{inh} R^{-1/3}$, where $l_{inh}$ is the characteristic scale of inhomogeneity. Since we assume that $R = \mathcal{O}(\epsilon^{-3/2})$ we have $l_{inh} R^{-1/3} = \mathcal{O}(\epsilon^{1/2} l_{inh})$. Similar to Sect. 4.3, it is convenient to introduce a stretching variable $\xi = \epsilon^{-1/2} x$ inside the Alfvén dissipative layer.

We can rewrite Eqs. (4.5)–(4.14) using the stretching variable, however, in the interest of being concise, we only display the equations we use explicitly, which are the normal component of induction and the perpendicular component of momentum

$$\epsilon^{1/2} (V - w) \frac{\partial b_x}{\partial \theta} + \epsilon^{1/2} (B_0 \cos\alpha + b_z) \frac{\partial u}{\partial \theta} + \epsilon\eta \left( \frac{\partial^2 b_x}{\partial \xi^2} + \epsilon \frac{\partial^2 b_x}{\partial \theta^2} \right) = 0, \tag{5.12}$$

$$\begin{aligned} \frac{1}{\overline{\rho}} \left[ \epsilon^{1/2} \frac{\partial P}{\partial \theta} \sin\alpha + \frac{b_x}{\mu_0} \frac{\partial b_\perp}{\partial \xi} + \frac{\epsilon^{1/2}}{\mu_0} (B_0 \cos\alpha + b_z) \frac{\partial b_\perp}{\partial \theta} \right] \\ = -\epsilon^{1/2} (V - w) \frac{\partial v_\perp}{\partial \theta} + u \frac{\partial v_\perp}{\partial \xi} - \epsilon \frac{\eta_1}{\overline{\rho}} \left( \frac{\partial^2 v_\perp}{\partial \xi^2} + \epsilon \frac{\partial^2 v_\perp}{\partial \theta^2} \right), \end{aligned} \tag{5.13}$$

In Sect 4.3, we used the stretched versions of Eqs (4.5)–(4.14) to find the relationships between variables in each successive order of approximation, which (for the first order of approximation) are given by Eqs (4.17)–(4.20). Additionally, Eqs (5.12) and (5.13) are used to help derive the equations governing the mean shear flow inside the dissipative layer. Inside the Alfvén dissipative layer, Eqs (5.5) and (5.6) for the generated mean flow are transformed to

$$\begin{aligned} \epsilon \frac{\eta_1}{\overline{\rho}} \frac{d^2 U_\perp}{d\xi^2} = \left\langle u \frac{\partial v_\perp}{\partial \xi} \right\rangle - \frac{1}{\mu_0} \left\langle \frac{b_x}{\overline{\rho}} \frac{\partial b_\perp}{\partial \xi} \right\rangle + \epsilon^{1/2} \left[ \left\langle \nu_\| \frac{\partial v_\perp}{\partial \theta} \right\rangle \cos\alpha - \frac{B_0 \cos\alpha}{\mu_0} \left\langle \frac{1}{\overline{\rho}} \frac{\partial b_\perp}{\partial \theta} \right\rangle \right. \\ \left. - \left\langle \frac{1}{\overline{\rho}} \frac{\partial P}{\partial \theta} \right\rangle \sin\alpha - \frac{\cos\alpha}{\mu_0} \left\langle \frac{b_\|}{\overline{\rho}} \frac{\partial b_\perp}{\partial \theta} \right\rangle + \frac{\sin\alpha}{\mu_0} \left\langle \frac{b_\perp}{\overline{\rho}} \frac{\partial b_\perp}{\partial \theta} \right\rangle \right], \end{aligned} \tag{5.14}$$

$$\epsilon\frac{\eta_1}{\overline{\rho}}\frac{d^2U_\parallel}{d\xi^2}=\left\langle u\frac{\partial v_\parallel}{\partial\xi}\right\rangle-\frac{1}{\mu_0}\left\langle\frac{b_x}{\overline{\rho}}\frac{\partial b_\parallel}{\partial\xi}\right\rangle+\epsilon^{1/2}\left[\left\langle v_\parallel\frac{\partial v_\perp}{\partial\theta}\right\rangle\cos\alpha+\left\langle\frac{1}{\overline{\rho}}\frac{\partial P}{\partial\theta}\right\rangle\cos\alpha\right.$$
$$\left.-\frac{B_0\cos\alpha}{\mu_0}\left\langle\frac{1}{\overline{\rho}}\frac{\partial b_\parallel}{\partial\theta}\right\rangle-\frac{\cos\alpha}{\mu_0}\left\langle\frac{b_\parallel}{\overline{\rho}}\frac{\partial b_\parallel}{\partial\theta}\right\rangle+\frac{\sin\alpha}{\mu_0}\left\langle\frac{b_\perp}{\overline{\rho}}\frac{\partial b_\parallel}{\partial\theta}\right\rangle-\frac{1}{\mu_0}\frac{dB_0}{dx}\left\langle\frac{b_x}{\overline{\rho}}\right\rangle\right]. \quad (5.15)$$

In Chapter 4 we found that large variables ($\widetilde{v}_\perp$, $b_\perp$) inside the dissipative layer are expanded in the form of Eq. (3.39), whereas small variables ($P$, $p$, $\rho$, $u$, $\widetilde{v}_\parallel$, $b_x$, $b_\parallel$) expand in the form of Eq. (3.19). The variables $v_\perp$ and $v_\parallel$ are expanded in series of the same form as $\widetilde{v}_\perp$ and $\widetilde{v}_\parallel$, hence we expand $U_\perp$ and $U_\parallel$ as

$$U_\perp=\epsilon U_\perp^{(2)}+\ldots,\quad U_\parallel=\epsilon U_\parallel^{(1)}+\ldots. \quad (5.16)$$

We have chosen the superscripts in Eq. (5.16) in such a way that

$$v_\perp^{(n)}=\widetilde{v}_\perp^{(n)}+U_\perp^{(n)},\quad v_\parallel^{(n)}=\widetilde{v}_\parallel^{(n)}+U_\parallel^{(n)}. \quad (5.17)$$

Recall that, on substituting these expansions into the stretched versions of Eqs (4.5)–(4.14) we found a linear homogeneous system of equations for the variables with superscript '1' in the first order approximation. Then, in the second order approximation, after eliminating all variables with superscript '1' in favour of $\widetilde{v}_\perp^{(1)}$ and $P^{(1)}$ using Eqs (4.17)–(4.20), and satisfying the compatibility condition, we derived the equation governing resonant Alfvén waves inside the dissipative layer given by Eq. (4.23).

Inserting the expansions (3.19), (3.39) and (5.16) into Eqs (5.14) and (5.15) and collecting terms proportional to $\epsilon$, we have

$$\frac{\eta_1}{\rho_{0_a}}\frac{d^2U_\perp^{(2)}}{d\xi^2}=\left\langle u^{(1)}\frac{\partial\widetilde{v}_\perp^{(2)}}{\partial\xi}+u^{(2)}\frac{\partial\widetilde{v}_\perp^{(1)}}{\partial\xi}\right\rangle-\frac{1}{\mu_0\rho_{0_a}}\left\langle b_x^{(1)}\frac{\partial b_\perp^{(2)}}{\partial\xi}+b_x^{(2)}\frac{\partial b_\perp^{(1)}}{\partial\xi}\right\rangle+\cos\alpha\left\langle\widetilde{v}_\parallel^{(1)}\frac{\partial\widetilde{v}_\perp^{(1)}}{\partial\theta}\right\rangle$$
$$-\frac{\cos\alpha}{\mu_0\rho_{0_a}}\left\langle b_\parallel^{(1)}\frac{\partial b_\perp^{(1)}}{\partial\theta}\right\rangle+\frac{B_{0_a}\cos\alpha}{\mu_0\rho_{0_a}^2}\left\langle\rho^{(1)}\frac{\partial b_\perp^{(1)}}{\partial\theta}\right\rangle+\frac{\xi}{\mu_0\rho_{0_a}^2}\left(\frac{d\rho_0}{dx}\right)_a\left\langle b_x^{(1)}\frac{\partial b_\perp^{(1)}}{\partial\xi}\right\rangle, \quad (5.18)$$

$$\frac{\eta_1}{\rho_{0_a}}\frac{d^2U_\parallel^{(1)}}{d\xi^2}=\frac{\sin\alpha}{\mu_0\rho_{0_a}}\left\langle b_\perp^{(1)}\frac{\partial b_\parallel^{(1)}}{\partial\theta}\right\rangle+\sin\alpha\left\langle\widetilde{v}_\parallel^{(1)}\frac{\partial\widetilde{v}_\perp^{(1)}}{\partial\theta}\right\rangle-\frac{1}{\mu_0\rho_{0_a}}\left\langle b_x^{(1)}\frac{\partial b_\parallel^{(1)}}{\partial\xi}\right\rangle. \quad (5.19)$$

In deriving Eqs (5.18) and (5.19) we have utilized the fact that

$$\left\langle\frac{\partial f}{\partial\theta}\right\rangle=\left\langle f\frac{\partial f}{\partial\theta}\right\rangle=\left\langle\frac{\partial g}{\partial\theta}\right\rangle=\left\langle g\frac{\partial g}{\partial\theta}\right\rangle=0,$$

which follows directly from Eq. (5.1) [and Eqs (5.2) and (5.3)]. Here $f$ is any small variable and $g$ is any large variable. Now we use Eqs (4.17)–(4.20) to eliminate terms on the right-hand sides of Eqs. (5.18) and (5.19) in favour of $\widetilde{v}_\perp^{(1)}$ and $P^{(1)}$ to leave

$$\frac{\eta_1}{\rho_{0_a}}\frac{d^2U_\perp^{(2)}}{d\xi^2}=\left\langle u^{(1)}\frac{\partial\widetilde{v}_\perp^{(2)}}{\partial\xi}+u^{(2)}\frac{\partial\widetilde{v}_\perp^{(1)}}{\partial\xi}\right\rangle-\frac{1}{\mu_0\rho_{0_a}}\left\langle b_x^{(1)}\frac{\partial b_\perp^{(2)}}{\partial\xi}+b_x^{(2)}\frac{\partial b_\perp^{(1)}}{\partial\xi}\right\rangle$$
$$+\frac{1}{\rho_{0_a}}\left(\frac{d\rho_0}{dx}\right)_a\left\langle u^{(1)}\frac{\partial\left(\xi\widetilde{v}_\perp^{(1)}\right)}{\partial\xi}\right\rangle-\frac{1}{B_{0_a}}\left(\frac{dB_0}{dx}\right)_a\left\langle u^{(1)}\widetilde{v}_\perp^{(1)}\right\rangle, \quad (5.20)$$

$$\frac{\eta_1}{\rho_{0_a}}\frac{d^2U_\parallel^{(1)}}{d\xi^2} = -\frac{V\sin\alpha}{\rho_{0_a}v_{A_a}^2\cos\alpha}\left\langle \widetilde{v}_\perp^{(1)}\frac{dP^{(1)}}{d\theta}\right\rangle. \tag{5.21}$$

Averaging the governing equation (4.23) and substituting it into Eq. (5.21) we obtain

$$\frac{d^2U_\parallel^{(1)}}{d\xi^2} = -\frac{V(\eta_1+\rho_{0_a}\eta)}{\eta_1 v_{A_a}^2\cos\alpha}\left\langle \widetilde{v}_\perp^{(1)}\frac{\partial^2\widetilde{v}_\perp^{(1)}}{\partial\xi^2}\right\rangle, \tag{5.22}$$

which constitutes the equation that governs the generated mean flow inside the dissipative layer parallel to the magnetic field lines. In order to derive the equivalent equation for the generated mean flow perpendicular to the magnetic field lines we we note that Eqs (5.12) and (5.13) in the second order approximation lead to

$$u^{(2)} + \frac{Vb_x^{(2)}}{B_{0_a}\cos\alpha} = \frac{\eta\sin\alpha}{V}\frac{\partial\widetilde{v}_\perp^{(1)}}{\partial\xi} - \frac{\xi u^{(1)}}{B_{0_a}}\left(\frac{dB_0}{dx}\right)_a. \tag{5.23}$$

$$\rho_{0_a}\frac{\partial\widetilde{v}_\perp^{(2)}}{\partial\theta} + \frac{B_{0_a}\cos\alpha}{\mu_0 V}\frac{\partial b_\perp^{(2)}}{\partial\theta} = -\frac{\sin\alpha}{V}\frac{dP^{(1)}}{d\theta} - \frac{\eta_1}{V}\frac{\partial^2\widetilde{v}_\perp^{(1)}}{\partial\xi^2} + \left[\frac{B_{0_a}}{\mu_0 v_{A_a}^2}\left(\frac{dB_0}{dx}\right)_a - \left(\frac{d\rho_0}{dx}\right)_a\right]\xi\frac{\partial\widetilde{v}_\perp^{(1)}}{\partial\theta}, \tag{5.24}$$

Substituting Eq. (4.23) into Eq. (5.24) we obtain

$$\frac{\partial\widetilde{v}_\perp^{(2)}}{\partial\xi} + \frac{B_{0_a}\cos\alpha}{\mu_0\rho_{0_a}V}\frac{\partial b_\perp^{(2)}}{\partial\xi} = \left[\frac{\eta_1\Delta_a}{V^2(\eta_1+\rho_{0_a}\eta)} + \frac{1}{B_{0_a}}\left(\frac{dB_0}{dx}\right)_a - \frac{1}{\rho_{0_a}}\left(\frac{d\rho_0}{dx}\right)_a\right]\frac{\partial\left(\xi\widetilde{v}_\perp^{(1)}\right)}{\partial\xi}. \tag{5.25}$$

On substitution of Eqs (5.23) and (5.25) into Eq. (5.20) we produce

$$\frac{\eta_1}{\rho_{0_a}}\frac{d^2U_\perp^{(2)}}{d\xi^2} = \frac{\eta\sin\alpha}{V}\left\langle\left(\frac{\partial\widetilde{v}_\perp^{(1)}}{\partial\xi}\right)^2\right\rangle + \frac{\eta_1}{V^2(\eta_1+\rho_{0_a}\eta)}\frac{\partial}{\partial\xi}\left(\Delta_a\xi\left\langle u^{(1)}\widetilde{v}_\perp^{(1)}\right\rangle\right). \tag{5.26}$$

It follows directly from Eqs. (4.20) and (4.23) that

$$\frac{\Delta_a\xi}{V^2}\left\langle u^{(1)}\widetilde{v}_\perp^{(1)}\right\rangle = -\frac{\sin\alpha}{\rho_{0_a}V}\left\langle u^{(1)}P^{(1)}\right\rangle - \frac{(\eta_1+\rho_{0_a}\eta)}{\rho_{0_a}V}u^{(1)}\int\left\langle\frac{\partial^2\widetilde{v}_\perp^{(1)}}{\partial\xi^2}\right\rangle d\theta \tag{5.27}$$

and

$$\left\langle P^{(1)}\frac{\partial u^{(1)}}{\partial\xi}\right\rangle = (\eta_1+\rho_{0_a}\eta)\left\langle\widetilde{v}_\perp^{(1)}\frac{\partial^2\widetilde{v}_\perp^{(1)}}{\partial\xi^2}\right\rangle. \tag{5.28}$$

Using Eq. (5.26) along with Eqs (5.27)–(5.28) we find the equation governing the generated mean shear flow inside the dissipative layer perpendicular to the magnetic field lines is

$$\frac{d^2U_\perp^{(2)}}{d\xi^2} = \frac{\rho_{0_a}\eta\sin\alpha}{\eta_1 V}\left\langle\left(\frac{\partial\widetilde{v}_\perp^{(1)}}{\partial\xi}\right)^2\right\rangle - \frac{\sin\alpha}{V}\left\langle\widetilde{v}_\perp^{(1)}\frac{\partial^2\widetilde{v}_\perp^{(1)}}{\partial\xi^2}\right\rangle - \frac{1}{V}\left\langle\int\frac{\partial^3\widetilde{v}_\perp^{(1)}}{\partial\xi^3}d\theta\right\rangle. \tag{5.29}$$

## 5.5 Connection formulae

To derive the jump in the derivative of the parallel component of the mean velocity across the dissipative layer we remember from Eq. (5.9) that $V_\parallel^\pm$ are constants and the superscripts '–' and

'+' refer to $x < 0$ and $x > 0$, respectively. This means that

$$V_{\parallel}^{+} - V_{\parallel}^{-} = \lim_{\xi\to\infty} \frac{dU_{\parallel}^{(1)}}{d\xi} - \lim_{\xi\to-\infty} \frac{dU_{\parallel}^{(1)}}{d\xi} = -\frac{V(\eta_1 + \rho_{0_a}\eta)}{\eta_1 v_{A_a}^2 \cos\alpha} \int_{-\infty}^{\infty} \left\langle \left( \frac{\partial \widetilde{v}_{\perp}^{(1)}}{\partial \xi} \right)^2 \right\rangle d\xi. \tag{5.30}$$

In a similar fashion, we find the jump in the derivative of the perpendicular component of the mean velocity across the dissipative layer to be

$$V_{\perp}^{+} - V_{\perp}^{-} = \lim_{\xi\to\infty} \frac{dU_{\perp}^{(1)}}{d\xi} - \lim_{\xi\to-\infty} \frac{dU_{\perp}^{(1)}}{d\xi} = \frac{(\eta_1 + \rho_{0_a}\eta)\sin\alpha}{\eta_1 V} \int_{-\infty}^{\infty} \left\langle \left( \frac{\partial \widetilde{v}_{\perp}^{(1)}}{\partial \xi} \right)^2 \right\rangle d\xi. \tag{5.31}$$

Outside the dissipative layer we have the following approximate equalities:

$$U_{\perp} \simeq \epsilon^{1/2} U_{\perp}^{(0)}(x), \quad U_{\parallel} \simeq \epsilon^{1/2} U_{\parallel}^{(0)}(x). \tag{5.32}$$

Let us introduce the new dimensionless variables

$$\sigma_a = \delta_a^{-1} x = \epsilon^{1/2} \delta_a^{-1} \xi, \quad q_a = \frac{\epsilon^{1/2} k \delta_a}{V} \widetilde{v}_{\perp}^{(1)}, \text{ where } \delta_a = \left[ \frac{V}{k|\Delta_a|} \left( \frac{\overline{\eta}_1}{\rho_{0_a}} + \overline{\eta} \right) \right]^{1/3}. \tag{5.33}$$

Here $\delta_a$ is the width of the anisotropic Alfvén dissipative layer and $k = 2\pi/L$. Equations (5.30) and (5.31) can be rewritten in these new variables as

$$\left[ \frac{dU_{\parallel}}{dx} \right] = -\frac{\rho_{0_a}|\Delta_a|\cos\alpha}{2\pi\overline{\eta}_1} \int_0^L d\theta \int_{-\infty}^{\infty} \left( \frac{\partial q_a}{\partial \sigma_a} \right)^2 d\sigma_a, \tag{5.34}$$

$$\left[ \frac{dU_{\perp}}{dx} \right] = \frac{\rho_{0_a}|\Delta_a|\sin\alpha}{2\pi\overline{\eta}_1} \int_0^L d\theta \int_{-\infty}^{\infty} \left( \frac{\partial q_a}{\partial \sigma_a} \right)^2 d\sigma_a. \tag{5.35}$$

These equations are implicit connection formulae and, as such, they must be solved in conjunction with the dimensionless version of Eq. (4.23), namely,

$$\mathrm{sgn}(\Delta_a)\sigma_a \frac{\partial q_a}{\partial \theta} + k \frac{\partial^2 q_a}{\partial \sigma_a^2} = -\frac{k \sin\alpha}{\rho_{0_a}|\Delta_a|} \frac{dP_a}{d\theta}, \tag{5.36}$$

where the notation $P_a = P(x_a = 0)$ is introduced. We note that Eqs (5.34) and (5.35) imply that at $\alpha = 0, \pi/2$ the jumps are zero, which is to be expected, since at these values of $\alpha$ there is no Alfvén resonance present [note that for Eq.(5.34) we have to solve the integral to discover that the jump is zero - however Eq. (5.44) shows this explicitly].

In fact, Eqs (5.34) and (5.35) can be solved explicitly, since the governing equation (5.36) is linear. It has been shown by, e.g. Goossens (1994); Erdélyi (1997) that the solution of the governing equation can be found in terms of the so-called F and G functions. In order to find the solutions to Eqs (5.34) and (5.35) we need to find $\widetilde{v}_{\perp}^{(1)}$ in order to obtain $q_a$. In cartesian coordinates, this was recently accomplished by Ruderman (2009) where he found that

$$\widetilde{v}_{\perp} = \frac{iVP\sin\alpha}{\rho_{0_a}\delta_a|\Delta_a|} F(\sigma_a), \tag{5.37}$$

where $F(\sigma_a)$ is given by Eq. (2.48) with $r$ substituted with $\sigma_a$. Substituting Eq. (5.37) into Eqs.

(5.34) and (5.35) leads to

$$\left[\frac{dU_{\parallel}}{dx}\right] = -\frac{k^2 \sin^2\alpha\cos\alpha}{2\pi\overline{\eta}_1 \rho_{0_a}|\Delta_a|}\int_0^L P^2\, d\theta \int_{-\infty}^{\infty}\left|\frac{dF}{d\sigma_a}\right|^2 d\sigma_a, \tag{5.38}$$

$$\left[\frac{dU_{\perp}}{dx}\right] = \frac{k^2 \sin^3\alpha}{2\pi\overline{\eta}_1 \rho_{0_a}|\Delta_a|}\int_0^L P^2\, d\theta \int_{-\infty}^{\infty}\left|\frac{dF}{d\sigma_a}\right|^2 d\sigma_a. \tag{5.39}$$

We can rewrite the integrals on the right-hand sides of Eqs (5.38) and (5.39) as

$$\int_{-\infty}^{\infty}\left|\frac{dF}{d\sigma_a}\right|^2 d\sigma_a = \int_{-\infty}^{\infty} d\sigma_a \int_0^{\infty} \widetilde{\phi} e^{i\widetilde{\phi}\sigma_a - \widetilde{\phi}^3/3}\, d\widetilde{\phi} \int_0^{\infty} \widetilde{\lambda} e^{-i\widetilde{\lambda}\sigma - \widetilde{\lambda}^3/3}\, d\widetilde{\lambda}, \tag{5.40}$$

where the tilde denotes the inclusion of the $\mathrm{sgn}(\Delta_a)$ and differentiates them from other variables, from this point onwards we drop the tilde notation. Here we are calculating the absolute value of the derivative, and so we use complex conjugates. If we change the order the integration we obtain

$$\int_{-\infty}^{\infty}\left|\frac{dF}{d\sigma_a}\right|^2 d\sigma_a = \int_0^{\infty} \phi e^{-\phi^3/3}\, d\phi \times \int_0^{\infty} \lambda e^{-\lambda^3/3}\, d\lambda \times \int_{-\infty}^{\infty} e^{-i\sigma_a(\lambda-\phi)}\, d\sigma_a. \tag{5.41}$$

The third integral in Eq. (5.41) is the definition of the delta function, $\delta(\lambda-\phi)$, so we can write Eq. (5.41) as

$$\int_{-\infty}^{\infty}\left|\frac{dF}{d\sigma_a}\right|^2 d\sigma_a = \int_0^{\infty} \phi e^{-\phi^3/3}\, d\phi \times \int_0^{\infty} \lambda e^{-\lambda^3/3} \cdot 2\pi\delta(\lambda-\phi) d\lambda. \tag{5.42}$$

Since the integral of the delta function is always unity, we arrive at

$$\int_{-\infty}^{\infty}\left|\frac{dF}{d\sigma_a}\right|^2 d\sigma_a = 2\pi\int_0^{\infty} \phi^2 e^{-2\phi^3/3}\, d\phi = -\pi e^{-2\phi^3/3}\Big|_0^{\infty} = \pi, \tag{5.43}$$

implying that Eqs (5.38) and (5.39) reduce to

$$\left[\frac{dU_{\parallel}}{dx}\right] = -\frac{k^2 \sin^2\alpha\cos\alpha}{2\overline{\eta}_1 \rho_{0_a}|\Delta_a|}\int_0^L P^2\, d\theta, \quad \left[\frac{dU_{\perp}}{dx}\right] = \frac{k^2 \sin^3\alpha}{2\overline{\eta}_1 \rho_{0_a}|\Delta_a|}\int_0^L P^2\, d\theta. \tag{5.44}$$

Equation (5.44) contains the explicit connection formulae for the jumps in the derivatives of the mean shear flow across the anisotropic Alfvén dissipative layer. They are explicit because we are considering a driven problem, and hence $P$ is assumed to be known.

If we take $\alpha = \pi/4$ we have the following approximation

$$\left[\frac{dU_{\parallel}}{dx}\right] = -\left[\frac{dU_{\perp}}{dx}\right] \simeq \frac{\epsilon^{1/2} V}{l_{inh}}, \tag{5.45}$$

and these values can be seen as jumps in vorticity. Here we have used the obvious estimates $|\Delta_a| = \mathcal{O}(V^2/l_{inh})$, $P = \mathcal{O}(\epsilon V^2 k l_{inh})$ and $\overline{\eta}_1 = \mathcal{O}(\epsilon^{3/2} V l_{inh})$. In order to find the profiles of the components of the generated mean shear flow we need to impose boundary conditions far away from the Alfvén dissipative layer. For example, if there are rigid walls at $x = \pm a$ where the condition of adhesion has to be satisfied, then the components of the generated mean flow take

the simple form

$$U_{\parallel} = \begin{cases} \left[\frac{dU_{\parallel}}{dx}\right]\frac{x-a}{2}, & x > 0, \\ -\left[\frac{dU_{\parallel}}{dx}\right]\frac{x+a}{2}, & x < 0, \end{cases} \qquad U_{\perp} = \begin{cases} \left[\frac{dU_{\perp}}{dx}\right]\frac{x-a}{2}, & x > 0, \\ -\left[\frac{dU_{\perp}}{dx}\right]\frac{x+a}{2}, & x < 0. \end{cases} \tag{5.46}$$

With the estimate given by Eq. (5.45) and the simple mean flow profiles in Eq. (5.46) we can calculate the expected mean flow generated outside the anisotropic Alfvén dissipative layer in the solar upper chromosphere and solar corona. For example, if the incoming wave has a dimensionless amplitude of $\epsilon = \mathcal{O}(10^{-4})$, then the predicted mean shear flow is of the order of $10\text{kms}^{-1}$ in both the upper chromosphere and corona. Here we have assumed that the characteristic scale of inhomogeneity ($l_{inh}$) is $10^2$m in the upper chromosphere and $10^3$m in the corona. This generated flow can be superimposed on existing flow, so it is difficult to observe. These results should be used with caution, when applied to the solar atmosphere. We have assumed that outside the dissipative layer the plasma is homogeneous and infinite, and clearly the solar atmosphere is neither, so, since all flows are entirely governed by the boundary conditions, the flow generated may be less than predicted or may even be stopped entirely.

## 5.6 Conclusions

In the present chapter we have completed the nonlinear theory of resonant Alfvén waves in dissipative layers in a one-dimensional (1-D) planar geometry. In Chapter 4 we showed that even though nonlinearity and dispersion are considered the equation governing resonant Alfvén waves in the Alfvén dissipative layer is always linear (provided $\epsilon \ll R^{-1/3}$). However, we neglected the second manifestation of nonlinearity at resonance; the generation of mean shear flows outside the dissipative layer. This flow is produced by the nonlinear interaction of harmonics inside the dissipative layer and may still exist even though the governing equation inside the dissipative layer is linear.

We have shown that outside the dissipative layer a mean flow is generated parallel to the magnetic surfaces. The flow has an amplitude proportional to $\epsilon^{1/2}$, and depends linearly on $x$. The derivatives of the velocity of the generated mean flow have a nonzero jump across the dissipative layer determined by Eq (5.44). When $\alpha = \pi/4$ the magnitude of the jumps can be estimated as $\epsilon^{1/2} V l_{inh}^{-1}$, where $V$ is the phase speed of the incoming wave and $l_{inh}$ is the characteristic scale of inhomogeneity. For typical conditions in the solar upper chromosphere and corona the magnitude of the jumps in the derivatives of mean shear flow velocity would be of the order of $10\text{s}^{-1}$. From this, and the simple flow profiles given by Eq. (5.46), we predict a mean flow outside the dissipative layer (generated by resonant absorption) with an amplitude of the order of $10\text{kms}^{-1}$ in the solar upper chromosphere and corona.

The magnitude of the jumps in the derivatives of the mean flow were found to depend on the phase speed ($V$), the characteristic scale of inhomogeneity ($l_{inh}$) and the dimensionless amplitude of oscillation ($\epsilon$) far away from the Alfvén dissipative layer. Even though simple estimations allowed us to approximate the magnitude of the shear flows, the results in the present chapter should be used with caution. The present analysis has been carried out for magnetic configurations that are homogeneous and infinite in the direction of wave propagation outside the Alfvén dissipative layer. This situation can only take place in laboratory devices (such as tokamaks). In

the solar atmosphere, magnetic configurations are bounded and / or inhomogeneous in the direction of wave propagation. These additional boundary conditions may reduce (or even prevent) the generation of mean shear flows by resonant absorption.

It is worth mentioning that when an Alfvén resonance is present there may exist a slow resonance coupled to it. If this happens (and the timescales of development are comparable), both resonances will generate their own mean shear flows which could become superimposed. This may enhance the flow through constructive superposition, but equally, they may interact destructively leaving a reduced overall combined generated mean shear flow. In other words, it is possible to see a more efficient coupled dissipative layer create more heating, but actually generate a smaller amplitude mean shear flow compared with two separate dissipative layers.

If the boundary conditions allow the generation of mean shear flows by resonant absorption in the solar atmosphere, we would expect to see these flows superimposed on existing large scale motions. It is speculated that these mean shear flows (if set up) superimposed on existing bulk motion of the plasma would produce turbulent motions and create a Kelvin–Helmholtz instability (KHI) along the Alfvén dissipative layer. A KHI instability may already exist due to the shear velocity field of Alfvén waves as was shown by Ofman and Davila (1995); Terradas et al. (2008). The generation of mean shear flow would survive the instability due to the velocity shear and, hence, will still contribute to the bulk motion causing larger shear, and perhaps creating a secondary instability. Either way, the KHI would distort the dissipative layer, locally enhancing the dissipation (due to enhanced transport coefficients), which in turn would produce greater amplitude mean shear flows. This process of feedback would continue until either; (i) the wave is dissipated, or (ii) the turbulence destroys the dissipative layer. Either way, the turbulence would allow greater absorption and achieve heating over a greater area (here the development of turbulent eddies can be seen as a means of heat transport).

The resonant absorption itself may not produce the heating we see in the solar corona, but we believe it is likely that these dissipative layers are created and KHI are formed. The KHI might be able to trigger small scale reconnection events (nanoflaring) if the mean shear flows produced by resonant absorption become strong enough. However, further study and observations are required before we can make more definitive investigations.

# 6

# Nonlinear resonant absorption of fast magnetoacoustic waves in strongly anisotropic and dispersive plasmas

*The nonlinear theory of driven magnetohydrodynamics (MHD) waves in strongly anisotropic and dispersive plasmas, developed for slow resonance in Chapter 3 and Alfvén resonance in Chapter 4, is used to study the weakly nonlinear interaction of fast magnetoacoustic (FMA) waves in a one-dimensional planar plasma. The magnetic configuration consists of an inhomogeneous magnetic slab sandwiched between two regions of semi-infinite homogeneous magnetic plasmas. Laterally driven FMA waves penetrate the inhomogeneous slab interacting with the localized slow or Alfvén dissipative layer and are partly reflected, dissipated and transmitted by this region. The nonlinearity parameter defined by Eq. (2.58) is assumed to be small and a regular perturbation method is used to obtain analytical solutions in the anisotropic slow dissipative layer. We find that the effect of dispersion in the slow dissipative layer is to further decrease the coefficient of energy absorption, compared to its standard weakly nonlinear counterpart, along with the generation of higher harmonics in the outgoing wave in addition to the fundamental one. The absorption of external drivers at the Alfvén resonance is described within the linear MHD with great accuracy. We also, briefly, investigate the effect of equilibrium flow on the resonant absorption of FMA waves in anisotropic dissipative layers. The results of the present chapter were published in Physics of Plasmas (Clack and Ballai, 2009b).*

*No nature except an extraordinary one could ever easily formulate a theory.*
**(Plato** 429 – 347**BC)**

## 6.1 Introduction

The problem of interacting fast magnetoacoustic (FMA) waves with different magnetic structures is not only important in the context of astrophysics and solar physics, but also in laboratory plasma devices. Space and laboratory plasmas are highly non-uniform and dynamical systems and as a consequence they are a natural medium for magnetohydrodynamic (MHD) waves. As discussed before, in the context of solar and space physics, the process of resonant coupling of waves provides a means of extracting wave energy and converting the energy into heat by, e.g. dissipation.

Many studies of resonant absorption have been attempted (see, e.g. Davila, 1987; Ruderman et al., 1997c; Ballai et al., 1998a; Erdélyi, 1998; Erdélyi and Ballai, 1999; Peter and Vocks, 2003), but considered only the sound (or slow) and Alfvén waves as excellent candidates for coronal heating. Alfvén waves can only carry energy along the magnetic field lines and slow waves are only able to carry $1-2\%$ of energy under coronal (low plasma-$\beta$) conditions. However, FMA waves might have an important role in explaining the coronal temperatures, as has been shown by, e.g. Čadež et al. (1997); Csík et al. (1998). One of the critical features of FMA waves is their ability to propagate across the magnetic field, a feat not matched by the slow or Alfvén waves.

Recall that in Sect. 1.3 we discussed that for all AC heating mechanisms to occur a wave has to arrive at a region of interest. We stated that the waves, in this case FMA waves, can arrive from the photosphere below due to magnetic shuffling. The energy flux density of FMA waves required for significant heating is of the order of 100 $\mathrm{Jm^{-2}s^{-1}}$ at the base of the corona. This is not entirely inconsistent with the upper limit on acoustic waves of 10 $\mathrm{Jm^{-2}s^{-1}}$ (see, e.g. Athay and White, 1978), provided the magnetic field at the base is sufficiently large, e.g. $> 10^{-3}$T. However, we did discuss that it is possible for the FMA waves (along with Alfvén and slow waves) to be produced within the corona itself, a process known as *nanoflaring* (or flaring, in general). The production of waves within the corona alleviates many of the constraints on finding sufficient energy in waves to provide the heating for the corona.

Unfortunately, there are still a few questions to be answered here. Nanoflaring, so far, has only been observed in one study by Reale et al. (2009). The lack of observations could be due to the nanoflares' highly localized nature. Even if we extend the theory to readily observable events, such as microflares, blinkers, etc., we cannot be certain of the energy requirement for heating being met by explosive events (see, e.g. Aschwanden et al., 1999b). We, however, assume the amount of energy required for heating is available in the magnetic energy stored by the shuffling of the footpoints in the photosphere. Hence, the necessary supplementary heating may come from reconnection driven, locally generated MHD waves (see, e.g. Erdélyi and Ballai, 2001). Studies by Roussev et al. (2001a,b,c) have carried out numerical simulations, experiments and observations of explosive events where reconnection has excited and driven FMA waves, but did not comment on the dissipation of the waves produced.

The aim of the present chapter is to study the nonlinear (linear) resonant interaction of externally driven FMA waves with the slow (Alfvén) dissipative layer in strongly anisotropic and dispersive static plasmas. The governing equations and jump conditions, derived earlier in Chapters 3 and 4, will be used to study the efficiency of absorption at the slow and Alfvén resonance.

## 6.2 Governing equations and assumptions

The dynamics and absorption of the waves will be studied in a Cartesian coordinate system. The equilibrium state is shown in Figure 6.1. The configuration consists of an inhomogeneous magnetized plasma $0 < x < x_0$ (Region II) sandwiched between two semi-infinite homogeneous magnetized plasmas $x < 0$ and $x > x_0$ (labelled as Regions I and III, respectively). This model was chosen as theoretical results earlier in the present thesis are ready to be applied in this form. Our intention is to have a model which gives us the trend in the absorption of an incident wave on a magnetic structure. It is obvious that real magnetic structures are far more complicated (and far from being fully understood), however, the magnetic field has been simplified to be unidirectional in order to make the model more transparent, such that the role of the dispersion at the resonance and the change in the absorption can be investigated more fully, and compared to previous studies. We took inspiration for this model from studies such as, e.g. Roberts (1981b); Edwin and Roberts (1982); Ruderman et al. (1997c); Ballai et al. (1998a); Ballai (2000); Ruderman (2000); Erdélyi and Ballai (2001).

The equilibrium density and pressure are denoted by $\rho$ and $p$. The equilibrium magnetic field, **B**, is unidirectional and lies in the $yz-$plane (just as in previous chapters). In what follows the subscripts $'e'$, $'0'$ and $'i'$ denote the equilibrium quantities in the three regions (Regions I, II, III, respectively). The components of the equilibrium magnetic field are given in Eq (3.3) and all equilibrium quantities are continuous at the boundaries of Region II, so they satisfy the equation of total pressure balance

$$p_e + \frac{B_e^2}{2\mu_0} = p_0(x) + \frac{B_0^2(x)}{2\mu_0} = p_i + \frac{B_i^2}{2\mu_0}. \tag{6.1}$$

It follows from the equation of total pressure that the density ratio between Regions I and III satisfy the relation

$$\frac{\rho_i}{\rho_e} = \frac{2c_{S_e}^2 + \gamma v_{A_e}^2}{2c_{S_i}^2 + \gamma v_{A_i}^2}, \tag{6.2}$$

where the squares of the Alfvén and sound speed are given in Sect. 2.5. We have replaced the subscript $'0'$ with $'e'$ for Region I and $'i'$ for Region III. We consider a hot magnetized plasma such that $c_{S_i}^2 > c_{S_e}^2$, and $v_{A_i}^2 > v_{A_e}^2$.

The objective of the present chapter is to study (i) the combined effect of nonlinearity and dispersion on the interaction of incoming *fast waves* with *anisotropic slow dissipative layers* and (ii) the interaction of incoming *fast waves* with *anisotropic Alfvén dissipative layers*. We, therefore, have two different criteria to be satisfied in order that resonant absorption takes place. First of all, we need to assume that there is no overlap between the slow and Alfvén continua, i.e. $\min[\omega_A(r)] - \max[\omega_C(r)] > 0$. For interaction of FMA waves with the slow dissipative layer we assume that the frequency of the incoming fast wave is within the slow continuum of the inhomogeneous plasma, so that there is a slow resonant position at $x = x_c$ in Region II. Interactions with the Alfvén dissipative layer leads to the assumption that the frequency of the incoming fast wave is within the Alfvén continuum of the inhomogeneous plasma, so that there is an Alfvén resonant point at $x = x_a$ in Region II. At the slow resonance, this leads to the inequality,

$$c_{T_e} < \frac{\omega}{k} < c_{T_i}, \tag{6.3}$$

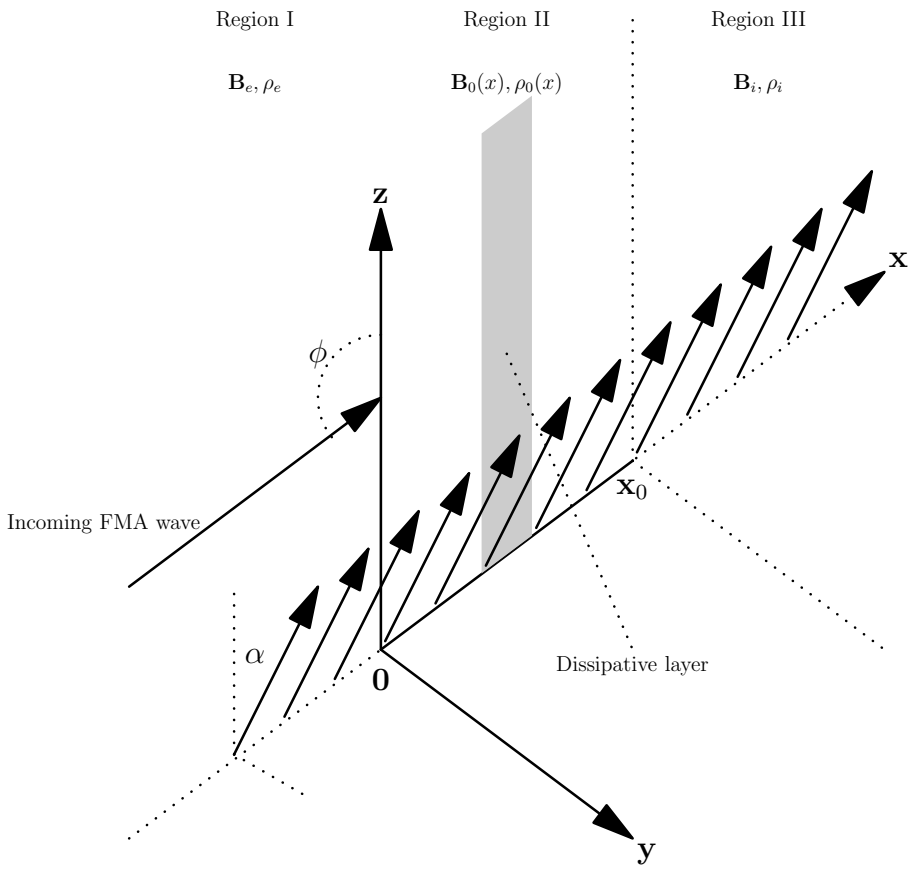


Figure 6.1: Illustration of the equilibrium state. Regions I ($x < 0$) and III ($x > x_0$) contain a homogeneous magnetized plasma and Region II ($0 < x < x_0$) an inhomogeneous magnetized plasma. The shaded strip shows the dissipative layer embracing the ideal resonant position at $x_a$ or $x_c$.

while at the Alfvén resonance, we have

$$v_{A_e} < \frac{\omega}{k} < v_{A_i}. \tag{6.4}$$

Here $\omega$ is the frequency of the incoming fast wave and $k = (k_x^2 + k_z^2)^{1/2}$ is the wave number. Even though, in principle, when a slow resonance occurs in this manner an Alfvén resonance is also present we ignore the Alfvén resonance that occurs alongside the slow resonance as this would complicate the analysis and obscure the results associated with the slow resonance. We study the Alfvén resonance separately to the slow resonance. We note that the Alfvén resonance would, in simple terms, act to *restrict the energy* available at the slow resonance. In this way we can treat the two resonances separately. We intend to address the issue of coupled resonances in Chapter 7, where we will show that the governing equations derived here remain the same (meaning the work here is valid), however, the interaction of the waves between the resonant positions changes the absorption of wave energy.

In an attempt to remove other effects from the analysis we consider the incoming fast wave to be entirely in the $xz-$plane, i.e. $k_y = 0$. In Ruderman et al. (1997c) it is suggested that aligning the equilibrium magnetic field with the $z-$axis will remove the Alfvén resonance (if we consider planar waves) from the analysis of the slow resonance, however, this is not possible nor necessary

here. The dispersion is dependent on the angle ($\alpha$) between the equilibrium magnetic field and the $z-$axis , hence if $\alpha = 0$ the dispersion effects disappear, and we recover the governing equation derived by Ballai et al. (1998b).

Inequalities (6.3) and (6.4) guarantee that the slow and Alfvén resonances appears in Region II when studying in the upper chromosphere and the solar corona, respectively. The resonant positions, therefore, are defined mathematically as $\omega_c = kc_T(x_c)\cos\alpha$ and $\omega_a = kv_A(x_a)\cos\alpha$, which is identical to their definitions in Chapters 3 and 4. The inequalities (6.3) and (6.4) also provides us with some information about the plasma condition. First, in conjunction with Eq. (6.2) we obtain that

$$\frac{\rho_i}{\rho_e} = \frac{2c_{S_e}^2 + \gamma v_{A_e}^2}{2c_{S_i}^2 + \gamma v_{A_i}^2} < 1. \tag{6.5}$$

Hence, the plasma in region III is more rarefied than in Region I, with $c_{T_e} < c_{T_i}$ and the plasma in Region III is hotter than the plasma in Region I.

The dispersion relation for the impinging propagating fast waves takes the form (see, e.g. Ballai, 2000; Erdélyi and Ballai, 2001)

$$\frac{\omega^2}{k^2} = \frac{1}{2}\left\{\left(v_A^2 + c_S^2\right) + \left[\left(v_A^2 + c_S^2\right)^2 - 4v_A^2 c_S^2\cos^2\phi\right]^{1/2}\right\}, \tag{6.6}$$

where $\phi$ is the angle between the direction of propagation and the background magnetic field within the $xz-$plane and $\mathbf{k} = k_x\mathbf{e}_x + k_z\mathbf{e}_z$. For the sake of simplicity, we denote $\kappa_e$ as the ratio $k_x/k_z$. Since the equilibrium magnetic field in the $xz-$plane is aligned with the $z-$axis, the dispersion relation (6.6) becomes

$$\frac{\omega^2}{k^2} = \frac{1}{2}\left\{\left(v_A^2 + c_S^2\right) + \left[\left(v_A^2 + c_S^2\right)^2 - 4\frac{v_A^2 c_S^2}{1+\kappa_e^2}\right]^{1/2}\right\}, \tag{6.7}$$

where $1 + \kappa_e^2 = 1/\cos^2\phi$.

We assume that the plasma is *strongly* magnetized in the three regions, such that the conditions $\omega_{i(e)}\tau_{i(e)} \gg 1$ are satisfied. Due to the strong magnetic field, transport processes are derived from Braginskii's stress tensor (see Sect. 2.4). As we deal with two separate types of resonances (slow and Alfvén), we will need to choose the particular dissipative process which is most efficient for these waves. Recall that for slow waves, it is a good approximation to retain only the first term of Braginksii's expression for viscosity, given by Eq. (2.29). In addition, in the solar upper atmosphere slow waves are sensitive to thermal conduction so we have to include $\mathcal{L} = \nabla\cdot\mathbf{q}$ in Eq. (2.7), however, as explained by Ruderman et al. (1996), we do not include thermal radiation. We must also include dispersion due to Hall conduction at the slow resonance, as shown by Appendix A. On the other hand, since Alfvén waves are transversal and incompressible they are affected by the second and third components of Braginskii's stress tensor, provided by Eq. (2.30). Finally, Alfvén waves are efficiently damped by finite electrical conductivity, which becomes anisotropic under coronal conditions. The parallel and perpendicular components, however, only differ by a factor of 2, so we will only consider one of them without loss of generality. All other transport mechanisms can be neglected (see Sect. 2.4).

The dynamics of nonlinear resonant MHD waves in anisotropic and dispersive plasmas was studied in Chapters 3 and 4. We derived the governing equations and connection formulae necessary to study resonant absorption in slow / Alfvén dissipative layers. The efficiency of dissi-

pation, when studying anisotropic slow dissipative layers, in an anisotropic plasma is given by the (compressional) viscous Reynolds number and the Péclet number, combining to define the compressional total Reynolds number, defined in Eq. (2.54). The efficiency of dissipation, when studying anisotropic Alfvén dissipative layers is measured in a slightly different way. Now dissipative processes are described by the shear viscous Reynolds number and the magnetic Reynolds number, combining to define the shear total Reynolds number, provided by Eq. (2.55).

As we have stated a few times now, under chromospheric and coronal conditions $R \gg 1$, which means that dissipation is only important inside the dissipative layer. Far away from the dissipative layer amplitudes are small, therefore we can use the linear ideal MHD equations to describe the plasma motions far from the resonant position. These equations can be reduced to a system of coupled first order PDE's for the total pressure perturbation and the normal component of the velocity shown in Eq. (3.20). Inside the thin dissipative layers (where the dynamics is described by the nonlinear and dissipative MHD equations) embracing the ideal resonant surfaces ($x = x_c$ or $x = x_a$) we must use the governing equations derived in Chapters 3 and 4. The characteristic thickness of the anisotropic slow dissipative layer, $\delta_c$, is given by Eq. (3.55), while the characteristic thickness of the anisotropic Alfvén dissipative layer, $\delta_a$, is written in Eq. (5.33).

Here we need to make a note: the two nonlinearity parameters defined by Eqs (2.58) and (2.57) are different not only in their form but also in the values the total Reynolds numbers take. In the case of slow waves, the compressional total Reynolds number that corresponds to a characteristic length of 200Mm, a speed of 200kms$^{-1}$, a density of $10^{-13}$kgm$^{-3}$ and a compressional viscosity coefficient of $5 \times 10^{-2}$kgm$^{-1}$s$^{-1}$ is $R_c \approx 80$. Alfvén waves are efficiently damped by shear viscosity which is given by the second and third coefficients of the Bragisnkii's tensor. Since $\eta_1 = \eta_0/(\omega_i\tau_i)^2$ and under coronal conditions $\omega_i\tau_i$ is of the order of $10^5$, we obtain that the coefficient of shear viscosity is about 10 orders of magnitude smaller than the coefficient of compressional viscosity. Now, using the characteristic speed of 1000kms$^{-1}$, the shear total Reynolds number used in calculating the nonlinear parameter in the case of Alfvén nonlinearity is $R_a \approx 4 \times 10^{12}$.

The dimensionless governing equation inside the anisotropic slow dissipative layer is contained in Eq. (3.60). In the governing equation, the first term appears due to the inhomogeneity in the cusp speed, the second term describes the nonlinearity of waves, the third term stands for the dissipative effects while the last term on the left-hand side describes the nonlinear dispersive effects generated after taking into account Hall currents. The term on the right-hand side can be considered as a driver. We also note that $q_c(\sigma_c, \theta)$ is the dimensionless component of velocity parallel to the equilibrium magnetic field. The dimensionless equation governing wave dynamics in the anisotropic Alfvén dissipative layer is provided by Eq. (5.36). Here $q_a(\sigma_a, \theta)$ is the dimensionless component of velocity perpendicular to the equilibrium magnetic field.

When studying resonant MHD waves, we are generally not interested in the solution inside the dissipative layer and can consider the dissipative layer as a surface of discontinuity. Instead, we solve the system (3.20) and match the solutions at the boundaries of the discontinuity using connection formulae. These connection formulae determine the jumps in $u$ and $P$ across the dissipative layer. In the context of solar plasmas, it was shown that the first connection formula, for both the slow and Alfvén resonance, is $[P] = 0$, where the square brackets denote the jump across the dissipative layer. The jump condition for the total pressure will take a more complicated form for a more complex magnetic configuration (e.g. twist). The second connection formula for slow resonance can only be written in the implicit form of Eq. (3.65). In an attempt to follow the same procedure utilized for finding solutions at the slow resonance we can write the jump in the nor-

mal component of velocity for the Alfvén resonance in an implicit form. For the sake of brevity, we do not show the derivation here, but it follows the procedure to find the jump in the normal component of velocity completed in Sect. 3.4. This jump is given by

$$[u_a] = \frac{V \sin\alpha}{k} \mathcal{P} \int_{-\infty}^{\infty} \frac{\partial q_a}{\partial \theta} \, d\sigma_a. \tag{6.8}$$

Finally, we should note some critical assumption we make to allow analytical progress. From the very beginning we must assume that the nonlinearity parameter in Eq. (2.58) is small so that regular perturbation theory can be applied at the slow resonance. We also assume that the inhomogeneous region is thin in comparison with the wavelength of the impinging wave, i.e. $kx_0 \ll 1$. Ruderman (2000) investigated the absorption of sound waves at the slow dissipative layer in the limit of strong nonlinearity. In his analysis nonlinearity dominated dissipation in the *resonant layer* which embraces the dissipative layer. He concluded that nonlinearity decreases absorption in the long wavelength approximation, but increases it at intermediate values of $kx_0$, however, the increase is never more than 20%. To the best of our knowledge, at present, we cannot solve the governing equation (3.60) in the limit of strong nonlinearity due to the nonlinear dispersive term, therefore we restrict our analysis to the weak nonlinear limit. We mention that no such assumptions are needed for studying the Alfvén dissipative layer since the governing equation (5.36) is linear.

## 6.3 Solutions outside the dissipative layer

In what follows we derive a solution for the system (3.20) in Regions I, II and III. In Region II we only find the solution outside the dissipative layers. Section 6.4 is devoted to finding a solution to Eq. (3.60) inside the anisotropic slow dissipative layer and Sect. 6.5 is used to find a solution to Eq. (5.36) inside the anisotropic Alfvén dissipative layer. Outside the dissipative layers the solutions take identical forms because they are governed by the same equation.

### 6.3.1 Region I

The solution of Eq. (3.20) in Region I is given in the form of an incoming and outgoing fast wave of the form

$$P = \epsilon \left\{ p_e \cos\left[k\left(\theta + \kappa_e x\right)\right] + A \cos\left[k\left(\theta - \kappa_e x\right)\right] \right\}, \tag{6.9}$$

$$u = \frac{\epsilon \kappa_e V}{\rho_e \left(V^2 - v_{A_e}^2 \cos^2\alpha\right)} \left\{ p_e \cos\left[k\left(\theta + \kappa_e x\right)\right] - A \cos\left[k\left(\theta - \kappa_e x\right)\right] \right\}, \tag{6.10}$$

where $\epsilon \ll 1$ is the dimensionless amplitude of perturbation far from the dissipative layer. The frequency of the incoming wave is given by Eq. (6.7) and must lie within the slow or Alfvén continuum depending on which dissipative layer we are studying. The first term in the braces in Eqs (6.9) and (6.10) describes the incoming wave, while the second term describes the outgoing wave which will be obtained in Sect. 6.4 for anisotropic slow dissipative layers and in Sect. 6.5 for anisotropic Alfvén dissipative layers.

### 6.3.2 Region II

In Region II, the equation for the total pressure, $P$, is obtained by eliminating $u$ from the system (3.20),

$$\widetilde{F}\frac{\partial}{\partial x}\left[\frac{1}{\rho_0\left(V^2-v_A^2\cos^2\alpha\right)}\frac{\partial P}{\partial x}\right]=\frac{\partial^2 P}{\partial\theta^2}, \tag{6.11}$$

where

$$\widetilde{F}(x)=\frac{\rho_0(x)\left[v_A^2(x)+c_S^2(x)\right]\left[V^2-v_A^2(x)\cos^2\alpha\right]\left[V^2-c_T^2(x)\cos^2\alpha\right]}{V^4-V^2\left[v_A^2(x)+c_S^2(x)\right]+v_A^2(x)c_S^2(x)\cos^2\alpha}.$$

Since we have assumed that $kx_0\ll 1$, the ratio of the right-hand side and the left-hand side is of the order of $k^2x_0^2$. It follows that

$$\frac{\partial P}{\partial x}=\rho_0\left(V^2-v_A^2\cos^2\alpha\right)f(\theta)+\mathcal{O}(k^2x_0^2), \tag{6.12}$$

where the function $f(\theta)$ is determined by the second equation of (3.20) and the boundary conditions at $x=0$. Equation (6.12) yields

$$P=\widetilde{P}(\theta)+f(\theta)\int_0^x\rho_0\left[V^2-v_A^2\cos^2\alpha\right]dx+\mathcal{O}(k^2x_0^2). \tag{6.13}$$

The function $\widetilde{P}(\theta)$ has to be determined by the boundary conditions at $x=0$. It can be shown that, because $[P]=0$, the functions $f(\theta)$ and $\widetilde{P}(\theta)$ take the same values throughout Region II. Noting that the second term in Eq. (6.13) is of the order of $kx_0$ we can express $P$ in a simplified form as

$$P=\widetilde{P}(\theta)+(kx_0)\,P'(x,\theta)+\mathcal{O}(k^2x_0^2). \tag{6.14}$$

### 6.3.3 Region III

To derive the governing equation for Region III we eliminate the normal component of the velocity from the system (3.20) to arrive at

$$\frac{\partial^2 P}{\partial x^2}+\kappa_i^2\frac{\partial^2 P}{\partial\theta^2}=0, \tag{6.15}$$

where $\kappa_i^2$ is defined as

$$\kappa_i^2=-\frac{V^4-V^2\left(c_{S_i}^2+v_{A_i}^2\right)+c_{S_i}^2v_{A_i}^2\cos^2\alpha}{\left(c_{S_i}^2+v_{A_i}^2\right)\left(V^2-c_{T_i}^2\cos^2\alpha\right)}. \tag{6.16}$$

Since, for anisotropic slow dissipative layers, $V<c_{T_i}\cos\alpha$, it follows that $\kappa_i^2>0$. It also follows that for anisotropic Alfvén dissipative layers $\kappa_i^2>0$ because $V>c_{T_i}\cos\alpha>v_{A_e}\cos\alpha$. Therefore, Eq. (6.15) is an elliptical differential equation and the wave motion is evanescent in Region III. In reality, if $\kappa_i^2<0$, there could be wave leakage. The existence of wave leakage depends on the profile of the slow and Alfvén speeds in the inhomogeneous region (Region II). For simplicity, we have assumed that the slow and Alfvén resonances take place at a single location (obviously different for the two resonances), which means the profiles of the slow and Alfvén speeds are monotonically increasing inside Region II. Should we have a more complex model, the possibility of wave leakage would need to be taken into account.

## 6.4 Weak nonlinear solution inside the slow dissipative layer

Since we are not able to solve the governing equation (3.60) inside the anisotropic slow dissipative layer analytically, we consider the limit of weak nonlinearity ($N_c^2 \ll 1$). In accordance with this assumption we rewrite the governing equation (3.60) and the jump condition (3.65) as

$$\sigma_c \frac{\partial \overline{q}_c}{\partial \theta} + \epsilon^{-1} \zeta \left( \frac{\Lambda}{\Psi} \right) \overline{q}_c \frac{\partial \overline{q}_c}{\partial \theta} - \epsilon^{-1} \zeta \frac{\partial \overline{q}_c}{\partial \sigma_c} \frac{\partial \overline{q}_c}{\partial \theta} - k^{-1} \frac{\partial^2 \overline{q}_c}{\partial \theta^2} = - \frac{V^4}{\rho_{0_c} v_{A_c}^4 |\Delta_c| x_0} \frac{dP_c}{d\theta}, \tag{6.17}$$

$$[u_c] = - \frac{V x_0}{\cos^2 \alpha} \mathcal{P} \int_{-\infty}^{\infty} \frac{\partial \overline{q}_c}{\partial \theta} \, d\sigma_c, \tag{6.18}$$

where

$$\overline{q}_c = \frac{q_c}{k x_0}, \quad \zeta = \frac{k x_0 D_d^2 \Psi}{R_c^4}, \quad D_d^2 = \epsilon R_c^4 = R_c^2 N_c^2. \tag{6.19}$$

Note that $\zeta$ is of the order of $\epsilon R_c^2$, the ratio $(\Lambda/\Psi)$ is of the order of unity and $\overline{q}_c$ is of the order of $\epsilon$. In what follows we drop the bar notation on the dimensionless variable $q_c$.

We proceed by using a regular perturbation method and look for solutions in the form

$$f = \epsilon \sum_{n=1}^{\infty} \zeta^{n-1} f_n, \tag{6.20}$$

where $f$ represents any of the quantities $P$, $u$ and $q$.

### 6.4.1 First order approximation

In the first order approximation, from Eq. (6.17), we obtain

$$\sigma \frac{\partial q_{1_c}}{\partial \theta} - k^{-1} \frac{\partial^2 q_{1_c}}{\partial \theta^2} = - \frac{V^4}{\rho_{0_c} v_{A_c}^4 |\Delta_c| x_0} \frac{dP_{1_c}}{d\theta}. \tag{6.21}$$

Since the total pressure, $P$, is continuous throughout the dissipative layer *and* is periodical with respect to $\theta$, we look for a solution in the form

$$g_1 = \Re(\hat{g}_1 e^{ik\theta}), \tag{6.22}$$

where $g_1$ represents $P_1$, $u_1$ and $q_{1_c}$ and $\Re$ indicates the real part of a quantity.

In Region I the solutions for the pressure and velocity exactly recover the results found in linear theory, i.e.

$$\hat{P}_1 = p_e e^{ik\kappa_e x} + A_{1_c} e^{-ik\kappa_e x}, \quad \hat{u}_1 = \frac{\kappa_e V \left( p_e e^{ik\kappa_e x} - A_{1_c} e^{-ik\kappa_e x} \right)}{\rho_e \left( V^2 - v_{A_e}^2 \cos^2 \alpha \right)}, \tag{6.23}$$

where $A_{1_c}$ (and subsequent values of $A_{i_c}$) is the amplitude of the outgoing wave. The first terms of the right-hand side of $\hat{P}_1$ and $\hat{u}_1$ represent the incoming wave, while the second terms are the outgoing (reflected) wave. The continuity of the total pressure perturbation at $x = 0$ and $x = x_0$ in combination with Eq. (6.14) yields $\hat{P}_1$, in Region II, as

$$\hat{P}_1 = p_e + A_{1_c} + (k x_0) \hat{h}_1, \tag{6.24}$$

where $\hat{h}_n = \hat{h}_n(x) = \hat{P}'_n(x) - \hat{P}'_n(0), \quad n \geq 1$. The solution in Region III is obtained by using Eqs (3.20), (6.15) and (6.24) with the continuity conditions at $x = x_0$. The solution takes the form

$$\hat{P}_1 = \left\{p_e + A_{1_c} + (kx_0)\hat{h}_1\right\} e^{-k\kappa_i(x-x_0)}, \quad \hat{u}_1 = \frac{i\kappa_i V\left\{p_e + A_{1_c} + (kx_0)\hat{h}_1\right\}}{\rho_i\left(V^2 - v_{A_i}^2\cos^2\alpha\right)} e^{-k\kappa_i(x-x_0)}. \quad (6.25)$$

Utilizing the fact that $\hat{u}_1$ is continuous at $x = 0$ and $x = x_0$, and employing Eqs (3.20) and (6.24) we find that the jump in the normal component of velocity across the dissipative layer is

$$[\hat{u}_1] = \frac{i\kappa_i V(p_e + A_{1_c})}{\rho_i\left(V^2 - v_{A_i}^2\cos^2\alpha\right)} - \frac{\kappa_e V(p_e - A_{1_c})}{\rho_e\left(V^2 - v_{A_e}^2\cos^2\alpha\right)} - ikV\left(p_e + A_{1_c}\right)\mathcal{P}\int_0^{x_0}\frac{1}{\widetilde{F}(x)}\,dx - ikV(kx_0)\mathcal{P}\int_0^{x_0}\frac{\hat{h}_1(x)}{\widetilde{F}(x)}\,dx, \quad (6.26)$$

where the expression of $\widetilde{F}(x)$ is given by Eq. (3.21).

Solving Eq. (6.21) reveals $\hat{q}_{1_c}$ to be

$$\hat{q}_{1_c} = -\frac{V^4\left(p_e + A_{1_c}\right)\{1 + \mathcal{O}(kx_0)\}}{\rho_{0_c} v_{A_c}^2 |\Delta_c| x_0\left(\sigma_c - i\right)}. \quad (6.27)$$

Substitution of Eq. (6.27) into Eq. (6.18) leads to another definition of the jump in the normal component of velocity across the anisotropic slow dissipative layer, namely,

$$[\hat{u}_{1_c}] = \frac{-\pi k V^5\left(p_e + A_{1_c}\right)\{1 + \mathcal{O}(kx_0)\}}{\rho_{0_c} v_{A_c}^4 |\Delta_c|\cos^2\alpha}. \quad (6.28)$$

Comparing Eqs. (6.26) and (6.28) we obtain that

$$A_{1_c} = -p_e\frac{\tau_c - \mu + i\upsilon}{\tau_c + \mu + i\upsilon} + \mathcal{O}(k^2x_0^2), \quad (6.29)$$

where

$$\tau_c = \frac{\pi k V^5}{\rho_{0_c} v_{A_c}^4 |\Delta_c|\cos^2\alpha}, \quad \mu = \frac{\kappa_e V}{\rho_e\left(V^2 - v_{A_e}^2\cos^2\alpha\right)},$$
$$\upsilon = \frac{\kappa_i V}{\rho_i\left(V^2 - v_{A_i}^2\cos^2\alpha\right)} - kV\mathcal{P}\int_0^{x_0}\frac{1}{\widetilde{F}(x)}\,dx. \quad (6.30)$$

When deriving Eq. (6.29) we have employed the estimate that

$$k\mathcal{P}\int_0^{x_0}\frac{\hat{h}_n(x)}{\widetilde{F}(x)}\,dx = \mathcal{O}(kx_0). \quad (6.31)$$

The quantity $A_{1_c}$ is complex which means that the outgoing (reflected) wave has a phase alteration compared with the incoming wave. The *true amplitude* of the outgoing wave is given by $\widetilde{A}_{1_c} = (A_{1_c(r)}^2 + A_{1_c(im)}^2)^{1/2}$ (where the subscripts 'r' and 'im' mean the real and imaginary parts, respectively). The Fourier analysis allows $A_{1_c}$ to be complex. In general, a complex value of $A_{n_c}$ means the true amplitude of the outgoing harmonic is defined as above and a phase of the outgoing wave is shifted by $\tan^{-1}(A_{n_c(im)}^2/A_{n_c(r)}^2)$. This definition of $A_{n_c}$ applies to all subsequent orders of approximation.

In the studies by Ruderman et al. (1997c) and Ballai et al. (1998a) a similar procedure was

carried out. Our results are similar with theirs if we consider $B_e = 0$ and $\alpha = 0$. This conclusion is not surprising because the first order approximation with respect to $\zeta$ coincides with linear theory. In addition, dispersion due to the Hall effect at the slow resonance does not alter linear theory, since dispersion effects appear as a nonlinear term in the governing equation.

### 6.4.2 Second order approximation

Nonlinear effects start to be important from the second order approximation onwards, but they are always due to the nonlinear combination of lower order harmonics. In this order of approximation Eq. (6.17) is reduced to

$$\sigma_c \frac{\partial q_{2_c}}{\partial \theta} - k^{-1} \frac{\partial^2 q_{2_c}}{\partial \theta^2} = -\frac{V^4}{\rho_{0_c} v_{A_c}^4 |\Delta_c| x_0} \frac{dP_{2_c}}{d\theta} - q_{1_c} \frac{\partial q_{1_c}}{\partial \theta} + \frac{\partial q_{1_c}}{\partial \sigma_c} \frac{\partial q_{1_c}}{\partial \theta}. \tag{6.32}$$

Taking advantage of the form of the first order approximation terms enables us to rewrite the second term on the right-hand side of this equation as

$$q_{1_c} \frac{\partial q_{1_c}}{\partial \theta} = \Re \left( \frac{ik}{2} \hat{q}_{1_c}^2 e^{2ik\theta} \right). \tag{6.33}$$

Since the nonlinear terms are proportional to $\Re\left(e^{2ik\theta}\right)$, it is appropriate to seek a solution of the form

$$g_2 = \Re \left( \hat{g}_2 e^{2ik\theta} \right), \tag{6.34}$$

where $g_2$ represents any of the functions $P_2$, $u_2$ and $q_{2_c}$.

Using the same techniques as in the first order approximation, it is straightforward to find the jump in the normal component of velocity in Region II as

$$[\hat{u}_{2_c}] = \frac{i\kappa_i V A_{2_c}}{\rho_i \left(V^2 - v_{A_i}^2 \cos^2\alpha\right)} + \frac{\kappa_e V A_{2_c}}{\rho_e \left(V^2 - v_{A_e}^2 \cos^2\alpha\right)} - 2ikVA_{2_c} \mathcal{P} \int_0^{x_0} \frac{1}{\widetilde{F}(x)}\, dx - 2ikV(kx_0)\mathcal{P} \int_0^{x_0} \frac{\hat{h}_2(x)}{\widetilde{F}(x)}\, dx. \tag{6.35}$$

Using Eqs (6.27) and (6.33) we can solve Eq.(6.32) to obtain

$$\hat{q}_{2_c} = -\frac{1}{\sigma_c - 2i} \left[ \frac{V^4 A_{2_c}}{\rho_{0_c} v_{A_c}^4 |\Delta_c| x_0} + \frac{V^8 \left(p_e + A_{1_c}\right)^2 (1 + 4\Omega_2)}{4\rho_{0_c}^2 v_{A_c}^8 |\Delta_c|^2 x_0^2 (\sigma_c - i)^2} \right], \tag{6.36}$$

where $\Omega_2 = 1/(\sigma_C - i)$ is the additional factor due to the nonlinear dispersion (as are all subsequent values of $\Omega_i$, $i > 2$). We substitute the expression for $\hat{q}_{2_c}$ into Eq. (6.18) to find

$$[\hat{u}_{2_c}] = -\frac{2\pi k V^5 A_{2_c}}{\rho_{0_c} v_{A_c}^4 |\Delta_c| \cos^2\alpha}, \tag{6.37}$$

where the terms of the order of $k^2 x_0^2$ are not indicated. To calculate $A_{2_c}$ we compare the jump in the normal component of velocity across the anisotropic slow dissipative layer defined by Eqs (6.35) and (6.37). This leads to

$$A_{2_c} = \mathcal{O}(k^2 x_0^2). \tag{6.38}$$

This result implies that all quantities in the second order approximation (with respect to $\zeta$) are

zero outside the dissipative layer up to an accuracy of $\mathcal{O}(kx_0)$. With this restriction the outgoing wave remains monochromatic in the second order approximation. This result coincides with the results of Ruderman et al. (1997c), Ballai et al. (1998a),Erdélyi and Ballai (2001) and Ruderman (2000) [which is especially surprising because in this paper nonlinearity is strong].

### 6.4.3 Third order approximation

The third order approximation with respect to $\zeta$ is governed by

$$\sigma_c \frac{\partial q_{3_c}}{\partial \theta} - k^{-1} \frac{\partial^2 q_{3_c}}{\partial \theta^2} = -\frac{V^4}{\rho_{0_c} v_{A_c}^4 |\Delta_c| x_0} \frac{dP_{3_c}}{d\theta} - \frac{\partial (q_{1_c} q_{2_c})}{\partial \theta} + \frac{\partial q_{1_c}}{\partial \sigma_c} \frac{\partial q_{2_c}}{\partial \theta} + \frac{\partial q_{2_c}}{\partial \sigma_c} \frac{\partial q_{1_c}}{\partial \theta}. \quad (6.39)$$

Taking into account the form of the solutions in the previous two orders of approximation we can rewrite the second term on the right-hand side of Eq. (6.39) as

$$\frac{\partial (q_{1_c} q_{2_c})}{\partial \theta} = \frac{k}{2} \Re \left( 3i \hat{q}_{1_c} \hat{q}_{2_c} e^{3ik\theta} + i \hat{q}_{1_c}^* \hat{q}_{2_c} e^{ik\theta} \right), \quad (6.40)$$

where $q_{n_c} = \Re \left( \hat{q}_{n_c} e^{ink\theta} + \hat{q}_{n_c}^* e^{-ink\theta} \right)$ and the asterisk denotes a complex conjugate. This result inspires us to seek solutions in the third order approximation in the form

$$g_3 = \Re \left( \hat{g}_{31} e^{ik\theta} + \hat{g}_{33} e^{3ik\theta} \right), \quad (6.41)$$

where $g_3$ represents $P_3$, $u_3$ and $q_{3_c}$.

In Region I we obtain the solutions

$$\hat{P}_{31} = A_{31_c} e^{-ik\kappa_e x}, \quad \hat{u}_{31} = -\frac{\kappa_e V A_{31_c} e^{-ik\kappa_e x}}{\rho_e \left( V^2 - v_{A_e}^2 \cos^2 \alpha \right)}, \quad (6.42)$$

$$\hat{P}_{33} = A_{33_c} e^{-3ik\kappa_e x}, \quad \hat{u}_{33} = -\frac{\kappa_e V A_{33_c} e^{-3ik\kappa_e x}}{\rho_e \left( V^2 - v_{A_e}^2 \cos^2 \alpha \right)}. \quad (6.43)$$

Using the same method as in the first and second order approximations we find the amplitudes of total pressure perturbations to be

$$\hat{P}_{31} = A_{31_c} + (kx_0) \hat{h}_{31}, \quad \hat{P}_{33} = A_{33_c} + (kx_0) \hat{h}_{33}. \quad (6.44)$$

As a result, the normal velocities and pressure perturbations in region III, take the form

$$\hat{P}_{31} = \left\{ A_{31_c} + (kx_0) \hat{h}_{31} \right\} e^{-k\kappa_i (x - x_0)}, \quad \hat{u}_{31} = \frac{i\kappa_i V \left\{ A_{31_c} + (kx_0) \hat{h}_{31} \right\}}{\rho_i \left( V^2 - v_{A_i}^2 \cos^2 \alpha \right)} e^{-k\kappa_i (x - x_0)}, \quad (6.45)$$

$$\hat{P}_{33} = \left\{ A_{33_c} + (kx_0) \hat{h}_{33} \right\} e^{-3k\kappa_i (x - x_0)}, \quad \hat{u}_{33} = \frac{i\kappa_i V \left\{ A_{33_c} + (kx_0) \hat{h}_{33} \right\}}{\rho_i \left( V^2 - v_{A_i}^2 \cos^2 \alpha \right)} e^{-3k\kappa_i (x - x_0)}. \quad (6.46)$$

In a similar manner as the first and second order approximations, we find that the jumps in the

normal component of velocity across the anisotropic slow dissipative layer to be

$$[\hat{u}_{31_c}] = \frac{i\kappa_i V A_{31_c}}{\rho_i\left(V^2 - v_{A_i}^2\cos^2\alpha\right)} + \frac{\kappa_e V A_{31_c}}{\rho_e\left(V^2 - v_{A_e}^2\cos^2\alpha\right)} - ikVA_{31_c}\mathcal{P}\int_0^{x_0}\frac{1}{\widetilde{F}(x)}\,dx - ikV(kx_0)\mathcal{P}\int_0^{x_0}\frac{\hat{h}_{31}(x)}{\widetilde{F}(x)}\,dx, \quad (6.47)$$

$$[\hat{u}_{33_c}] = \frac{i\kappa_i V A_{33_c}}{\rho_i\left(V^2 - v_{A_i}^2\cos^2\alpha\right)} + \frac{\kappa_e V A_{33_c}}{\rho_e\left(V^2 - v_{A_e}^2\cos^2\alpha\right)} - 3ikVA_{33_c}\mathcal{P}\int_0^{x_0}\frac{1}{\widetilde{F}(x)}\,dx - 3ikV(kx_0)\mathcal{P}\int_0^{x_0}\frac{\hat{h}_{33}(x)}{\widetilde{F}(x)}\,dx. \quad (6.48)$$

To find $\hat{q}_{31_c}$ and $\hat{q}_{33_c}$ we must exploit Eqs (6.27), (6.36) and (6.40) to solve Eq. (6.39). The calculation is analogous to the first and second order approximation calculations and we arrive at the solutions

$$\hat{q}_{31_c} = -\frac{V^4 A_{31_c}}{\rho_{0_c} v_{A_c}^4 |\Delta_c| x_0\,(\sigma_c - i)} - \frac{V^{12}\,(p_e + A_{1_c})\,|p_e + A_{1_c}|^2\,(1 + 2\Omega_{31})}{8\rho_{0_c}^3 v_{A_c}^{12}|\Delta_c|^3 x_0^3\,(\sigma_c - i)^2\,(\sigma_c - 2i)\,(\sigma_c^2 + 1)}, \quad (6.49)$$

$$\hat{q}_{33_c} = -\frac{V^4 A_{33_c}}{\rho_{0_c} v_{A_c}^4 |\Delta_c| x_0\,(\sigma_c - 3i)} - \frac{V^{12}\,(p_e + A_{1_c})^3\,(3 + 2\Omega_{33})}{24\rho_{0_c}^3 v_{A_c}^{12}|\Delta_c|^3 x_0^3\,(\sigma_c - i)^3\,(\sigma_c - 2i)\,(\sigma_c - 3i)}, \quad (6.50)$$

where $\Omega_{31}$ and $\Omega_{33}$ are given by

$$\Omega_{31} = \Omega_2\frac{\sigma_c^3 - (8+7i)\sigma_c^2 - (11+12i)\sigma_c - (44-5i)}{(\sigma_c - 2i)\,(\sigma_c^2 + 1)},$$

$$\Omega_{33} = \Omega_2^2\frac{11\sigma_c^2 + (24-32i)\sigma_c - (21+44i)}{(\sigma_c - 2i)}.$$

We substitute these expressions for $\hat{q}_{31_c}$ and $\hat{q}_{33_c}$ to find a second definition for the jump in the normal component of velocity across the dissipative layer (up to an accuracy of $kx_0$)

$$[\hat{u}_{31_c}] = -\frac{\pi k V^5 A_{31_c}}{\rho_{0_c} v_{A_c}^4 |\Delta_c|\cos^2\alpha} + \frac{\pi k V^{13}\,(p_e + A_{1_c})\,|p_e + A_{1_c}|^2\,(27 - 8i)}{96\rho_{0_c}^3 v_{A_c}^{12}|\Delta_c|^3 x_0^2\cos^2\alpha}, \quad (6.51)$$

$$[\hat{u}_{33_c}] = -\frac{3kV^5 A_{33_c}}{\rho_{0_c} v_{A_c}^4 |\Delta_c| x_0}. \quad (6.52)$$

Similar to the first two orders of approximation, we can compare Eqs (6.47) and (6.48) with (6.51) and (6.52), respectively, to find the coefficients $A_{31_c}$ and $A_{33_c}$

$$A_{31_c} = \frac{p_e^3\tau_c^3\mu^3\,(27 - 8i)\cos^4\alpha}{12\pi^2 V^2 k^2 x_0^2\,(\mu + i\upsilon)^2\,(\mu^2 + \upsilon^2)}, \quad A_{33_c} = \mathcal{O}(k^2x_0^2). \quad (6.53)$$

When calculating $A_{31_c}$ we have used the estimates

$$\tau_c = \mathcal{O}(kx_0), \quad kV\mathcal{P}\int_0^{x_0}\frac{1}{\widetilde{F}(x)}\,dx = \mathcal{O}(kx_0),$$

and retain only the terms of lowest order with respect to $kx_0$, as we have assumed that $kx_0 \ll 1$.

Equation (6.53) illustrates that with an accuracy of up to $\mathcal{O}(kx_0)$ the outgoing (reflected) wave remains monochromatic in the third order of approximation (with respect to $\zeta$). Nevertheless, there is a slight alteration to the amplitude of the fundamental harmonic of the outgoing wave from $A_{1_c}$ to $A_{1_c} + \zeta^2 A_{31_c}$. These results coincide, qualitatively, with the findings of, e.g. Ruderman et al. (1997c); Ballai et al. (1998a); Erdélyi and Ballai (2001), however, $A_{31_c}$ is quantitatively larger than that of previous studies and has an imaginary component. This implies that the amplitude of the harmonic is greater and the phase of the correction is changed when compared with those studies. The expression for $A_{31_c}$, Eq. (6.53), is different to the ones they obtained because of the inclusion of dispersion through the Hall current.

### 6.4.4 Higher order approximations

In the fourth order of approximation the outgoing (reflected) wave becomes non-monochromatic. This means the energy from this order of approximation no longer contribute to the fundamental harmonic, but to a higher one. In the fourth order approximation Eq. (6.17) gives

$$\sigma_c \frac{\partial q_{4_c}}{\partial \theta} - k^{-1} \frac{\partial^2 q_{4_c}}{\partial \theta^2} = -\frac{V^4}{\rho_{0_c} v_{A_c}^4 |\Delta_c| x_0} \frac{dP_{4_c}}{d\theta} + \frac{\partial q_{2_c}}{\partial \sigma_c} \frac{\partial q_{2_c}}{\partial \theta} - \frac{\partial}{\partial \theta}\left( q_{1_c} q_{3_c} + \frac{1}{2} q_{2_c}^2 \right) + \frac{\partial q_{1_c}}{\partial \sigma_c} \frac{\partial q_{3_c}}{\partial \theta} + \frac{\partial q_{3_c}}{\partial \sigma_c} \frac{\partial q_{1_c}}{\partial \theta}. \quad (6.54)$$

We can rewrite the third term on the right-hand side of Eq. (6.54) using our knowledge about the first three orders of approximation, so

$$\frac{\partial}{\partial \theta}\left( q_{1_c} q_{3_c} + \frac{1}{2} q_{2_c}^2 \right) = k\Re\left\{ i\left( \hat{q}_{1_c} \hat{q}_{31_c} + \hat{q}_{1_c}^* \hat{q}_{33_c} \right) e^{2ik\theta} + i\left( 2\hat{q}_{1_c} \hat{q}_{33_c} + \hat{q}_{2_c}^2 \right) e^{4ik\theta} \right\}. \quad (6.55)$$

Equation (6.55) contains terms proportional to $e^{2ik\theta}$ and $e^{4ik\theta}$, so we can anticipate the solution to Eq. (6.54) to be of the form

$$g_4 = \Re\left( \hat{g}_{42} e^{2ik\theta} + \hat{g}_{44} e^{4ik\theta} \right), \quad (6.56)$$

where $g_4$ represents $P_4$, $u_4$ and $q_{4_c}$. We calculate the fourth order approximation to demonstrate that nonlinearity and dispersion in the anisotropic slow dissipative layer generates overtones in the outgoing (reflected) fast wave. For brevity, we shall only derive the terms proportional to $e^{2ik\theta}$, but for completeness we note that it can be shown that terms proportional to $e^{4ik\theta}$ are only present in the solution inside the dissipative layer.

Using the continuity conditions at $x = 0$ and $x = x_0$ we find the jump in the normal component of velocity across the dissipative layer to be

$$[\hat{u}_{42_c}] = \frac{i\kappa_i V A_{42_c}}{\rho_i \left( V^2 - v_{A_i}^2 \cos^2\alpha \right)} + \frac{\kappa_e V A_{42_c}}{\rho_e \left( V^2 - v_{A_e}^2 \cos^2\alpha \right)} - 2ikV A_{42_c} \mathcal{P} \int_0^{x_0} \frac{1}{\widetilde{F}(x)}\, dx - 2ikV(kx_0) \mathcal{P} \int_0^{x_0} \frac{\hat{h}_2(x)}{\widetilde{F}(x)}\, dx. \quad (6.57)$$

It is straightforward, but longwinded, to derive $\hat{q}_{42_c}$, so we skip all intermediate steps and give

the result

$$\hat{q}_{42_c} = \frac{-1}{\sigma_c - 2i}\left\{\frac{V^4 A_{42_c}}{\rho_{0_c} v_{A_c}^4 |\Delta_c| x_0} + \frac{V^8 (p_e + A_{1_c}) A_{31_c} (1+\Omega_2)}{2\rho_{0_c} v_{A_c}^8 |\Delta_c|^2 x_0^2 (\sigma_c - i)^2} + \frac{V^{16} (p_e + A_{1_c})^2 |p_e + A_{1_c}|^2 (12 - \Omega_{42})}{96\rho_{0_c}^4 v_{A_c}^{16} |\Delta_c|^4 x_0^4 (\sigma_c - i)^3 (\sigma_c - 3i)(\sigma_c^2 + 1)}\right\}, \quad (6.58)$$

with $\Omega_{42} = f(\sigma_c)$, where $f(\sigma_c) \to 0$ as $\sigma_c \to \infty$, is the contribution due to the Hall effect. As $\Omega_{42}$ is messy, longwinded and not essential for forthcoming calculations, its exact form is not given here. The substitution of $\hat{q}_{42_c}$ into Eq. (6.18) yields

$$[\hat{u}_{42_c}] = -\frac{2\pi k V^5 A_{42_c}}{\rho_{0_c} v_{A_c}^4 |\Delta_|} \cos^2\alpha + 0.082 \times \frac{\pi k V^{17} (p_e + A_{1_c})^2 |p_e + A_{1_c}|^2}{\rho_{0_c}^4 v_{A_c}^{16} |\Delta_c|^4 x_0^3} \cos^2\alpha, \quad (6.59)$$

Comparing Eqs. (6.57) and (6.59) we obtain that

$$A_{42_c} = 1.279 \times \frac{p_e^4 \tau_c^4 \mu^4 \cos^6\alpha}{\pi^3 V^3 k^3 x_0^3 (\mu + i\upsilon)^3 (\mu^2 + \upsilon^2)}. \quad (6.60)$$

Here we have used the same estimations that were utilized for calculating $A_{31_c}$ in the third order approximation and retain only the largest order terms with respect to $kx_0$. It is clear from this result that the outgoing wave becomes non-monochromatic in the fourth order approximation. We can also observe that the second harmonic appears in addition to the fundamental mode. This result parallels the results obtained by, e.g. Ruderman et al. (1997c); Ballai et al. (1998a). However, Eq. (6.60) shows that the *phase* is inverted and the *amplitude* of the second harmonic is approximately 30 times greater than theirs due to the presence of the Hall effect. Remember, though, that this amplitude is multiplied by a very small term, $\zeta^3$, which means the overall correction is very small.

Continuing calculations to even higher order approximations it can be shown that the higher order harmonics (third, fourth, etc.) are generated in the outgoing (reflected) fast wave. The pressure perturbation of the outgoing wave can be written as

$$P' = \epsilon \Re\left\{\sum_{n=1}^{\infty} \overline{A}_{n_c} e^{ink(\theta - \kappa_e x)}\right\}. \quad (6.61)$$

The second harmonic only appears in the outgoing wave in the fourth order approximation, whereas, higher harmonics appear in higher orders of approximation. This implies that the estimate $\overline{A}_{n_c} = \mathcal{O}(\zeta^3),\ n \geq 2$ is valid.

## 6.5 Solution inside the Alfvén dissipative layer

We can find the jump in the normal component of velocity at the Alfvén resonance explicitly, however, in an attempt to follow the procedure in the Sect. 6.4 (and to verify the theory), we proceed to use the implicit form of the jump conditions. As the governing equation (5.36) is linear we only need to calculate one order of approximation.

Although the Alfvén resonant position is at $x = x_a$, compared with $x = x_c$ for the slow resonant position, we can use some of the same formulae as in Sect. 6.4. First, we look for a

solution in the form of $g_1 = \Re(\hat{g}_1 e^{ik\theta})$. In Region I, we use Eq. (6.23) to represent the pressure and normal component of velocity perturbations. For Region II, due to the first connection formula, $[P] = 0$, we can write the pressure perturbation as Eq. (6.24). We also find that Eq. (6.25) can be used to represent the pressure and normal component of velocity perturbations in Region III. The fact we can employ the same equations (as in slow resonance) in the three regions leads to one of the definitions of the jump in the normal component of velocity over the anisotropic Alfvén dissipative layer being defined as Eq. (6.26). It should come as no surprise that this definition of the jump across the anisotropic Alfvén dissipative layer coincides with the jump across the anisotropic slow dissipative layer in the first order approximation. We are using linear theory to obtain both expressions and are not looking inside the, respective, dissipative layers', so the forms should be identical.

To find $\hat{q}_a$, so that we find the other definition of the jump in $u_a$, requires a different approach to the one used in the Sect. 6.4. After Fourier analyzing Eq. (5.36), we are left with

$$i\sigma\hat{q}_a - \frac{d^2\hat{q}_a}{d\sigma_a^2} = \frac{ik\sin\alpha}{\rho_{0_a}|\Delta_a|}P_a. \tag{6.62}$$

To solve Eq. (6.62) we introduce the Fourier transform with respect to $\sigma_a$:

$$\mathcal{F}[f(\sigma_a)] = \int_{-\infty}^{\infty} f(\sigma_a)e^{-i\sigma_a r}\, d\sigma_a. \tag{6.63}$$

Then from Eq. (6.62) we have

$$\frac{d\mathcal{F}[\hat{q}_a]}{dr} - r^2\mathcal{F}[\hat{q}_a] = -\frac{2\pi ik\sin\alpha\,(p_e + A_a)}{\rho_{0_a}|\Delta_a|}\delta(r), \tag{6.64}$$

where $\delta(r)$ is the delta-function. We find that the solution to Eq. (6.64) that is bounded for $|r| \to \infty$ is

$$\mathcal{F}[\hat{q}_a] = \frac{2i\pi k\sin\alpha(p_e + A_a)}{\rho_{0_a}|\Delta_a|}H(-r)e^{r^3/3}. \tag{6.65}$$

Here $H(r)$ denotes the Heaviside function. It was shown by Ruderman et al. (1997c) that

$$\mathcal{P}\int_{-\infty}^{\infty} f(\sigma_a)\, d\sigma_a = \frac{1}{2}\left(\lim_{r\to+0}\mathcal{F}[f] + \lim_{r\to-0}\mathcal{F}[f]\right). \tag{6.66}$$

With the aid of Eqs. (6.8), (6.65) and (6.66) we find that

$$[\hat{u}_a] = -\frac{\pi kV(p_e + A_a)\sin^2\alpha}{\rho_{0a}|\Delta_a|}. \tag{6.67}$$

Comparing Eqs. (6.26) and (6.67) we derive that

$$A_a = -p_e\frac{\tau_a - \mu + i\upsilon}{\tau_a + \mu + i\upsilon} + \mathcal{O}(k^2x_0^2), \tag{6.68}$$

where

$$\tau_a = \frac{\pi kV\sin^2\alpha}{\rho_{0_a}|\Delta_a|}, \tag{6.69}$$

and $\mu$ and $\upsilon$ have their forms given by Eq. (6.30). However, their values are different for the two resonances.

## 6.6 Coefficient of wave energy absorption

The coefficient of wave absorption is defined as

$$\Gamma = \frac{\Pi_{in} - \Pi_{out}}{\Pi_{in}}, \tag{6.70}$$

where $\Pi_{in}$ and $\Pi_{out}$ are the normal components of the energy fluxes, averaged over a period, of the incoming and outgoing waves, respectively. It is straightforward to obtain that

$$\Gamma = 1 - \frac{1}{p_e^2}\sum_{n=1}^{\infty} |\overline{A}_n|^2 \approx \Gamma_L + \zeta^2 \Gamma_{ND}, \tag{6.71}$$

where $\Gamma_L$ is the linear coefficient of wave absorption and $\Gamma_{ND}$ is the nonlinear and dispersive correction. Note that $\Gamma_{ND}$ is multiplied by the small factor $\zeta^2$ which means that this term will provide small corrections to linear results (a normal result, bearing in mind that we are dealing with weakly nonlinear waves).

Carrying out a series of simple calculations we find at the slow resonance, in agreement with linear theory, that

$$\Gamma_{L_c} = \frac{4\tau_c \mu}{\mu^2 + \upsilon^2} + \mathcal{O}(k^2 x_0^2). \tag{6.72}$$

The coefficient $\Gamma_{ND}$ is defined as

$$\Gamma_{ND} = -\frac{2}{p_e^2}\Re\{A_1^* A_{31}\}, \tag{6.73}$$

which can be rewritten using Eqs (6.29) and (6.53) as

$$\Gamma_{ND_c} = -\frac{27 p_e^2 \tau_c^3 \mu^3 \cos^4\alpha}{6\pi^2 V^2 k^2 x_0^2 (\mu^2 + \upsilon^2)^2} + \mathcal{O}(k^2 x_0^2). \tag{6.74}$$

Both $\Gamma_{L_c}$ and $\Gamma_{ND_c}$ are of the order of $kx_0$. This result is qualitatively the same as Ruderman et al. (1997c); Ballai et al. (1998a) results, however, the nonlinear correction is different. In fact, it is 27 times larger due to the Hall current having a dominant effect around the resonance. Moreover, the dispersion in the anisotropic slow dissipative layer causes a further reduction in the coefficient of energy absorption, in comparison to the nonlinear regime alone. We calculate the jump in the normal component of velocity across the anisotropic slow dissipative layer

$$[u_c] = -2p_e\tau_c\mu\left\{\left[1 - \zeta^2\frac{p_e\tau_c^2\mu^2\cos^4\alpha}{24\pi^2 k^2 x_0^2(\mu^2+\upsilon^2)}\right]\Re\left(\frac{e^{ik\theta}}{\mu+i\upsilon}\right) - \zeta^2\frac{p_e\tau_c^2\mu^2\cos^4\alpha}{24\pi^2 k^2 x_0^2(\mu^2+\upsilon^2)}\Re\left(\frac{(26-8i)e^{ik\theta}}{\mu+i\upsilon}\right)\right\}, \tag{6.75}$$

This result shows that nonlinearity and dispersion indeed reduces the absolute value of the velocity jump, reflecting the decrease in energy absorption.

At the Alfvén resonance dynamics can be described within the linear framework. Hence, using Eqs (6.68) and (6.71) we obtain that

$$\Gamma_a = \frac{4\tau_a\mu}{(\tau_a+\mu)^2 + \upsilon^2}. \tag{6.76}$$

Finally, we can calculate the jump in the normal component of velocity across the anisotropic Alfvén dissipative layer

$$[u_a] = -2p_e\tau_a\mu\Re\left(\frac{e^{ik\theta}}{\tau_a+\mu+i\upsilon}\right). \tag{6.77}$$

In Chapter 7 we shall numerically analyze the coefficient of wave energy absorption at both the slow and Alfvén resonances.

## 6.7 Effect of Equilibrium Flows

Satellite observations show that the solar plasma is characterized by a high degree of dynamics. The plasma is moving on a wide range of time scales. In order to have a more accurate description of wave heating in the solar atmosphere the observed large scale motions should be included. We discuss, briefly, the effect an equilibrium background motion has on the theory. In what follows, we illustrate the alterations in the theory of resonant heating when either a simple *homogeneous* or *inhomogeneous* flow is present.

Hollweg (1990) showed that, for an incompressible linear plasma in planar geometry, the damping or excitation of *surface waves* can be strongly influenced by an equilibrium shear flow. Erdélyi (1998) studied the effect of bulk motion on resonant Alfvén waves in coronal loops and found that a *steady* state can either efficiently enhance or decrease the wave energy dissipation depending on the relative direction of the bulk and wave motions. The absorption of FMA waves in the presence of a field-aligned equilibrium flow in the *linear* regime was investigated by Csík et al. (1998) and they also found a smooth variation of the wave energy absorption coefficient relative to the equilibrium flow. The effect of an equilibrium flow on nonlinear resonant MHD waves in isotropic plasmas was studied by Ballai and Erdélyi (1998). The generalized connection formulae and modified solutions due to shear equilibrium flows were determined.

Let us consider an equilibrium flow in an anisotropic and dispersive plasma. Let us introduce the Doppler shifted phase velocity of the waves;

$$\mathcal{V} = V - v_0\cos\alpha, \tag{6.78}$$

where $\mathbf{v}_0$ is the equilibrium flow speed and for simplicity it is taken to be parallel to the equilibrium magnetic field. The slow resonant position is now determined by the condition $\mathcal{V}^2 = c_T^2(x_c)\cos^2\alpha$, while the Alfvén resonant position is $\mathcal{V}^2 = v_A^2(x_a)\cos^2\alpha$. The first main effect of the equilibrium flow is the introduction of a mode shifting due to the coupling between the localized slow or Alfvén waves and the equilibrium flow. We consider the *homogeneous* flow to be defined as

$$\mathbf{v}_0 = \begin{cases} 0, & x<0, \\ \mathbf{v}_0, & x>0, \end{cases} \tag{6.79}$$

and the *inhomogeneous* flow to be given by

$$\mathbf{v}_0 = \begin{cases} 0, & x<0, \\ \mathbf{v}_0(x), & x>0, \end{cases} \tag{6.80}$$

where the spatial dependence of $\mathbf{v}_0$ is assumed to be a monotonically increasing linear function. We do not give all the details of how to derive the modified absorption rate due to the presence of equilibrium flows, since the procedure is identical to the one shown in Sect. 6.4 and 6.5.

The modified coefficient of wave energy absorption, at the slow resonance, is obtained as

$$\Gamma_c = \frac{4\tau_c\mu}{\mu^2+\upsilon^2} - \zeta^2\frac{27p_e^2\tau_c^3\mu^3\cos^4\alpha}{6\pi^2\mathcal{V}^2k^2x_0^2\left(\mu^2+\upsilon^2\right)^2}, \tag{6.81}$$

where, for the *homogeneous* flow we have

$$\tau_c = \frac{\pi k\mathcal{V}^5}{\rho_{0_c}v_{A_c}^4|\Delta_c|\cos^2\alpha}, \quad \mu = \frac{\kappa_e\mathcal{V}}{\rho_e\left(V^2-v_{A_e}^2\cos^2\alpha\right)}$$

$$\upsilon = \frac{\kappa_i\mathcal{V}}{\rho_i\left(\mathcal{V}^2-v_{A_i}^2\cos^2\alpha\right)} - k\mathcal{V}\mathcal{P}\int_0^{x_0}\frac{1}{\widetilde{F}(x)}\,dx, \tag{6.82}$$

and for the *inhomogeneous* flow $\tau_c$ and $\upsilon$ are as in Eq. (6.82), but $\mu$ is given as

$$\mu = \frac{\kappa_e V}{\rho_e\left(V^2-v_{A_e}^2\cos^2\alpha\right)}. \tag{6.83}$$

This is in complete agreement with Ballai and Erdélyi (1998) and Erdélyi and Ballai (2001).

In the case of the Alfvén resonance, the coefficient of wave energy absorption if found to be in the form of Eq. (6.76). The quantities $\mu$ and $\upsilon$ take the same form as at the slow resonance, i.e. Eq. (6.82) in a homogeneous flow and Eq. (6.83) in an inhomogeneous flow, however, $\tau_a$ is prescribed by

$$\tau_a = \frac{\pi k\mathcal{V}\sin^2\alpha}{\rho_{0_a}|\Delta_a|}. \tag{6.84}$$

## 6.8 Conclusions

In the present chapter we have investigated (i) the effect of nonlinearity and dispersion on the interaction of fast magnetoacoustic (FMA) waves with a one-dimensional inhomogeneous magnetized plasma with strongly anisotropic transport processes in the slow dissipative layer (ii) the interaction of FMA waves with Alfvén dissipative layers. The study is based on the nonlinear theory of slow resonance in strongly anisotropic and dispersive plasmas developed in Chapter 3 and the theory of Alfvén resonance developed in Chapter 4. Additionally, we investigated the effect of equilibrium flows on the resonant absorption.

We have assumed that (i) the thickness of the slab containing the inhomogeneous plasma (Region II) is small in comparison with the wavelength of the incoming fast wave (i.e. $kx_0 \ll 1$); and (ii) the nonlinearity in the dissipative layer is weak - the nonlinear term in the equation describing the plasma motion in the slow dissipative layer can be considered as a perturbation and nonlinearity gives only a correction to the linear results.

Applying a regular perturbation method, analytical solutions in the slow dissipative layer are obtained in the form of power expansions with respect to the nonlinearity parameter $\zeta$. Our main results are the following: nonlinearity in the dissipative layer generates higher harmonic contributions to the outgoing (reflected) wave in addition to the fundamental one (in agreement with, e.g. Ballai et al., 1998a; Erdélyi and Ballai, 2001). The dispersion does not alter this, however, the phase and amplitude of some of the higher harmonics are different from the standard nonlinear counterpart (see discussions before). Dispersion in the slow dissipative layer further decreases the coefficient of the wave energy absorption. The factor of alteration to the *nonlinear* correction

of the coefficient of wave absorption due to dispersion is 2600%. Remember, however, that the nonlinear correction is multiplied by the small parameter $\zeta^2$, so the effect to the overall coefficient of wave energy absorption is still small.

Calculating the coefficient of wave absorption at the Alfvén resonance confirms the linear theory of the past and verifies the approach taken to be correct. As our physical set-up of the problem (for the Alfvén resonance) matches the typical conditions found in the solar corona, hence, these results can be applied to it. The equilibrium state of the problem (for the slow resonance) can match conditions found in the upper chromosphere, where FMA waves may interact with slow dissipative layers, and if the reduction in the coefficient of wave energy absorption persists to the strong nonlinear case (as with the long wavelength approximation found by Ruderman, 2000) dispersion may have further implications to the resonant absorption in the solar atmosphere.

In the next chapter we shall theoretically and numerically investigate coupled resonances, which builds from the work in the present chapter to obtain a more realistic model for a solar physical description. In addition, we will numerically analyze the absorption of fast waves at the Alfvén resonance as a possible scenario of the interaction of global fast waves (modelling EIT waves) and coronal loops.

# 7

# Numerical analysis of resonant absorption of FMA waves due to coupling into the slow and Alfvén continua

*In Chapter 6 we investigated the resonant absorption of fast magnetoacoustic (FMA) waves at slow and Alfvén dissipative layers in anisotropic and dispersive plasmas. In the present chapter we extend the study to investigate coupled resonances. A coupled resonance occurs when two different resonances are in close proximity to each other, causing the incoming wave to act as though it has been influenced by the two resonances simultaneously. Numerical results are analyzed to determine the coefficient of wave energy absorption at both the slow and Alfvén resonance positions, as well as at the coupled resonance. The results are based on the two simplifying assumptions that (i) nonlinearity is weak, and (ii) the thickness of the inhomogeneous layer is small in comparison to the wavelength of the wave, i.e. we apply the so-called long wavelength approximation. In order to cast both resonances together, the coefficient of wave energy absorption at the coupled resonance is derived and analyzed for conditions typical for the solar chromosphere. Our investigation shows that the wave energy absorption is heavily dependent on the angle of the incident wave in combination with the angle of the equilibrium magnetic field with respect to the vertical direction. The results of the present chapter have been submitted to Astron. Astrophys. (Clack et al., 2009a).*

*If I have been able to see further, it was only because I stood on the shoulders of giants.*
**(Isaac Newton** 1643 – 1727**)**

## 7.1 Introduction

The complicated interaction of the motion of plasma with the magnetic fields is one of the most interesting processes in the solar atmosphere. A highly non-uniform and dynamical system, such as the solar atmosphere, is a perfect medium for magnetohydrodynamic (MHD) waves. These waves are able to transport momentum and energy which can be dissipated. One of the many possibilities of the conversion of the energy to heat is through resonant absorption. The existence of resonant absorption is due to the coupling of global waves and oscillations to local waves in a non-ideal and inhomogeneous plasma.

It is well known (and discussed in Sect. 6.1) that in order to have acceptable heating by FMA waves coming from lower regions (e.g. generated by convective motions below the photosphere), the waves should not be reflected by the steep rise of the Alfvén and / or slow wave speed with height, nor should they become evanescent. However, this is difficult to prevent. On the other hand, to interact resonantly with the slow waves, FMA waves would only have to propagate to the upper chromosphere, since the ratio between characteristic speeds (slow and Alfvén) is much smaller than in the solar corona. Only the high-frequency waves of the full FMA spectrum can reach the corona (with periods of a few tens of seconds). The energy flux density of fast waves at the bottom of the corona required for significant heating is not inconsistent with the upper limit on acoustic waves (Athay and White, 1978). There is an alternative to the FMA waves propagating from the photosphere towards the solar corona. FMA waves (as well as slow and Alfvén waves) may be generated locally in the chromosphere and corona by, e.g. phenomena involving magnetic reconnection. It was suggested by Parker (1988) that shuffling the magnetic field in the solar atmosphere (by convective motion in lower regions) builds up magnetic stresses which can be released through, e.g. reconnection providing the energy to maintain the high temperature of the solar upper atmosphere (see, e.g. Roussev et al., 2001a,b,c). It is known that reconnection events can produce (amongst other things) waves.

The present chapter has three major aims. First, is to (numerically) study the nonlinear resonant interaction of FMA waves coupled to the slow continua in strongly anisotropic and dispersive plasmas (conditions typical of the solar upper chromosphere). Secondly, to numerically investigate the resonant absorption of FMA waves at the Alfvén resonance for conditions typically found in the solar corona. Finally, we numerically analyse the resonant absorption of FMA waves at a coupled (slow and Alfvén ) resonance. The present chapter takes advantage of the analytical study presented in Chapter 6, where we derived the coefficient of wave energy absorption for FMA waves at the two separate slow and Alfvén resonances. We use a simplified slab geometry throughout the chapter, where an inhomogeneous and dissipative magnetic slab is sandwiched by two semi-infinite homogeneous plasma regions.

## 7.2 The equilibrium and assumptions

The magnetic and density topology of the solar atmosphere is highly complex and, therefore, there are many degrees of freedom. However, to make our investigation tractable mathematically, we study the interaction of incident FMA waves in a one-dimensional plasma. The dynamics and absorption of the waves will be studied in a Cartesian coordinate system. The equilibrium configuration is similar to that in Chapter 6 (see Fig. 6.1) and consists of an inhomogeneous and dissipative magnetised plasma $0 < x < x_0$ (Region II) sandwiched between two semi-infinite

homogeneous magnetised plasmas $x < 0$ and $x > x_0$ (Regions I and III, respectively). The equilibrium magnetic field, **B**, is unidirectional and lies in the $yz-$plane. In what follows we use the same subscript notations as in the previous chapter, namely, the subscripts 'e', '0' and 'i' denoting the equilibrium quantities in the three regions (Regions I, II, III, respectively). All equilibrium quantities are continuous at the boundaries of Region II, and they satisfy the equation of total pressure balance, which prescribes that the density ratio between Regions I and III satisfy the relation (6.2).

We consider an equilibrium such that the plasma in Region III is both hotter and more rarefied than in Region I and assume a simple monotonic linear profile for all variables in Region II. This choice provides a single unique resonant surface for both the slow and Alfvén resonances. The objective of the present chapter is to study the resonant absorption of FMA waves at slow and Alfvén dissipative layers. We have two cases which we wish to investigate. First, we study the absorption of fast waves at Alfvén resonance as a possible scenario of the interaction of global fast waves (modelling EIT waves) and coronal loops. Secondly, we analyse the absorption of fast waves at the slow resonance as a possible scenario for heating in the upper chromosphere. When a fast wave interacts with a slow resonance, an Alfvén resonance is also present. We consider this in our analysis and study the total (i.e. coupled) absorption in the inhomogeneous layer.

In an attempt to remove other effects from the analysis we consider the incoming fast wave to be entirely in the $xz-$plane, i.e. $k_y = 0$. The resonant positions are located where the global fast wave speed coincides with that of the local slow / Alfvén speed. The dispersion relation for the impinging propagating fast waves takes the form of Eq. (6.7). We assume the plasma is *strongly* magnetized in the three regions, such that the conditions $\omega_{i(e)}\tau_{i(e)} \gg 1$ are satisfied. Due to the strong magnetic field, we are bound by similar transport processes as considered in Chapter 6. Thus, for slow waves, it is a good approximation to retain only the first term of Braginksii's expression for viscosity, namely compressional viscosity, and thermal conduction. In addition, the dispersion due to Hall currents is included. Alfvén waves are transversal and incompressible so they are affected by the second and third components of Braginskii's stress tensor, shear viscosity, and finite electrical conductivity. All other transport mechanisms can be neglected. For further details we refer to Sect. 2.4 and 6.2.

The dynamics of nonlinear resonant MHD waves in anisotropic and dispersive plasmas was studied in chapters 3 and 4 where we derived the governing equations and connection formulae necessary to study resonant absorption in slow / Alfvén dissipative layers. In Chapter 6 we analytically studied the interaction of fast waves with the slow and Alfvén resonances and derived the coefficients of wave energy absorption. We intentionally overlooked the complication of an Alfvén resonance being present at the same time as the slow resonance. In the present chapter, however, we include both resonances. These conditions would be typical of the upper chromosphere where the plasma-$\beta$ goes from being larger than unity to becoming smaller than unity, retaining the monotonic dependence of characteristic speeds in the inhomogeneous layer.

The key assumptions we use in the present chapter in order to facilitate analytical progress are connected to the strength of nonlinearity and the wavelength of the incoming wave. First, from the very beginning we assume that nonlinearity, at the slow resonance, is weak. We apply this restriction as we cannot solve Eq. (3.60) analytically, in the limit of strong nonlinearity. Secondly, we assume that the thickness of the inhomogeneous region (Region II) is thin in comparison to the wavelength of the impinging fast wave, i.e. $kx_0 \ll 1$, which has two implications. The first is to enable us to neglect terms of the order of $k^2x_0^2$ (and above) in the calculations. The

second consequence is more subtle. To have a coupled resonance, the incoming FMA wave must resonantly interact with an Alfvén resonance and be partially transmitted and then resonantly interact with a slow resonance. On one hand, if the Alfvén and slow resonance are more than one wavelength, $k^{-1}$, apart the transmitted wave will have decayed by the time it reaches the slow resonance. On the other hand, if the Alfvén and slow resonance are within one wavelength[1] of each other then the transmitted wave will be able to interact with the slow resonance. So, if an environment is set up such that both an Alfvén and a slow resonance occur within the inhomogeneous region the distance between the resonances, $x_1$, must satisfy the condition $x_1 < x_0$. Hence, we have $kx_0 \ll 1 \Rightarrow x_0 \ll k^{-1} \Rightarrow x_1 \ll k^{-1}$.

We will use the same governing equations, absorption coefficients and results as obtained in Chapter 6. We will only derive new results necessary to investigate the processes at the coupled resonance.

## 7.3 Coefficient of wave energy absorption

To derive the coefficient of wave energy absorption we follow the procedure presented in Chapter 6. The basic premise is that one single monochromatic wave (the FMA wave) interacts with the inhomogeneous layer and one (or more) wave leaves it. The difference of the energy flux entering and leaving the resonance quantifies the energy resonantly absorbed inside the inhomogeneous region. This energy can then be converted into heat by dissipation. The coefficient of wave energy absorption is just the *percentage* of the energy entering the inhomogeneous region that is resonantly absorbed.

For simplicity, in the present chapter, we restrict ourselves to a static equilibrium. As shown in Chapter 4, at the Alfvén resonance the wave dynamics is described by linear theory. Therefore, the incoming monochromatic FMA wave is partly reflected, transmitted and dissipated. The reflected wave is monochromatic, with amplitude $A_a$, and the transmitted wave from the inhomogeneous region carries no energy because it is decaying (see, e.g. Goossens, 1994; Goossens et al., 1995; Goossens and Ruderman, 1995; Tirry and Goossens, 1995). The coefficient of wave energy absorption of FMA waves at the Alfvén resonance is given by Eq. (6.76), where $\tau_a$ is provided by Eq. (6.69)

At the slow resonance the dynamics is governed by the nonlinear equation (3.60). Similar to the Alfvén resonance, the incoming FMA wave is partly reflected, transmitted and dissipated. The transmitted wave is decaying similar to the Alfvén resonance, however, the reflected wave includes higher harmonics in addition to the fundamental mode. Using the approximation of weak nonlinearity, in the first order of approximation, we find the fundamental mode of the reflected wave. In the second order approximation, we obtain that the higher harmonics are of the order of $k^2x_0^2$, which are subsequently neglected as our analysis is restricted to terms proportional to $kx_0$. In the third order of approximation, we find an additional contribution to the reflected fundamental mode due to nonlinearity and dispersion. Higher order approximations result in non-monochromatic harmonics which are subsequently ignored. The coefficient of wave energy absorption of fast magnetoacoustic waves at the slow resonance is given by the addition of Eqs

[1]We want the distance to be much less than one wavelength so that we can assume the transmitted wave loses no energy before interacting with the slow resonance. Distances over one wavelength results in the energy lost by the transmitted wave become very large and non-negligible.

(6.72) and (6.73) resulting in

$$\Gamma_c = \frac{4\tau_c \mu}{\mu^2 + \upsilon^2} - \zeta^2 \frac{27 p_e^2 \tau_c^3 \mu^3 \cos^4 \alpha}{6\pi^2 V^2 k^2 x_0^2 \left(\mu^2 + \upsilon^2\right)^2} + \mathcal{O}(k^2 x_0^2), \tag{7.1}$$

where $\tau_c$, $\mu$ and $\upsilon$ are given by Eq. (6.30) and $\zeta$, defined by Eq. (6.19), is assumed to be small.

Equations (6.76) and (7.1) involve variables that need some explanation. The variable $\kappa_e = \pm \tan\phi$ is the angle at which the impinging FMA makes with the $z-$axis, while the sign of the variable $\kappa_i$, defined as

$$\kappa_i = \sqrt{-\frac{V^4 - V^2\left(c_{S_i}^2 + v_{A_i}^2\right) + c_{S_i}^2 v_{A_i}^2 \cos^2\alpha}{\left(c_{S_i}^2 + v_{A_i}^2\right)\left(V^2 - c_{T_i}^2 \cos^2\alpha\right)}}, \tag{7.2}$$

gives the condition of wave leakage in region II. If the terms inside the square root of Eq. (7.2) are negative, $\kappa_i$ is imaginary and Eq. (6.15) is no longer an elliptical equation, which corresponds to wave leakage. The Cauchy principal part, $\mathcal{P}$, is used in $\upsilon$ [see Eq. (6.30)] because the integral is divergent at infinity. The function $\widetilde{F}^{-1}(x)$ originates after solving the ideal linear MHD equations in region II and is obtained from Eq. (3.21).

As mentioned earlier, the previously discussed coefficients of wave energy absorption (taken separately) do not give the complete picture. In principle, every time a FMA wave interacts with a slow resonance an Alfvén resonance is also present (it is easy to show that under coronal conditions, the vise-versa statement is not true). Usually, to avoid this problem we would align the magnetic field with the $z-$axis, and since $\partial/\partial y = 0$ the Alfvén resonance would vanish. However, to include Hall currents (which provides dispersive effects at the slow resonance) we must have an angle between the $z-$axis and the equilibrium magnetic field. In an attempt to tackle this problem, we investigate the interaction of FMA waves with an inhomogeneous region that contains *both* a slow and an Alfvén resonance. To carry this out analytically, we must assume that the thickness of the inhomogeneous region is much smaller than the wavelength of the incoming wave, i.e. $kx_0 \ll 1$ (see discussion at the end of Sect. 7.2). We also assume that there is a single and unique slow and Alfvén resonance, (this assumption can be relaxed later).

To find the coefficient of wave energy absorption at a coupled resonance the procedure is identical to that carried out in Sect. 6.4, so we write out our findings rather than presenting all calculations in detail. First, we found that, at a coupled resonance, in the first order approximation (i.e. deriving the fundamental mode form), we cannot decouple the Alfvén and slow reflected waves. This is in agreement with Woodward and McKenzie (1994a,b) who state that when Hall currents are present the slow and Alfvén modes cannot always be decoupled. Even though these studies were investigating stationary waves, we believe the same applies here with resonant absorption, specifically, if we approximate that the wave interacts with both resonances simultaneously. The amplitude of the reflected wave in the first order of approximation is derived as

$$A_a + A_{1_c} = -p_e \frac{\tau - \mu + i\upsilon}{\tau + \mu + i\upsilon}, \tag{7.3}$$

where $\tau = \tau_a + \tau_c$, and $\mu$ and $\upsilon$ are given by Eq. (6.30). In higher order approximations we find that the Alfvén resonance has no contribution to the amplitudes of the reflected waves. In particular, the addition to the fundamental mode due to nonlinearity and dispersion is identical to that found when no Alfvén resonance is present, which is to be expected, since the dynamics

at the Alfvén resonance is linear and, therefore, should have no contribution to nonlinear effects.

The coefficient of wave energy absorption is given by Eq. (6.71) where $\overline{A}_n$ denotes the *total* amplitude of the reflected wave in a particular order of approximation. Calculating the coefficient of wave energy absorption of FMA waves inside the inhomogeneous region we find that (in the long wavelength approximation)

$$\Gamma = \frac{4\tau\mu}{(\tau+\mu)^2+\upsilon^2} - \zeta^2 \frac{27 p_e^2 \tau_c^3 \mu^3 \cos^4\alpha}{6\pi^2 V^2 k^2 x_0^2 \left(\mu^2+\upsilon^2\right)^2} + \mathcal{O}(k^2 x_0^2). \tag{7.4}$$

In the next section, we will numerically analyse the coefficient of wave energy absorption and, in particular, we investigate what is the significance of the angle of the incident wave and the inclination of the ambient magnetic field on the absorption of wave energy at the coupled resonance.

## 7.4 Numerical results

Before proceeding to the mentioned analysis of the wave energy absorption, it is instructive to consider the contributions to $\tau$ due to the slow and Alfvén resonances. We can easily calculate what percentage of $\tau$ comes from each resonance by studying Eq. (7.4). Immediately it is clear that the nonlinear term comes wholly from the slow resonance, as we have already discussed. The linear term is a combination of the resonant absorption due to the slow and Alfvén resonance. The percentage contributions of each resonance is found by calculating $\tau_c/\tau$ (% of slow contribution) and $\tau_a/\tau$ (% of Alfvén contribution). Using Eqs (6.30), (6.69) and (7.4) we obtain

$$\frac{\tau_c}{\tau} = \frac{K_1}{K_1+K_2}, \quad \frac{\tau_a}{\tau} = \frac{K_2}{K_1+K_2}, \tag{7.5}$$

where

$$K_1 = \rho_{0_a} |\Delta_a| V^4, \quad K_2 = \rho_{0_c} v_{A_c}^4 |\Delta_c| \sin^2\alpha \cos^2\alpha. \tag{7.6}$$

The particular form of Eq. (7.5) depends entirely on the choice of profile for the equilibrium quantities inside the inhomogeneous layer. For our analysis, in Region II (the inhomogeneous region) we have chosen a monotonically increasing linear profile for all equilibrium quantities (including characteristic speeds) of the form $f(x) = f(0) + x/x_0[f(x_0) - f(0)]$. Using the values $v_{A_e} = 28\ \mathrm{kms}^{-1}$, $c_{S_e} = 34\ \mathrm{kms}^{-1}$, $v_{A_i} = 156\ \mathrm{kms}^{-1}$, $c_{S_i} = 65\ \mathrm{kms}^{-1}$ and $\rho_e = 5\times10^{-11}\ \mathrm{kgm}^{-3}$ for characteristic speeds we can obtain the variations given by Fig. 7.1.

Figure 7.1 shows the percentage contribution to the quantity $\tau$ due to the slow (left) and Alfvén resonance (right). It is easily seen that $\phi$ does not have much effect on the contributions, however, $\alpha$ has a marked effect. At $\alpha = 0$, there is no contribution from the Alfvén resonance - which is to be expected since, for this particular inclination, global oscillations cannot resonantly interact with local Alfvén modes. As the angle $\alpha$ increases the contribution due to the Alfvén resonance increases rapidly (and accordingly the contribution from the slow resonance decreases), and by $\alpha = \pi/4$ the Alfvén resonance contributes 80% of the absorbed energy. At $\alpha = \pi/2$ the slow resonance disappears, and so its contribution drops to zero.

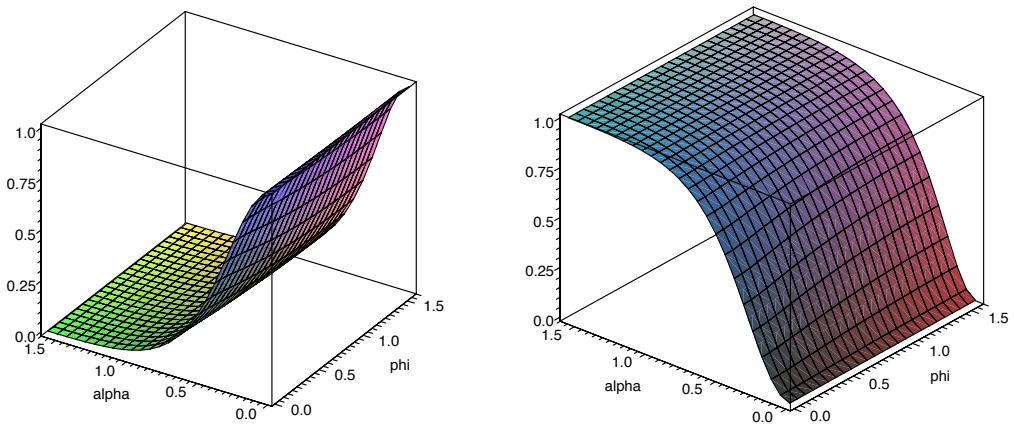


Figure 7.1: Percentage contribution to $\tau$ in the coupled resonance due to the slow resonance (left) and the Alfvén resonance (right) in terms of the wave incident angle, $\phi$, and the inclination angle of the magnetic field, $\alpha$.

### 7.4.1 Alfvén resonance: Modelling the interaction of EIT waves with coronal loops

Fast waves that are generated by the convection motion and propagate upwards are reflected by the strong density gradients in the upper chromosphere, so just a tiny proportion of FMA waves are able to reach the corona. Fast waves, however, can be generated in the corona by, e.g. flaring processes, in particular coronal mass ejections (CMEs). Global disturbances generated by CMEs, known as EIT (Extreme ultraviolet Imaging Telescope) waves, are believed to be FMA waves (Ballai et al., 2005) propagating in the quiet Sun. In their propagation, EIT waves interact with active region loops setting them into motion. The present section is devoted to the study of resonant coupling of FMA waves (modelling EIT waves) with local Alfvén waves in coronal loops. One major problem identified with the model we would like to use is that the EIT waves have very low speeds ($300 - 500$ kms$^{-1}$) compared with the accepted Alfvén speed outside coronal loops (1200 kms$^{-1}$). The problem associated with the speed of EIT waves could be resolved by assuming a steady rise in temperature and magnetic field strength as an active region is approached. The rise in temperature increases the sound speed, while the increase in strength of magnetic field will cause the Alfvén speed to grow. Hence, the FMA wave speed will increase as it is a combination of the sound and Alfvén speeds. As the gradients are not steep enough to cause shocks or reflection, the EIT waves are accelerated to the local speeds as they approach active regions.

Another assumption our model relies on is that $v_{A_i} > v_{A_e}$, i.e. the Alfvén speed in Region I is less than that in Region III. Since we can only solve $\widetilde{F}(x)$ when we assume monotonic functions inside the inhomogeneous region we have to chose whether these functions will increase or decrease. If the functions decrease in the inhomogeneous region there will be no absorption since the FMA waves will never resonantly interact with the local Alfvén waves. However, if the functions increase, we do achieve resonant interactions of the two modes. A more accurate model of reality at a coronal loop's edge would be a complicated non-monotonic function that both increases and decreases the local equilibrium parameters which could create resonant interactions. Essentially, there would be several resonant positions inside the inhomogeneous region, however, we cannot

analytically solve such a model at present (due to the form that $\widetilde{F}(x)$ would take). Therefore, to provide a valuable insight of resonant absorption at coronal loops, we choose an unrealistic but tractable model. Mathematically, the above restriction can be easily represented by the condition that $\max[v_A(x)] > v_{A_e}$ where $x \in (0, x_0]$. In addition, for a single unique resonance we need to impose the constraint $dv_A(x)/dx \neq 0$, $x \in (0, x_0)$. It is also clear, from the outset, that under coronal conditions ($\beta \ll 1$) FMA waves will never resonantly interact with local slow waves.

To simulate conditions typical of the solar corona we consider $v_{Ae} = 1200\,\mathrm{kms}^{-1}$, $c_{Se} = 200\,\mathrm{kms}^{-1}$, $v_{Ai} = 1400\,\mathrm{kms}^{-1}$, $c_{Si} = 250\,\mathrm{kms}^{-1}$ and $\rho_e = 1.33 \times 10^{-12}\,\mathrm{kgm}^{-3}$. We select $k = 5 \times 10^{-8}\,\mathrm{m}^{-1}$ such that the incoming FMA wave has a period of about 100 s (consistent with observed EIT waves in the solar corona). It should be mentioned that the analysis presented in Fig. 7.2 is valid for any k as long as the dimensionless quantity $kx_0$ satisfies the condition $kx_0 \ll 1$.

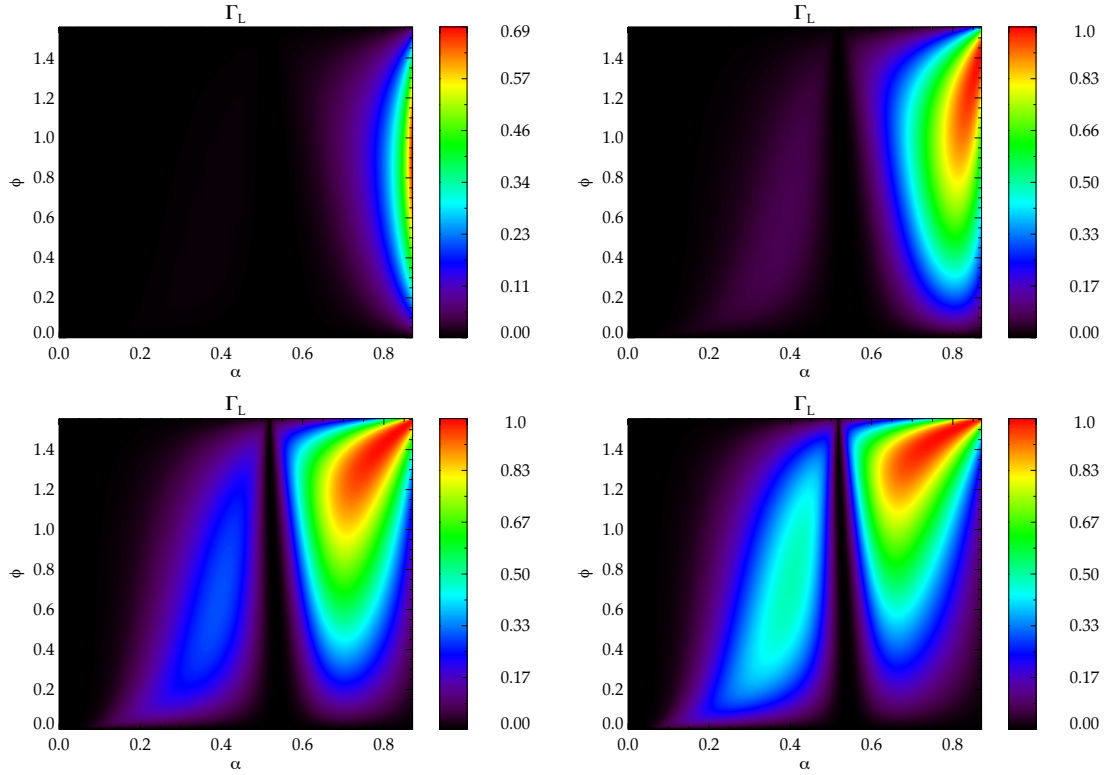


Figure 7.2: The wave energy absorption coefficient of FMA waves at the Alfvén resonance. Here we have $v_{Ae} = 1200\,\mathrm{kms}^{-1}$, $c_{Se} = 200\,\mathrm{kms}^{-1}$, $v_{Ai} = 1400\,\mathrm{kms}^{-1}$, $c_{Si} = 250\,\mathrm{kms}^{-1}$ and $\rho_e = 1.33 \times 10^{-12}\,\mathrm{kgm}^{-3}$. The dimensionless quantity, $kx_0$, takes the values (from top left to bottom right) 0.01, 0.1, 0.5 and 1.0, respectively.

Figure 7.2 gives the wave energy absorption coefficient for $kx_0 = 0.01$, 0.1, 0.5 and 1.0 (the last one not being fully consistent with our assumptions, but illustrates the trend). The angle of the incoming FMA wave, $\phi$, takes values between 0 and $\pi/2$, while the angle of the equilibrium magnetic field, $\alpha$, only varies between 0 and $\pi/4$, because beyond this point the integrals calculated are divergent and the numerical analysis cannot resolve the Cauchy principal part. The coefficient of wave energy absorption should take a value between 0 and 1, and can be thought of the percentage of incoming wave energy transferred to local Alfvén waves by resonance. We recognize that the plasma is unstable when the value of the coefficient of wave energy absorption

is negative, provided a flow exists. The plasma can also create over-reflection, and we observe this in the coefficient of wave energy absorption when the value becomes greater than unity. Both the phenomena of over-reflection and instabilities occur for $\alpha > \pi/4$.

The first thing to notice, about Fig. 7.2, is that as $kx_0$ increases so does the coefficient of wave energy absorption. In the same way, the area over which absorption can take place is also increasing. In general, we can state that the most efficient absorption occurs at angles of inclination of $\phi$ which are larger than $\pi/4$, while the most efficient absorption with respect to $\alpha$ changes depending on $kx_0$. The larger the value of $kx_0$ the less influential $\alpha$ becomes on the most efficient absorption regions. At approximately $\alpha = \pi/5 \approx 0.63$ the absorption drops to zero for all values of $kx_0$ and $\phi$, which could be explained by the inhomogeneous layer becoming *transparent* to the incoming wave, a phenomenon that cannot be explained by the present model (further study is needed to find out whether it is a numerical artefact or a physical property).

It is also clear from Fig. 7.2 that FMA waves are absorbed efficiently at the Alfvén resonance, which is encouraging when thinking about EIT waves within the solar corona. The EIT waves could be absorbed by Alfvén resonances present in / or near coronal loops (arcades). In some cases all of the energy of the incoming wave can be absorbed, and dissipated by, e.g. viscosity. The variation in absorption due to combinations of $\alpha$ and $\phi$ may help explain why when an incoming wave impacts a coronal arcade, some loops oscillate more than others and some loops dim and while others get brighter. When the frequency of the incoming FMA wave does not fall within the frequencies of the Alfvén continuum the energy of the incident wave is, likely to be, transferred to the coronal loop as kinetic energy, thereby setting the loop into oscillation. These oscillations are studied in the framework of coronal seismology for the purposes of field and plasma diagnostics.

We note here that, if the density is varied (within reasonable parameters), the absorption is changed only slightly. If we change the density so it is really high or low (for the solar corona) the absorption starts dramatically changing, eventually leading to a breakdown of the numerical analysis. We do not show any plots of the variation of the absorption coefficient with density because the values at which the coefficient of wave energy absorption is noticeably changed are not consistent with observation of the solar corona (or chromosphere). The last significant variables to discuss are the equilibrium wave speeds. The wave speeds here have been selected to be consistent with the environment of the solar corona. However, we know that there is a plethora of wave speeds available in the inhomogeneous plasma of the corona. We have tested different values of equilibrium speeds, and the overall pattern of absorption is identical to that found in Fig. 7.2, and the absorption coefficient remained relatively similar to those discussed above.

### 7.4.2 Coupled resonance: Modelling chromospheric absorption

To model a coupled resonance, we consider a slow and an Alfvén resonance so close together that they are both able to interact with the incoming FMA wave (so-called coupled resonance). This means that we will lower our applicability region to the denser chromosphere. To match conditions typical of the chromosphere we have taken the values $v_{Ae} = 28\ \mathrm{kms}^{-1}$, $c_{Se} = 34\ \mathrm{kms}^{-1}$, $v_{Ai} = 156\ \mathrm{kms}^{-1}$, $c_{Si} = 65\ \mathrm{kms}^{-1}$ and $\rho_e = 3.99 \times 10^{-11}\ \mathrm{kgm}^{-3}$. The specific values of equilibrium quantities can be changed, however, the overall trend of absorption will remain the same as shown here. The nonlinear correction to linear absorption at the coupled resonance comes solely from the slow resonance (as the Alfvén resonance can be described by linear theory) and is very

small when compared to the linear absorption coefficient (in line with the weak nonlinear limit imposed in the derivations). In Figs 7.3–7.6 we display the linear coefficient of wave energy absorption for the slow, Alfvén and coupled resonance for comparison and we show the nonlinear correction to the coupled resonance for values of $kx_0 = 0.01$, $kx_0 = 0.1$, $kx_0 = 0.5$ and $kx_0 = 1.0$, with the last value of $kx_0$ not being fully consistent with the assumption of the long wavelength approximation, but illustrates the overall trend.

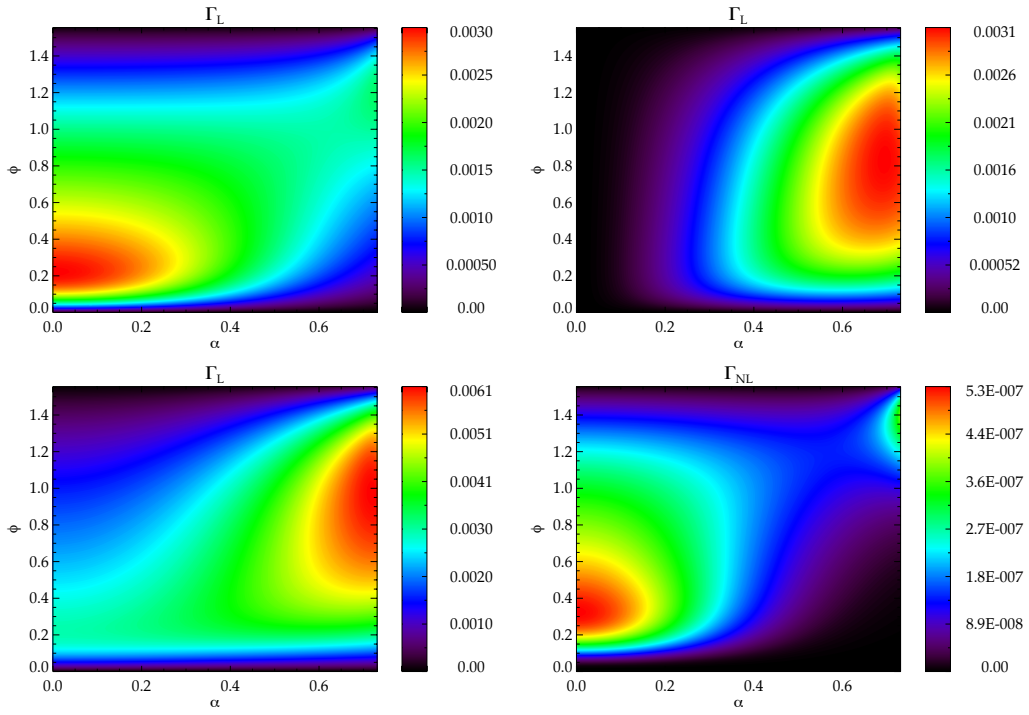


Figure 7.3: Comparison of the linear absorption at the slow (top left), Alfvén (top right) and coupled (bottom left) resonances for $kx_0 = 0.01$. We also show the nonlinear absorption for the coupled (and slow) resonance.

The first striking result to notice about Figs 7.3–7.6 is how similar they appear compared to each other. The first three figures are fully valid using the method presented in the present chapter, while the last one is not strictly valid. We have truncated the abscissa at $\alpha = 6\pi/25$, because the integrals become divergent and the numerical analysis cannot resolve the Cauchy principal part.

In all of Figs 7.3–7.6 the bottom right plot describes the nonlinear coefficient of wave energy absorption, which are incredibly small (under the conditions presented here). The reason for such small values, in these cases, is that the ratio of magnetic and plasma pressures (the plasma-$\beta$) has a value smaller than unity. When $\beta \ll 1$ the plasma kinetic pressure is low and, by extension, [examine Eq. (7.4)] so is the nonlinear coefficient of wave energy absorption. In addition, the nonlinear coefficient must be multiplied by the very small parameter $\zeta^2$. Therefore, the nonlinear correction of wave energy absorption at coupled resonances in the chromosphere is truly tiny in comparison to the linear wave energy absorption and acts to decrease the total coefficient of wave energy absorption.

In general, we can state that the greatest linear wave energy absorption at the slow resonance occurs at small values of $\phi$ ($0 < \phi < 0.3$) and small to moderate values of $\alpha$ ($0.1 < \alpha < 0.6$),

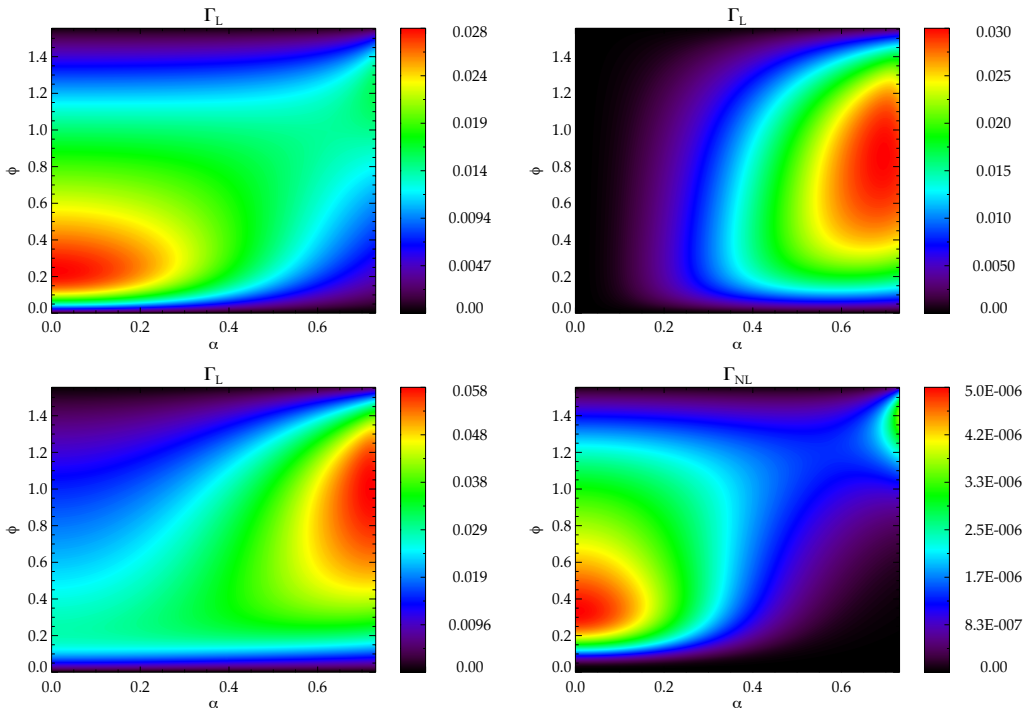


Figure 7.4: The same as Fig. 7.3, but here the coefficient of wave energy absorption is plotted for $kx_0 = 0.1$.

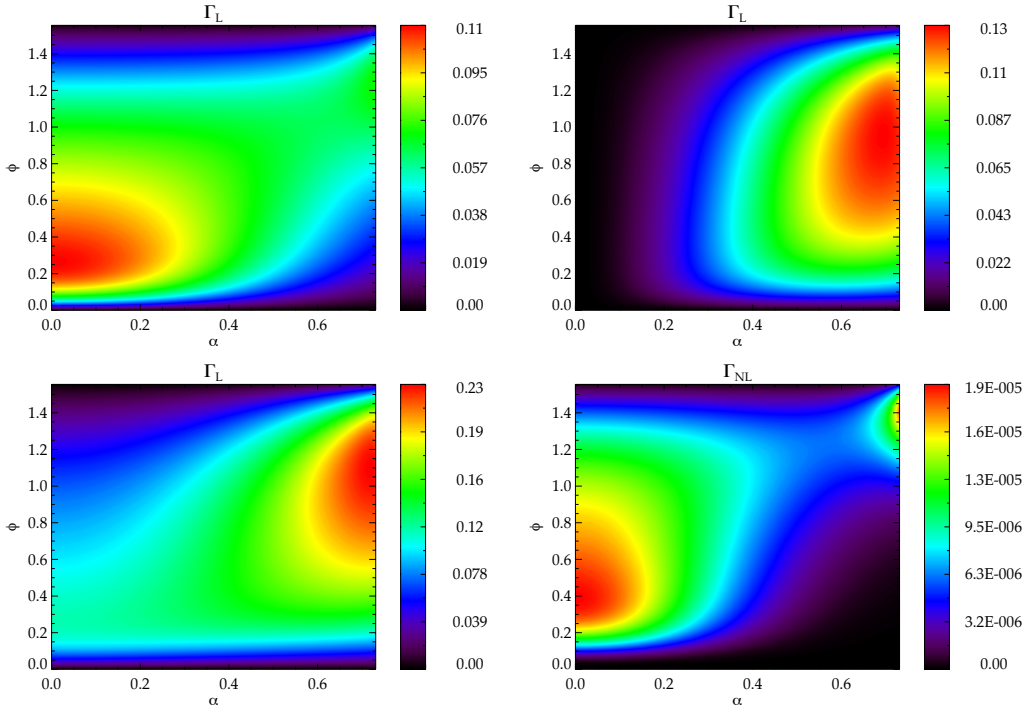


Figure 7.5: The same as Fig. 7.3, but here the coefficient of wave energy absorption is plotted for $kx_0 = 0.5$.

whereas the the greatest linear wave energy absorption at the Alfvén resonance occurs at moderate values of $\alpha$ ($0.6 < \alpha < 0.8$) and a wide range of values of $\phi$ ($0.2 < \phi < 1.2$). For all values of

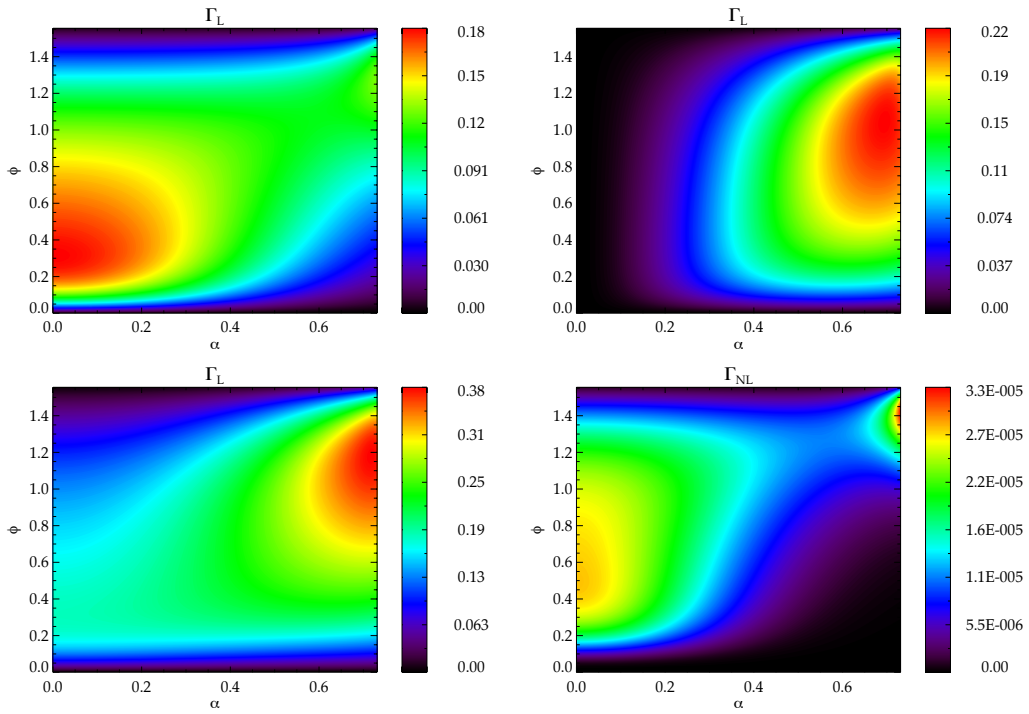


Figure 7.6: The same as Fig. 7.3, but here the coefficient of wave energy absorption is plotted for $kx_0 = 1.0$.

$kx_0$ a larger percentage of energy is absorbed at the Alfvén resonance compared to the slow resonance, which is indicated by the coefficient of wave energy absorption having greater values at the Alfvén resonance. We can also state that increasing $kx_0$ produces more absorption (of course up to the point where the mathematical model becomes invalid).

The most interesting feature of these plots is the coupled resonance. When there is no absorption at both the slow and Alfvén resonance, the absorption at the coupled resonance is also zero and if there is absorption at only one of the slow or Alfvén resonance the coefficient of wave energy absorption at the coupled resonance is identical to the value at the single resonance. However, more interestingly, when there is absorption at both the single Alfvén and slow resonance the absorption at the coupled resonance is always *greater* than the sum of the two single absorption coefficients. The greater coefficient of wave energy absorption at the coupled resonance compared to the two single resonances implies that there is more energy available for heating the plasma. We shall use Fig. 7.5 to clarify what we have just explained. At the values of, e.g. $\alpha = 0, \phi = \pi/2$ in all three plots we can clearly see the coefficient of wave energy absorption is zero. When, e.g. $\alpha = 0, \phi = 0.4$ the coefficient of wave energy absorption at the Alfvén resonance is zero, while at the slow and coupled resonance it is 0.11. If we change the angles such that, e.g. $\alpha = 6\pi/25, \phi = 1.0$ the coefficient of wave energy absorption at the slow, Alfvén and coupled resonances are 0.067, 0.13 and 0.23, respectively, hence it is clear that $0.23 > 0.13 + 0.067 = 0.197$. The same procedure can be carried out at any values of $\alpha$ and $\phi$ where there is absorption at both the single Alfvén and slow resonances.

There is also clear evidence in these plots that the efficiency at which FMA waves are absorbed at the Alfvén resonance under chromospheric conditions is far lower that in the coronal counterpart.

## 7.5 Conclusions

In the present chapter, we have investigated the absorption of fast magnetoacoustic (FMA) waves at individual and coupled slow and Alfvén resonances. We have derived the wave energy absorption coefficient analytically by applying the long wavelength approximation ($kx_0 \ll 1$). Analytical results for the absorption at the separate slow and Alfvén resonances found in Chapter 6 were numerically analysed.

We have shown that the absorption of incoming FMA waves depends heavily on the combination of the angle of incidence of the wave ($\phi$) and the angle of the equilibrium magnetic field ($\alpha$). At some combinations of $\phi$ and $\alpha$, the quantity $\kappa_i^2 < 0$ which reduces absorption to zero, because the incident FMA wave can *leak* passed the resonances. Normally, the inhomogeneous layer is translucent to waves, but occasionally when the conditions are right, the inhomogeneous layer can become transparent so that they can pass through without undergoing resonant absorption.

We introduced the concept of coupled resonances which could be critical for the heating of the solar upper atmosphere, because FMA waves propagate throughout the solar atmosphere. When FMA waves interact with a slow resonance, an Alfvén resonance is *always* present as well (as long as there is an angle between the magnetic field and the direction of wave propagation). We believe this is the most likely form of resonant absorption in the upper chromosphere. In the corona, the Alfvén (and hence FMA) waves speeds are much larger then the slow speed, so just an Alfvén resonance is present when a FMA wave is incident on an inhomogeneous plasma layer. The governing equations for the slow and Alfvén resonances are derived considering nonlinearity, and even though nonlinearity only slightly decreases the resonant absorption, in comparison to linear theory, it provides a device by which the heated plasma can be transported: the *mean shear flow*, creating turbulence, which can distort the inhomogeneous layer (see, e.g. Ofman and Davila, 1995; Clack and Ballai, 2009a), enhancing absorption and transporting heated plasma away from the resonance.

We assumed, for simplicity, that the equilibrium quantities inside the inhomogeneous layer increased monotonically, which, in reality, is not always the case. If we allow the equilibrium quantities to vary non-monotonically, the situation is changed. If we still use the long wavelength approximation, the calculations are almost identical to the ones produced in the present chapter. However, instead of one position for the Alfvén and slow resonances (different for each one) there could be several. Again, we would not be able to separate the individual outgoing waves, but the collective outgoing wave would be defined exactly as Eq. (7.3), where $\tau$ would equal the addition of all the $\tau_c$s and $\tau_a$s associated with the different resonant points. The form of the $\tau_c$s and $\tau_a$s would be identical to Eqs. (6.30) and (6.69), respectively, though the quantities would take different values corresponding to the different resonant positions. In general, this would produce greater absorption of wave energy inside the inhomogeneous layer, creating further heating possibility.

Extreme ultraviolet (EUV) observations of active regions showed that, when coronal arcades oscillate under the influence of an external driver, some of the loops oscillate more than others, some of the loops do not oscillate at all and some become *dimmer* in the wavelength that they have been observed in. Part of this behaviour can be explained by the varying strength of the magnetic field inside the loops, however, this is not fully satisfactory. We *speculate* that this phenomenon is predominately created by resonant absorption. The varying conditions allow for varying degrees of resonant absorption. The loops that oscillate the most do not have the conditions necessary for

resonant absorption, so the incident waves just transfer their kinetic energy to the loops. Other loops have the right conditions for resonant absorption, and some even have the conditions for multiple resonant positions. These loops will oscillate less, because the wave energy is being absorbed. The loops with the conditions for multiple resonances will oscillate the least (possibly not at all) as more and more energy of the wave is deposited. These loops should either get *brighter* or *dimmer*, since the loops are only observed in a single wavelength. If a loop *brightens*, the plasma is emitting more intensely in the filter's wavelength, but if a loop *dims* the loop could be getting either cooler or hotter, as the plasmas emissions move out of the filter's range. This explanation covers all the observed properties of some coronal arcade oscillations, and could explain why they are damped so quickly. The speculation must be viewed with caution as the heating due to absorption is likely to take place over a small area, in comparison to the width of the loop.

We wish to add a note of possible caution to our results. We have two main assumptions in creating our model (not including the monotonic functions inside the inhomogeneous layer, discussed earlier). First is the long wavelength approximation; if we relax this assumption and consider intermediate wavelengths then the FMA wave will always experience the influence of the Alfvén resonance first, and since the inhomogeneous layer is *nearly* always translucent to the incoming FMA wave no interaction with the slow resonance will occur. On the other hand, this does not affect the Alfvén resonance. Secondly, since we used the equations derived in Chapter 6, we assumed weak nonlinearity; we studied in this limit because the governing equation is unsolvable analytically for arbitrary degrees of nonlinearity. The findings of Ruderman (2000) showed that in the limit of strong nonlinearity the coefficient of resonant absorption is qualitatively the same as in the weak nonlinear limit (with the difference never being greater than 20%). As explained above, intermediate values of wavelength disable the slow interaction anyway. Furthermore, strong nonlinearity does not alter the Alfvén resonance.

Finally, we mention further work that we feel needs to be carried out. The work presented here must be extended to higher dimensions. At present, it is only a 1-D model and the solar atmosphere is, obviously, far more complex than this. The analytically obtained results show trends that must be built on in more realistic models and have the results verifiably observed.

# 8
# Summary and conclusions

*In the present chapter we draw the Thesis to an end, summarizing and reviewing the conclusions from each of the individual chapters. Furthermore, we shall describe some further work that can be carried out in the field of nonlinear resonant absorption. We also discuss the limitations and applicability of the research presented in the Thesis. The subject of my research is laterally driven resonant absorption of MHD waves in completely ionized and hot plasmas. In solar plasmas, the spectral theory predicts the existence of two resonances: Alfvén and slow. In the case of the slow resonance we investigated the effect of Hall currents on nonlinear resonant waves. At the Alfvén resonance we found the upper limit of linear theory and calculated the mean shear flow generated by resonant absorption. We then studied the absorption of fast magnetoacoustic waves at Alfvén and slow resonances. Finally, we introduced the concept of coupled Alfvén and slow resonances (in the context of chromospheric heating) and numerically analysed the resonant absorption of FMA waves at these coupled resonances.*

*Nobody of any real culture, for instance, ever talks nowadays about the beauty of sunset. Sunsets are quite old fashioned. To admire them is a distinct sign of provincialism of temperament. Upon the other hand they go on.*
**(Oscar Wilde** 1854 — 1900**)**

## 8.1 Summary

The Sun is the most important celestial body for mankind's existence and has been studied continuously for centuries. During the ongoing research many questions have been [believed to be] answered, e.g. how the Sun creates energy, what is the Sun's life cycle, what is the Sun made of, etc., however, many more problems still remain unsolved. One such conundrum is the very high temperatures achieved in the solar corona. The observational evidence of heating requirements suggests that the complex magnetic field plays a vital role in all heating processes. The heating process we considered in the present Thesis is resonant absorption, which is not only a viable mechanism for supplying some of the heating requirement for coronal active regions, but can also play a role in energy transfer in lower regions of the Sun such as the chromosphere and even the photosphere. Recently, resonant absorption was proposed to be the mechanism responsible for damping of oscillations in coronal magnetic structures, making resonant absorption one of the cornerstones of coronal seismology.

Resonant absorption in an inhomogeneous magnetized plasma can occur whenever the frequency of an externally driven wave matches a local plasma frequency, which causes resonant energy transfer between the two systems. If the plasma is dissipative the resonantly transferred energy can be efficiently damped (by, e.g. resistivity or viscosity) to create heating. In the presence of a resonant surface, some wave parameters can become divergent which results in the increase of amplitude of resonant waves. The increasing amplitudes can cause a breakdown of linear theory. In solar plasmas, where the dynamics is described within the framework of MHD, there are two possible kinds of resonances: Alfvén and slow. The existence of these resonances is rooted in the behaviour of eigenoscillations of plasmas with inhomogeneities in the transversal direction with respect to the ambient magnetic field. The present Thesis investigated the mathematical description of resonances. At the slow resonance we investigated the effect of Hall currents (generating nonlinear dispersion) on nonlinear resonant waves. At the Alfvén resonance we found the upper limit of linear theory and calculated the mean shear flow generated by resonant absorption. We then studied the absorption of fast magnetoacoustic waves at Alfvén and slow resonances. Finally, we introduced the concept of coupled Alfvén and slow resonances (in the context of chromospheric heating) and numerically analysed the resonant absorption of FMA waves at these coupled resonances.

The first two chapters of the present Thesis introduced the Sun and all of the critical concepts required for the rest of the Thesis. We discussed the structure of the Sun, along with some of it's basic properties. The importance of the magnetic field was explained and magnetohydrodynamic waves were introduced giving, first, observational evidence and, then, theoretical explanation of their existence. Chapter 2 described the MHD equations and explained the assumptions used to obtain them and, also, the concepts of resonant absorption, anisotropy, dispersion, nonlinearity and the methodology for deriving governing equations were explained. In addition, for completeness, we described the procedure for finding the resonant interactions of linear slow MHD waves (presented by, e.g. Sakurai et al., 1991b; Goossens and Ruderman, 1995) and reproduced the nonlinear governing equation describing resonant slow waves in isotropic plasmas first derived by Ruderman et al. (1997d). Nonlinearity needs to be considered when studying resonant absorption because the near-resonant behaviour of some equilibrium quantities is divergent which causes local wave amplitudes to grow and in turn may lead to a breakdown in linear theory.

The nonlinear theory of resonant slow waves in strongly anisotropic and dispersive plasmas

was presented in Chapter 3. Ballai et al. (1998b) investigated slow dissipative layers in anisotropic plasmas, however, they neglected the dispersion due to Hall currents, which is inconsistent with the condition that the plasma is highly anisotropic [$\omega_{e(i)}\tau_{e(i)} \gg 1$, where $\omega_{e(i)}$ is the electron (ion) frequency and $\tau_{e(i)}$ is the mean electron (ion) collision time], because under these conditions it is essential to consider the off-diagonal terms of the conductivity tensor (Hall currents). It was shown in Chapter 3 that dispersion effects due to Hall currents are of the same order of magnitude as nonlinearity and dissipation inside the anisotropic dissipative layer. Outside the dissipative layer the results of the chapter coincided with all previous studies of resonant slow waves because the wave dynamics is described by linear and ideal theory far from the resonance (outside the dissipative layer) and the dispersion due to Hall conduction is a nonlinear term (only considered important in the dissipative layer). The chapter concludes that dispersion due to Hall currents at the slow resonance in strongly anisotropic plasmas results in the addition of a nonlinear term describing the dispersion compared with the result of Ballai et al. (1998b). Indeed the governing equation described by Ballai et al. (1998b) can be thought of a special case of Eq. (3.60) when dispersion due to Hall currents is negligible. The form of the jump in total pressure and the implicit connection formula for the normal velocity are similar to those previously found (see, e.g. Ruderman et al., 1997d; Ballai et al., 1998b), however, due to the difference in the governing equation the magnitude of the jump in the normal component of velocity will be changed.

The limit of linear theory for resonant Alfvén waves in space plasmas was considered in Chapter 4. Nonlinear theories of resonant absorption have mainly dealt with the slow resonance because slow waves are more affected by nonlinearity despite the fact that Alfvén waves are more likely to contribute to the process of heating. In Chapter 4, we investigated whether a nonlinear theory (similar to that produced for the slow resonance) could be derived in an isotropic or anisotropic dispersive plasma. It was found that a nonlinear theory could not be produced (using the standard method) and that dispersion due to Hall currents is negligible. We went on to estimate the upper limit for the applicability of linear theory of resonant Alfvén waves and we found that, in all space plasmas, linear theory is an accurate approximation provided that the dimensionless amplitude of variables far away from the resonance satisfies the condition $\epsilon \ll R_a^{-1/3}$ (where $R_a$ is the total Reynolds number at the Alfvén resonance). We accomplished the task by showing that the nonlinear corrections are always much smaller than the linear approximation and, in addition, the second order corrections are magnetoacoustic in nature and, therefore, are not resonant. If it were assumed that $\epsilon \geq R_a^{-1/3}$, our approach would become invalid and a new technique would be required. The most important conclusion of Chapter 4 was that the well-known linear theory is always applicable to resonant Alfvén waves in space plasmas when the incoming wave dynamics is described by linear theory far away from the resonance (otherwise the full nonlinear MHD equations have to be solved over the entire domain).

Chapter 5 was aimed to study the mean shear flows generated by nonlinear resonant Alfvén waves. Even though the wave dynamics at the Alfvén resonance are governed by linear theory, nonlinearity has a second manifestation which is the generation of a mean shear flow parallel to the magnetic surfaces outside the dissipative layer. The characteristic velocity of the flow is proportional to $\epsilon^{1/2}$ where $\epsilon$ is the dimensionless amplitude of perturbations far from the resonant surface. The jumps in the derivative of velocity parallel and perpendicular to the ambient magnetic field are derived in explicit form. The mean shear flow can create a Kelvin–Helmholtz instability (KHI) at the dissipative layer which would be in addition to the KHI that might exist due to the velocity field of the resonant Alfvén waves. The results of Chapter 5 have to be used

with caution when applied to the solar atmosphere because in deriving the mean shear flows we assumed that the plasma is homogeneous and infinite outside the dissipative layer when neither is a truly accurate description.

In Chapter 6 we devoted our time to the nonlinear resonant absorption of fast magnetoacoustic (FMA) waves in strongly anisotropic and dispersive plasmas. We employed the governing equations and jump conditions across the resonances derived in Chapters 3 and 4. The equilibrium consisted of an inhomogeneous region sandwiched between two semi-infinite regions of homogenous plasmas. In order to make the problem mathematically tractable, there were two important assumptions made in Chapter 6, the first was that the width of the inhomogeneous region was thin in comparison to the wavelength of the incoming FMA wave, i.e. we employed the so-called long wavelength approximation ($kx_0 \ll 1$) which enabled us to neglect terms of the order of $k^2x_0^2$ or larger. The second main assumption is that nonlinearity is weak, i.e. dissipation dominates nonlinearity (and dispersion) and a regular perturbation technique was used when dealing with nonlinear terms. These assumptions allowed us to to find analytical solutions to the governing equations. The weak nonlinear solution inside the slow dissipative layer was found and can be considered to be a small correction to the linear result. In the first order approximation the fundamental mode of the reflected wave was found, in the second order approximation terms were of the order of $k^2x_0^2$ so were neglected, while in the third order approximation we found a correction to the fundamental mode due to nonlinearity and dispersion. Finally, we obtained that even higher order approximations resulted in non-monochromatic harmonics, and therefore were neglected. At the Alfvén resonance the solution to the governing equation is found in terms of the fundamental mode. We then found the coefficient of wave energy absorption at both the slow and Alfvén resonance (separately). The coefficient at the slow resonance has a small nonlinear correction which decreases the overall absorption in comparison to the linear absorption coefficient. In the final section of Chapter 6 we, briefly, investigated the effect of equilibrium flows on the coefficient of wave energy absorption. The result of the equilibrium flows considered was a Doppler shifted phase velocity included in the definition of the coefficient of wave energy absorption.

Chapter 7 focuses on the numerical analysis of the resonant absorption of FMA waves due to coupling into the slow and Alfvén continua. The assumptions used in Chapter 6 were also applied to Chapter 7. The long wavelength assumption gives the additional benefit that the slow and Alfvén resonance are close enough together to produce a *coupled* resonance (an Alfvén resonance followed by a slow resonance that can both interact with the incoming wave). We also had to impose a further condition that equilibrium quantities inside the inhomogeneous layer are monotonic increasing functions which, although not fully realistic, made the problem tractable from a mathematical point of view. We derived the coefficient of wave energy absorption at a so-called *coupled resonance*. We showed that the outgoing (reflected) wave from a coupled resonance has both slow and Alfvén contributions, however, these components cannot be decoupled. We modelled the interaction of EIT waves with coronal loops and found that the interactions can produce efficient resonant absorption, however, the absorption is very dependent on the angle of inclination of the impinging wave ($\phi$) and the angle of inclination of the ambient magnetic field ($\alpha$). We also modelled chromospheric absorption using coupled resonances. We showed that coupled resonances produce more efficient absorption than the two single resonances alone, however, under the conditions considered, the absorption rate is still fairly low. The absorption coefficient is again heavily dependent on the variables $\alpha$ and $\phi$.

## 8.2 Further possible research on nonlinear resonant waves

The present Thesis has answered some important unresolved problems within the realm of resonant absorption. While solving the problems contained within the present Thesis we have uncovered more questions that still need answering. In our analysis we intentionally overlooked a few facts in order to make the analytical analysis tractable, however, the omitted ingredients could play an important role. The research presented in the Thesis could be expanded along the following lines.

The investigations presented in Chapters 3 and 4 completed the governing equations for resonant slow and Alfvén waves in a one-dimensional planar plasma using the single-fluid approximation. To extend this work we would have to do one (or combination) of the following:

- Calculate the governing equations when there is a slight dependence on the $y-$coordinate, such that the problem becomes quasi-2D. The addition of a small dependence on $y$ would allow the wave to take more than a plane polar shape and would provide a more accurate description of waves in the solar atmosphere. The role of the dependence is unclear, but warrants investigation.

- Derive the nonlinear governing equations for the slow and Alfvén resonance using the two-fluid approximation which would result in separate equations for the electrons and protons. The investigation would have to establish which scale is larger: dissipation or inertia. If the scale of dissipation is larger than the scale of inertia then the single-fluid approximation is adequate, however, if the converse is true we need a two-fluid approximation. Some work has been carried out on two-fluids with regards to ULF pulsations in the Earth's magnetosphere by, e.g. Wright and Allan (1996) where it was shown that the scales of dissipation and inertia play a vital role in determining the effects of a two-fluid approximation.

- Produce an analytical nonlinear theory for resonant Alfvén waves where the waves inside the dissipative layer can have a large amplitude (and small amplitude far away from the resonance) and not cause a breakdown in the validity of the approach taken. The new theory would be a more realistic model of the solar atmosphere.

The results of Chapter 5 provide an insight into the generated mean shear flow outside the dissipative layer. Similar work was carried out for the slow resonance by, e.g. Ruderman et al. (1997d). Possible extensions of this work are:

- Calculate the generated mean shear flow at the slow and Alfvén resonance in a two-fluid approximation. The two-fluid approximation could cause different flows for the ions and electrons.

- Derive the governing equations for the generated mean shear flow in a two-dimensional topology. The extra degree of freedom could create additional effects not yet discovered, clearly shown by solar wind measurements.

Chapters 6 and 7 calculated the wave energy absorption of monochromatic waves at the slow, Alfvén and the introduced coupled resonances. The work could be continued by:

- Extend the limits of validity to include the short and intermediate wavelength approximations and discover how this would affect the coefficient of wave energy absorption.

- Have a non-monotonic function for equilibrium quantities inside the inhomogeneous region. The function would need to be simple and smooth enough to allow mathematical tractability, but more realistic than the model presented.
- Have a non-monochromatic wave impinging on the inhomogeneous layer. The non-monochromatic wave is a far more realistic model for waves present in the solar atmosphere.
- Significant work should be focussed on the timescales for the development (and longevity) of resonant layers. The work would show whether or not the coupled slow and Alfvén resonances can supplement heating in the solar chromosphere.
- Further research should take into account the effect of mean shear flows produced by the velocity field of resonant Alfvén waves and by considering nonlinearity (as well as equilibrium flow effects) on the dissipative layer when investigating resonant absorption.

The further research proposed here is work that will extend the envelope on the theory of resonant absorption and if carried out would determine the feasibility of resonant absorption as a supplementary heating source for the solar corona.

# References


Acton, L. W., Wolfson, C. J., Joki, E. G., Culhane, J. L., Rapley, C. G., Bentley, R. D., Gabriel, A. H., Phillips, K. J. H., Hayes, R. W., and Antonucci, E. (1981). X-ray line widths and coronal heating. *Astrophys. J.*, 244:L137.

Alfvén, H. (1950). *Cosmical electrodynamics*. Clarendon Press, Oxford.

Andries, J., Goossens, M., Hollweg, J. V., Arregui, I., and Doorsselaere, T. V. (2005). Coronal loop oscillations. Calculation of resonantly damped MHD quasi-mode kink oscillations of longitudinally stratified loops. *Astron. Astrophys.*, 430:1109.

Aschwanden, M. J. (2003). Review of coronal oscillations - An observer's view. *NATO Advanced Research Workshops, 16-20 Sept 2002, Budapest, Hungary*.

Aschwanden, M. J. (2004). *Physics of the solar corona: an introduction*. Springer, Praxis.

Aschwanden, M. J., Bastian, T. S., and Gary, D. E. (1992). 180th AAS Meeting. In *Am. Astron. Soc.*, volume 24 of *BAAS*, page 802.

Aschwanden, M. J., Fletcher, L., Schrijver, C. J., and Alexander, D. (1999a). Coronal loop oscillations observed with the transition region and coronal explorer. *Astrophys. J.*, 520:880.

Aschwanden, M. J., Kosugi, T., Hanaoka, Y., Nishio, M., and Melrose, D. B. (1999b). Quadrupolar magnetic reconnection in solar flares. I. Three-dimensional geometry inferred from Yohkoh observations. *Astrophys. J.*, 526:1026.

Aschwanden, M. J., Nightingale, R. W., Andries, J., Goossens, M., and Doorsselaere, T. V. (2003). Observational tests of damping by resonant absorption in coronal loop oscillations. *Astrophys. J.*, 598:1375.

Athay, R. G. (1976). *The solar chromosphere and corona: quiet sun*. D. Reidel, Dordrecht.

Athay, R. G. and White, O. R. (1978). Chromospheric and coronal heating by sound waves. *Astrophys. J*, 526:1026.

Ballai, I. (2000). *Nonlinear resonant slow MHD waves in the solar atmosphere*. PhD thesis, Katholieke Universiteit Leuven.

Ballai, I., Douglas, M., and Marcu, A. (2008). Forced oscillations of coronal loops driven by EIT waves. *Astron. Astrophys.*, 488:1125.

Ballai, I. and Erdélyi, R. (1998). Resonant absorption of nonlinear slow MHD waves in isotropic steady plasmas - I. Theory. *Sol. Phys.*, 180:65.

Ballai, I., Erdélyi, R., and Goossens, M. (2000). Linear and nonlinear resonant interaction of sound waves in dissipative layers. *J. Plasma Phys.*, 64:579.

Ballai, I., Erdélyi, R., and Hargreaves, J. (2006). Slow magnetohydrodynamic waves in stratified and viscous plasmas. *Phys. Plasmas*, 13:042108.

Ballai, I., Erdélyi, R., and Pintér, B. (2005). On the nature of coronal EIT waves. *Astrophys. J.*, 633:L145.

Ballai, I., Erdélyi, R., and Ruderman, M. S. (1998a). Interaction of sound waves with slow dissipative layers in anisotropic plasmas in the approximation of weak nonlinearity. *Phys. Plasmas*, 5:2264.

Ballai, I., Ruderman, M. S., and Erdélyi, R. (1998b). Nonlinear theory of slow dissipative layers in anisotropic plasmas. *Phys. Plasmas*, 5:252.

Ballai, I., Thelen, J. C., and Roberts, B. (2003). Solitary waves in a Hall solar wind plasma. *Astron. Astrophys.*, 404:701.

Balogh, A. and Thompson, M. J. (2009). Introduction to solar magnetism: the early years. *Space Sci. Rev.*, 144:1.

Banerjee, D., Erdélyi, R., Oliver, R., and O'Shea, E. (2007). Present and future observing trends in atmospheric magnetoseismology. *Sol. Phys*, 246:3.

Baranov, V. B. and Ruderman, M. S. (1974). Waves in a plasma with Hall dispersion. *Fluid Dyn.*, 9:421.

Beckers, J. M. and Tallant, P. E. (1969). Chromospheric inhomogeneities in sunspot umbrae. *Sol. Phys*, 7:351.

Belien, A. J. C., Martens, P. C. H., and Keppens, R. (1999). Coronal heating by resonant absorption: the effects of chromospheric coupling. *Astrophys. J.*, 526:478.

Belmonte-Beitia, J., Pérez-García, V. M., Vekslerchik, V., and Torres, P. J. (2007). Lie symmetries and solitons in nonlinear systems with spatially inhomogeneous nonlinearities. *Phys. Rev. Lett.*, 98:064102.

Bender, C. M. and Országh, S. A. (1991). *Advanced methods for scientists and engineers: asymptotics*. Springer-Verlag, New York.

Biermann, L. (1946). The meaning of chromospheric turbulence and the UV excess of the Sun. *Die Naturwissenschaften*, 33:118.

Birn, J., Fletcher, L., Hesse, M., and Neukirch, T. (2009). Energy release and transfer in solar flares: simulations of three-dimensional reconnection. *Astrophys. J.*, 695:1151.

Biskamp, D. (1986). Magnetic reconnection via current sheets. *Phys. Fluids*, 29:1520.

Braginskii, S. I. (1965). Transport processes in a plasma. *Rev. Plasma Phys.*, 1:205.

Chandran, B. D. G. (2008). Weakly turbulent magnetohydrodynamic waves in compressible low-$\beta$ plasmas. *Phys. Rev. Lett.*, 101:235004.

Chapman, S. (1954). The viscosity and thermal conductivity of a completely ionized gas. *Astrophys. J.*, 120:151.

Chen, L. and Hasegawa, A. (1974). Plasma heating by spatial resonance of Alfvén wave. *Phys. Fluids*, 17:1399.

Cheng, C.-C., Doeschek, G. A., and Feldman, U. (1979). The dynamical properties of the solar corona from intensities and line widths of EUV forbidden lines of SI VIII, Fe XI, and Fe XII. *Astrophys. J.*, 227:1037.

Chitre, S. M. and Davila, J. M. (1991). The resonant absorption of p-modes by sunspots with twisted magnetic fields. *Astrophys. J.*, 371:785.

Clack, C. T. M. and Ballai, I. (2008). Nonlinear theory of resonant slow waves in anisotropic and dispersive plasmas. *Phys. Plasmas*, 15:082310.

Clack, C. T. M. and Ballai, I. (2009a). Mean shear flows generated by nonlinear resonant Alfvén waves. *Phys. Plasmas*, 16:072115.

Clack, C. T. M. and Ballai, I. (2009b). Nonlinear resonant absorption of fast magnetoacoustic waves in strongly anisotropic and dispersive plasmas. *Phys. Plasmas*, 16:0402305.

Clack, C. T. M., Ballai, I., and Douglas, M. (2009a). Resonant absorption of fast magnetoacoustic waves due to coupling into the slow and Alfvén continua in the solar atmosphere. *Astron. Astrophys.*, in press.

Clack, C. T. M., Ballai, I., and Ruderman, M. S. (2009b). On the validity of nonlinear Alfvén resonance in space plasmas. *Astron. Astrophys.*, 494:317.

Cowling, T. G. (1976). *Magnetohydroynamics*. Adam Hilger, Bristol.

Csík, A., Čadež, V. M., and Goossens, M. (1998). Effects of mass flow on resonant absorption and on over-reflection of magnetosonic waves in low-$\beta$ solar plasmas. *Astron. Astrophys.*, 339:215.

Das, M., Vogel, S. N., Verdoes, K., Gijs, A., O'Dea, C. P., and Baum, S. A. (2005). BIMA millimeter-wave observations of the core-jet and molecular gas in the FR I radio galaxy NGC 3801. *Astrophys. J.*, 629:757.

Davila, J. M. (1987). Heating of the solar corona by the resonant absorption of Alfvén wave. *Astrophys. J.*, 317:215.

DeForest, C. E. and Gurman, J. B. (1998). Observation of quasi-periodic compressive caves in solar polar plumes. *Astrophys. J.*, 501:L217.

DeGroof, A. and Goossens, M. (2000). Randomly driven fast waves in coronal loops. II. with coupling to Alfvén waves. *Anstron. Astrophys.*, 356:724.

DeGroof, A., Paes, K., and Goossens, M. (2002). Fast and Alfvén waves driven by azimuthal footpoint motions. I. Periodic driver. *Anstron. Astrophys.*, 386:681.

DePontieu, B., McIntosh, S. W., Carlsson, M., Hansteen, V. H., Tarbell, T. D., Schrijver, C. J., Title, A. M., Shine, R. A., Tsuneta, S., Katsukawa, Y., Ichimoto, K., Suematsu, Y., Shimizu, T., and Nagata, S. (2007). Chromospheric Alfvénic waves strong enough to power the solar wind. *Science*, 318:1574.

Deubner, F. L. (1975). Observations of low wavenumber nonradial eigenmodes of the sun. *Sol. Phys*, 44:371.

DiMauro, M. P. (2008). Helioseismology. *Astrophysics and Space Sciences Transactions*, 4:13.

Dmitruk, P. and Gómez, D. O. (1999). Scaling law for the heating of solar coronal loops. *Astrophys. J.*, 527:L63.

Dobrowolny, M., Mangeney, A., and Veltri, P. (1980). Fully developed anisotropic hydromagnetic turbulence in interplanetary space. *Phys. Lett. Rev.*, 45:144.

Doschek, G. A., Vanhoosier, M. E., Bartoe, J.-D. F., and Feldman, U. (1976). The emission-line spectrum above the limb of the quiet sun - 1175-1940Å. *Astrophys. J. Supp. Ser.*, 31:417.

Dymova, M. V. and Ruderman, M. S. (2006). Resonantly damped oscillations of longitudinally stratified coronal loops. *Astron. Astrophys.*, 457:1059.

Edwin, P. M. and Roberts, B. (1982). Wave propagation in a magnetically structured atmosphere III: the slab in a magnetic environment. *Sol. Phys*, 76:239.

Edwin, P. M. and Roberts, B. (1983). Wave propagation in a magnetic cylinder. *Sol. Phys*, 88:179.

Edwin, P. M. and Roberts, B. (1986). The Benjamin–Ono–Burgers equation: an application in solar physics. *Wave motion*, 8:151.

Elfimov, A. (2000). Icpp: Alfvén wave heating and current drive. In *42nd annual meeting of the APS division of plasma physics combined with the 10th international congress on plasma physics*, Québec City, Canada. Physics Institute, Brazil, American Physical Society.

Erdélyi, R. (1996). *Resonant absorption of MHD waves in visco-resistive plasmas: applications to the solar atmosphere*. PhD thesis, Katholieke Universiteit Leuven.

Erdélyi, R. (1997). Analytical solutions for cusp resonance in dissipative MHD. *Sol. Phys.*, 171:49.

Erdélyi, R. (1998). Resonant absorption of Alfvén waves in steady coronal loops. *Solar Phys.*, 180:213.

Erdélyi, R. (2004). Coronal heating: heating in the solar atmosphere. *Astron. Geophys.*, 45:34.

Erdélyi, R. (2006). Magnetic coupling of waves and oscillations in the lower solar atmosphere: can the tail wag the dog? *Royal Society of London Transactions Series A*, 364:351.

Erdélyi, R. (2008). *Waves and oscillations in the solar atmosphere*. World Scientific, Singapore.

Erdélyi, R. and Ballai, I. (1999). Resonant absorption of nonlinear slow MHD waves in isotropic steady plasmas - II. Application: resonant acoustic waves. *Sol. Phys.*, 186:67.

Erdélyi, R. and Ballai, I. (2001). Nonlinear resonant absorption of fast magnetoacoustic waves due to coupling into slow continua in the solar atmosphere. *Astron. Astrophys.*, 368:662.

Erdélyi, R. and Ballai, I. (2007). Heating of the solar and stellar coronae: a review. *Astron. Nachrichten*, 328:726.

Erdélyi, R. and Fedun, V. (2007). Solitary wave propagation in solar flux tubes. *Phys. Plasmas*, 13:032902.

Erdélyi, R. and Goossens, M. (1995). Resonant absorption of Alfvén waves in coronal loops in visco-resistive MHD. *Astron. Astrophys.*, 294:575.

Erdélyi, R. and Morton, R. J. (2009). Magnetohydrodynamic waves in a compressible magnetic flux tube with elliptical cross-section. *Astron. Astrophys.*, 494:295.

Erdélyi, R. and Taroyan, Y. (2008). Hinode EUV spectroscopic observations of coronal oscillations. *Astron. Astrophys.*, 489:L49.

Fedun, V., Ruderman, M. S., and Erdélyi, R. (2008). Generation of short-lived large-amplitude magnetohydrodynamic pulses by dispersive focusing. *Physics Letters A*, 372:6107.

Feldman, U., Doschek, G. A., Vanhoosier, M. E., and Purcell, J. D. (1976). The emission-line spectrum above the limb of a solar coronal hole - 1175-1940 Å. *Astrophys. J. Supp. Ser.*, 31:445.

Galtier, S. (2009). Wave turbulence in magnetized plasmas. *Non. Proc. in Geophys.*, 16:83.

Goedbloed, J. P. (1975). Spectrum of ideal magnetohydrodynamics of axisymmetric toroidal systems. *Phys. Fluids*, 18:1258.

Goedbloed, J. P. (1983). Lecture notes on ideal magnetohydrodynamics. *Rijnhuizen Report*, page 83.

Goedbloed, J. P. (1984). Plasma-vacuum interface problems in magnetohydrodynamics. *Physica D*, 12:107.

Golub, L. and Pasachoff, J. M. (1997). *The solar corona*. Cambridge University Press, Cambridge, UK.

Goossens, M. (1994). Alfvén wave heating. *Space Sci. Rev.*, 68:51.

Goossens, M., Andries, J., and Arregui, I. (2006). Damping of magnetohydrodynamic waves by resonant absorption in the solar atmosphere. *Royal Society of London Transactions Series A*, 364:433.

Goossens, M., Andries, J., and Aschwanden, M. J. (2002). Coronal loop oscillations. An interpretation in terms of resonant absorption of quasi-mode kink oscillations. *Astron. Astrophys.*, 394:L39.

Goossens, M., Arregui, I., Ballester, J. L., and Wang, T. J. (2008). Analytic approximate seismology of transversely oscillating coronal loops. *Astron. Astrophys.*, 484:851.

Goossens, M., Hollweg, J. V., and Sakurai, T. (1992). Resonant behaviour of MHD waves on magnetic flux tubes. III - Effect of equilibrium flow. *Solar Phys.*, 138:233.

Goossens, M. and Poedts, S. (1992). Linear resistive magnetohydrodynamic computations of resonant absorption of acoustic oscillations in sunspots. *Astrophys. J.*, 384:348.

Goossens, M. and Ruderman, M. S. (1995). Conservation laws and connection formulae for resonant MHD waves. *Phys. Scr.*, T60:171.

Goossens, M., Ruderman, M. S., and Hollweg, J. V. (1995). Dissipative MHD solutions for resonant Alfvén waves in 1-dimensional magnetic flux tubes. *Solar Phys.*, 157:75.

Grossmann, M. and Tataronis, J. (1973). Decay of MHD waves by phase mixing. *Zeitschrift für Physik*, 261:217.

Hasegawa, A. and Chen, L. (1976). Kinetic processes in plasma heating by resonant mode conversion of Alfvén wave. *Phys. Fluids*, 19:1924.

Hasegawa, A. and Uberoi, C. (1982). *The Alfvén wave*. U.S. Department of Energy, Washington D.C., USA.

Hassler, D. M., Rottman, G. J., Shoub, E. C., and Holzer, T. E. (1990). Line broadening of MG X 609 and 625 A coronal emission lines observed above the solar limb. *Astrophys. J.*, 348:L77.

Heyvaerts, J. and Priest, E. R. (1983). Coronal heating by phase-mixed shear Alfvén waves. *Astron. Astrophys.*, 117:220.

Hollweg, J. V. (1984). Resonances of coronal loops. *Astrophys. J.*, 277:392.

Hollweg, J. V. (1985). Viscosity in a magnetized plasma - Physical interpretation. *J. Geophys. Res.*, 90:7620.

Hollweg, J. V. (1987). Resonant absorption of magnetohydrodynamic surface waves - Physical discussion. *Astrophys. J.*, 312:880.

Hollweg, J. V. (1988). Resonance absorption of solar p-modes by sunspots. *Astrophys. J.*, 335:1005.

Hollweg, J. V. (1990). Heating of the solar corona. *Comput. Phys. Rep.*, 12:205.

Hollweg, J. V. and Yang, G. (1988). Resonance absorption of compressible magnetohydrodynamic waves at thin 'surfaces'. *J. Geophys. Res.*, 93:5423.

Huba, J. D. (1995). Hall magnetohydrodynamics in space and laboratory plasmas. *Phys. Plasmas*, 2:2504.

Ionson, J. A. (1978). Resonant absorption of Alfvénic surface waves and the heating of solar coronal loops. *Astrophys. J.*, 226:650.

Ionson, J. A. (1985). Coronal heating by resonant (A.C.) and nonresonant (D.C.) mechanisms. *Astron. Astrophys.*, 146:199.

Jain, R., Browning, P., and Kusano, K. (2006). Nonlinear effects on magnetic energy release by forced magnetic reconnection: long wavelength perturbations. *Phys. Plasmas*, 13:052902.

Jess, D. B., Mathioudakis, M., Erdélyi, R., Crockett, P. J., Keenan, F. P., and Christian, D. J. (2009). Alfvén waves in the lower solar atmosphere. *Science*, 323:1582.

Kai, K. and Takayanagi, A. (1973). Interferometer observation of pulsating sources associated with a type IV solar radio burst. *Solar Phys.*, 29:461.

Karpen, J. T., Dahlburg, R. B., and Davila, J. M. (1994). The effects of Kelvin–Helmholtz instability on resonance absorption layers in coronal loops. *Astrophys. J.*, 421:372.

Keppens, R., Bogdan, T. J., and Goossens, M. (1994). Multiple scattering and resonant absorption of p-modes by fibril sunspots. *Astrophys. J.*, 436:372.

King, D. B., Nakariakov, V. M., Deluca, E. E., Golub, L., and McClements, K. G. (2003). Propagating EUV disturbances in the solar corona: two-wavelength observations. *Astron. Astrophys*, 404:L1.

Korzennik, S. G. (2008). Current status of asteroseismology. *Advances in Space Research*, 41:897.

Leibacher, J. W. and Stein, R. F. (1971). A new description of the solar five-minute oscillation. *Astrophys. Lett.*, 7:191.

Leighton, R. B., Noyes, R. W., and Simon, G. W. (1962). Velocity fields in the solar atmosphere. I - Preliminary report. *Astrophys. J.*, 135:474.

Li, B. and Li, X. (2007). Propagation of non-Wentzel-Kramers-Brillouin Alfvén waves in a multi-component solar wind with differential ion flow. *Astrophys. J.*, 661:1222.

Lighthill, M. J. (1960). Studies on magnetohydrodynamic waves and other anisotropic wave motions. *Phil. Trans. Roy. Soc.*, 252:397.

Lites, B. W. (1988). Photoelectric observations of chromospheric sunspot oscillations. V - Penumbral oscillations. *Astrophys. J.*, 334:1054.

Lou, Y.-Q. (1990). Viscous magnetohydrodynamic modes and p-mode absorption by sunspots. *Astrophys. J.*, 350:452.

Mann, G. (1995). Simple magnetohydrodynamic waves. *J. Plasma Phys.*, 53:109.

Mariska, J., Warren, H., Williams, D., and Watanabe, T. (2008). Observations of Doppler shift oscillations with the EUV imaging spectrometer on Hinode. *Astrophys. J.*, 681:L41.

Mariska, J. T. (1992). *The solar transition region*. Cambridge University Press, New York.

Mariska, J. T., Feldman, U., and Doschek, G. A. (1979). Nonthermal broadening of extreme ultraviolet emission lines near the solar limb. *Astrophys. J.*, 73:361.

Matthaeus, W. H., Oughton, S., Pontius, D. H., and Zhou, Y. (1994). Evolution of energy-containing turbulent eddies in the solar wind. *J. Geophys. Res.*, 99:19267.

Miteva, R., Zhelyazkov, I., and Erdélyi, R. (2004). Hall-magnetohydrodynamic surface waves in solar wind flow-structures. *New J. phys.*, 6:14.

Mocanu, G., Marcu, A., Ballai, I., and Orza, B. (2008). The problem of phase mixed shear Alfvén waves in the solar corona revisited. *Astron. Nachrichten*, 329:780.

Nakariakov, V. M., Ofman, L., Deluca, E. E., Roberts, B., and Davila, J. M. (1999). TRACE observation of damped coronal loop oscillations: implications for coronal heating. *Science*, 285:862.

Nakariakov, V. M. and Oraevsky, V. N. (1995). Resonant interactions of modes in coronal magnetic flux tubes. *Sol. Phys.*, 160:289.

Nakariakov, V. M. and Roberts, B. (1999). Solitary autowaves in the magnetic tubes. *Phys. Lett. A*, 254:314.

Nakariakov, V. M., Roberts, B., and Murawski, K. (1997). Alfvén wave phase mixing as a source of fast magnetosonic waves. *Sol. Phys.*, 175:93.

Nakariakov, V. M. and Verwichte, E. (2005). Coronal waves and oscillations. *L. Rev. Solar Phys.*, 2:3.

Nayfeh, A. H. (1981). *Introduction to perturbation techniques*. Wiley–Interscience, New York.

Nocera, L. and Ruderman, M. S. (1998). On the steady state of nonlinear quasiresonant Alfvén oscillations in one-dimensional magnetic cavity. *Astron. Astrophys.*, 340:287.

Ofman, L. and Davila, J. M. (1995). Nonlinear resonant absorption of Alfvén waves in three dimensions, scaling laws, and coronal heating. *J. Geophys. Res.*, 100:23427.

Ofman, L., Davila, J. M., and Steinolfson, R. S. (1994). Nonlinear studies of coronal heating by the resonant absorption of Alfvén waves. *Geophys. Res. Lett.*, 21:2259.

Ofman, L. and Wang, T. J. (2008). Hinode observations of transverse waves with flows in coronal loops. *Astron. Astrophys.*, 482:L9.

Ogata, K. (2003). *System dynamics (4th edition)*. Prentice Hall, New Jersey, USA.

O'Shea, E., Banerjee, D., and Doyle, J. G. (2007). A statistical study of wave propagation in coronal holes. *Astron. Astrophys.*, 463:713.

O'Shea, E. and Doyle, J. G. (2009). On oscillations found in an active region with EIS on Hinode. *Astron. Astrophys.*, 494:355.

Osterbrock, D. E. (1961). The heating of the solar chromosphere, plages, and corona by magneto-hydrodynamic waves. *Astrophys. J.*, 134:347.

Parker, E. N. (1972). Topological dissipation and the small-scale fields in turbulent gases. *Astrophys. J.*, 174:499.

Parker, E. N. (1988). Nanoflares and the solar X-ray corona. *Astrophys. J.*, 330:474.

Parker, E. N. (1993). Resistive dissipation and magnetic field topology in the stellar corona. *Astrophys. J.*, 407:342.

Parker, E. N. (2009). Solar magnetism: the state of our knowledge and ignorance. *Space Sci. Rev.*, 144:15.

Pbroks13 (2009). The Sun. `http://en.wikipedia.org/wiki/Sun`.

Peter, H. and Vocks, C. (2003). Heating the magnetically open ambient background corona of the Sun by Alfvén waves. *Astron. Astrophys.*, 411:L481.

Piddington, J. H. (1956). Solar atmospheric heating by hydromagnetic waves. *MNRAS*, 116:314.

Poedts, S., Belien, A. J. C., and Goedbloed, J. P. (1994). On the quality of resonant absorption as a coronal loop heating mechanism. *Solar Phys.*, 151:271.

Poedts, S., Goossens, M., and Kerner, W. (1989). Numerical simulation of coronal heating by resonant absorption of Alfvén waves. *Sol. Phys.*, 123:83.

Poedts, S., Goossens, M., and Kerner, W. (1990a). On the efficiency of coronal loop heating by resonant absorption. *Astrophys. J.*, 360:279.

Poedts, S., Goossens, M., and Kerner, W. (1990b). On the efficiency of coronal loop heating by resonant absorption. *Solar Phys.*, 360:279.

Poedts, S., Goossens, M., and Kerner, W. (1990c). Temporal evolution of resonant absorption in solar coronal loops. *Comput. Phys. Commun.*, 59:95.

Poedts, S., Kerner, W., and Goossens, M. (1990d). Numerical simulation of the stationary state of periodically driven coronal loops. *Comput. Phys. Commun.*, 59:75.

Pokhotelov, O. A., Onishchenko, O. G., Balikhin, M. A., Stenflo, L., and Shukla, P. K. (2007). Magnetosonic solitons in space plasmas: dark or bright solitons? *J. Plasma Phys.*, 73:981.

Porter, L. J., Klimchuk, J. A., and Sturrock, P. A. (1994). The possible role of high-frequency waves in heating solar coronal loops. *Astrophys. J.*, 435:482.

Priest, E. R. (1984). *Solar magnetohydrodynamics*. Springer, Berlin.

Priest, E. R. (1997). Three-dimensional magnetic reconnection in the solar corona. *Phys. Plasmas*, 4:1945.

Priest, E. R. and Forbes, T. G. (1992). Magnetic flipping - Reconnection in three dimensions without null points. *J. Geophys. Res.*, 97:1521.

Reale, F., Testa, P., Klimchuk, J. A., and Susanna, P. (2009). Evidence of widespread hot plasma in a nonflaring coronal active region from Hinode/X-Ray telescope. *Astrophys. J.*, 698:756.

Robbrecht, E., Verwichte, E., Berghmans, D., Hochedez, J. F., Poedts, S., and Nakariakov, V. M. (2001). Slow magnetoacoustic waves in coronal loops: EIT and TRACE. *Astron. Astrophys.*, 370:591.

Roberts, B. (1981a). Wave propagation in a magnetically structured atmosphere I: surface waves at a magnetic interface. *Sol. Phys*, 69:27.

Roberts, B. (1981b). Wave propagation in a magnetically structured atmosphere II: waves in a magnetic slab. *Sol. Phys*, 69:39.

Roberts, B. (1987). On the magnetohydrodynamic solitons in jets. *Astrophys. J.*, 318:590.

Roberts, B. (1988). *Cometary and solar plasma physics: solar magnetohydrodynamics*. World Scientific, Singapore.

Roberts, B., Edwin, P. M., and Benz, A. O. (1984). On coronal oscillations. *Astrophys. J.*, 279:857.

Roberts, B. and Mangeney, A. (1982). Solitons in solar magnetic flux tubes. *Monthly Notices, RAS*, 198:3280.

Roussev, I., Doyle, J. G., Galsgaard, K., and Erdélyi, R. (2001a). Modelling of solar explosive events in 2D environments. III - Observable consequences. *Astron. Astrophys.*, 380:719.

Roussev, I., Galsgaard, K., Erdélyi, R., and Doyle, J. G. (2001b). Modelling of explosive events in the solar transition region in a 2D environment. I - General reconnection jet dynamics. *Astron. Astrophys.*, 370:298.

Roussev, I., Galsgaard, K., Erdélyi, R., and Doyle, J. G. (2001c). Modelling of explosive events in the solar transition region in a 2D environment. II - Various MHD experiments. *Astron. Astrophys.*, 375:228.

Ruderman, M. S. (1976). Waves in a nonuniform plasma with Hall dispersion. *Fluid Dyn.*, 11:762.

Ruderman, M. S. (1987). Stability of quasi-longitudinally propagating solitons in a Hall-dispersion plasma. *Fluid Dyn.*, 22:229.

Ruderman, M. S. (2000). Interaction of sound waves with an inhomogeneous magnetized plasma in a strongly nonlinear resonant slow-wave layer. *J. Plasma Phys.*, 63:43.

Ruderman, M. S. (2002). DNLS equation for large-amplitude solitons propagating in an arbitrary direction in a high-$\beta$ Hall plasma. *J. Plasma Phys.*, 67:271.

Ruderman, M. S. (2009). Resonant magnetohydrodynamic waves in high-beta plasmas. *Phys. Plasmas*, 16:042109.

Ruderman, M. S., Berghmans, D., Goossens, M., and Poedts, S. (1997a). Direct excitation of resonant torsional Alfvén waves by footpoint motions. *Astron. Astrophys.*, 320:305.

Ruderman, M. S. and Goossens, M. (1993). Nonlinearity effects on resonant absorption of surface Alfvén waves in incompressible plasmas. *Sol. Phys.*, 143:69.

Ruderman, M. S. and Goossens, M. (1996). Slow resonant MHD waves in one-dimensional magnetic plasmas with anisotropic viscosity and thermal conductivity. *Astrophys. J.*, 471:1015.

Ruderman, M. S., Goossens, M., Ballester, J. L., and Oliver, R. (1997b). Resonant Alfvén waves in coronal arcades driven by footpoint motions. *Astron. Astrophys.*, 328:361.

Ruderman, M. S., Goossens, M., and Hollweg, J. V. (1997c). Nonlinear theory of the interaction of sound waves with an inhomogeneous magnetized plasma in the resonant slow wave layer. *Phys. Plasmas*, 4:91.

Ruderman, M. S., Hollweg, J. V., and Goossens, M. (1997d). Nonlinear theory of resonant slow waves in dissipative layers. *Phys. Plasmas*, 4:75.

Ruderman, M. S., Nakariakov, V. M., and Roberts, B. (1998). Alfvén wave phase mixing in two-dimensional open magnetic configurations. *Astron. Astrophys.*, 338:1118.

Ruderman, M. S., Oliver, R., Erdélyi, R., Ballester, J. L., and Goossens, M. (2000). Slow surface wave damping in plasmas with anisotropic viscosity and thermal conductivity. *Astron. Astrophys.*, 354:261.

Ruderman, M. S. and Roberts, B. (2002). The damping of coronal loop oscillations. *Astrophys. J.*, 577:475.

Ruderman, M. S., Tirry, W., and Goossens, M. (1995). Non-stationary resonant Alfvén surface waves in one-dimensional magnetic plasmas. *Phys. Plasmas*, 54:129.

Ruderman, M. S., Verwichte, E., Erdélyi, R., and Goossens, M. (1996). Dissipative instability of the MHD tangential discontinuity in magnetized plasmas with anisotropic viscosity and thermal conductivity. *J. Plasma Phys.*, 56:285.

Rui-Xiang, X., Min, W., Shou-Biao, S., Chun, X., Wei-Hua, L., and Yi-Hua, Y. (2003). Observational evidence for solar coronal decimetric radio pulsations with very short periods. *Astron. Astrophys.*, 27:426.

Saba, J. L. R. and Strong, K. T. (1991). Coronal dynamics of a quiescent active region. *Astrophys. J.*, 375:789.

Sakurai, T., Goossens, M., and Hollweg, J. V. (1991a). Resonant behaviour of magnetohydrodynamic waves on magnetic flux tubes - part two. *Sol. Phys.*, 133:247.

Sakurai, T., Goossens, M., and Hollweg, J. V. (1991b). Resonant behaviour of MHD waves on magnetic flux tubes. I - Connection formulae at the resonant surfaces. *Sol. Phys.*, 133:227.

Sarkar, A. and Walsh, R. W. (2008). Hydrodynamic simulation of a nanoflare-heated multistrand solar atmospheric loop. *Astrophys. J.*, 683:516.

Schatzman, E. (1949). The heating of the solar corona and chromosphere. *Ann. d. Astrophys.*, 12:203.

Spitzer, L. (1962). *Physics of fully ionized gases*. Interscience, New York.

Spruit, H. C. (1981). Equations for thin flux tubes in ideal MHD. *Astron. Astrophys.*, 102:129.

Spruit, H. C. and Bogdan, T. J. (1992). The conversion of p-modes to slow modes and the absorption of acoustic waves by sunspots. *Astrophys. J.*, 391:L109.

Spruit, H. C. and Roberts, B. (1983). Magnetic flux tubes on the Sun. *Nature*, 304:401.

Sydorenko, D., Rankin, R., and Kabin, K. (2008). Nonlinear effects in the ionospheric Alfvén resonator. *J. Geophys. Res.*, 113:A10206.

Tataronis, J. and Grossmann, M. (1973). Decay of MHD waves by phase mixing. *Zeitschrift für Physik*, 261:203.

Terradas, J., Andries, J., and Goossens, M. (2007). Coronal loop oscillations : energy considerations and initial value problem. *Astron. Astrophys.*, 469:1135.

Terradas, J., Arregui, I., Oliver, R., Ballester, J. L., Andries, J., and Goossens, M. (2008). Resonant absorption in complicated plasma configurations: applications to multistranded coronal loop oscillations. *Astrophys. J.*, 679:1611.

Thomas, J. H. (1985). Hydromagnetic waves in the photosphere and chromosphere. *Theoretical Problems in High Resolution Solar Physics*, MPA 212:126.

Thompson, M. J. (2006). Magnetohelioseismology. *Royal Society of London Transactions Series A*, 364:297.

Thompson, M. J. and Zharkov, S. (2008). Recent developments in local helioseismology. *Sol. Phys*, 251:225.

Tirry, W. J., Berghmans, D., and Goossens, M. (1997). Temporal evolution of resonant absorption in coronal loops. Excitation by footpoint motions normal to the magnetic surfaces. *Astron. Astrophys.*, 322:329.

Tirry, W. J. and Goossens, M. (1995). Dissipative MHD solutions for resonant Alfvén waves in two-dimensional poloidal magnetoplasmas. *J. Geophys. Res.*, 100:23687.

Tomczyk, S., McIntosh, S. W., Keil, S. L., Judge, P. G., Schad, T., Seeley, D. H., and Edmondson, J. (2007). Alfvén waves in the solar corona. *Science*, 317:1577.

Čadež, V. M., Csík, A., Erdélyi, R., and Goossens, M. (1997). Absorption of magnetosonic waves in presence of resonant slow waves in the solar atmosphere. *Astron. Astrophys.*, 326:1241.

Ulrich, R. K. (1970). The five-minute oscillations on the solar surface. *Astrophys. J.*, 162:993.

van Ballegooijen, A. A. (1985). Electric currents in the solar corona and the existence of magnetostatic equilibrium. *Astrophys. J.*, 298:421.

van Doorsselaere, T., Nakariakov, V. M., and Verwichte, E. (2008). Detection of waves in the solar corona: kink or Alfvén? *Astrophys. J.*, 461:L73.

van Eester, D., Goossens, M., and Poedts, S. (1991). Analytical study of plasma heating by resonant absorption of the modified external kink mode. *J. Plasmas Phys.*, 45:3.

Vasheghani, F. S., van Doorsselaere, T., Verwichte, E., and Nakariakov, V. M. (2009). Propagating transverse waves in soft X-ray coronal jets. *Astron. Astrophys.*, 498:L29.

Vasquez, B. J. (2005). Resonant absorption of an Alfvén wave: hybrid simulations. *J. Geophys. Res.*, 110:A10S10.

Walsh, R. W. and Ireland, J. (2003). The heating of the solar corona. *Astron. Astrophys. Review*, 12:1.

Wang, T. J., Ofman, L., and Davila, J. M. (2009). Propagating slow magnetoacoustic waves in coronal loops observed by Hinode/EIS. *Astrophys. J.*, 696:1448.

Wang, X. Y. and Lin, Y. (2003). Generation of nonlinear Alfvén and magnetosonic waves by beam-plasma interaction. *Phys. Plasmas*, 10:3528.

Wentzel, D. G. (1977). On the role of hydromagnetic waves in the corona and the base of the solar wind. *Sol. Phys.*, 52:163.

Woodward, T. I. and McKenzie, J. F. (1994a). Stationary MHD waves modified by Hall current coupling - I. Cold compressible flow. *Planet Space Sci.*, 42:463.

Woodward, T. I. and McKenzie, J. F. (1994b). Stationary MHD waves modified by Hall current coupling - II. Incompressible flow. *Planet Space Sci.*, 42:481.

Wright, A. N. and Allan, W. (1996). Are two-fluid effects relevant to ULF pulsations? *J. Geophys. Res.*, 101:24991.

Young, P. R., Klimchuk, J. A., and Mason, H. E. (1999). Temperature and density in a polar plume - measurements from CDS/SOHO. *Astron. Astrophys.*, 350:286.

Zirin, H. and Stein, A. (1972). Observations of running penumbral waves. *Astron. Astrophys.*, 178:L85.

Zirker, B. J. (1993). Photospheric vortices and coronal heating. *Sol. Phys*, 147:47.

# A

# The derivation of the Hall term in the induction equation for resonant slow and Alfvén waves in dissipative layers

In this appendix we will derive the components of the Hall term in the induction equations and study the conditions under which this extra effect is important. The parallel component of the magnetic field perturbation dominates the other components in the slow dissipative layer. In contrast, in the Alfvén dissipative layer the perpendicular component of the magnetic field perturbation dominates the other components. When studying resonant slow waves we find that the Hall term contains the first derivative of this parallel component of the magnetic field perturbation with respect to $z$, whereas the first term of Braginskii's viscosity tensor contains the second derivative of the parallel component of the magnetic field perturbation with respect to $z$. As a result the Hall term can be of the same order or larger than the dissipative term when considering resonant slow waves in the anisotropic dissipative layer.

For resonant Alfvén waves the situation is different; we will show that it is a good approximation for typical conditions throughout the solar atmosphere to neglect the Hall conduction when investigating resonant Alfvén waves. The main reasons qualitatively are as follows. When we are in the lower solar atmosphere (e.g. solar photosphere) the Hall conduction is much smaller than the direct conduction since the product of the electron gyrofrequency ($\omega_e$) and collision time ($\tau_e$) is less than unity (see, e.g. Priest, 1984). For the upper atmosphere (e.g. chromosphere, corona), where the product $\omega_e\tau_e$ is greater than unity, the Hall conduction has to be considered. However, when the Hall terms are derived, the largest terms in the perpendicular direction relative to the ambient magnetic field cancel leaving only higher order approximation terms which are far smaller than the direct conduction and since the dominant dynamics of resonant Alfvén waves in dissipative layer resides in the components of velocity and magnetic field perturbation in the perpendicular direction relative to the background magnetic field we can neglect the Hall conduction completely from the analysis without affecting the governing equation.

The generalized Ohm's law including the Hall term can be written as (see, e.g. Priest, 1984;

Clack and Ballai, 2008)

$$\mathbf{E} = -\mathbf{v} \times \mathbf{B} + \frac{1}{\widetilde{\sigma}}\mathbf{j} + \frac{1}{en_e}\mathbf{j} \times \mathbf{B}, \tag{A-1}$$

where $\mathbf{E}$ is the electric field, $\mathbf{j}$ the density of the electrical current, $n_e$ the electron number density, $e$ the electron charge and $\widetilde{\sigma}$ the electrical conductivity. Here the electrical conductivity is given by

$$\widetilde{\sigma} = \frac{n_e e^2 m_e^{-1}}{\tau_e^{-1} + \tau_n^{-1}}, \tag{A-2}$$

with $m_e$ the electron mass, $\tau_e$ the electron collision time and $\tau_n$ the neutral collision time. The density of electrical current and magnetic induction ($\mathbf{B}$) are related by Ampére's law

$$\mathbf{j} = \frac{1}{\mu_0}\nabla \times \mathbf{B}, \tag{A-3}$$

For a fully-ionized, collision-dominated, plasma Eq. (A-2) reduces to

$$\widetilde{\sigma} \approx \frac{n_e e^2 \tau_e}{m_e}, \tag{A-4}$$

with, in accordance to Spitzer (1962), the electron collision time being

$$\tau_e = 2.66 \times 10^5 \frac{T^{3/2}}{n_e \ln \Lambda} \mathrm{s}, \tag{A-5}$$

where $T$ is the temperature and $\ln \Lambda$ is the Coulomb logarithm (here taken to be 22). From Eq. (A-5), $\tau_e$ changes from $9.4 \times 10^{-8}$s in the upper photosphere to $1.4 \times 10^{-2}$s in the solar corona. On the other hand, $\omega_e$ changes from $1.8 \times 10^{10}\mathrm{s}^{-1}$ in the upper photosphere to $1.8 \times 10^{8}\mathrm{s}^{-1}$ in the solar corona. As a consequence the Hall parameter ($\omega_e \tau_e$) changes from $1.69 \times 10^3$ in the upper photosphere to $2.52 \times 10^6$ in the solar corona. Since $\omega_e \tau_e \gg 1$, the Hall term cannot be completely neglected in the upper photosphere nor the solar corona for either the resonant slow or Alfvén waves.

In the slow dissipative layer, Hall conduction and compressional viscosity dwarf the direct conduction, so we estimate the relative importance of the Hall term to the compressional viscous term. In the case of the Alfvén dissipative layer, shear viscosity and direct conduction are of the same order of magnitude. Hence, we compare the relative importance of the Hall conduction to the direct conduction. To do this we employ a more sophisticated analysis similar to the analysis presented by, e.g. Ruderman et al. (1997d); Clack and Ballai (2008); Clack et al. (2009b). The generalized induction equation (including Hall and direct conduction) is

$$\frac{\partial \mathbf{B}}{\partial t} = \nabla \times (\mathbf{v} \times \mathbf{B}) + \overline{\eta}\nabla^2 \mathbf{B} + \frac{1}{\mu_0 e}\nabla \times \left(\frac{1}{n_e}\mathbf{B} \times \nabla \times \mathbf{B}\right). \tag{A-6}$$

In what follows we assume that the ionization coefficient is constant, so that $n_e$ is proportional to $\overline{\rho}$, and in particular $n_e^{-1}\nabla n_e = \overline{\rho}^{-1}\nabla\overline{\rho}$. Equations (3.19) and (3.39) provide the following estimations in the slow dissipative layer:

$$u = \mathcal{O}(\epsilon), \quad v_\perp = \mathcal{O}(\epsilon), \quad \rho = \mathcal{O}(\epsilon^{1/2}), \quad v_\parallel = \mathcal{O}(\epsilon^{1/2}), \quad b_\parallel = \mathcal{O}(\epsilon^{1/2}), \tag{A-7}$$

where $\epsilon$ still denotes the dimensionless amplitude of oscillations far away from the slow dissipa-

tive layer. Similarly, Eqs (3.19) and (3.39) provide the following estimates in the Alfvén dissipative layer:

$$u = \mathcal{O}(\epsilon), \quad b_x = \mathcal{O}(\epsilon), \quad b_\parallel = \mathcal{O}(\epsilon), \quad v_\parallel = \mathcal{O}(\epsilon), \quad v_\perp = \mathcal{O}(\epsilon^{1/2}), \quad b_\perp = \mathcal{O}(\epsilon^{1/2}). \tag{A-8}$$

The thickness of the dissipative layers divided by the characteristic scale of inhomogeneity is $\delta_c/l_{inh} = \delta_a/l_{inh} = \mathcal{O}(\epsilon^{1/2})$. This gives rise to

$$l_{inh}\frac{\partial \pi}{\partial x} = \mathcal{O}(\epsilon^{-1/2}\pi), \quad l_{inh}\frac{\partial \pi}{\partial z} = \mathcal{O}(\pi), \quad l_{inh}^2\frac{\partial^2 \pi}{\partial z^2} = \mathcal{O}(\pi), \tag{A-9}$$

where $\pi$ denotes any of the quantities; $u$, $\rho$, $v_\parallel$, $b_\parallel$ in the slow dissipative layer; or $u$, $b_x$, $b_\parallel$, $b_\perp$, $v_\perp$ in the Alfvén dissipative layer. Since the first terms in the expansions of $b_\perp$ (and $v_\perp$) in the slow dissipative layer, and $v_\parallel$ in the Alfvén dissipative layer, are independent of $x$ it follows that

$$l_{inh}\frac{\partial \hat{\pi}}{\partial x} = \mathcal{O}(\hat{\pi}), \quad l_{inh}\frac{\partial \hat{\pi}}{\partial z} = \mathcal{O}(\hat{\pi}), \quad l_{inh}^2\frac{\partial^2 \hat{\pi}}{\partial x^2} = \mathcal{O}(\epsilon^{-1/2}\hat{\pi}), \tag{A-10}$$

where $\hat{\pi}$ represents $b_\perp$ and $v_\perp$ in the slow dissipative layer and denotes $v_\parallel$ in the Alfvén dissipative layer.

We now need to calculate the components of the Hall term from Eq. (A-6) normal to the magnetic surfaces (the $x-$direction) and in the magnetic surfaces parallel and perpendicular to the equilibrium magnetic field lines. We use Eqs (A-9) and (A-10) in order to estimate all the terms and then we only retain the largest ones. In the slow dissipative layer, the components of the Hall term in the induction equation reduce to

$$H_x = \frac{B_0 \cos\alpha \sin\alpha}{\mu_0 e n_e}\frac{\partial^2 b_\parallel}{\partial z^2} + \ldots, \quad H_\perp = \frac{B_0 \cos\alpha}{\mu_0 e n_e}\frac{\partial^2 b_\parallel}{\partial x \partial z} + \ldots,$$

$$H_\parallel = \frac{B_0 \sin\alpha}{\rho_0 \mu_0 e n_e}\frac{\partial b_\parallel}{\partial z}\frac{\partial \rho}{\partial x} + \ldots. \tag{A-11}$$

Whereas, in the Alfvén dissipative layer the largest components of the Hall term in the induction equation are

$$H_x = \frac{B_0 \cos^2\alpha}{\mu_0 e n_e}\frac{\partial^2 b_\perp}{\partial z^2} + \ldots, \quad H_\parallel = -\frac{B_0 \cos\alpha}{\mu_0 e n_e}\frac{\partial^2 b_\perp}{\partial z \partial x} + \ldots,$$

$$H_\perp = \frac{B_0}{\mu_0 e n_e}\left(\frac{1}{B_0}\frac{dB_0}{dx}\frac{\partial b_x}{\partial x} + \cos\alpha\frac{\partial^2 b_\parallel}{\partial z \partial x}\right) + \ldots, \tag{A-12}$$

where the dots indicate terms much smaller than those shown.

To find the relative importance of the Hall conduction we must find the largest terms of Braginskii's viscosity tensor (for the slow dissipative layer) and the largest terms of the direct conduction tensor (for the Alfvén dissipative layer). The dominant components of the Braginskii tensor acting in the normal and perpendicular directions relative to the equilibrium magnetic field are the second and third ones (describing shear viscosity). Since they are of the same order, for the purpose of our estimations it is enough to consider $\overline{\eta}_1$ only. Braginskii's viscosity tensor, in the slow dissipative layer, simplifies to (see derivation in Appendix B)

$$\overline{\eta}_1(\nabla \cdot S_1)_x = \overline{\eta}_1\frac{\partial^2 u}{\partial x^2} + \ldots, \quad \overline{\eta}_1(\nabla \cdot S_1)_\perp = \overline{\eta}_1\frac{\partial^2 v_\perp}{\partial x^2} + \ldots,$$

$$\overline{\eta}_0(\nabla\cdot S_0)_{\parallel}=\overline{\eta}_0\cos\alpha\left(2\cos\alpha\frac{\partial^2 v_{\parallel}}{\partial z^2}-\frac{\partial^2 u}{\partial x\partial z}\right)+\ldots. \tag{A-13}$$

It should be stated that $\overline{\eta}_0 \gg \overline{\eta}_1$ and $\overline{\eta}_0(\nabla\cdot S_1)_x=\overline{\eta}_0(\nabla\cdot S_1)_{\perp}=0$. We now need to calculate the components of the vector of the resistive term. We use Eqs (A-9) and (A-10) in order to estimate all the terms and we only retain the largest ones. As a result we have

$$\overline{\eta}\nabla^2 B_x=\overline{\eta}\frac{\partial^2 b_x}{\partial x^2}+\ldots,\quad \overline{\eta}\nabla^2 B_{\parallel}=\overline{\eta}\frac{\partial^2 b_{\parallel}}{\partial x^2}+\ldots,\quad \overline{\eta}\nabla^2 B_{\perp}=\overline{\eta}\frac{\partial^2 b_{\perp}}{\partial x^2}+\ldots. \tag{A-14}$$

With the aid of Eqs (A-7), (A-9) and (A-10) we obtain, for the slow dissipative layer, the ratios

$$\frac{H_x}{\overline{\eta}_1(\nabla\cdot S_1)_x}\sim\epsilon^{1/2}\frac{\overline{\chi}}{\overline{\eta}_1},\quad \frac{H_{\perp}}{\overline{\eta}_1(\nabla\cdot S_1)_{\perp}}\sim\epsilon^{-1/2}\frac{\overline{\chi}}{\overline{\eta}_1},\quad \frac{H_{\parallel}}{\overline{\eta}_0(\nabla\cdot S_0)_{\parallel}}\sim\frac{\overline{\chi}}{\rho_0\overline{\eta}_0}, \tag{A-15}$$

where $\overline{\chi}=\overline{\eta}\omega_e\tau_e$ is the coefficient of Hall conduction and $\overline{\eta}=(\widetilde{\sigma}\mu_0)^{-1}$ is the magnetic diffusivity. Strictly speaking, even the diffusivity is anisotropic in the solar corona, but the parallel and perpendicular components only differ by a factor of 2. It has been noted that magnetic diffusivity is much much smaller that the compressional viscosity in the solar corona. However, in the coefficient of Hall conduction ($\overline{\chi}=\overline{\eta}\omega_e\tau_e$) we observe that the magnetic diffusivity is multiplied by the product $\omega_e\tau_e$, which is very large in the solar corona ($10^4-10^6$). Moreover, if we look at the parallel component of Eq. (A-15) we see that the coefficient of Hall conduction is divided by the density, which is very small under solar coronal conditions. Therefore, the parallel component of the Hall term in the induction equation becomes very important in the slow dissipative layer. The Hall terms in the normal and perpendicular direction relative to the background magnetic field are included here for completeness, but they do not play a role in the equation governing resonant slow waves (i.e. can be left out completely and will not alter the result shown). This is attributed to the fact that the dominant dynamics of resonant slow waves is in the parallel direction relative to the ambient magnetic field.

Using Eqs (A-8)–(A-10) we obtain, for the Alfvén dissipative layer, the ratios

$$\frac{H_x}{\overline{\eta}\nabla^2 B_x}\sim\epsilon^{1/2}\omega_e\tau_e,\quad \frac{H_{\parallel}}{\overline{\eta}\nabla^2 B_{\parallel}}\sim\omega_e\tau_e,\quad \frac{H_{\perp}}{\overline{\eta}\nabla^2 B_{\perp}}\sim\epsilon\omega_e\tau_e. \tag{A-16}$$

For the Hall conduction to be significant in the direction of the dominant dynamics of resonant Alfvén waves (i.e. in the perpendicular direction) we must have $\epsilon\omega_e\tau_e\gtrsim 1$. This is plausible for the solar upper atmosphere. If this condition holds, then we must consider the Hall term in the induction equation. However, if the perpendicular component of Eq. (A-16) is expanded using Eq. (3.19), we obtain

$$\epsilon^{3/2}\eta\left\{\frac{1}{B_0}\left(\frac{dB_0}{dx}\right)\frac{\partial b_x^{(1)}}{\partial\xi}+\cos\alpha\frac{\partial^2 b_{\parallel}^{(1)}}{\partial\theta\partial\xi}\right\}+\mathcal{O}(\epsilon^2). \tag{A-17}$$

It should be noted that in deriving Eq. (A-17) we have used the assumption that $\epsilon\omega_e\tau_e=\mathcal{O}(1)$. The terms inside the braces are of the same order as the direct conduction. Hence, they would be expected to appear in the governing equation. When substituting for $b_x^{(1)}$ and $b_{\parallel}^{(1)}$ using Eqs

(4.17) and (4.18), respectively, it is found that the terms inside the brackets cancel in the form

$$\frac{\cos\alpha}{V}\left(\frac{dB_0}{dx}\right)\frac{\partial u^{(1)}}{\partial \xi} - \frac{\cos\alpha}{V}\left(\frac{dB_0}{dx}\right)\frac{\partial u^{(1)}}{\partial \xi} = 0. \tag{A-18}$$

Equation (A-18) shows that the Hall term in the perpendicular component of induction is always smaller than the direct conduction in the solar atmosphere. The normal and parallel components of the Hall conduction are, in fact, larger than the perpendicular component. Nevertheless they play no role in derivation of the governing equation of resonant Alfvén waves in dissipative layer. The parallel component is the largest of the three components and this is to be expected as the Hall effect is strongest at right angles to the dominant wave motion. This is in complete agreement with Eq. (A-15) which found the largest Hall effect was in the perpendicular component of Hall conduction, which is at right angles to the dominant dynamics of resonant slow waves.

In summary, for resonant Alfvén waves in dissipative layers, it is a good approximation to neglect the Hall term in the induction equation. This approximation holds throughout the entire solar atmosphere. On the other hand, we have shown for resonant slow waves in dissipative layers that the Hall term in the parallel direction relative to the ambient magnetic field ($H_{\parallel}$) must be included when $\omega_e\tau_e \gg 1$ because it is the same order of magnitude (or larger) than the compressional viscous term.

# B

# Braginskii's viscosity tensor and the derivation of largest terms

In this Appendix, we shall derive the largest terms of Braginskii's viscosity tensor when studying resonant slow and Alfvén waves inside anisotropic dissipative layers. Braginskii's viscosity tensor comprises of five terms. Its divergence can be written as (see, e.g. Braginskii, 1965)

$$\nabla \cdot \mathbf{S} = \overline{\eta}_0 \nabla \cdot \mathbf{S}_0 + \overline{\eta}_1 \nabla \cdot \mathbf{S}_1 + \overline{\eta}_2 \nabla \cdot \mathbf{S}_2 - \overline{\eta}_3 \nabla \cdot \mathbf{S}_3 - \overline{\eta}_4 \nabla \cdot \mathbf{S}_4, \tag{B-1}$$

We should stress that the terms proportional to $\overline{\eta}_0$, $\overline{\eta}_1$ and $\overline{\eta}_2$ in Eq. (B-1) describe viscous dissipation, while terms proportional to $\overline{\eta}_3$ and $\overline{\eta}_4$ are non-dissipative and describe the wave dispersion related to the finite ion gyroradius, therefore, they will be ignored in what follows.

The quantities $\mathbf{S}_0$, $\mathbf{S}_1$ and $\mathbf{S}_2$ are given by Eqs (2.23)–(2.25). The first viscosity coefficient ($\overline{\eta}_0$) has the following approximate expression (see, e.g. Ruderman et al., 2000)

$$\overline{\eta}_0 = \frac{\rho_0 k_B T_0 \tau_i}{m_p}, \tag{B-2}$$

where $\rho_0$ and $T_0$ are the equilibrium density and pressure, $m_p$ is the proton mass, $k_B$ the Boltzmann constant and $\tau_i$ the ion collision time. The other viscosity coefficients depend on the quantity $\omega_i \tau_i$, where $\omega_i$ is the ion gyrofrequency. When $\omega_i \tau_i \gg 1$ the coefficients in Eq. (B-1) are given by the approximate expressions

$$\overline{\eta}_1 = \frac{\overline{\eta}_0}{4\left(\omega_i \tau_i\right)^2}, \; \overline{\eta}_2 = 4\overline{\eta}_1. \tag{B-3}$$

The viscosity described by the sum of the second and third terms in Eq. (B-1) is the shear viscosity. For typical coronal conditions $\omega_i \tau_i$ is of the order of $10^5 - 10^6$, so according to Eq. (B-3) the term proportional to $\overline{\eta}_0$ in Eq. (B-1) is much larger than the second and third terms. This is true for the slow resonance, however, it has been long understood that the compressional viscosity does not remove the Alfvén singularity (see, e.g. Erdélyi and Goossens, 1995; Mocanu et al., 2008; Clack et al., 2009b) while shear viscosity does.

First, we shall calculate the components of the compressional viscosity. We will use the notation of parallel and perpendicular components as defined in Sect. 2.7. It is straightforward to obtain that

$$\overline{\eta}_0 \left(\nabla \cdot \mathbf{S}_0\right)_x = 0, \quad \overline{\eta}_0 \left(\nabla \cdot \mathbf{S}_0\right)_\perp = 0, \tag{B-4}$$

$$\overline{\eta}_0 \left(\nabla \cdot \mathbf{S}_0\right)_\parallel = \overline{\eta}_0 \cos\alpha \left(2\frac{\partial^2 v_\parallel}{\partial z^2}\cos\alpha - \frac{\partial^2 u}{\partial x \partial z} + \frac{\partial^2 v_\perp}{\partial z^2}\sin\alpha\right). \tag{B-5}$$

The shear viscosity, as stated above, is the sum of the second and third terms of Eq. (B-1). To evaluate these terms we use the approximate expression for $\overline{\eta}_1$ and $\overline{\eta}_2$ given by Eq. (B-3). As a result we obtain

$$\overline{\eta}_1 \left[\left(\nabla \cdot \mathbf{S}_1\right)_x + 4\left(\nabla \cdot \mathbf{S}_2\right)_x\right] = \overline{\eta}_1 \left[\frac{\partial^2 u}{\partial x^2} + (1 + 3\cos^2\alpha)\frac{\partial^2 u}{\partial z^2} + 4\frac{\partial^2 v_\parallel}{\partial x \partial z}\cos\alpha\right], \tag{B-6}$$

$$\begin{aligned}\overline{\eta}_1 \left[\left(\nabla \cdot \mathbf{S}_1\right)_\perp + 4\left(\nabla \cdot \mathbf{S}_2\right)_\perp\right] = \overline{\eta}_1 \Bigg[&\frac{\partial^2 v_\perp}{\partial x^2} + \left(4 - 3\sin^2\alpha - 16\sin^6\alpha\right)\frac{\partial^2 v_\perp}{\partial z^2} \\ &+ 4\sin\alpha\cos\alpha\left(4\sin^4\alpha - 1\right)\frac{\partial^2 v_\parallel}{\partial z^2}\Bigg],\end{aligned} \tag{B-7}$$

$$\begin{aligned}\overline{\eta}_1 \left[\left(\nabla \cdot \mathbf{S}_1\right)_\parallel + 4\left(\nabla \cdot \mathbf{S}_2\right)_\parallel\right] = 4\overline{\eta}_1 \Bigg\{&\frac{\partial^2 v_\parallel}{\partial x^2} + \left[1 + \cos^2\alpha\left(4\sin^4\alpha - 1\right)\right]\frac{\partial^2 v_\parallel}{\partial z^2} \\ &+ \frac{\partial^2 u}{\partial x \partial z}\cos\alpha - \left(4\sin^4\alpha + 1\right)\frac{\partial^2 v_\perp}{\partial z^2}\cos\alpha\sin\alpha\Bigg\}.\end{aligned} \tag{B-8}$$

Equations (B-4)–(B-8) are complicated, but we can simplify them further by taking the largest term only in each equation.

When studying resonant slow waves we can take the largest term proportional to $\overline{\eta}_0$ for the parallel direction, and the largest terms from Eqs (B-6) and (B-7), as the compressional viscosity in the normal and perpendicular directions are zero. This results in Braginskii's viscosity tensor, at the slow resonance, being approximated to

$$\left(\nabla \cdot \mathbf{S}\right)_x \approx \overline{\eta}_1 \left(\frac{\partial^2 u}{\partial x^2} + 4\frac{\partial v_\parallel}{\partial x \partial z}\cos\alpha\right), \tag{B-9}$$

$$\left(\nabla \cdot \mathbf{S}\right)_\perp \approx \overline{\eta}_1 \left[\frac{\partial^2 v_\perp}{\partial x^2} + 4\sin\alpha\cos\alpha\left(4\sin^4\alpha - 1\right)\frac{\partial^2 v_\parallel}{\partial z^2}\right], \tag{B-10}$$

$$\left(\nabla \cdot \mathbf{S}\right)_\parallel \approx 2\overline{\eta}_0 \frac{\partial^2 v_\parallel}{\partial z^2}\cos^2\alpha. \tag{B-11}$$

Even though Eqs (B-9) and (B-10) look complicated they appear for completeness. Since the dominant dynamics of resonant slow waves resides in the components of velocity and magnetic field perturbations parallel to the ambient magnetic field we can set $\left(\nabla \cdot \mathbf{S}\right)_x = \left(\nabla \cdot \mathbf{S}\right)_\perp = 0$ without loss of generality.

At the Alfvén resonance, the viscosity in the parallel direction it would, at first, seem obvious that the largest term will be proportional to $\overline{\eta}_0$ rather than $\overline{\eta}_1$. However, some of the variables

proportional to $\overline{\eta}_1$ have derivatives with respect to $x$ which produce enormous gradients in the anisotropic Alfvén dissipative layer when there is a transversal inhomogeneity, hence some of the terms proportional to $\overline{\eta}_1$ are of the same order as or larger than the terms proportional to $\overline{\eta}_0$. It is also important to note that in the first order approximation the second and third terms on the right-hand side of Eq. (B-4) cancel [see Eq. 4.20]. For the normal and perpendicular components of viscosity, the treatment is slightly simpler. The compressional viscosity is zero, and as derivatives with respect to $z$ are much small that derivatives with respect to $x$, we can select the largest term proportional to $\overline{\eta}_1$ by observation. Therefore, the viscosity tensor, at the Alfvén resonance, can be approximated by

$$(\nabla \cdot \mathbf{S})_x \approx \overline{\eta}_1 \frac{\partial^2 u}{\partial x^2}, \quad (\nabla \cdot \mathbf{S})_\perp \approx \overline{\eta}_1 \frac{\partial^2 v_\perp}{\partial x^2}, \quad (\nabla \cdot \mathbf{S})_\parallel \approx 4\overline{\eta}_1 \frac{\partial^2 v_\parallel}{\partial x^2}. \tag{B-12}$$

Equations (B-9)–(B-11) give an appropriate approximation to Braginskii's viscosity tensor when studying nonlinear resonant slow waves in anisotropic dissipative layers and Eq. (B-12) is the appropriate approximation to Braginskii's viscosity tensor when investigating nonlinear resonant Alfvén waves in anisotropic dissipative layers. It is interesting to note that the terms in Eq. (B-12) are identical to the largest terms when considering isotropic viscosity. Obviously, compressional viscosity cannot remove the Alfvén singularity since Eq. (B-4) is identically zero.